Economic Model Predictive Control and Time-Varying Systems

Von der Universität Bayreuth
zur Erlangung des Grades eines

Doktors der Naturwissenschaften (Dr. rer. nat.)

genehmigte Abhandlung

von

Simon Pirkelmann

aus Bayreuth

Acknowledgments

First of all, I would like to thank my PhD supervisor Prof. Dr. Lars Grüne for his continuous excellent supervision and support in academic matters, the many opportunities for international scientific exchange and also for his trust and the freedom in being able to pursue seemingly unrelated side projects.

Furthermore, I would like to thank Prof. Dr. Matthias Müller, who helped me to get started in the early phase of my doctorate and also agreed to evaluate this thesis as a second reviewer and contributed numerous improvements. I would also like to thank the other members of the examination board Prof. Jörg Rambau and Prof. Anton Schiela.

I thank the members of the Chair of Applied Mathematics for the good relationship in the past years - both professionally and privately: Dr. Robert Baier, Dr. Michael Baumann, Dr. Philipp Braun, Matthias Höger, Dr. Georg Müller, Julian Ortiz Lopez, Bastian Pötzl, Manuel Schaller, Tobias Sproll, Dr. Marleen Stieler, Matthias Stöcklein, as well as my office mates Arthur Fleig and Lisa Krügel. Special thanks go to Dr. Thomas Jahn, who sparked in me an interest in the more practical aspects of mathematics, and of course, to the kind soul of the chair, Sigrid Kinder, who tenaciously masters all bureaucratic difficulties, always with a smile on her lips.

I would also like to thank the DFG project partners Dr. Julian Andrej, Prof. Dr. Thomas Meurer, Prof. Dr. Stefan Volkwein and, in particular, Dr. Luca Mechelli, from whom I learned a lot in countless meetings of varying degrees of productivity. Furthermore, to Dr. David Angeli I say thank you for giving me the opportunity for an extended visit at Imperial College in London.

Away from work, there are a number of people who accompanied me during my doctorate. Quite literally, the people of the university running group, with whom I ran hundreds of kilometers together, clearing my head of math by simply putting one foot in front of the other, especially Frank Berger, Matthias Biber, Sophia Koch, Philipp Meier, Leonie Schlicht, Leonie Schulze, and Martin Wessel.

In addition, the great people of the TransitionHaus and the imaginaerraum, who have always been an inspiration and stimulus for me to develop myself in many ways beyond the university, above all Tobias Eckert, Daniel Heinlein, David Kienle, Stephan Messlinger, Valentin Ochs, Matthias Stachowski, and Nico Stuhlmüller.

Abstract

This thesis contributes to a better understanding of the method of model predictive control (MPC) for time-varying systems. Time-varying systems are used to describe physical phenomena in numerous technical applications. The interior temperature of a building can, for example, be described by such a time-varying system because it is influenced by the daily and nightly fluctuations of the outside temperature and the weather. MPC can be used to compute efficient operating strategies of buildings (i.e. when to heat or to cool) and thereby reduce overall energy consumption. With regard to the urgently needed reduction of CO_2 emissions in the building sector, a deeper understanding of this method is indispensable to develop more powerful algorithms.

In time-varying systems, optimal system behavior can generally be very complex and, in particular, does not have to occur at an equilibrium or periodic trajectory. This makes it necessary to adequately characterize optimal trajectories in the time-varying setting, which is achieved by considering a modified notion of optimality. Based on this, conditions are derived under which the cost of the MPC closed-loop are approximately optimal, i.e. almost equal to the costs of an optimal solution trajectory on infinite time horizon. For a sufficiently large MPC horizon length, the optimal system behavior can in principle be approximated arbitrarily well. In this context, the so-called turnpike property and a continuity property of the optimal value function are of particular importance. In addition, it is shown that under the additional assumption of strict dissipativity the MPC trajectory tends towards the vicinity of an optimal operating trajectory.

Furthermore, it is examined whether the assumptions made are reasonable and can be explicitly proven or observed in simulations for systems in practice. For this purpose, central results of the work are illustrated by the example of a convection-diffusion equation. Moreover, two methods for optimal control of variations of this equation are presented.

Finally, a performance estimator for time-invariant MPC is presented, which serves to monitor the controller performance at run-time.

Zusammenfassung

Die vorliegende Arbeit leistet einen Beitrag dazu, die Methode der Modellprädiktiven Regelung (MPC) für zeitvariante Systeme besser zu verstehen. Zeitvariante Systeme dienen zur Beschreibung von physikalischen Phänomenen in zahlreichen technischen Anwendungen. Die Innentemperatur eines Gebäudes kann z.B. durch ein solches zeitveränderliches System beschrieben werden, da sie durch die tageszeitlichen Schwankungen der Außentemperatur und durch das Wetter beeinflusst wird. Mit MPC können effiziente Betriebsstrategien von Gebäuden (d.h. wann geheizt bzw. gekühlt werden soll) berechnet und dadurch der Energieverbrauch insgesamt gesenkt werden. Im Hinblick auf die dringend nötigen Reduktion von CO_2 Emissionen im Gebäudesektor ist ein tieferes Verständnis dieser Methode unabdingbar, etwa um leistungsfähigere Algorithmen zu entwickeln.

Bei zeitvarianten System kann optimales Systemverhalten im Allgemeinen sehr komplex ausfallen und muss insbesondere nicht an einem Gleichgewicht oder einer periodischen Trajektorie auftreten. Dies erfordert eine geeignete Charakterisierung optimaler Trajektorien im zeitvarianten Fall, was durch die Einführung eines modifizierten Optimalitätsbegriffs erreicht wird. Darauf aufbauend werden in der Arbeit Bedingungen hergeleitet, unter denen die Kosten der Trajektorien des geschlossenen MPC Regelkreises annährend optimal sind, d.h. nahezu den Kosten einer Lösungstrajektorie auf unendlichem Zeithorizont entsprechen. Für hinreichend große MPC Horizontlänge kann das optimale Systemverhalten im Prinzip beliebig gut approximiert werden. In diesem Zusammenhang kommen der sogenannten Turnpike Eigenschaft und einer Stetigkeitseigenschaft der optimalen Wertefunktion besondere Bedeutung zu. Zusätzlich wird gezeigt, dass unter der zusätzlichen Annahme von strikter Dissipativität die MPC Trajektorie in eine Umgebung der optimalen Systemtrajektorie strebt.

Weiterhin wird untersucht, ob bei Systemen in der Praxis die getroffenen Annahmen sinnvoll sind und explizit nachgewiesen bzw. mit Hilfe von Simulationen beobachtet werden können. Zu diesem Zweck werden zentrale Ergebnisse der Arbeit anhand des Beispiels einer Konvektions-Diffusions-Gleichung illustriert. Auch werden dazu zwei Verfahren zur optimalen Steuerung von Varianten dieser Gleichung vorgestellt.

Abschließend wird in der Arbeit ein Güteschätzer für zeitinvariante MPC vorgestellt, der dazu dient die Regelgüte zur Laufzeit zu überwachen.

Contents

1 | Introduction

1.1 Motivation and scope of the thesis

When it comes to bringing a room to a comfortable temperature, the average person chooses a rather intuitive strategy: If it's too cold, you turn up the heat, and if it's too hot, you open a window or switch on the air conditioning. Generally, this decision is made spontaneously, based on the momentarily perceived discomfort, and without thinking about how the outside temperature will change in the future.
It is easy to imagine that this is not the most energy-efficient method, as heating or cooling might run unnecessarily long, or could sometimes even have been avoided entirely if only one would have thought about the changing demand a little earlier. Even though this waste of energy may be small on an individual level, it constitutes a considerable savings potential when aggregated. In times of climate change, the obvious question is how to harness this potential, especially since the building sector is a significant contributor to carbon emissions [2].
Apart from structural changes, such as better insulation or the installation of more economical heating, ventilation and air conditioning (HVAC) systems, there is great potential for savings by more efficient and demand-driven operation of existing systems [1]. With the increasing spread of the Internet of Things and the ensuing proliferation of networked sensors and actuators, smart energy management of buildings can make a serious, pragmatic, and viable contribution to reducing the carbon footprint and also lower energy costs.

A promising approach to achieving improvements in the operation of buildings is model-based control. It relies on a mathematical model describing, for example, how the inside temperature behaves when the outside temperature changes, or how different types of heaters or insulation affect energy consumption. Nowadays, building models exist on various scales from the simplest energy balance models to complex fluid dynamic models based on physical principles [22, 38, 105, 111]. With the help of such models, model-based control can make predictions about the evolution of the temperature from which optimal heating or cooling strategies can be identified. This can also take into account the weather forecast for the coming days as well as variable energy prices and building occupancy. The goal is to find an optimal operation strategy on an arbitrarily long (essentially infinite) time horizon.

A well-established model-based control method is Model Predictive Control (MPC) [31, 50,96], sometimes also termed Receding Horizon Control. MPC breaks the problem on the infinite horizon down to finite sub-problems by optimizing predictions only on relatively short time horizons (say, several hours in advance in the context of HVAC). After solving the first sub-problem, one starts to implement the optimal control strategy, but at regular intervals (e.g., after one hour) the optimization procedure is carried out again on an appropriately shifted horizon. This approach offers great flexibility to incorporate newly acquired data (updated demands, temperature measurements, weather or price forecasts) to which the controller adjusts automatically. Another advantage of MPC is that it allows explicit consideration of state constraints such as allowed minimum and maximum temperatures.

In the industry, MPC was initially mainly used to control processes that can be described by linear systems or have relatively slow dynamics [40, 93, 94], but today the method is successfully applied to systems of ever-increasing size and complexity due to the availability of more powerful computers [19, 26, 27, 32, 64, 103].

In many cases, the successes in the industrial application of MPC have been enabled by a deepened mathematical understanding of the method. For many system classes, conditions could be derived allowing to determine whether MPC works for a given system or not (see e.g. the survey articles [30, 35] for recent advances in the context of economic MPC). Nevertheless, there are still a number of open questions, especially for the case of time-varying systems. This is relevant for the problem of energy-efficient building operation since a building can be regarded as such a time-varying system. To fully exploit the vast potential MPC offers for such applications, it is necessary to better understand the method also for time-varying systems. This thesis contributes to answering some of the open questions.

1.2   Outline and contribution

Chapter 2 - Fundamentals of Model Predictive Control

In the next chapter, we give a short introduction to the basics of control theory and introduce the MPC method. In addition, we present well-known MPC results both in the context of classical MPC as well as economic MPC. These include guarantees for the stability of MPC closed-loop trajectories and (sub-)optimality estimates for performance of the MPC solutions. We also summarize the central assumptions which are required for obtaining these results. Of these, two assumptions will play a particularly important role throughout the thesis: the turnpike property and a certain continuity assumption of the optimal value function.

Chapter 3 - Optimal control of the convection-diffusion equation

Theoretical results obtained in this thesis will be illustrated by means of numerical simulations of heat-convection systems. The physics of such systems can be modeled by a convection-diffusion partial differential equation (PDE). In this chapter, we introduce two variants of this PDE.

In the first variant, we consider a boundary controlled convection-diffusion equation. This setting could be interpreted as a room where the room temperature is subject to changing outside temperatures and can additionally be influenced by a controllable heating or cooling system. The goal is to keep the temperature inside the room within certain limits by adjusting the heating and cooling accordingly. To achieve this, we introduce a PDE constrained optimal control problem.

For the second setting, we assume that, additionally, controllable ventilation (e.g. a fan) is available. This also leads to an optimal control problem, but, in contrast to the first one, it is bilinear which complicates the theoretical analysis.

For both approaches, we present numerical methods for solving the corresponding optimal control problems. In the case of the bilinear optimal control problem, we describe how the problem is discretized and formulate a finite-dimensional optimization problem that can be solved by standard nonlinear optimization tools. For the other case, we apply a primal-dual active set method constituting a function space optimization approach to solve the problem.

Chapter 4 - MPC Results for time-varying systems

In this chapter, we extend results from Chapter 2 to MPC for time-varying systems. We will see that the time-variance raises new fundamental questions about the optimality of solutions. As a result, existing performance and stability results for time-invariant control systems do not directly apply.

We introduce *overtaking optimality* which is necessary for a well-defined optimality notion in the time-varying setting. It allows to generalize the concept of an optimal equilibrium, referred to as *optimal trajectory* in the time-varying context. These optimal trajectories represent particular trajectories on which a time-varying system should operate in order to achieve the best performance in the long run.

In contrast to Chapter 2, we consider modified turnpike and continuity assumptions which enable us to recover performance estimates of the MPC solutions in the time-varying case. The second part of the chapter aims to prove stability of the MPC trajectories, more specifically, to show that they converge to an optimal trajectory. By employing a time-varying strict dissipativity assumption, we show that it becomes possible to construct a Lyapunov function for the MPC controlled system by augmenting the optimal value function of the MPC optimization problem. This implies P-practical asymptotic stability of the optimal trajectory, meaning that the MPC trajectory will converge to a neighborhood of the optimal trajectory.

The results in the chapter are accompanied by several examples.

Chapter 5 - Analytical and numerical approaches for checking turnpike and continuity assumptions

The purpose of this chapter is to examine whether the assumptions made in Chapter 4, in particular, the turnpike property, continuity of the optimal value function, and strict dissipativity, are realistic and can be observed in practical systems.
First, it is shown that both the turnpike property and the continuity of the optimal value function can be derived from strict dissipativity provided that an additional controllability assumption is satisfied. This allows to explicitly verify the assumptions for the case of a simple example.
In the second part of the chapter, a convection-diffusion system inspired by a more realistic scenario is considered. For this setting, numerical simulations are used to demonstrate that optimal open-loop trajectories of the system show typical turnpike behavior. Furthermore, we present numerical evidence for the continuity of the optimal value function in the vicinity of the optimal trajectory.

Chapter 6 - Online MPC performance estimates

Another contribution of this thesis is a new performance estimate for time-invariant economic MPC. At the beginning of the chapter, it is shown that existing MPC performance estimates based on a relaxed dynamic programming inequality do not provide a satisfactory estimate for economic cost functions. Instead, an alternative approach is proposed which examines the improvement of the MPC cost between consecutive MPC steps and derives from this a quantitative estimate for the deviation of the optimal performance. This makes it possible to monitor the performance of the MPC trajectory at run-time for economic MPC. At the end of the chapter, the practical application of the estimator is illustrated using a numerical example.

2 | Fundamentals of Model Predictive Control

In this chapter, we give a brief introduction to the fundamentals of control theory and repeat key results of classical and economic model predictive control which we will expand on in the course of the thesis. We will also establish the notation that will be employed throughout the thesis.

2.1 Background of control theory

We consider the discrete-time control system

$$x(k + 1) = f(x(k), u(k)) \text{ for } k \in \mathbb{N}_0 \tag{2.1}$$

with state $x(k) \in X$ and control $u(k) \in U$.

Starting from an initial state $x(0) = x_0$, an iterative application of the map f with controls $u = (u(0), u(1), \ldots)$ yields a sequence of states $(x(0), x(1), x(2), \ldots)$. This sequence is called state trajectory and is denoted by $x_u(\cdot; x_0)$.

Control theory in general addresses the question of how to select the controls u so that the state x (or an output of the system) exhibits a desired behavior. This behavior can be very versatile. For instance, one could demand that the state approaches a certain predefined state and stays there. This is referred to as *stability*. Another example would be to prevent the state from entering a certain region in order to guarantee safe operation. The concrete formulation depends on the respective application.

Often the desired behavior can be described by an optimal control problem. For this we consider a so-called stage cost function $\ell : X \times U \to \mathbb{R}$, which assigns a value to each pair of state and control. The stage costs are summed up along a trajectory of the system:

$$J_\infty(x_0, u) := \sum_{k=0}^{\infty} \ell(x_u(k; x_0), u(k)) \tag{2.2}$$

We call this function infinite horizon cost functional. By selecting ℓ in such a way that every deviation from a desired state x_e is penalized, the goal of stability of the state trajectory can be formulated as an optimal control problem. The cost functional thus quantifies the

difference of the trajectory of the system from the desired state for all times. The goal is
to find a control sequence $u \in U^\infty$ that minimizes this difference:

$$\begin{aligned} &\underset{u \in U^\infty}{\text{minimize }} J_\infty(x_0, u) \\ &\text{s.t. } x(k+1) = f(x(k), u(k)), \quad x(0) = x_0. \end{aligned}$$
(2.3)

Likewise, it is possible to allow only certain states or controls. This is done in the form of
constraints of the optimal control problem. Let $\mathbb{X}$ and $\mathbb{U}$ denote the sets of allowed states
and controls, respectively. Furthermore,

$$\mathbb{U}^\infty(x_0) := \{u \in \mathbb{U}^\infty | x_u(k; x_0) \in \mathbb{X} \text{ for all } k \in \mathbb{N}_0\}$$
(2.4)

is the set of all admissible controls for which the state trajectory remains admissible.
The optimal control problem with constraints then reads:

$$\begin{aligned} &\underset{u \in \mathbb{U}^\infty(x_0)}{\text{minimize }} J_\infty(x_0, u) \\ &\text{s.t. } x(k+1) = f(x(k), u(k)), \quad x(0) = x_0 \text{ for all } k \in \mathbb{N}. \end{aligned}$$
(2.5)

In any case, an optimization problem must be solved on an infinite horizon, which in
general is challenging. Model Predictive Control is a method for solving such problems by
reducing the complexity of the problem in time.

2.2   Model Predictive Control

The basic idea of Model Predictive Control (MPC) is to truncate the optimization horizon
after a finite number of time steps $N \in \mathbb{N}$. This means that only the cost functional

$$J_N(x_0, u) := \sum_{k=0}^{N-1} \ell(x_u(k; x_0), u(k))$$
(2.6)

is optimized on a finite horizon over the set of admissible control sequences

$$\mathbb{U}^N(x_0) := \{u \in \mathbb{U}^N | x_u(k; x_0) \in \mathbb{X} \text{ for all } k \in \{0, \dots, N-1\}\}.$$
(2.7)

The resulting optimal control sequence is denoted by u_{N,x_0}^*. Only the first part of this
control sequence is then used as a control in the system. Afterwards the horizon is shifted
one step ahead and the optimization is carried out again at the next time on the shifted
horizon. Since this can be continued indefinitely, in this way a trajectory on an infinite
horizon is obtained.
In Algorithm 2.1 the procedure is summarized and in Figure 2.1 the idea is visualized.
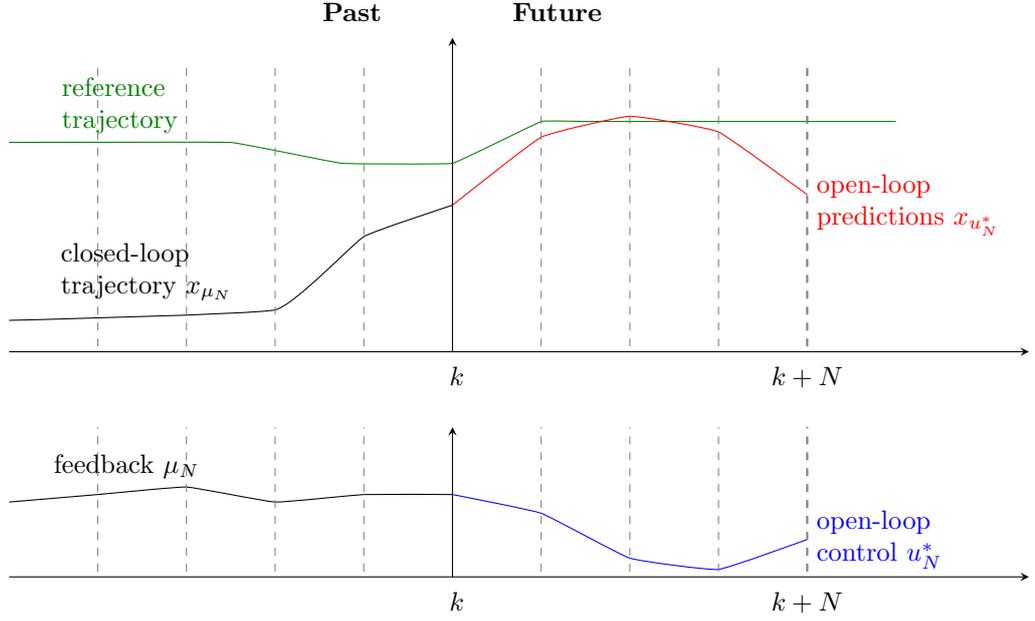
Figure 2.1: The figure illustrates the MPC principle. The upper part of the figure shows the evolution of the state trajectory, while the lower part shows the controls. At each time instant k predictions of state and control are computed by solving an optimal control problem up to time $k+N$ (yielding open-loop predictions of the state (depicted in red) and the control (depicted in blue)). Through successive implementation of the first part of the optimal control sequence the feedback μ_N and the corresponding closed-loop trajectory x_{μ_N} are obtained.

Algorithm 2.1 (MPC algorithm)

For each time instant $k = 0, 1, \dots$:

(1) *Measure the current state $x = x(k)$ of the system.*

(2) *Solve the optimal control problem*

$$\min_{u \in \mathbb{U}^N(x)} J_N(x, u)$$
$$x(k+1) = f(x(k), u(k)) \qquad \text{for all } k \in \{0, \dots, N-1\}, \tag{2.8}$$
$$x(0) = x,$$

in order to obtain the optimal control sequence $u^*_{N,x}$.

(3) *Apply the first element of $u^*_{N,x}$ as a control to the system during the next sampling period, i.e. use the feedback law $\mu_N(x) := u^*_{N,x}(0)$.*

(4) *Set $k := k+1$ and go to (1).*

The trajectory $x_{u_N^*}$ associated with the solution of the MPC optimization problem (2.8) is referred to as the MPC open-loop trajectory.

Since the state of the system is measured in each MPC step and a control is computed depending on the current initial state, MPC is a feedback control method. The MPC feedback is called μ_N. The resulting trajectory is called MPC closed-loop trajectory and denoted by $x_{\mu_N}(\cdot; x_0)$.

Remark 2.2 (Terminal conditions)

The literature often distinguishes between MPC with and without terminal conditions. In MPC with terminal conditions, the optimization problem in the MPC algorithm is modified such that an additional terminal cost term is added to the cost functional, or it is required that the final state of each MPC open-loop solution ends up in some terminal region. The inclusion of such terminal ingredients facilitates the convergence proofs and can even benefit the numerical solution of the MPC problems if terminal conditions are chosen in a way that adds more information to the problem [50, Section 7.4], [74].

In contrast, without terminal conditions no terminal costs or terminal regions are considered. From a theoretical point of view, this complicates the convergence proofs compared the case with terminal conditions, where approximate optimality and stability of the MPC closed-loop trajectory are relatively easy to derive. However, the design of suitable terminal ingredients (especially a Lyapunov function as terminal cost) is generally difficult. Thus, avoiding them simplifies the implementation of the MPC algorithm, at the cost of a more intricate convergence analysis.

Since in the course of the thesis we will only study MPC schemes without terminal conditions, the subsequent results focus on the case of MPC without terminal conditions. For further details on MPC with terminal conditions we refer to [8, 10, 25, 50, 96, 110]. $\diamond$

2.3   Essential MPC stability and performance results

In this section, we will present well-known results both for stabilizing and economic MPC. Of particular interest is the question which properties the closed-loop trajectory has and especially how it behaves compared to the solution of the optimal control problem (2.5) on the infinite horizon. To answer this, we consider the nominal MPC closed-loop system which is obtained by substituting the MPC feedback μ_N into (2.1):

$$x_{\mu_N}(k+1, x_0) = f(x_{\mu_N}(k, x_0), \mu_N(x_{\mu_N}(k, x_0))) \tag{2.9}$$

In order to evaluate the performance of the MPC closed-loop trajectory, the closed-loop costs are an important indicator. These are defined by

$$J_\infty^{cl}(x_0, \mu_N) := \sum_{k=0}^{\infty} \ell(x_{\mu_N}(k, x_0), \mu_N(x_{\mu_N}(k, x_0))). \tag{2.10}$$

We want to compare these costs with the best possible cost of the problem on the infinite horizon. To this end, we define the optimal value function of the problem (2.5):

$$V_\infty(x) := \inf_{u \in \mathbb{U}^\infty(x)} J_\infty(x, u) \tag{2.11}$$

To analyze stability and performance, the optimal value function for the MPC optimal control problem (2.8) on finite horizon is also useful. It is given by:

$$V_N(x) := \inf_{u \in \mathbb{U}^N(x)} J_N(x, u). \tag{2.12}$$

2.3.1 Stabilizing MPC

Historically, MPC was first applied to stabilization or tracking problems where an a priori given trajectory should be followed. In the most basic case, this trajectory is simply an equilibrium of the system.

Definition 2.3 (Equilibrium)
An equilibrium of the system (2.1) *is a pair* (x_e, u_e) *which satisfies*

$$x_e = f(x_e, u_e). \tag{2.13}$$

To achieve tracking, the cost functional is chosen such that it penalizes the distance to the desired equilibrium. From a mathematical point of view, this means that the stage cost is positive definite with regard to the equilibrium, i.e. that the following applies

$$\ell(x_e, u_e) = 0 \text{ and } \ell(x, u) > 0 \text{ for all } (x, u) \in X \times U \text{ with } x \neq x_e. \tag{2.14}$$

In classical MPC applications, stability of the MPC closed-loop trajectory is particularly important. For the characterization of stability we introduce the following comparison functions.

Definition 2.4 (Comparison functions)
We define the following classes of functions:

$$\mathcal{K} := \{\alpha : \mathbb{R}_0^+ \to \mathbb{R}_0^+ \mid \alpha \text{ is continuous and strictly increasing with } \alpha(0) = 0\}$$

$$\mathcal{K}_\infty := \{\alpha : \mathbb{R}_0^+ \to \mathbb{R}_0^+ \mid \alpha \in \mathcal{K} \text{ unbounded }\}$$

$$\mathcal{L} := \{\delta : \mathbb{R}_0^+ \to \mathbb{R}_0^+ \mid \delta \text{ is continuous and strictly decreasing with } \lim_{t \to \infty} \delta(t) = 0\}$$

$$\mathcal{KL} := \{\beta : \mathbb{R}_0^+ \times \mathbb{R}_0^+ \to \mathbb{R}_0^+ \mid \beta \text{ is continuous, } \beta(\cdot, t) \in \mathcal{K}, \beta(r, \cdot) \in \mathcal{L}\}$$

Loosely speaking, stability means that the distance between the MPC trajectory and the equilibrium tends to zero as time progresses. Throughout the thesis, we will use the shorthand notation

$$|x|_y := \|x - y\|$$

to measure the distance of two states x and y in some appropriate norm $\|\cdot\|$. Stability of the closed-loop trajectory is characterized by the following property.

Definition 2.5 (Asymptotic stability)
Let x_e be an equilibrium for the nominal closed-loop system (2.9). Then x_e is called locally asymptotically stable if there exist $\eta > 0$ and a function $\beta \in \mathscr{KL}$ such that the inequality

$$|x_{\mu_N}(k, x_0)|_{x_e} \leq \beta(|x_0|_{x_e}, k) \tag{2.15}$$

holds for all $x_0 \in \mathscr{B}_\eta(x_e)$ and all $k \in \mathbb{N}_0$, where $\mathscr{B}_\eta(x_e)$ is a ball with radius η around the equilibrium x_e.

Conditions for stability of tracking type MPC controllers are well understood by now (see the monographs [50, 96] for a comprehensive overview). For stabilizing MPC, establishing convergence of the closed-loop trajectory to the equilibrium relies on the fact that the optimal value function V_N of the MPC problem is a Lyapunov function. It has long been known that the existence of a Lyapunov function implies stability. We refer to [67, 99] for an introduction to Lyapunov theory from the perspective of continuous-time systems.

In classical MPC, perhaps the most well-known result is that stability of the MPC closed-loop trajectories can be expected provided the optimization horizon is sufficiently large and the stage cost satisfies suitable assumptions.

For our purposes, we will only mention one particular result in detail. It was developed in [58] and establishes suboptimality estimates along MPC closed-loop trajectories.

Theorem 2.6 (cf. [58, Proposition 3])
Consider a feedback law $\mu_N : X \to U$ and its associated trajectory $x_{\mu_N}(\cdot, x_0)$ with initial value $x(0) = x_0 \in X$. If there exists a function $V_N : X \to \mathbb{R}_0^+$ satisfying

$$V_N(x(k)) \geq \alpha \ell(x(k), \mu_N(x(k))) + V_N(f(x(k), \mu_N(x(k)))) \tag{2.16}$$

for some $\alpha \in (0, 1]$ and all $k \in \mathbb{N}_0$ then the relation

$$V_\infty(x(k)) \leq J_\infty^{cl}(x(k), \mu_N) \leq \frac{1}{\alpha} V_N(x(k)) \leq \frac{1}{\alpha} V_\infty(x(k)) \tag{2.17}$$

holds for all $k \in \mathbb{N}_0$.

This result allows to compare MPC controllers with different horizon lengths to an optimal controller on infinite horizon based on their *degree of suboptimality*, described by the quantity α. We will come back to it later in Chapter 6 where it forms the basis for online performance estimates for the MPC closed-loop trajectory.

2.3.2 Economic MPC

In contrast to stabilizing MPC, in economic MPC the performance (i.e. the cost of the MPC closed-loop) is often of greater importance than stability of the trajectories. This does not mean that stability becomes irrelevant, but that we do not a priori decide on a reference trajectory. Instead, we let the controller figure out the optimal behavior on its own. This presents the main advantage economic MPC offers over stabilizing MPC.

In classical MPC, the equilibrium (or reference trajectory) to be stabilized must be known in advance. Usually, it stems from additional knowledge about the system and higher-level design criteria, or it is determined by preceding optimization problems. However, optimal behavior of the trajectories in the sense that they yield good performance can be quite complex. This can complicate the design of stabilizing MPC controllers when there is no knowledge of optimal system behavior, most notably in the time-variant case which we will investigate in Chapter 4. Consequently, unlike in classical MPC, no reference trajectory is prescribed in economic MPC. Instead, it will emerge implicitly from the solution of the MPC algorithm. The stage cost is now regarded as given data originating from the underlying (usually economic) problem. Thus, one works directly with the economic stage cost.

From a mathematical point of view, the main difference lies in the fact that the economic stage cost is not necessarily positive definite with respect to a particular equilibrium. As a consequence, the results for stabilizing MPC can no longer be applied.

The survey articles [30, 35] give a comprehensive overview of the recent advances and future challenges of economic MPC. For the purpose of this thesis we will primarily focus on stability, optimality and transient optimality of the MPC closed-loop solutions. The key concepts for doing so are presented in the following, along the lines of [43, 44, 57]. Later on, in Chapter 4, we seek to obtain comparable results for MPC for time-varying systems. To simplify the presentation, we will only outline the central results and omit preparatory lemmas. For further details, we refer to the original publications.

In what follows, we will restrict our analysis to optimal equilibria as defined below.

Definition 2.7 (Optimal Equilibrium)
An equilibrium (x_e^*, u_e^*) is called optimal equilibrium if it holds that

$$\ell(x_e^*, u_e^*) \leq \ell(x_e, u_e) \text{ for all equilibria } (x_e, u_e) \in \mathbb{X} \times \mathbb{U}. \tag{2.18}$$

It should be noted that the existence of an optimal equilibrium does not necessarily imply that it is the best way to control the process. Instead, it is merely required that the optimal equilibrium has the lowest cost among all equilibria. In case the optimal way of controlling the process occurs in fact at an equilibrium, we speak of optimal operation at steady state. The case of optimal steady-state operation has been studied extensively, cf. the works [10, 83, 85], resulting in the characterization of necessary and sufficient conditions for optimal steady-state operation involving dissipativity (which we will introduce below). There also exists a number of extensions for more general types of optimal operation. We will mention some of these at the end of the chapter.

The following assumptions form the basis for establishing performance and convergence of economic MPC trajectories. In the first assumption we use the notation $\#S$ in order to indicate the cardinality of the set S.

Assumption 2.8 (Turnpike property)
Consider system (2.1) *with an optimal equilibrium according to Definition 2.7. We assume the following holds:*

(a) *There exists a function $\sigma \in \mathscr{L}$ such that for each optimal trajectory $x_{u_{N,x}^*}(k,x)$, $x \in \mathbb{X}$ and all $N, P \in \mathbb{N}$, $P \leq N$, there is a set $\mathcal{Q}(x,P,N) \subseteq \{0,\ldots,N\}$ with $\#\mathcal{Q}(x,P,N) \leq P$ elements such that*

$$|x_{u_{N,x}^*}(k,x)|_{x_e^*} \leq \sigma(P) \tag{2.19}$$

for all $k \notin \mathcal{Q}(x,P,N)$.

(b) *There exists a function $\rho \in \mathscr{L}$ such that each optimal trajectory $x_{u_{\infty,x}^*}(k,x)$, $x \in \mathbb{X}$ and all $P \in \mathbb{N}$, there is a set $\mathcal{Q}(x,P,\infty) \subseteq \mathbb{N}_0$ with $\#\mathcal{Q}(x,P,N) \leq P$ elements such that*

$$|x_{u_{\infty,x}^*}(k,x)|_{x_e^*} \leq \rho(P) \tag{2.20}$$

for all $k \notin \mathcal{Q}(x,P,\infty)$.

This assumption is referred to as the turnpike property. Part (a) describes the behavior of open-loop solutions of the MPC optimal control problems (2.8), requiring that they are most of the time close to the optimal equilibrium x_e^*. Part (b) demands the same for infinite horizon optimal trajectories associated with (2.5), which essentially corresponds to a convergence assumption for the trajectories on the infinite horizon.

A second assumption is a continuity property of the optimal value functions V_N.

Assumption 2.9 (Continuity property of V_N)
Assume there exists an open ball $\mathscr{B}_\varepsilon(x_e^*)$, $\varepsilon > 0$, around the equilibrium and functions $\eta \in \mathscr{K}_\infty$, $\omega \in \mathscr{L}$ such that for all $x \in \mathscr{B}_\varepsilon(x_e^*) \cap \mathbb{X}$ and all $N \in \mathbb{N} \cup \{\infty\}$ the optimal value functions V_N satisfy

$$|V_N(x) - V_N(x_e^*)| \leq \gamma_V(|x|_{x_e^*}) + \omega(N). \tag{2.21}$$

Using these assumptions it can be shown that MPC approximates the cost of an infinite horizon optimal trajectory.

Theorem 2.10 (cf. [44, Theorem 4.4])
If Assumptions 2.8 and 2.9 hold and V_∞ is bounded on $\mathbb{X}$, then the inequality

$$J_M^{cl}(x,\mu_N) + V_\infty(x_{\mu_N}(M)) \leq V_\infty(x) + M\delta(N) \tag{2.22}$$

holds for all $M \in \mathbb{N}$ and all sufficiently large $N \in \mathbb{N}$ with a function $\delta \in \mathscr{L}$.

An interpretation of this theorem is that the MPC trajectory is the initial piece of an approximately optimal infinite horizon trajectory. To see this, realize that inequality (2.22) states that the cost of the MPC closed-loop trajectory up to time M together with the infinite horizon optimal cost from the final state $x_{\mu_N}(M)$ (i.e. the left-hand side of (2.22)) is lower than the infinite horizon optimal cost $V_\infty(x)$, at least up to the error term $M\delta(N)$. A direct consequence of the above result is that an extension of the horizon leads to better approximation properties of the MPC controller, since the error term $\delta \in \mathscr{L}$ decreases

with increasing N. Note that the error term also depends on M. While in principle this means that for $M \to \infty$ the performance measure $J_M^{cl}(x, \mu_N)$ may not be finite, we can still guarantee an upper bound on the long term average performance $\frac{1}{M} J_M^{cl}(x, \mu_N)$, cf. [44, Remark 4.5].

Unfortunately, the approach from classical MPC, where the optimal value function V_N can be used as a Lyapunov function, does not directly transfer to economic MPC, due to the lack of sign definiteness of V_N in the economic case. However, stability can also be established for economic MPC, at least for strictly dissipative systems.

Assumption 2.11 (Strict dissipativity)
The optimal control problem (2.8) *is strictly dissipative, i.e. there exists a function* $\alpha_\ell \in \mathcal{K}_\infty$ *and a storage function* $\lambda : X \to \mathbb{R}$ *such that*

$$\ell(x, u) + \lambda(x) - \lambda(f(x, u)) - \ell(x_e^*, u_e^*) \geq \alpha_\ell(\|x - x_e^*\|) \tag{2.23}$$

holds for all $x \in \mathbb{X}$.

If strict dissipativity holds, the storage function λ can be used to define a modified stage cost function

$$\tilde{\ell}(x, u) = \ell(x, u) + \lambda(x) - \lambda(f(x, u)) - \ell(x_e^*, u_e^*). \tag{2.24}$$

The stability proof relies on the fact that even though ℓ is not necessarily positive definite with respect to the equilibrium x_e^*, the modified cost $\tilde{\ell}$ is, which then also transfers over to the optimal value function of the problem with the modified cost. Thus, in this way it is possible to recover a Lyapunov function. However, it comes at a price as the stability notion is slightly weakened compared to Definition 2.5.

Definition 2.12 (Practical asymptotic stability)
An equilibrium x_e *of the closed-loop system* (2.9) *is called practically asymptotically stable w.r.t.* $\varepsilon > 0$ *on a set* $S \subseteq \mathbb{X}$ *with* $x_e \in S$ *if there exists* $\beta \in \mathcal{K}\mathcal{L}$ *such that*

$$\|x_{\mu_N}(k, x) - x_e\| \leq \max\{\beta(\|x - x_e\|, k), \varepsilon\} \tag{2.25}$$

holds for all $x \in S$ *and all* $k \in \mathbb{N}$.

In addition to strict dissipativity we assume the following.

Assumption 2.13 (Continuity and compactness)
The state and control constraint set $\mathbb{X}$ *and* $\mathbb{U}$ *are compact, the functions* f, ℓ *and* λ *are continuous,* λ *is Lipschitz continuous on a ball* $\mathcal{B}_\delta(x_e^*)$ *around* x_e^* *and* $\tilde{\ell}$ *satisfies the inequality*

$$\tilde{\ell}(x, u) \leq \alpha(\|x - x_e^*\|) + \alpha(\|u - u_e^*\|) \tag{2.26}$$

for all $x \in \mathbb{X}$, $u \in \mathbb{U}$ *and a suitable* $\alpha \in \mathcal{K}_\infty$.

Assumption 2.14 (Local controllability)
There is $\varepsilon > 0$, $M \in \mathbb{N}$ and $C > 0$ such that for all $x \in \mathscr{B}_\varepsilon(x_e^*)$ there exists $u_1 \in \mathbb{U}^M(x)$, $u_2 \in \mathbb{U}^M(x_e^*)$ with

$$x_{u_1}(M, x) = x_e^*, \; x_{u_2}(M, x_e^*) = x \tag{2.27}$$

and

$$\max\{\|x_{u_1}(k, x) - x_e^*\|, \|x_{u_2}(k, x_e^*) - x_e^*\|, \|u_1(k) - u_e^*\|, \|u_2(k) - u_e^*\|\} \le C\|x - x_e^*\| \tag{2.28}$$

for $k = 0, 1, \ldots, M - 1$.

Assumption 2.15 (Finite time controllability)
For $\varepsilon > 0$ from Assumption 2.14 there is $K \in \mathbb{N}$ such that for each $x \in \mathbb{X}$ there is $k \le K$ and $u \in \mathbb{U}^k(x)$ with

$$x_u(k, x) \in \mathscr{B}_\varepsilon(x_e^*). \tag{2.29}$$

With these assumptions, one can prove convergence of the MPC closed-loop trajectory towards the optimal equilibrium x_e^* in the sense of Definition 2.12.

Theorem 2.16 (Practical asymptotic stability of the MPC closed-loop, cf. [57, Theorem 3.7])
Consider a strictly dissipative economic MPC problem satisfying Assumptions 2.13 - 2.15. Then the equilibrium (x_e^*, u_e^*) is practically asymptotically stable for the MPC closed-loop system (2.9) w.r.t. $\varepsilon \to 0$ as the horizon $N \to \infty$.

As a final result, we mention that it is also possible to prove transient optimality, meaning that among all trajectories converging to a neighborhood of the optimal equilibrium x_e^*, the ones generated by MPC are the ones with the lowest cost, at least up to certain error terms.

Theorem 2.17 (Transient optimality, cf. [57, Theorem 4.1])
Assume that x_e^* is practically asymptotically stable on a set $S \subseteq \mathbb{X}$ w.r.t. $\varepsilon = \varepsilon(N)$ for the economic MPC closed-loop system. Assume further that there exists $\alpha_\lambda \in \mathscr{K}_\infty$ with $|\lambda(x)| \le \alpha_\lambda(\|x - x_e^*\|)$ for all $x \in \mathbb{X}$. Let $\varepsilon_{K,N} := \|x_{\mu_N}(K, x) - x_e^*\| \le \max\{\beta(\|x - x_e^*\|, K), \varepsilon(N)\}$ and let $\mathbb{U}_{\varepsilon_{K,N}}^K := \{u \in \mathbb{U}^K(x) | x_u(K, x) \in \mathscr{B}_{\varepsilon_{K,N}}(x)\}$. Then the inequality

$$J_K^{cl}(x, \mu_N) \le \inf_{u \in \mathbb{U}_{\varepsilon_{K,N}}^K} J_K(x, u) + \alpha_V(\varepsilon_{K,N}) + 2\alpha_\lambda(\varepsilon_{K,N}) + K\delta(N) \tag{2.30}$$

holds for all $K, N \in \mathbb{N}$ and all $x \in S$.

It should be noted that the first two error terms vanish as K and N tend towards infinity. However, this is not clear for the last error term $K\delta(N)$.

To summarize, the key concepts used in the analysis for economic MPC are the turnpike property and continuity of the optimal value functions. Together with strict dissipativity, these properties allow to prove the existence of a Lyapunov function and thus to conclude asymptotic stability of the MPC closed-loop trajectories and certain performance estimates. In Chapter 4 we will generalize and extend the central Theorems 2.10 and 2.16 to the time-varying case.

2.3.3 Extensions

There exists a number of extensions related to the results presented before, some of which we briefly mention here.

Periodic optimal operation:
The first extension addresses the fact that the optimal operation does not have to occur at an equilibrium. Indeed, the optimal behavior can also be, e.g., periodic and even more general types like complex chaotic regimes are conceivable, even though we are not aware of any examples of this in the literature.

The case of periodic optimal operation has been investigated in [84]. The most noteworthy result in this work is the observation that the default MPC scheme from Algorithm 2.1 does not necessarily result in optimal closed-loop performance. Whether this happens rather depends on the period length P of the optimal periodic trajectory (called orbit). In order to guarantee convergence of the MPC closed-loop to the optimal periodic orbit, one can apply a multi-step MPC scheme. In this scheme, not only the very first control of the open-loop control sequence is implemented in the system but the open-loop control sequence is applied for a total of M steps before the horizon gets shifted and the optimization is carried out anew. It was shown in [84] that if the step length of the MPC method is chosen such that it matches the period length of the optimal periodic orbit, i.e. $M = P$, then the MPC closed-loop will converge to this orbit yielding near-optimal performance.

Other works investigating optimal periodic systems include [109, 110] as well as [10]. Out of these, the last one is particularly interesting since it contains a practical example of a chemical reactor which is optimally operated at a periodic trajectory.

Application of turnpike properties:
Assumption 2.8 (the turnpike property) is increasingly recognized as a valuable tool, both in the structural analysis of optimal control problems as well as for the improvement of numerical methods.

An example of the latter is a new adaptive discretization scheme for MPC open-loop solutions developed in [56]. It exploits the fact that open-loop trajectories hardly change when close to the turnpike and that an accurate estimation of only the initial piece of the open-loop solution suffices when applying MPC. The adaptive discretization reduces computation time and memory load of the MPC optimal control problems while maintaining high accuracy for the relevant parts of the open-loop.

Other recent results [34, 37] extend the concept of turnpike behavior from equilibria to general non-stationary trajectories. For mechanical systems, this allows to identify elementary pieces of optimal control trajectories called motion primitives or trims, connecting different configurations of the system. These trims can be assembled into a library of solutions for intermediate optimal control problems which, in turn, can be efficiently searched for an optimal path between two arbitrary configurations.

Connection between turnpike property and dissipativity:

While numerical observations suggest that turnpike phenomena are prevalent in applications, their rigorous verification is still challenging. In this context, strict dissipativity (see Assumption 2.11) plays an important role, since there exists a strong connection between strict dissipativity and the turnpike property as first observed in [43], identifying strict dissipativity as a sufficient condition for the turnpike property.

This connection was further explored in [48], where it was shown that strict dissipativity is not only a sufficient but, in certain cases, also a necessary condition for the turnpike property, i.e., under appropriate assumptions the turnpike property implies strict dissipativity.

For particular classes of systems, the connection between dissipativity and the turnpike property allows to explicitly verify the presence of the turnpike property. In [23] the case of linear systems with convex stage costs is considered, in which case an exponential turnpike result can be deduced. These results were extended in [45] to also allow for state and control constraints and more recently to non-convex (indefinite) stage cost functions in [15].

In Chapter 5, we will explore the link between dissipativity and the turnpike property further in the context of time-varying systems.

3 | Optimal control of the convection-diffusion equation

We will supplement the theoretical results developed in the course of this thesis by numerical examples. Several of these examples involve different variations of the convection-diffusion equation, a particular parabolic partial differential equation (PDE). This chapter aims to introduce this PDE and to present the numerical methods for its optimal control. We consider two different scenarios of the convection-diffusion equation. In the first scenario we consider a 1D domain with boundary control and a controlled convection term. This results in a bilinear optimal control problem, which is solved via a *first-discretize-then-optimize* approach.

Secondly, we consider the equation on a 2D domain without controlled convection. Instead, we assume the velocity field is given, e.g. by a solution of the Navier-Stokes equations. For this setting, we apply a function space optimization method implemented in [76].

3.1 The convection-diffusion equation

The convection-diffusion equation models the transport of particles, energy or other physical quantities within a system by convective and diffusive processes. The equation plays an important role in the explanation of physical phenomena in many fields like hydrology [12], climate modeling [42] or magnetohydrodynamics [24][1]. For our purposes, the equation serves as a simplified model of the dispersion of heat in a room by conductive heat transfer (i.e. radiation) on the one hand and convective transfer induced by a velocity field (i.e. air flow) on the other hand.

Let $\Omega \subset \mathbb{R}^d$, $d \in \{1, 2\}$, be a domain, $T > 0$ and define $Q := (0, T) \times \Omega$. We denote $H := L^2(\Omega)$, $V := H^1(\Omega)$, and consider the space

$$L^2(0, T; V) := \{v : [0, T] \to V \mid \int_0^T \|v(t)\|_V^2 \, dt < \infty\} \tag{3.1}$$

---

[1]In some of these fields, the equation appears under different names such as *advection-diffusion equation* or *drift-diffusion equation*.

of square integrable functions from $[0, T]$ to V. Let

$$W(0, T) := \{\varphi \in L^2(0, T; V) | \ \varphi_t \in L^2(0, T; V')\}, \tag{3.2}$$

where V' is the dual space of V and φ_t is the (distributional) time derivative of φ. The convection-diffusion equation reads

$$y_t(t, x) - \alpha \Delta y(t, x) + v(t, x) \nabla y(t, x) = 0 \qquad \text{almost everywhere (a.e.) on } Q \tag{3.3a}$$

$$y(0, x) = y_0(x) \qquad\qquad \text{a.e. in } \Omega \tag{3.3b}$$

where $y : Q \to \mathbb{R}$ is the temperature, $\alpha \in \mathbb{R}$ is the diffusion coefficient, $v : [0, T] \to \Omega$ is a velocity field and $y_0 : \Omega \to \mathbb{R}$ is the initial temperature distribution. According to equation (3.3a), the change of heat y_t depends on diffusive parts $\alpha \Delta y(t, x)$ and convective parts $v(t, x) \nabla y(t, x)$ subject to a given velocity field $v(t, x)$.

3.1.1   Boundary conditions

The temperature within the room Ω is subject to variations of the temperature on the outside. This is modeled by the following boundary conditions:

$$\alpha \frac{\partial y}{\partial n}(t, s) + \gamma_{out} y(t, s) = \delta_{out} y_{out}(t) \text{ a.e. on } \Sigma_{out} := (0, T) \times \Gamma_{out} \tag{3.4a}$$

$$\alpha \frac{\partial y}{\partial n}(t, s) + \gamma_c y(t, s) = \delta_c u_i(t) \qquad \text{a.e. on } \Sigma_{c_i} := (0, T) \times \Gamma_{c_i}, i \in \{1, \dots, m\} \tag{3.4b}$$

The boundary is partitioned into a part Γ_{out} where some outside temperature is prescribed and control boundaries Γ_{c_i}, $i \in \{1, \dots, m\}$, where we can influence the temperature by heating and cooling. The functions $u_i : [0, T] \to \mathbb{R}$, $i \in \{1, \dots, m\}$, and $y_{out} : [0, T] \to \mathbb{R}$ specify the temperature on the respective parts of the boundary. The coefficients $\gamma_{out}, \gamma_c, \delta_{out}, \delta_c \geq 0$ can be used to model different types of heat transfer across the boundary. For example, by choosing $\gamma_c = \delta_c \gg \alpha$ we can approximate a Dirichlet boundary condition for the state which means that we can set the temperature at the boundary directly. Conversely, choosing $\gamma_c = 0$ corresponds to a Neumann boundary condition which would imply that the control defines the flux of heat across the boundary. An illustration of a 2D domain on a unit square with a single control boundary at $x_2 = 0$ can be found in Figure 3.1.

3.1.2   Problem statement

We want to control the system governed by the convection-diffusion equation such that the temperature $y(t, x)$ remains within certain lower and upper bounds $\underline{y}(t, x)$ and $\overline{y}(t, x)$. At the same time, the control effort (corresponding to the amount of energy supplied to the system) should be minimized. From a control perspective, we will consider two fundamentally different versions of the problem.
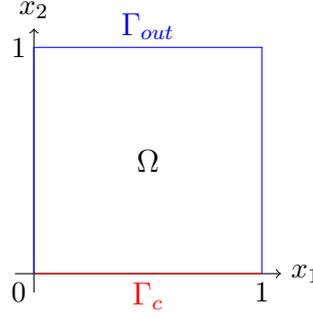
Figure 3.1: Example illustration of the domain and boundaries. A single control boundary Γ_c is shown in red and the other boundary Γ_{out} is shown in blue.

Boundary heating

In the first version, the only control action happens at the boundary through the control $u \in \mathcal{U} := L^2(0, T; \mathbb{R}^m)$, $m \in N$. In this case, our goal can be expressed by the following PDE optimal control problem:

$$
\min_{y,u} J(y, u) = \frac{\sigma_T}{2} \int_{\Omega} (y(T, x) - y_T(x))^2 \, dx + \frac{\sigma_Q}{2} \int_0^T \int_{\Omega} (y(t, x) - y_Q(t, x))^2 \, dx \, dt
$$
$$
+ \frac{\sigma_u}{2} \sum_{i=1}^m \int_0^T (u_i(t))^2 \, dt
$$
(3.5)

$$
\text{subject to (s.t.) } (3.3), (3.4)
$$
$$
\underline{u}(t) \leq u_i(t) \leq \overline{u}(t), \ i \in \{1, \ldots, m\} \quad \text{a.e. on } (0, T)
$$
$$
\underline{y}(t, x) \leq y(t, x) \leq \overline{y}(t, x) \quad \text{a.e. on } (0, T) \times \Omega_y
$$

where $y_Q \in L^2(0, T; H)$, $y_T \in H$, parameters $\sigma_Q, \sigma_T \geq 0$, $\sigma_1, \ldots, \sigma_m > 0$ and $\Omega_y \subset \Omega$ is a subdomain where the temperature bounds $\underline{y}, \overline{y} \in C(\overline{Q})$ should be enforced. This setting has been studied in [76], where a numerical solution based on a primal-dual-active-set method was implemented. We will discuss this setting later on in this chapter.

Controlled convection term

Alternatively, we can additionally permit control of the velocity field $v(t, x)$ which could be interpreted as, e.g., an adjustable ventilating fan inside the room. This is expressed by adding a second control variable $w \in \mathcal{W} := L^2(0, T; \mathbb{R})$ that determines the magnitude of the velocity field. Formally, we introduce a mapping $v : \mathcal{W} \to L^\infty(0, T; L^\infty(\Omega, \mathbb{R}^d))$ which maps each control value $w(t)$ to a velocity field $v(w)(t) \in L^\infty(\Omega, \mathbb{R}^d)$.

In this case, the optimal control problem is augmented to:

$$
\begin{aligned}
\min_{y,u,w} J(y,u,w) =& \frac{\sigma_T}{2} \int_\Omega (y(T,x) - y_T(x))^2 \, dx + \frac{\sigma_Q}{2} \int_0^T \int_\Omega (y(t,x) - y_Q(t,x))^2 \, dx \, dt \\
& + \frac{\sigma_u}{2} \sum_{i=1}^m \int_0^T (u_i(t))^2 \, dt + \frac{\sigma_w}{2} \int_0^T (w(t))^2 \, dt
\end{aligned}
$$

$$
\begin{aligned}
\text{s.t. } & (3.3), (3.4) \\
& \underline{u}(t) \le u_i(t) \le \overline{u}(t), \ i \in \{1, \ldots, m\} \quad \text{a.e. on } (0,T) \\
& \underline{w}(t) \le w(t) \le \overline{w}(t), \quad\quad\quad\quad\quad\quad\ \text{a.e. on } (0,T) \\
& \underline{y}(t,x) \le y(t,x) \le \overline{y}(t,x) \quad\quad\quad\quad\quad \text{a.e. on } (0,T) \times \Omega_y
\end{aligned}
\tag{3.6}
$$

with $\sigma_w > 0$. Naturally, this gives the controller more leeway but at the same time it renders the problem bilinear which complicates the analytical treatment. In particular, it can no longer be solved directly by the method from [76] because of the different optimality conditions due to the bilinear structure. For this reason, a different path was chosen for the solution of the bilinear optimal control problem based on a first-discretize-then-optimize approach.

It should be remarked that optimality conditions for bilinear control of convection-diffusion equations have been developed in [13], albeit without boundary control and in absence of state constraints. Presumably, it should be possible to extend these ideas to our setting which would allow to solve the first scenario with the method from [76] as well.

3.1.3 Derivation of the weak form

Before we come to the numerical methods for solving the above problems, we derive the weak form of the PDE (3.3). This weak (or variational) formulation of the equation will serve as the basis for the numerical discretization by the Finite Element method.

In the derivation, we will only consider the case with the controlled velocity field $v(w)(t,x)$ and remark that the derivation for uncontrolled convection term $v(t,x)$ works analogously. To enhance readability, below we will omit the arguments t and x of the functions. The weak form is obtained by the following steps. First, we formally multiply equation (3.3) with a test function $\varphi \in V$ and integrate over the domain Ω:

$$
\int_\Omega \frac{d}{dt} y\varphi \, dx - \alpha \int_\Omega \Delta y \varphi \, dx + \int_\Omega (v(w) \cdot \nabla y)\varphi \, dx = 0. \tag{3.7}
$$

Using integration by parts in space and substituting the boundary conditions (3.4) we obtain

$$
\begin{aligned}
& \int_\Omega \frac{d}{dt} y\varphi \, dx + \alpha \int_\Omega \nabla y \cdot \nabla \varphi \, dx + \int_\Omega (v(w) \cdot \nabla y)\varphi \, dx \\
& + \gamma_{out} \int_{\Gamma_{out}} y\varphi \, ds - \delta_{out} y_{out} \int_{\Gamma_{out}} \varphi \, ds + \sum_{i=1}^m \gamma_c \int_{\Gamma_{c_i}} y\varphi \, ds - \delta_c u_i \int_{\Gamma_{c_i}} \varphi \, ds = 0.
\end{aligned}
\tag{3.8}
$$

Reordering by terms dependent and independent of y yields

$$\int_\Omega \frac{\mathrm{d}}{\mathrm{d}t} y\varphi \, dx + \alpha \int_\Omega \nabla y \cdot \nabla\varphi \, dx + \int_\Omega (vw \cdot \nabla y)\varphi \, dx + \gamma_{out} \int_{\Gamma_{out}} y\varphi \, ds + \sum_{i=1}^m \gamma_c \int_{\Gamma_{c_i}} y\varphi \, ds$$

$$= \delta_{out} y_{out} \int_{\Gamma_{out}} \varphi \, ds + \sum_{i=1}^m \delta_c u_i \int_{\Gamma_{c_i}} \varphi \, ds.$$

In order to shorten the notation, for $\varphi, \psi \in V$ let

$$\langle \varphi, \psi \rangle_{L^2(\Omega)} := \int_\Omega \varphi\psi \, dx \tag{3.9}$$

and introduce the functionals $\mathscr{F}(t) : V \to V'$, $\mathscr{B} : \mathbb{R}^m \to V'$

$$\langle \mathscr{F}(t), \varphi \rangle_{V',V} := \delta_{out} y_{out}(t) \int_{\Gamma_{out}} \varphi \, ds$$

$$\langle \mathscr{B}u(t), \varphi \rangle_{V',V} := \sum_{i=1}^m \delta_c u_i(t) \int_{\Gamma_{c_i}} \varphi \, ds$$

as well as $A : \mathscr{W} \to L^\infty(0, T; L(V, V'))$

$$\langle A(w)(t)\varphi, \psi \rangle_{V',V} := \alpha \int_\Omega \nabla\varphi \cdot \nabla\psi \, dx + \int_\Omega (v(w)(t) \cdot \nabla\varphi)\psi \, dx$$

$$+ \gamma_{out} \int_{\Gamma_{out}} \varphi\psi \, ds + \sum_{i=1}^m \gamma_c \int_{\Gamma_{c_i}} \varphi\psi \, ds \tag{3.10}$$

resulting in the variational equation

$$\frac{\mathrm{d}}{\mathrm{d}t} \langle y(t), \varphi \rangle_{L^2(\Omega)} + \langle A(w)(t)y(t), \varphi \rangle_{V',V} = \langle \mathscr{B}u(t), \varphi \rangle_{V',V} + \langle \mathscr{F}(t), \varphi \rangle_{V',V}. \tag{3.11}$$

We now call $y \in W(0, T)$ weak solution of the PDE (3.3) if it satisfies

$$\frac{\mathrm{d}}{\mathrm{d}t} \langle y(t), \varphi \rangle_{L^2(\Omega)} + \langle A(w)(t)y(t), \varphi \rangle_{V',V} = \langle \mathscr{B}u(t), \varphi \rangle_{V',V} + \langle \mathscr{F}(t), \varphi \rangle_{V',V},$$

$$\forall \varphi \in V \text{ a.e. on } (0, T)$$

$$y(0) = y_0 \text{ in } L^2(\Omega). \tag{3.12}$$

3.2 Solution with controlled convection term

We first consider the case where both the boundary heating u and the convection term v can be controlled. For simplicity, we restrict ourselves to a 1-dimensional domain $\Omega = [0, 1] \subset \mathbb{R}$ with a single control boundary Γ_c on the right and an uncontrollable outside temperature at the left boundary Γ_{out}. We want to constrain the temperature on the subinterval $\Omega_y := [\frac{1}{4}, \frac{3}{4}]$. An illustration of this setting can be found in Figure 3.2. Another simplification that is made is the assumption that the convection term acts uniformly on the domain, i.e., $v(w)(t, x) = v(w)(t) =: v_w(t) \in \mathbb{R}$ is independent of the position x.

$$\Omega$$

$$\Gamma_{out} \qquad \Omega_y \qquad \Gamma_c$$

Figure 3.2: Illustration of the domain and control boundaries as well as the subdomain Ω_y where the temperature constraints should be satisfied.

3.2.1   Galerkin spatial discretization

As the first step, we discretize equation (3.12) by a Galerkin method [7, 18, 41]. To this end, we consider a finite dimensional subspace $V_h \subset V$ and a basis of this space consisting of *trial functions* $\{\psi_i\}_{i=1}^L$, i.e., $V_h := \text{span}\{\psi_1, \ldots, \psi_L\}$. The idea is to approximate the functions $y(t)$ and the initial condition y_0 via

$$y_h(t, x) = \sum_{j=1}^L y_j(t)\psi_j(x), \tag{3.13}$$

$$y_{0,h}(x) = \sum_{j=1}^L y_{0,j}\psi_j(x), \tag{3.14}$$

with coefficients $y_j(t)$, $y_{0,j}$, $j \in \{1, \ldots, L\}$. These coefficients will be determined by solving a system of equations which is derived as follows. Inserting the approximations in the weak form (3.11) and considering only test functions $\psi_1, \ldots, \psi_L$ we obtain

$$\frac{\mathrm{d}}{\mathrm{d}t}\langle y_h(t), \psi_i\rangle_{L^2(\Omega)} + \langle A(w)(t)y_h(t), \psi_i\rangle_{V',V} = \langle \mathscr{B}u(t), \psi_i\rangle_{V',V} + \langle \mathscr{F}(t), \psi_i\rangle_{V',V}, \tag{3.15}$$
$$\forall i \in \{1, \ldots, L\} \text{ a.e. on } (0, T).$$

This yields a total of L equations, one for each test function ψ_i. We now consider the individual components in the above equation to obtain the mass and stiffness matrices as well as the right-hand side of the system of equations. Starting with the first term, we insert the definition of y_h to get

$$\frac{\mathrm{d}}{\mathrm{d}t}\langle y_h(t), \psi_i\rangle_{L^2(\Omega)} = \frac{\mathrm{d}}{\mathrm{d}t}\langle \sum_{j=1}^L y_j(t)\psi_j, \psi_i\rangle_{L^2(\Omega)} = \sum_{j=1}^L \frac{\mathrm{d}}{\mathrm{d}t}y_j(t)\underbrace{\int_\Omega \psi_j(x)\psi_i(x)\,dx}_{=:\mathbf{M}_{ji}} \tag{3.16}$$

for all $i \in \{1, \ldots, L\}$. Next, from the second term we get

$$
\langle A(w)(t)y_h(t), \psi_i \rangle_{V',V} = \langle A(w)(t) \sum_{j=1}^{L} y_j(t)\psi_j, \psi_i \rangle_{V',V}
$$

$$
= \sum_{j=1}^{L} y_j(t) \underbrace{\left(\alpha \int_{\Omega} \nabla \psi_j(x) \cdot \nabla \psi_i(x) \, dx + \gamma_{out} \int_{\Gamma_{out}} \psi_j(s)\psi_i(s) \, ds + \gamma_c \int_{\Gamma_c} \psi_j(s)\psi_i(s) \, ds \right)}_{=:\mathbf{A}_{ji}}
$$

$$
+ y_j(t)v_w(t) \underbrace{\int_{\Omega} \nabla \psi_j(x)\psi_i(x) \, dx}_{=:\mathbf{B^w}_{ji}}
$$

(3.17)

for $i \in \{1, \ldots, L\}$. Finally, the right-hand side of (3.15) yields

$$
\langle \mathscr{B}u(t), \psi_i \rangle_{V',V} + \langle \mathscr{F}(t), \psi_i \rangle_{V',V} = u(t) \underbrace{\delta_c \int_{\Gamma_c} \psi_i \, ds}_{=:\mathbf{b^u}_i} + y_{out}(t) \underbrace{\delta_{out} \int_{\Gamma_{out}} \psi_i \, ds}_{=:\mathbf{f^{out}}_i}, \quad i \in \{1, \ldots, L\}.
$$

(3.18)

In addition, we get L equations from the projection of the initial condition $y_0(x)$ to the space V_h:

$$
y_{0,i} = \int_{\Omega} y_0(x)\psi_i(x) \, dx, \quad i \in \{1, \ldots, L\}.
$$

(3.19)

Let us define the coefficient vectors

$$
\mathbf{y_h}(t) := (y_1(t), \ldots, y_L(t))^{\top}
$$

(3.20)

$$
\mathscr{y}_0 := (y_{0,1}, \ldots, y_{0,L})^{\top}.
$$

(3.21)

Then, for given data y_{out}, $\mathbf{y_0}$ and given controls u, w, we can compute an approximate solution of the PDE by solving the (nonlinear) ODE initial value problem

$$
\mathbf{M\dot{y}_h}(t) + \mathbf{Ay_h}(t) + v_w(t)\mathbf{B^w y_h}(t) = \mathbf{b^u}u(t) + \mathbf{f^{out}}y_{out}(t)
$$

$$
\mathbf{y_h}(0) = \mathscr{y}_0.
$$

(3.22)

So far we did not specify the choice of the basis of trial functions which span the finite dimensional subspace $V_h \subset V$. A popular way to choose them is using Finite Elements. An in-depth introduction to the Finite Element method can be found in [41, 71]. Briefly, for the method we subdivide the domain Ω into subsets K_i, e.g. by triangulation (which simplifies to subdivision by finite intervals in the 1D case). We then consider piecewise polynomial trial functions on each subset. This approach offers the advantage that the resulting mass and stiffness matrices are sparse which facilitates the numerical solution of the system.

3.2.2 Time discretization by implicit Euler method

To solve the ODE system (3.22) numerically, the system has to be discretized in time. We will apply the implicit Euler method for this purpose. Let $N \in \mathbb{N}$ and define the step size $h := \frac{T}{N} > 0$. We want to obtain a solution at the discrete time instances $t_k = kh$, $k \in \{0, \ldots, N\}$. For a general control system

$$
\begin{aligned}
\dot{y}(t) &= f(t, y(t), u(t)) \\
y(0) &= y_0,
\end{aligned}
\tag{3.23}
$$

the implicit Euler discretization computes approximations y_{k+1} of the state $y(t_{k+1})$ at the time points t_{k+1} by solving the (nonlinear) system

$$
y_{k+1} = y_k + h f(t_{k+1}, y_{k+1}, u_{k+1})
\tag{3.24}
$$

for each $k \in \{0, \ldots, N-1\}$, starting at time $k = 0$ with the initial state y_0. We assume that the controls u are piecewise constant, i.e., they are kept constant during the time interval $[t_k, t_{k+1})$, and identify u_k with the value of the function $u(t_k)$. The same holds for the controls $w_k = v_w(t_k)$ and the outside temperature $y_{out,k} = y_{out}(t_k)$.

Applying this discretization scheme to the system (3.22) and replacing the time derivative $\dot{\mathbf{y}}_\mathbf{h}$ by the difference quotient $\frac{\mathbf{y_{k+1}} - \mathbf{y_k}}{h}$ we obtain

$$
(\mathbf{M} + h\mathbf{A})\mathbf{y_{k+1}} + h w_{k+1}\mathbf{B^w}\mathbf{y_{k+1}} = \mathbf{M}\mathbf{y_k} + h(\mathbf{b^u}u_{k+1} + \mathbf{f^{out}}y_{out,k+1}).
\tag{3.25}
$$

Iteratively solving this system for each time step $k \in \{0, \ldots, N-1\}$ yields an approximation $\mathbf{y_{k+1}}$ of $\mathbf{y_h}(t_{k+1})$, which, in turn, corresponds to the spatial approximation of the PDE state $y(t_{k+1})$.

Remark 3.1 (Alternative discretization approaches)
The method presented above of first discretizing in space by Finite Elements followed by subsequent time discretization is also known as method of lines. There exist alternative approaches where essentially both time and space discretization are based on Galerkin methods [33]. This offers the advantage that optimality conditions translate directly from the continuous to the discrete level [14]. Moreover, a rigorous convergence analysis is available, as well as error estimates measuring the discrepancy between discrete and continuous solutions [80]. The approach is also suitable for efficient implementation with adaptive time and space grids [79].

3.2.3 Finite dimensional optimal control problem

Recall that we aim to solve the optimal control problem (3.6) numerically. In the previous sections, we have already described how the state equation is discretized using Finite

Elements and the Implicit Euler Method. What is left to discretize is the cost functional

$$J(y, u, w) = \frac{\sigma_T}{2} \int_\Omega (y(T, x) - y_T(x))^2 \, dx + \frac{\sigma_Q}{2} \int_0^T \int_\Omega (y(t, x) - y_Q(t, x))^2 \, dx \, dt$$
$$+ \frac{\sigma_u}{2} \int_0^T (u(t))^2 \, dt + \frac{\sigma_w}{2} \int_0^T (w(t))^2 \, dt. \tag{3.26}$$

For this, we replace the integrals over the domain Ω and over the time interval $[0, T]$ by discrete approximations. For functions $z \in L^2(\Omega)$ this can be achieved by approximating

$$\|z\|_{L^2(\Omega)}^2 = \int_\Omega (z(x))^2 \, dx \approx \mathbf{z_h}^\top \mathbf{M} \mathbf{z_h}, \tag{3.27}$$

where $\mathbf{z_h} = (z_0, \ldots, z_L)^\top$ is the coefficient vector of the Finite Element discretization of z and $\mathbf{M}$ is the mass matrix (see equation (3.16)). In addition, the time integral on the interval $[0, T]$ of a function $f(t)$ can be approximated using the (right) Riemann sum

$$\int_0^T f(t) \, dt \approx h \sum_{k=0}^{N-1} f(t_{k+1}). \tag{3.28}$$

By applying these discretizations to (3.26), we obtain the discretized cost functional

$$J_d(\mathbf{y}, \mathbf{u}, \mathbf{w}) = \frac{\sigma_T}{2} (\mathbf{y_N} - \mathbf{y_T})^\top \mathbf{M} (\mathbf{y_N} - \mathbf{y_T})$$
$$+ h \sum_{k=0}^{N-1} \left(\frac{\sigma_Q}{2} (\mathbf{y_k} - \mathbf{y_{Q,k}})^\top \mathbf{M} (\mathbf{y_k} - \mathbf{y_{Q,k}}) + \frac{\sigma_u}{2} u_k^2 + \frac{\sigma_w}{2} w_k^2 \right) \tag{3.29}$$

with $\mathbf{y} = (\mathbf{y_0}, \ldots, \mathbf{y_N})^\top$, $\mathbf{u} = (u_0, \ldots, u_{N-1})^\top$ and $\mathbf{w} = (w_0, \ldots, w_{N-1})^\top$.

The last issue to address is how the state constraints on y can be enforced. For this we make the assumption that we use linear Lagrange Finite Elements. In this case, the coefficients $(y_{k,1}, \ldots, y_{k,L}) = \mathbf{y_k}$ directly correspond to the value of the Finite Element approximation of $y(t_k)$ at the Finite Element nodes. Thus, we can constrain the state by demanding

$$\underline{\mathbf{y}}_{\mathbf{k,i}} \leq \mathbf{y_{k,i}} \leq \overline{\mathbf{y}}_{\mathbf{k,i}} \tag{3.30}$$

for each $k \in \{0, \ldots, N\}$ and $i \in \mathscr{I}_{\Omega_y}$, where $\underline{\mathbf{y}}_{\mathbf{k}}$ and $\overline{\mathbf{y}}_{\mathbf{k}}$ are the coefficient vectors of appropriate Finite Element representations of $\underline{y}$ and $\overline{y}$ and $\mathscr{I}_{\Omega_y}$ is the index set of Finite Element nodes in the subdomain Ω_y.

With all of the above, we can finally write down the fully discretized finite dimensional

optimization problem of (3.6):

$$\min_{\mathbf{y},\mathbf{u},\mathbf{w}} J_d(\mathbf{y}, \mathbf{u}, \mathbf{w}) = \frac{\sigma_T}{2}(\mathbf{y_N} - \mathbf{y_T})^\top \mathbf{M}(\mathbf{y_N} - \mathbf{y_T})$$

$$+ h \sum_{k=0}^{N-1} \left(\frac{\sigma_Q}{2}(\mathbf{y_k} - \mathbf{y_{Q,k}})^\top \mathbf{M}(\mathbf{y_k} - \mathbf{y_{Q,k}}) + \frac{\sigma_u}{2}u_k^2 + \frac{\sigma_w}{2}w_k^2 \right)$$

$$\text{s.t. } (\mathbf{M} + h\mathbf{A})\mathbf{y_{k+1}} + hw_{k+1}\mathbf{B^w}\mathbf{y_{k+1}} = \mathbf{My_k} + h(\mathbf{b^u}u_{k+1} + \mathbf{f^{out}}y_{out,k+1}), \quad k \in \{0, \ldots, N-1\},$$

$$\underline{\mathbf{y}}_{\mathbf{k,i}} \leq \mathbf{y_{k,i}} \leq \overline{\mathbf{y}}_{\mathbf{k,i}}, \qquad\qquad\qquad k \in \{0, \ldots, N\}, i \in \mathscr{I}_{\Omega_y},$$

$$\underline{u}_k \leq u_k \leq \overline{u}_k, \qquad\qquad\qquad k \in \{0, \ldots, N-1\},$$

$$\mathbf{y_0} = \mathscr{y}_0.$$

$$(3.31)$$

Observe that the equality constraints of the finite dimensional optimization problem are nonlinear due to the mixed terms $w_{k+1}\mathbf{B^w}\mathbf{y_{k+1}}$. For the numerical solution, we thus need a method capable of handling nonlinear equality constraints, as well as (in our case linear) inequality constraints. One option is to apply an interior point method (see [88]) such as the one implemented in the library `Ipopt` [104].

3.3 Solution without controlled convection term

We now return to the setting presented in problem (3.5) where the only control happens at the boundary and the velocity field $v(t, x)$ is regarded as given data. This exact setting has been studied in detail in [76]. Therein, the problem is solved using a Primal Dual Active Set Strategy (PDASS) [16, 63]. In this section, we will give a short overview of the method without delving into details. For these, we refer to [76, 77].

Recall that we have already derived the weak formulation of the PDE in Section 3.1.3, although for the more general case with a controlled convection term. In the present setting, we consider the bilinear form, which for $t \in (0, T)$ is defined by

$$a(t; \varphi, \psi) := \alpha \int_\Omega \nabla\varphi(x) \cdot \nabla\psi(x)\, dx + \int_\Omega (vt, x \cdot \nabla\varphi(x))\psi(x)\, dx + \gamma_{out} \int_{\Gamma_{out}} \varphi(s)\psi(s)\, ds$$

$$+ \sum_{i=1}^m \gamma_c \int_{\Gamma_{c_i}} \varphi(s)\psi(s)\, ds.$$

$$(3.32)$$

This leads to the weak form of the state equation:

$$\frac{\mathrm{d}}{\mathrm{d}t}\langle y(t), \varphi \rangle_{L^2(\Omega)} + a(t; y(t), \varphi) = \langle \mathscr{B}u(t), \varphi \rangle_{V',V} + \langle \mathscr{F}(t), \varphi \rangle_{V',V}, \forall \varphi \in V \text{ a.e. on } (0, T)$$

$$y(0) = y_0 \text{ in } L^2(\Omega).$$

$$(3.33)$$

Let us write down the optimal control problem (3.5) once more:

$$\min_{y,u} J(y,u) = \frac{\sigma_T}{2}\|y(T) - y_T\|_{L^2(\Omega)}^2 + \frac{\sigma_Q}{2}\int_0^T \|y(t) - y_Q(t)\|_{L^2(\Omega)}^2 \, dt \tag{3.34a}$$

$$+ \frac{\sigma_u}{2}\sum_{i=1}^m \|u_i\|_{L^2(0,T)}^2 \tag{3.34b}$$

subject to (3.33),

$$\underline{u}(t) \leq u_i(t) \leq \overline{u}(t), \; i \in \{1,\dots,m\} \text{ a.e. on } (0,T) \tag{3.34c}$$

$$\underline{y}(t,x) \leq y(t,x) \leq \overline{y}(t,x) \qquad \text{a.e. on } (0,T) \times \Omega_y \tag{3.34d}$$

The state constraints (3.34d) pose the largest difficulty to solving the optimal control problem since they lead to measure-valued Lagrange multipliers in the optimality conditions (cf. [76, Theorem 1.18]). One way to handle them is to apply a regularization, e.g., using a virtual control approach [69]. In this approach, the state constraints are replaced by mixed state-control constraints. In a slight abuse of notation, we introduce an additional control variable $w \in \mathscr{W} := L^2(0,T;H)$, noting that this new variable and the corresponding space should not be confused with their counterparts from the previous section. The task of the virtual control variable is to capture violations of the state constraints which are then penalized in an augmented cost functional. We choose a regularization parameter $\varepsilon > 0$ and replace the state constraint in problem (3.34) by the auxiliary control constraint

$$\underline{y}(t,x) \leq y(t,x) + \varepsilon w(t,x) \leq \overline{y}(t,x) \text{ a.e. in } \Omega \times (0,T).^2 \tag{3.35}$$

It can be written equivalently as

$$\underbrace{\frac{1}{\varepsilon}(\underline{y}(t,x) - y(t,x))}_{=:\underline{w}(t,x)} \leq w(t,x) \leq \underbrace{\frac{1}{\varepsilon}(\overline{y}(t,x) - y(t,x))}_{=:\overline{w}(t,x)} \text{ a.e. in } \Omega \times (0,T). \tag{3.36}$$

The cost functional is modified to

$$J_\varepsilon(y,u,w) = \frac{\sigma_T}{2}\|y(T) - y_T\|_{L^2(\Omega)}^2 + \frac{\sigma_Q}{2}\int_0^T \|y(t) - y_Q(t)\|_{L^2(\Omega)}^2 \, dt$$

$$+ \frac{\sigma_u}{2}\sum_{i=1}^m \|u_i\|_{L^2(0,T)}^2 + \frac{\sigma_w}{2}\|w\|_{\mathscr{W}}^2$$

with the regularization parameter $\sigma_w > 0$. As stated in [76, Theorem 1.39], the solution of problem (3.34) can be approximated by the solution of the following regularized optimal

---

²For ease of presentation, we omit the embedding operator $\mathscr{E} : W(0,T) \to \mathscr{W}$ to map from state space to the space of the virtual control w. The full details can be found in [77].

control problem:

$$
\begin{aligned}
&\min_{y,u,w} J_\varepsilon(y,u,w) \\
&\text{subject to } (3.3), (3.4) \\
&\quad \underline{u}(t) \le u_i(t) \le \overline{u}(t), \ i \in \{1,\dots,m\} \quad \text{a.e. on } (0,T) \\
&\quad \underline{w}(t,x) \le w(t,x) \le \overline{w}(t,x) \qquad\qquad \text{a.e. in } \Omega \times (0,T)
\end{aligned}
\tag{3.37}
$$

The above problem can be written in control-reduced form, i.e., the optimization is carried out only with respect to the control variables u and w. In this formulation, the state y is derived from the state $\hat{y}$ resulting from the uncontrolled dynamics and the (additive) influence of the control described by the control-to-state operator $\mathscr{S}$, i.e., $y = \hat{y} + \mathscr{S}u$. The resulting control-reduced problem reads

$$
\begin{aligned}
\min_{u,w} \hat{J}_\varepsilon(u,w) = {}& \frac{\sigma_T}{2} \|(\mathscr{S}u)(T) - (y_T - \hat{y}(T))\|^2_{L^2(\Omega)} + \frac{\sigma_Q}{2} \int_0^T \|(\mathscr{S}u)(t) - (y_Q(t) - \hat{y}(t))\|^2_{L^2(\Omega)} dt \\
&+ \frac{\sigma_u}{2} \sum_{i=1}^m \|u_i\|^2_{L^2(0,T;\mathbb{R})} + \frac{\sigma_w}{2}\|w\|^2_{\mathscr{W}} \\
&\quad \underline{u}(t) \le u_i(t) \le \overline{u}(t), \ i \in \{1,\dots,m\} \quad \text{a.e. on } (0,T) \\
&\quad \underline{w}(t,x) \le w(t,x) \le \overline{w}(t,x) \qquad\qquad \text{a.e. in } \Omega \times (0,T).
\end{aligned}
\tag{3.38}
$$

Necessary optimality conditions for the relaxed problem (3.38) have been derived in [77]. We state them in the following theorem.

Theorem 3.2 (First-order optimality conditions, cf. [77, Theorem 2.2])
Suppose the feasible set

$$
\mathscr{Z}_{ad}^\varepsilon = \{z = (u,w) \in \mathscr{U} \times \mathscr{W} \mid \underline{u} \le u_i \le \overline{u}, i \in \{1,\dots,m\}, \ \underline{w} \le w \le \overline{w}\}
\tag{3.39}
$$

is nonempty and that $z^* = (u^*, w^*)$ is the solution of problem (3.38) with associated optimal state $y^* = \hat{y} + \mathscr{S}u^*$. Then there exist unique Lagrange multipliers $p^* \in W(0,T)$ and $\beta^* \in \mathscr{W}$, $\mu^* = (\mu_i^*)_{1 \le i \le m} \in \mathscr{U}$ satisfying the dual equations

$$
-\frac{d}{dt}\langle p^*(t), \varphi \rangle_{L^2(\Omega)} + a(t; \varphi, p^*(t)) = \sigma_Q \langle (y_Q - y^*)(t), \varphi \rangle_{L^2(\Omega)} - \langle \beta^*(t), \varphi \rangle_{L^2(\Omega)}
$$
$$
\textit{for all } \varphi \in H^1(\Omega), \tag{3.40}
$$
$$
p^*(T) = \sigma_T(y_T - y^*(T)) \textit{ in } L^2(\Omega)
$$

a.e. in $[0,T]$ and the optimality system

$$
\begin{aligned}
\sigma_u u^* - \delta_c \int_{\Gamma_c} p^* \, ds + \mu^* = 0 \ \textit{in } L^2(0,T) \\
\sigma_w w^* + \varepsilon\beta^* = 0 \ \textit{in } L^2(0,T;L^2(\Omega)).
\end{aligned}
\tag{3.41}
$$

Moreover,

$$\beta^* = \max\{0, \beta^* + \eta(y^* + \varepsilon w^* - \overline{y})\} + \min\{0, \beta^* + \eta(y^* + \varepsilon w^* - \underline{y})\},$$
$$\mu^* = \max\{0, \mu^* + \eta_i(u_i^* - \overline{u})\} + \min\{0, \mu^* + \eta_i(u_i^* - \underline{u})\} \tag{3.42}$$

for $i = 1, \ldots, m$ and arbitrarily chosen $\eta, \eta_1, \ldots, \eta_m > 0$, where the max- and min-operations are interpreted componentwise in the pointwise everywhere sense.

The goal of the PDASS method is to compute a solution of the optimality system in the above theorem. For given $z = (u, w)$ consider the forward and backward solutions[3] of the state and adjoint equations

$$y(z) = \hat{y} + \mathcal{S}u, \quad p(z) = \hat{p} + \mathcal{A}_1 u - \frac{\sigma_w}{\varepsilon}\mathcal{A}_2 w \tag{3.43}$$

and let

$$\mu_i(z) = \delta_c \int_{\Gamma_c} p(z)ds - \sigma_u u_i, \ i = 1, \ldots, m \quad \text{and} \quad \beta(z) = -\frac{\sigma_w}{\varepsilon}w. \tag{3.44}$$

Define active and inactive sets as follows:

$$\underline{\mathcal{A}}_i^{\mathcal{U}}(z) := \{t \in [0, T] | \ \mu_i(z) + \sigma_u(u_i - \underline{u}) < 0 \text{ a.e.}\}, \quad i = 1, \ldots, m,$$
$$\overline{\mathcal{A}}_i^{\mathcal{U}}(z) := \{t \in [0, T] | \ \mu_i(z) + \sigma_u(u_i - \overline{u}) > 0 \text{ a.e.}\}, \quad i = 1, \ldots, m,$$
$$\underline{\mathcal{A}}^{\mathcal{W}}(z) := \{(t, x) \in Q | \ \beta(z) + \frac{\sigma_w}{\varepsilon^2}(y(z) + \varepsilon w - \underline{y}) < 0 \text{ a.e.}\},$$
$$\overline{\mathcal{A}}^{\mathcal{W}}(z) := \{(t, x) \in Q | \ \beta(z) + \frac{\sigma_w}{\varepsilon^2}(y(z) + \varepsilon w - \overline{y}) > 0 \text{ a.e.}\}, \tag{3.45}$$
$$\mathcal{I}_i^{\mathcal{U}}(z) := [0, T] \setminus (\underline{\mathcal{A}}_i^{\mathcal{U}}(z) \cup \overline{\mathcal{A}}_i^{\mathcal{U}}(z)), \quad i = 1, \ldots, m,$$
$$\mathcal{I}^{\mathcal{W}}(z) := Q \setminus (\underline{\mathcal{A}}^{\mathcal{W}}(z) \cup \overline{\mathcal{A}}^{\mathcal{W}}(z)).$$

The name of the PDASS method derives from the fact that the primal system (3.33) (i.e. the state equation) and the dual system (3.40) are solved simultaneously, while the active and inactive sets are keeping track of points where the constraints are violated. The solutions of the primal and dual systems are successively updated in order to eliminate these violations.

New control iterates $z^{k+1} = (u^{k+1}, w^{k+1})$ are computed by the solution of the following system

$$\delta_c \int_{\Gamma_c} b_i p^{k+1} ds - \sigma_u u_i^{k+1} = 0 \quad \text{in } \mathcal{I}_i^{\mathcal{U}}(z^k), \quad i = 1, \ldots, m,$$
$$u_i^{k+1} = \underline{u} \quad \text{in } \underline{\mathcal{A}}_i^{\mathcal{U}}(z^k), \quad i = 1, \ldots, m,$$
$$u_i^{k+1} = \overline{u} \quad \text{in } \overline{\mathcal{A}}_i^{\mathcal{U}}(z^k), \quad i = 1, \ldots, m, \tag{3.46}$$
$$w^{k+1} = 0 \quad \text{in } \mathcal{I}^{\mathcal{W}}(z^k),$$
$$y^{k+1} + \varepsilon w^{k+1} = \underline{y} \quad \text{in } \underline{\mathcal{A}}^{\mathcal{W}}(z^k),$$
$$y^{k+1} + \varepsilon w^{k+1} = \overline{y} \quad \text{in } \overline{\mathcal{A}}^{\mathcal{W}}(z^k).$$

---

[3]For brevity, we avoid giving the full definitions of the solution operators $\mathcal{S}, \mathcal{A}_1$ and $\mathcal{A}_2$. These can be found in [77, Section 2.2 + 2.3]

To solve this system, we first need to compute new iterates y^{k+1} and p^{k+1} of the state and of the adjoint, respectively. These are obtained by combining (3.44) and (3.46) to get

$$
u^{k+1} = \begin{cases} \frac{\delta_c}{\sigma_u} \int_{\Gamma_c} p^{k+1} ds & \text{in } \mathscr{I}_i^{\mathscr{U}}(z^k), \\ \underline{u} & \text{in } \underline{\mathscr{A}}_i^{\mathscr{U}}(z^k), \\ \overline{u} & \text{in } \overline{\mathscr{A}}_i^{\mathscr{U}}(z^k), \end{cases} \qquad \beta^{k+1} = -\frac{\sigma_w}{\varepsilon} w^{k+1} = \begin{cases} 0 & \text{in } \mathscr{I}^{\mathscr{W}}(z^k), \\ \frac{\sigma_w}{\varepsilon^2}(y^{k+1} - \underline{y}) & \text{in } \underline{\mathscr{A}}^{\mathscr{W}}(z^k), \\ \frac{\sigma_w}{\varepsilon^2}(y^{k+1} - \overline{y}) & \text{in } \overline{\mathscr{A}}^{\mathscr{W}}(z^k), \end{cases}
$$
(3.47)

for $i = 1, \ldots, m$, and substituting these into the primal and dual equations (3.33), (3.40). This leads to the (coupled) primal-dual system

$$
\frac{\mathrm{d}}{\mathrm{d}t} \langle y^{k+1}(t), \varphi \rangle_{L^2(\Omega)} + a(t; y^{k+1}(t), \varphi) - \delta_c \sum_{i=1}^m \chi_{\mathscr{I}_i^{\mathscr{U}}(z^k)}(t) \frac{\delta_c}{\sigma_u} \int_{\Gamma_c} p^{k+1} d\tilde{s} \int_{\Gamma_c} \varphi ds
$$
$$
= \langle \mathscr{F}(t), \varphi \rangle_{V', V} + \delta_c \sum_{i=1}^m \left(\chi_{\underline{\mathscr{A}}^{\mathscr{U}}(z^k)}(t) \underline{u}(t) + \chi_{\overline{\mathscr{A}}^{\mathscr{U}}(z^k)}(t) \overline{u}(t) \right) \int_{\Gamma_c} \varphi ds, \qquad \forall \varphi \in V \text{ a.e. on } (0, T),
$$
(3.48a)

$$
y^{k+1}(0) = y_0,
$$
(3.48b)

$$
-\frac{\mathrm{d}}{\mathrm{d}t} \langle p^{k+1}(t), \varphi \rangle_{L^2(\Omega)} + a(t; \varphi, p^{k+1}(t)) + \sigma_Q \langle y^{k+1}(t), \varphi \rangle_{L^2(\Omega)} + \frac{\sigma_w}{\varepsilon^2} \langle \left(\chi_{\underline{\mathscr{A}}^{\mathscr{W}}(z^k)}(t) + \chi_{\overline{\mathscr{A}}^{\mathscr{W}}(z^k)}(t) \right) y^{k+1}(t), \varphi \rangle_{L^2(\Omega)}
$$
$$
= \sigma_Q \langle y_Q(t), \varphi \rangle_{L^2(\Omega)} + \frac{\sigma_w}{\varepsilon^2} \langle \chi_{\underline{\mathscr{A}}^{\mathscr{W}}(z^k)}(t) \underline{y}(t) + \chi_{\overline{\mathscr{A}}^{\mathscr{W}}(z^k)}(t) \overline{y}(t), \varphi \rangle_{L^2(\Omega)} \qquad \forall \varphi \in V \text{ a.e. on } (0, T),
$$
(3.48c)

$$
p^{k+1}(T) = \sigma_T(y_T - y^{k+1}(T)),
$$
(3.48d)

where $\chi_{\mathscr{M}}$ denotes the characteristic function on the set $\mathscr{M}$.

Starting from an initial guess $z^0 = (u^0, w^0) \in \mathscr{U} \times \mathscr{W}$ of the solution, the PDASS method repeatedly solves the primal-dual system (3.48) and determines new active and inactive sets for each iterate. The method terminates, if at some point the sets no longer change from one iteration to the next. The PDASS method corresponds to a semi-smooth Newton method and thus features local super-linear convergence [65, 102].

The procedure is summarized in Algorithm 3.3.

Algorithm 3.3 (PDASS Algorithm)

1: *Choose starting values $z^0 = (u^0, w^0)$ and determine the corresponding state y^0 and adjoint p^0;*

2: *Set $k = 0$ and* `flag = false`;

3: *Compute the initial active and inactive sets $\underline{\mathscr{A}}_i^{\mathscr{U}}(z^0)$, $\overline{\mathscr{A}}_i^{\mathscr{U}}(z^0)$, $\mathscr{I}_i^{\mathscr{U}}(z^0)$ for $i = 1, \ldots, m$, and $\underline{\mathscr{A}}^{\mathscr{W}}(z^0)$, $\overline{\mathscr{A}}^{\mathscr{W}}(z^0)$, $\mathscr{I}^{\mathscr{W}}(z^0)$ according to (3.45);*

4: **while** `flag == false` **do**

5: 　　*Compute the solutions (y^{k+1}, p^{k+1}) of the primal-dual system (3.48);*

6:     Compute the new iterate $z^{k+1} = (u^{k+1}, w^{k+1})$ *according to* (3.46);
7:     Compute the new active and inactive sets $\underline{\mathscr{A}}_i^{\mathscr{U}}(z^{k+1})$, $\overline{\mathscr{A}}_i^{\mathscr{U}}(z^{k+1})$, $\mathscr{I}_i^{\mathscr{U}}(z^{k+1})$
       for $i = 1, \ldots, m$, *and* $\underline{\mathscr{A}}^{\mathscr{W}}(z^{k+1})$, $\overline{\mathscr{A}}^{\mathscr{W}}(z^{k+1})$, $\mathscr{I}^{\mathscr{W}}(z^{k+1})$ *according to* (3.45);
8:     **if** $\underline{\mathscr{A}}_i^{\mathscr{U}}(z^k) == \underline{\mathscr{A}}_i^{\mathscr{U}}(z^{k+1})$ *and* $\overline{\mathscr{A}}_i^{\mathscr{U}}(z^k) == \overline{\mathscr{A}}_i^{\mathscr{U}}(z^{k+1})$ *for all* $i = 1, \ldots, m$,
       and $\underline{\mathscr{A}}^{\mathscr{W}}(z^k) == \underline{\mathscr{A}}^{\mathscr{W}}(z^{k+1})$ *and* $\overline{\mathscr{A}}^{\mathscr{W}}(z^k) == \overline{\mathscr{A}}^{\mathscr{W}}(z^{k+1})$
       then
9:         `flag = true`
10:    **end if**
11:    Set $k = k + 1$;
12: **end while**

The method can be implemented using Finite Element and Implicit Euler methods for the discretization of the primal-dual system (3.48) as described in Sections 3.2.1 and 3.2.2.

3.4   Efficient implementation and extensions

In the following, we give some explanation on how the previously presented methods have been implemented, as well as ideas for possible improvements.

Software for Finite Element discretization
The triangulation and the assembly of the Finite Element matrices for the PDE examples later on in the thesis was performed by the libraries `FEniCS` [6] and `Firedrake` [95][4]. These libraries handle the translation of the variational formulation of the PDE to a system of equations which can be passed on to the backend linear algebra library or the optimization routine. They also provide interfaces to a number of linear algebra libraries, which enables us to choose between different solvers for the solution of the Finite Element systems.

Iterative solvers and preconditioning
Both (3.31) and the primal-dual system (3.48) in the PDASS algorithm rely on the solution of linear systems of equations. Although the system matrices are sparse (due to the compact support of the Finite Element basis functions), for a high number of Finite Element degrees of freedom this cannot be done efficiently using direct solvers. Instead, we employ iterative solvers. In practice, we opted for the Generalized minimal residual method (GMRES) implemented in the `PETSc` library[5].
Furthermore, for improving the speed of convergence, the method needs to be combined with a matrix preconditioner. The incomplete LU factorization (ILU) turned out to be a good choice.

---

[4]For the numerical computations in this thesis both libraries were used. `FEniCS` was used for the 1D setting in Example 4.42. `Firedrake` was used for the 2D convection-diffusion example in at the end of Chapter 6.
[5]See: `https://www.mcs.anl.gov/petsc/`

Proper Orthogonal Decomposition (POD)

Considerable speed-ups of the solution of the optimal control problem can be obtained by applying POD [59, 70]. In contrast to the Finite Element method, POD uses a different choice of basis functions for the approximation of the space V. The reduced order POD basis is generated from so-called snapshots of the system dynamics, which are obtained initially from a single solution of the optimal control problem using the full order Finite Element model.

While the resulting system matrices in the POD basis are no longer sparse, it generally suffices to use a significantly smaller number $\ell \ll L$ of POD basis functions, compared to the number of finite element nodes L, for obtaining the desired accuracy. Thus, instead of solving a high-dimensional sparse system, in POD we solve a low-dimensional dense system capturing the essential dynamics.

In the context of MPC, the initial control used for the generation of the snapshots may differ from controls at later time steps. Consequently, after some time the reduced order model may no longer be an appropriate approximation of the true dynamics. This makes it necessary to update the POD basis. For an in-depth introduction to the POD method, as well as strategies for handling the POD basis update we refer to [59, 70, 76, 78].

4 | MPC results for time-varying systems

In Chapter 2, we revisited existing results of classical and economic MPC for time-invariant systems. Now, we will turn to the more general case of control systems depending on time. This means that the system is affected by variables that change over time. Mathematically this implies that the transition function f of the control system now additionally depends on the time t (or the time index k) besides state x and control u. Additionally, time-varying behavior of a system can also be induced by a time-dependent stage cost function ℓ or a time-dependent constraint set (both for control and/or state).

Time-varying systems appear in many practical applications. Examples include both industrial applications like vehicles navigating dynamic environments [62], as well as applications with an economic background such as residential building control subject to time-varying electricity pricing [21, 86, 89]. We will particularly consider the latter example since it can exhibit all three of the factors mentioned above: time-varying dynamics (due to changing outside temperature), time-varying stage cost (dynamically priced electricity) and time-varying constraints (bounds for the temperature profile).

By adding the time-variance, new fundamental questions regarding the optimality of solutions arise. In the time-invariant setting, optimal equilibria were of particular importance because they represent points to operate the system at minimal costs. When considering time-varying systems the regime of optimal operation will generally no longer be an equilibrium but some non-stationary distinguished trajectory of the system. Such generalized regimes of optimal operation have already been studied in the time-invariant context, specifically for the case of optimal periodic operation [84], (possibly) non-periodic trajectories with an averaged performance criterion [28], and so-called optimal set operation where a system is optimally operated when the states of the system remain in a certain subset of the state space [73]. To classify non-stationary regimes of optimal operation in the time-varying context, we will introduce a modified notion of optimality, called *overtaking optimality*.

In the literature, it is often distinguished between MPC schemes with and without terminal conditions. When including terminal conditions like terminal constraint sets or a terminal cost in the formulation of the MPC problem, the proofs of convergence and stability of the MPC closed-loop trajectories are very elegant. For examples of this approach see, e.g., [8, 10, 25, 110]. However, the design of appropriate terminal ingredients is not straightforward already in the time-invariant setting, because usually knowledge of the

optimal regime of operation enters in their formulation. This is even more so in the time-varying case, where the optimal steering behavior can be arbitrarily complex and is in general not known a priori.

MPC schemes without terminal conditions, on the other hand, entirely avoid the use of terminal costs or terminal constraints. Thus, no prior knowledge of the optimal system behavior is required. For time-invariant systems, performance and stability of the MPC closed-loop trajectory have been shown for the case of optimal equilibria [43, 44, 57], and more generally for optimal periodic behavior [84]. Unfortunately, these results cannot be applied in the time-varying case directly. We will transfer the relevant assumptions from the time-invariant setting and modify them if necessary to recover performance and convergence of MPC solutions. In the next chapter, we will justify this by checking the plausibility of the new assumptions.

There exist some results considering time-varying economic MPC in continuous time [3, 4], particularly with time-varying stage cost as in the first reference. However, these rely on the design of terminal constraints which, as mentioned above, is challenging and can be avoided with our approach.

The results presented in this chapter comprise the outcomes of the papers [51] and [53].

4.1 Time-varying setting

Moving to time-varying systems leads to a number of notational changes compared to Chapter 2. Firstly, we get an additional parameter k for the time index in the control system

$$x(k+1) = f(k, x(k), u(k)), \quad x(0) = x, \tag{4.1}$$

now with $f : \mathbb{N}_0 \times X \times U \to X$. In this setting $k \in \mathbb{N}_0$ represents a time instant, $x(k) \in X$ is the state of the system at that time and $u(k) \in U$ is the control applied to the system during the next sampling interval.

In the notation of the state trajectory we now explicitly indicate the dependence on the initial time. Given a control sequence $u \in U^N$ we denote the state trajectory which results from iteratively applying (4.1) starting at initial time k_0 from an initial state $x_0 \in X$ by $x_u(\cdot; k_0, x_0)$. Only when it is clear from the context we may omit the initial time and instead write $x_u(\cdot, x_0)$ to abbreviate.

In addition, we allow the constraint sets to be time-varying as well and define $\mathbb{X}(k) \subseteq X$ to be the sets of admissible states at time k and $\mathbb{U}(k, x) \subseteq U$ as the sets of admissible control values for $x \in \mathbb{X}(k)$ for $k \in \mathbb{N}_0$. Accordingly, for $N \in \mathbb{N}$ the sets $\mathbb{U}^N(k, x)$ denote the admissible control sequences for initial state $x \in \mathbb{X}(k)$ up to time $k + N$, i.e. control sequences $u \in U^N$ satisfying

$$u(j) \in \mathbb{U}(k+j, x_u(j; k, x)) \text{ and } x_u(j+1; k, x) \in \mathbb{X}(k+j+1)$$

for all $j = 0, \ldots, N - 1$.

Finally, the stage cost $\ell : \mathbb{N}_0 \times X \times U \to \mathbb{R}$ may also be time-varying, which leads to a time dependent cost functional

$$J_N(k, x, u) = \sum_{j=0}^{N-1} \ell(k + j, x_u(j; k, x), u(j)).$$

and optimal value function

$$V_N(k, x) := \inf_{u \in \mathbb{U}^N(k,x)} J_N(k, x, u).$$

Our goal is to apply MPC to find a solution to an optimal control problem on the infinite horizon. More specifically, we want to compute a feasible control sequence $u \in \mathbb{U}^\infty(k, x)$ that minimizes the cost functional

$$J_\infty(k, x, u) = \sum_{j=0}^{\infty} \ell(k + j, x_u(j; k, x), u(j)) \tag{4.2}$$

At this point it is not clear that this is a well-defined problem (we will address this issue in the next section). Assuming a control sequence that minimizes (4.2) does exist we will denote it by u_∞^*. Moreover, we define the the infinite horizon optimal value function as follows:

$$V_\infty(k, x) := \inf_{u \in \mathbb{U}^\infty(k,x)} J_\infty(k, x, u).$$

In order to find an approximate solution to the problem on the infinite horizon we apply the following time-varying model predictive control algorithm:

Algorithm 4.1 *For each time instant $k = k_0, k_0 + 1, \ldots$:*

1. *Measure the current state $x = x(k)$ of the system.*

2. *Solve the optimal control problem*

$$\underset{u \in \mathbb{U}^N(k,x)}{minimize} \quad J_N(k, x, u). \tag{4.3}$$

   in order to obtain the optimal control sequence $u_{N,x}^*$.

3. *Apply the first element of $u_{N,x}^*$ as a control to the system during the next sampling period, i.e. use the feedback law $\mu_N(k, x) := u_{N,x}^*(0)$.*

4. *Set $k := k + 1$ and go to 1.*

In the sequel, we assume that a minimizer to the (finite horizon) MPC optimal control problem (4.3) always exists. We will denote it by u_N^*, or by $u_{N,x}^*$ in case we want to emphasize the dependence on the initial state x. Note that for this optimal control it holds that $V_N(k, x) = J_N(k, x, u_{N,x}^*)$.

By iteratively applying the feedback in each step, that is by setting

$$x(k+1) = f(k, x(k), \mu_N(k, x(k))), \tag{4.4}$$

we obtain the *closed-loop trajectory* of the system, which we will denote by $x_{\mu_N}(\cdot; k_0, x_0)$ for the initial value $x_0 = x(k_0) \in \mathbb{X}(k_0)$ at time $k_0 \in \mathbb{N}_0$. The cost of this closed-loop trajectory for L time steps is defined by

$$J_L^{cl}(k_0, x_0, \mu_N) := \sum_{j=0}^{L-1} \ell(k_0 + j, x_{\mu_N}(j; k_0, x_0), \mu_N(k_0 + j, x_{\mu_N}(j; k_0, x_0))). \tag{4.5}$$

The optimality proofs of the MPC closed-loop trajectory rely on the dynamic programming principle. In the course of this chapter we will apply the two versions of the finite and infinite dynamic programming principle which are stated below.

Theorem 4.2 (Finite horizon dynamic programming principle (cf. [50, Theorem 3.15]))
Consider the optimal control problem (4.3) with $x_0 \in \mathbb{X}$ and $k \in \mathbb{N}_0$, $N \in \mathbb{N}$. Let $u_N^*(\cdot) \in \mathbb{U}^N(k, x_0)$ be an optimal control sequence. Then for all $N \in \mathbb{N}$ and all $K = 1, \dots, N$ the equation

$$V_N(k, x_0) = \sum_{j=0}^{K-1} \ell(k + j, x_{u_N^*}(j, x_0), u_N^*(j)) + V_{N-K}(k + K, x_{u_N^*}(K, x_0)) \tag{4.6}$$

holds.

Theorem 4.3 (Infinite horizon dynamic programming principle (cf. [50, Theorem 4.4]))
Consider the optimal control problem (4.9) with $x_0 \in \mathbb{X}$ and $k \in \mathbb{N}_0$. Let $u_\infty^*(\cdot) \in \mathbb{U}^\infty(k, x_0)$ be an optimal control sequence. Then for all $K \in \mathbb{N}$ the equation

$$V_\infty(k, x_0) = \sum_{j=0}^{K-1} \ell(k + j, x_{u_\infty^*}(j, x_0), u_\infty^*(j)) + V_\infty(k + K, x_{u_\infty^*}(K, x_0)) \tag{4.7}$$

holds.

4.2   Overtaking optimality and optimal operation

The problem of minimizing the infinite horizon cost function (4.2) is not necessarily well-defined because for infinite optimal control sequences it is not at all clear for $J_\infty(k, x, u)$ to attain a finite minimum. In fact, with general stage cost the value of $J_\infty(k, x, u)$ may be infinite for all control sequences, so it is not directly possible to compare two control sequences based on their costs. An optimality criterion in the usual sense of $J_\infty(k, x, u^*) \leq J_\infty(k, x, u)$ for all u is not meaningful, since we have an infinite value on both sides of the inequality.
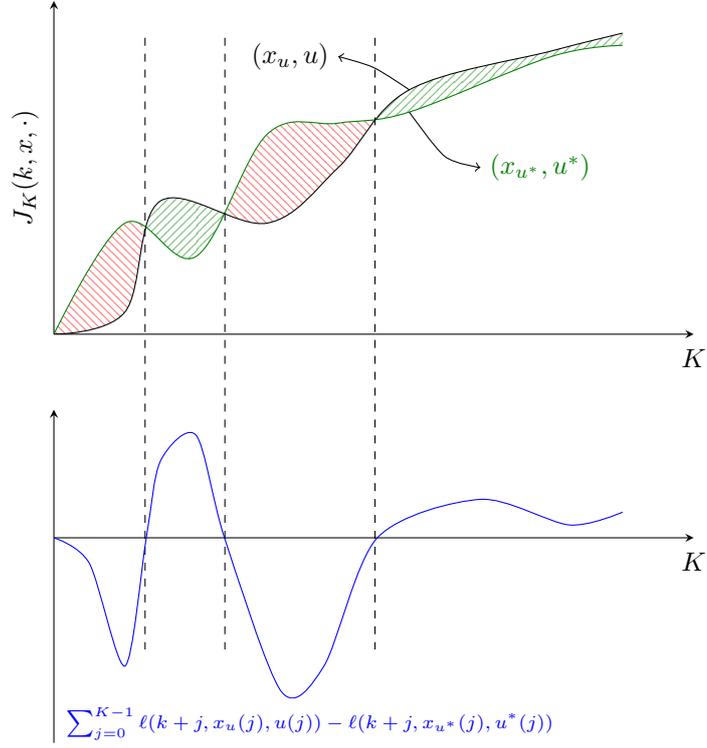
Figure 4.1: Graphical illustration of overtaking optimality.

For this reason, in the following we will clarify what we mean by "minimizing" in the context of infinite horizon optimal control. A remedy to the issues mentioned above is provided by considering an alternative optimality notion going back to Gale [39] in the context of mathematical economics. The key idea is to look at the difference of the cost of two control sequences instead of considering their total cost separately. Although both control sequences in themselves generate infinite costs, the difference between the two can still be finite. A control sequence is considered optimal if its cost is overtaken by the cost of any other control sequence at some point.

Definition 4.4 (Overtaking optimality)
Let $x \in \mathbb{X}(k)$ and consider a control sequence $u^* \in \mathbb{U}^\infty(k,x)$ with corresponding state trajectory $x_{u^*}(\cdot; k, x)$. The pair (x_{u^*}, u^*) is called overtaking optimal if

$$\liminf_{K \to \infty} \left(\sum_{j=0}^{K-1} \ell(k+j, x_u(j,x), u(j)) - \ell(k+j, x_{u^*}(j,x), u^*(j)) \right) \geq 0 \qquad (4.8)$$

for all $u \in \mathbb{U}^\infty(k,x)$.

A graphical illustration of this definition can be found in Figure 4.1. The upper part of the figure shows in green the cost of an overtaking optimal trajectory pair (x_{u^*}, u^*) and

in black the cost of a second (suboptimal) trajectory pair (x_u, u). Initially, the trajectory (x_u, u) produces smaller cost than (x_{u^*}, u^*). As the horizon increases the cost of the two trajectories alternates back and forth several times, until finally the overtaking optimal trajectory pair (x_{u^*}, u^*) prevails, yielding a lower cost than (x_u, u). Still, the individual cost of both trajectory grows unboundedly as $K \to \infty$, which makes them difficult to compare.

The lower part of the figure depicts in blue the difference of the cost of the two trajectories corresponding to the quantity considered in inequality (4.8). This quantity allows us to differentiate the two trajectories by checking if it ultimately becomes positive and stays that way as we take the $\liminf_{K \to \infty}$.

Definition 4.4 provides us with the ability to decide which of two infinite control sequences is better when both are starting from the same initial value x. The minimization in the following problem is to be understood in this overtaking optimal sense:

$$\underset{u \in \mathbb{U}^\infty(k,x)}{\text{minimize}} \; J_\infty(k, x, u) \tag{4.9}$$

In the next definition, the initial state is no longer fixed. Instead, we now look at all possible feasible trajectories of the system and choose from those the one that is optimal in the sense of Definition 4.4.

Definition 4.5 (Optimal operation)
Let $x \in \mathbb{X}(k)$ and consider a control sequence $u^* \in \mathbb{U}^\infty(k, x)$ with corresponding state trajectory $x^* = x_{u^*}(\cdot; k, x)$. We say the system (4.1) is optimally operated at (x^*, u^*) if

$$\liminf_{K \to \infty} \left(\sum_{j=0}^{K-1} \ell(k+j, x_u(j, x'), u(j)) - \ell(k+j, x^*(j), u^*(j)) \right) \geq 0 \tag{4.10}$$

for all $x' \in \mathbb{X}(k)$ and $u \in \mathbb{U}^\infty(k, x')$.

We will refer to the trajectory pair (x^*, u^*) as *optimal trajectory*. In the following, we will assume that an optimal trajectory of the system always exists. Similarly, we assume a solution of problem (4.9) exists, which will be denoted by u_∞^*.

It should be noted that there is no reason to assume that the optimal trajectory is unique. In fact, it is easy to devise examples where multiple optimal trajectories exist which all satisfy Definition 4.5. For our purposes, we will select one distinct optimal trajectory from the set of all optimal trajectories. The question of how this set can be classified remains open for now.

Remark 4.6
The idea of an optimal trajectory can be regarded as a generalization of an optimal equilibrium or an optimal periodic orbit that may occur in the case of time-invariant systems as has been observed e.g. in [84]. In the classical time-invariant setting, there may, for

example, exist an optimal equilibrium at which the system can be operated at minimal cost for an infinite horizon. Then, for any given initial condition, we want to find a control sequence that brings the state to the optimal equilibrium.

In the same way in our setting an optimal trajectory exhibits the best performance in the long run. The question is how this trajectory is connected to the solution of problem (4.9), i.e. the problem on the infinite horizon.

As we will see shortly, using appropriate assumptions we can prove that the solution of problem (4.9) converges to an optimal trajectory. This means we can reach the optimal operating behavior of a system by solving an infinite horizon optimal control problem.

Still, solving problems on an infinite horizon is difficult, which is why MPC is used to compute an approximate solution. ◇

Remark 4.7 (Alternatives to overtaking optimality)

Alternative approaches establish a well-defined optimality notion for problems on an infinite horizon either by considering only stage cost functions which are positive definite w.r.t. some a priori defined reference trajectory or by using discounting of the stage cost. The first approach is usually applied for tracking type problems where a reachable time-varying reference trajectory is known a priori. This is also the reason why it does not fit our setting since we cannot expect a priori knowledge of the optimal trajectory (x^*, u^*). Instead, this trajectory is implicitly defined by the interplay of dynamics, stage cost and constraints.

The idea of the second approach is to include a discount factor β^k, $0 < \beta < 1$ for the stage cost in the cost functional, i.e. by defining

$$J_\infty^{disc}(k, x, u) = \sum_{j=0}^{\infty} \beta^k \ell(k + j, x_u(j; k, x), u(j)). \tag{4.11}$$

Assuming boundedness of the stage cost function ℓ this then guarantees that the cost functionals $J_\infty^{disc}(k, x, u)$ are finite. It offers the advantage that the usual notion of optimality suffices and avoids the need for using overtaking optimality. The approach has its merits and is widely used, e.g. in [20, 49, 72], but the downside is that it changes the original problem causing the stage cost values in the near future to have more impact while distant costs hardly matter. As a consequence, effects of the control in the distant future are considered less important. In many real-world problems (e.g. involving sustainability issues) this behavior is undesirable since it trades short-term gains for long-term adverse effects. Conversely, in some problems, it may even pay off to put up with bigger cost in the near future in order to save in the long run. Thus it becomes hard to justify discounting, even if it simplifies the problem.

While one could argue that in the context of MPC a sort of discounting also happens implicitly via the truncation of the horizon, we still use the non-discounted cost functional together with overtaking optimality in order to characterize the optimal operating behavior in our setting. ◇

Using the overtaking optimality concept does of course not change the fact that the infinite horizon cost functional may be unbounded. However, we can introduce a shifted cost function for which we can then at least guarantee boundedness of the infinite horizon optimal value function.

Definition 4.8 (Shifted cost)
Let (x^*, u^*) be an optimal trajectory. We define the shifted stage cost as

$$\hat{\ell}(k, x(k), u(k)) := \ell(k, x(k), u(k)) - \ell(k, x^*(k), u^*(k)).$$

Correspondingly, the shifted cost functional is defined as

$$\hat{J}_N(k, x, u) := \sum_{j=0}^{N-1} \hat{\ell}(k + j, x_u(j; k, x), u(j)),$$

and shifted optimal value function is given by

$$\hat{V}_N(k, x) := \inf_{u \in \mathbb{U}^N(k,x)} \hat{J}_N(k, x, u).$$

In the same way for the infinite horizon we define

$$\hat{J}_\infty(k, x, u) := \sum_{j=0}^{\infty} \hat{\ell}(k + j, x_u(j; k, x), u(j))$$

and

$$\hat{V}_\infty(k, x) := \inf_{u \in \mathbb{U}^\infty(k,x)} \hat{J}_\infty(k, x, u).$$

It is easy to verify that for $\hat{V}_\infty$ the identity

$$\hat{V}_\infty(k, x^*(k)) = 0$$

holds for all $k \in \mathbb{N}_0$. Moreover, from the Definition 4.5 it follows that the inequality

$$\hat{V}_\infty(k, x) \geq 0 \tag{4.12}$$

holds for all $k \in \mathbb{N}$ and $x \in \mathbb{X}(k)$ (although $\hat{V}_N(k, x) < 0$ is possible).

Note that the optimal control trajectory of the shifted problem coincides with the optimal control trajectory of the original MPC problem (4.3). From an application point of view, this is important because we cannot assume knowledge of the optimal trajectory (x^*, u^*) for the solution of the MPC problems.

Without additional assumptions $\hat{V}_\infty(k, x)$ does not necessarily attain a finite value for all $x \in \mathbb{X}(k)$. This is only clear for the special choice of $x = x^*(k)$, i.e. for an initial value which is located on the optimal trajectory x^*.

In the next section, we will introduce two key assumptions that ensure finiteness of $\hat{V}_\infty(k, x)$ for all $x \in \mathbb{X}(k)$.
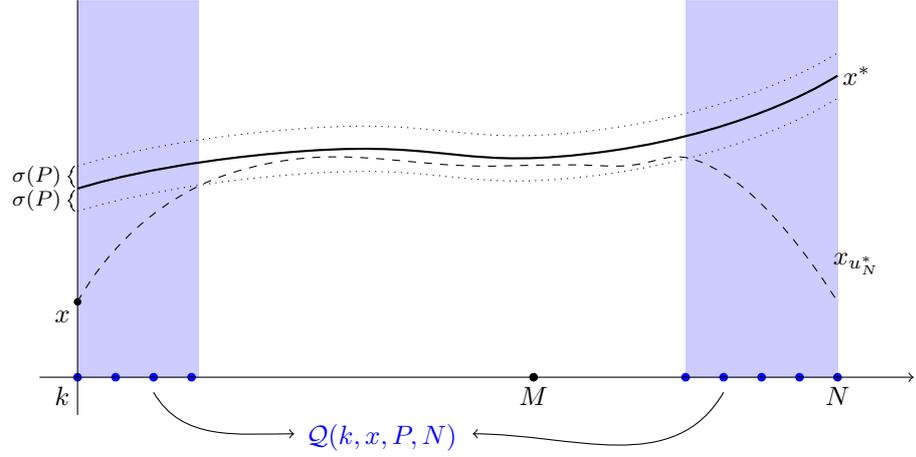
Figure 4.2: Finite horizon turnpike property for time-varying systems.

4.3 Time-varying turnpike and continuity assumptions

The first crucial assumption we make is the occurrence of the *turnpike property*. The version used here is a straightforward extension of the classical turnpike property for time-invariant systems which we introduced in Assumption 2.8 in Chapter 2. The main difference in our time-varying setting consists of working with a (now time-varying) optimal trajectory instead of an equilibrium.

The time-varying turnpike property demands that open-loop optimal trajectories spend most of their time in a neighborhood of the optimal pair (x^*, u^*) from Definition 4.5. To get an intuition of the turnpike property it is helpful to visualize it graphically. This is done in Figure 4.2 for the version on a finite time horizon. We invite the reader to refer to this illustration while studying the rather notation-heavy definition which follows.

Definition 4.9 (Turnpike property)
Consider a trajectory pair (x^*, u^*) at which the system (4.1) is optimally operated.

(a) *We say that an optimal control problem has the finite horizon turnpike property at (x^*, u^*) if the following holds:*
There exists $\sigma \in \mathscr{L}$ such that for each $k \in \mathbb{N}_0$, each optimal trajectory $x_{u_N^*}(\cdot, x)$, $x \in \mathbb{X}(k)$ and all $N, P \in \mathbb{N}$ there is a set $\mathcal{Q}(k, x, P, N) \subseteq \{0, \ldots, N\}$ with $\#\mathcal{Q}(k, x, P, N) \leq P$ elements and

$$|(x_{u_N^*}(M, x), u_N^*(M))|_{(x^*(k+M), u^*(k+M))} \leq \sigma(P)$$

for all $M \in \{0, \ldots, N\} \setminus \mathcal{Q}(k, x, P, N)$.

(b) *Similarly, an optimal control problem on the infinite horizon has the turnpike property, if there exists $\rho \in \mathscr{L}$ such that for each $k \in \mathbb{N}_0$, each optimal trajectory*

$x_{u_\infty^*}(\cdot, x)$, $x \in \mathbb{X}(k)$ *and all* $P \in \mathbb{N}$ *there is a set* $\mathcal{Q}(k, x, P, \infty) \subseteq \mathbb{N}_0$ *satisfying* $\#\mathcal{Q}(k, x, P, \infty) \leq P$ *elements and*

$$|(x_{u_\infty^*}(M, x), u_\infty^*(M))|_{(x^*(k+M), u^*(k+M))} \leq \rho(P)$$

for all $M \in \mathbb{N}_0 \setminus \mathcal{Q}(k, x, P, \infty)$.

Assumption 4.10 (Turnpike property for MPC problem)
We assume that the MPC problem from (4.3) *has the finite horizon turnpike property.*

Assumption 4.11 (Turnpike property for problem on infinite horizon)
We assume that the optimal control problem (4.9) *has the infinite horizon turnpike property.*

The turnpike property guarantees that the open-loop solutions on infinite and finite horizons are close to the optimal trajectory of the system, at least most of the time. While the turnpike property is a very convenient assumption it is at the same time not unreasonable. In the time-invariant framework turnpike properties of optimal control problems are abundant in practical problems, see e.g. [34, 36, 101].
In Chapter 5 we will investigate different ways to verify our extension of the turnpike property for a given system, both by numerical and analytic means.

Note that the infinite horizon turnpike property can also be regarded as a convergence assumption of the solution of the infinite horizon problem (4.9) to the optimal trajectory. This is evident because the turnpike property requires that the distance between the optimal trajectory and the trajectory generated by u_∞^* can only be large for a finite number of points that can only hold for a convergent trajectory.
The second important property for proving performance estimates for the MPC closed-loop is the continuity of the optimal value function.

Assumption 4.12 (Continuity property of the optimal value function)
We assume that the optimal value function $\hat{V}_N$ *is approximately continuous at* x^* *in the following uniform way:*
there exists a function $\gamma_V : \mathbb{R}_0^+ \times \mathbb{R}_0^+ \to \mathbb{R}_0^+$ *with* $\gamma_V(N, r) \to 0$ *if* $N \to \infty$ *and* $r \to 0$, *and* $\gamma_V(\cdot, r), \gamma_V(N, \cdot)$ *monotonous for fixed* r *and* N *such that for each* $k \in \mathbb{N}_0$ *and* $\varepsilon > 0$ *there is an open ball* $\mathscr{B}_\varepsilon(x^*(k))$ *around* $x^*(k)$ *and for all* $x \in \mathscr{B}_\varepsilon(x^*(k)) \cap \mathbb{X}(k)$ *and all* $N \in \mathbb{N}$ *the inequality*
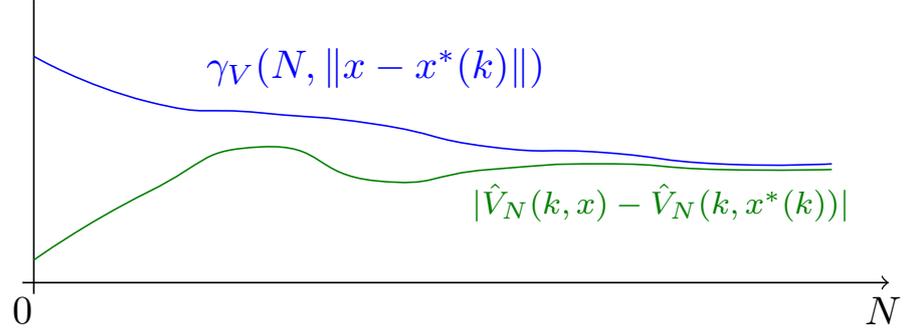
$$|\hat{V}_N(k, x) - \hat{V}_N(k, x^*(k))| \leq \gamma_V(N, |x|_{x^*(k)}) \tag{4.13}$$

holds.
In addition, we also assume approximate continuity of the optimal value function on the infinite horizon:
there exists a function $\omega_V \in \mathscr{K}_\infty$ *such that for each* $k \in \mathbb{N}_0$ *and* $\varepsilon > 0$ *there is an open ball* $\mathscr{B}_\varepsilon(x^*(k))$ *around* $x^*(k)$ *and for all* $x \in \mathscr{B}_\varepsilon(x^*(k)) \cap \mathbb{X}(k)$ *it holds*

$$|\hat{V}_\infty(k, x) - \hat{V}_\infty(k, x^*(k))| \leq \omega_V(|x|_{x^*(k)}). \tag{4.14}$$

(a) First component of γ_V as a function in N for fixed $x \in \mathscr{B}_\varepsilon(x^*(k))$. Since $\gamma_V(\cdot, \|x - x^*(k)\|)$ is monotonously decreasing in N this means the value $|\hat{V}_N(k, x) - \hat{V}_N(k, x^*(k))|$ must be bounded.
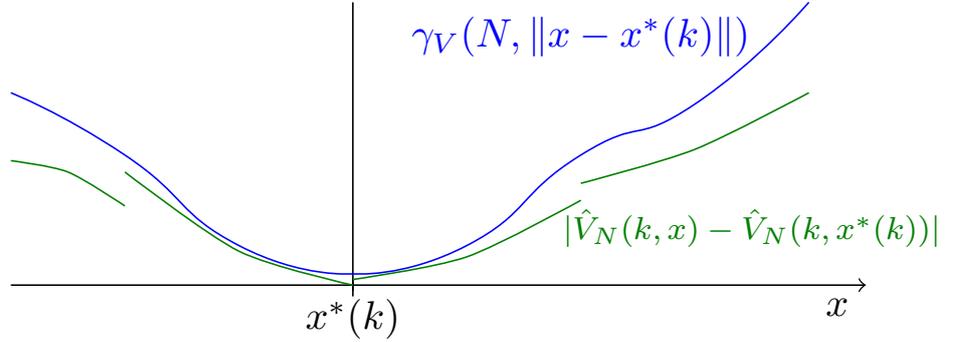
(b) The second component of γ_V as a function in x for fixed horizon length N. $\gamma_V(N, \cdot)$ increases monotonically with growing distance $\|x - x^*(k)\|$.

Figure 4.3: Graphical illustration of the continuity property for $\hat{V}_N$ from Assumption 4.12.

The assumption demands that the shifted optimal value function is approximately continuous in a neighborhood of the optimal trajectory. This means we assume that the optimal value function changes only by a small amount if we consider points x that are sufficiently close to $x^*(k)$. The term *"approximately"* in the above definition reflects the fact that for points away from the optimal trajectory small discontinuities of the optimal value function are permitted. Moreover, for any finite N bounded discontinuities of $\hat{V}_N$ are allowed even for points on the optimal trajectory. Figure 4.3b illustrates this idea. In addition, it is required that for fixed states x and $x^*(k)$ the gap in the optimal value functions can be bounded monotonically as we consider longer horizons N. This is shown in Figure 4.3a.

The following lemma shows that $\hat{V}_\infty$ assumes finite values for each $x \in \mathbb{X}(k)$ if the turnpike property and the continuity property of the optimal value functions hold.

Lemma 4.13 (Finiteness of the shifted optimal value function)
Assume that the infinite horizon turnpike property from Assumption 4.11 and the continuity property from Assumption 4.12 hold. Then for each $k \in \mathbb{N}_0$ and for each $x \in \mathbb{X}(k)$ the value $\hat{V}_\infty(k, x)$ is finite.

Proof. We note that because of (4.12) it is sufficient to show $\hat{V}_\infty(k, x) < \infty$. Let $k \in \mathbb{N}_0$ and $x \in \mathbb{X}(k)$. Consider the infinite horizon optimal control sequence u_∞^*. Pick $P \in \mathbb{N}$ such that $\rho(P) < \varepsilon$ with ε from Assumption 4.12.
Because the infinite horizon turnpike property holds we know that

$$|(x_{u_\infty^*}(j, x), u_\infty^*(j))|_{(x^*(k+j), u^*(k+j))} \leq \rho(P) < \varepsilon$$

for some $j \in \mathbb{N}_0$, in particular $x_{u_\infty^*}(j, x) \in \mathscr{B}_\varepsilon(x^*(k+j))$. Thus we can apply the continuity property from Assumption 4.12 which yields

$$|\hat{V}_\infty(k + j, x_{u_\infty^*}(j, x)) - \hat{V}_\infty(k + j, x^*(k + j))|$$
$$\leq \omega_V(\|x_{u_\infty^*}(j, x) - x^*(k + j)\|) < \omega_V(\varepsilon),$$

where we used the monotonicity of ω_V in the last inequality. Because $\hat{V}_\infty(k+j, x^*(k+j)) = 0$ (cf. the discussion after Definition 4.8) it follows that

$$|\hat{V}_\infty(k + j, x_{u_\infty^*}(j, x))| < \omega_V(\varepsilon).$$

From the optimality of $\hat{V}_\infty(k, x)$ it follows that

$$\hat{V}_\infty(k, x) \leq \hat{J}_j(k, x, u_\infty^*) + \hat{V}_\infty(k + j, x_{u_\infty^*}(j, x)).$$

The term $\hat{J}_j(k, x, u_\infty^*)$ is finite and thus we have a finite bound

$$|\hat{V}_\infty(k, x)| < |\hat{J}_j(k, x, u_\infty^*)| + |\omega_V(\varepsilon)|$$

which shows the assertion. $\qquad\qquad\qquad\qquad\qquad\qquad\qquad\qquad\qquad\square$

4.4   Performance estimates

In this section, we will address the question of how the cost of the MPC closed-loop compares to the cost of the optimal solution on an infinite horizon, i.e. the solution to problem (4.9). For problems in an economic setting, this is of particular interest, whereas the behavior of the state trajectory is of secondary importance. The main aim is to compute a solution that generates the lowest possible costs.
The literature often considers averaged costs of the MPC closed-loop. This has the downside that only a statement about the long term performance is possible, while the transient performance could be arbitrarily poor. For this reason, we will first consider the closed-loop cost directly without averaging. Afterwards, we can still extract a statement about the average cost from our result.
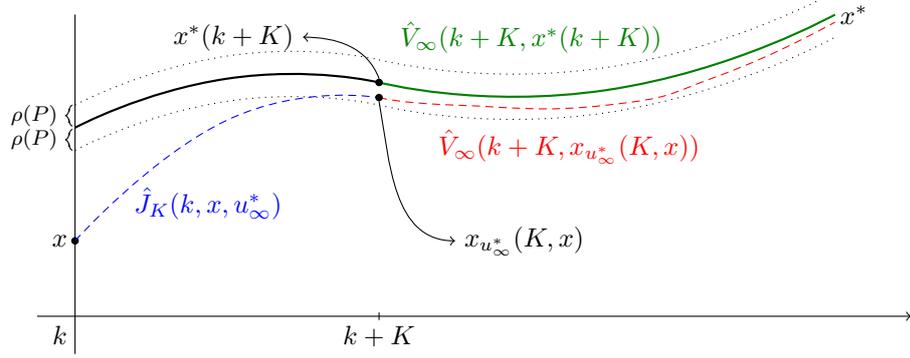
Figure 4.4: Graphical illustration of the proof of Lemma 4.14 (a).

4.4.1 Non-averaged performance

Before we can present our main result we will prove two preparatory lemmas. The first one states that the cost of the optimal trajectory evaluated along the complete horizon is approximately the same as the cost evaluated only up to some appropriately chosen time index K. The result applies to both the infinite and finite horizon optimal control trajectories, although for the latter an additional term appears.

Lemma 4.14 *(a) If the system has the infinite horizon turnpike property from Assumption 4.11 and the continuity property from Assumption 4.12 is satisfied, then the equation*

$$\hat{V}_\infty(k, x) = \hat{J}_K(k, x, u_\infty^*) + R_1(k, x, K) \tag{4.15}$$

holds with $|R_1(k, x, K)| \leq \omega_V(\rho(P))$ for all $k \in \mathbb{N}_0$, for all $x \in \mathbb{X}(k)$, all $N \in \mathbb{N}$, all sufficiently large $P \in \mathbb{N}$ and all $K \notin \mathcal{Q}(k, x, P, \infty)$.

(b) If the system has the finite horizon turnpike property from Assumption 4.10 and the continuity property from Assumption 4.12 is satisfied, then the equation

$$\hat{V}_N(k, x) = \hat{J}_K(k, x, u_N^*) + \hat{V}_{N-K}(k + K, x^*(k + K)) \\ + R_2(k, x, K, N) \tag{4.16}$$

holds with $|R_2(k, x, K, N)| \leq \gamma_V(N - K, \sigma(P))$ for all $k \in \mathbb{N}_0$, for all $x \in \mathbb{X}(k)$, all $N \in \mathbb{N}$, all sufficiently large $P \in \mathbb{N}$ and all $K \notin \mathcal{Q}(k, x, P, N)$.

Proof. (a) Let $k \in \mathbb{N}_0$ and $x \in \mathbb{X}(k)$. We begin with the proof of the infinite horizon case. A visual representation of this proof can be found in Figure 4.4.

The infinite horizon dynamic programming principle from Theorem 4.3 yields

$$\hat{V}_\infty(k, x) = \hat{J}_K(k, x, u_\infty^*) + \hat{V}_\infty(k + K, x_{u_\infty^*}(K, x))$$

for each $K \in \mathbb{N}_0$. This means equation (4.15) holds with $R_1(k, x, K) = \hat{V}_\infty(k + K, x_{u_\infty^*}(K, x))$. Chose $P \in \mathbb{N}$ sufficiently large such that $\rho(P) < \varepsilon$ with ρ from

Assumption 4.11 and ε from Assumption 4.12. Because we have $\hat{V}_\infty(k + K, x^*(k + K)) = 0$ and because of the continuity of $\hat{V}_\infty$ we get that

$$
\begin{aligned}
|R_1(k, x, K)| &= |\hat{V}_\infty(k + K, x_{u_\infty^*}(K, x)) - \hat{V}_\infty(k + K, x^*(k + K))| \\
&\leq \omega_V(\|x_{u_\infty^*}(K, x) - x^*(k + K)\|) \\
&\leq \omega_V(|(x_{u_\infty^*}(K, x), u_\infty^*(K))|_{(x^*(k+K), u^*(k+K))}) \\
&\leq \omega_V(\rho(P)),
\end{aligned}
$$

which holds for all $K \in \mathbb{N}$ with $K \notin \mathcal{Q}(k, x, P, \infty)$ and where we used the monotonicity of ω_V. This shows the assertion.

(b) In the finite horizon case the proof is similar. The dynamic programming principle (Theorem 4.2) yields

$$
\hat{V}_N(k, x) = \hat{J}_K(k, x, u_N^*) + \hat{V}_{N-K}(k + K, x_{u_N^*}(K, x))
$$

for $K \in \{0, \ldots, N\}$. Hence, (4.16) holds with

$$
R_2(k, x, K, N) = \hat{V}_{N-K}(k + K, x_{u_N^*}(K, x)) - \hat{V}_{N-K}(k + K, x^*(k + K)).
$$

Chose $P \in \mathbb{N}$ sufficiently large such that $\sigma(P) < \varepsilon$ holds for σ from Assumption 4.10 and ε from Assumption 4.12. Then we have

$$
\begin{aligned}
|R_2(k, x, K, N)| &= |\hat{V}_{N-K}(k + K, x_{u_N^*}(K, x)) - \hat{V}_{N-K}(k + K, x^*(k + K))| \\
&\leq \gamma_V(N - K, \|x_{u_N^*}(K, x) - x^*(k + K)\|) \\
&\leq \gamma_V(N - K, |(x_{u_N^*}(K, x), u_N^*(K))|_{(x^*(K+k), u^*(K+k))})
\end{aligned}
$$

using again the monotonicity of $\gamma_V(N - K, \cdot)$. For $K \notin \mathcal{Q}(k, x, P, N)$ it follows that $|R_2(k, x, K, N)| \leq \gamma_V(N - K, \sigma(P))$ and thus the assertion. $\qquad\square$

Next, we present a lemma showing that we can exchange finite and infinite horizon optimal control sequences in the shifted cost functional at the cost of a bounded error term, provided we choose the summation index K appropriately.

Lemma 4.15
If the system has the infinite and finite horizon turnpike properties from Assumptions 4.10 and 4.11 and the continuity property from Assumption 4.12 is satisfied, then the equation

$$
\hat{J}_K(k, x, u_\infty^*) = \hat{J}_K(k, x, u_N^*) + R_3(k, x, K, N)
$$

holds with $|R_3(k, x, K, N)| \leq \gamma_V(N - K, \rho(P)) + \gamma_V(N - K, \sigma(P)) + \omega_V(\sigma(P)) + \omega_V(\rho(P))$ for all $k \in \mathbb{N}_0$, all $N \in \mathbb{N}$, all sufficiently large $P \in \mathbb{N}$, all $x \in \mathbb{X}(k)$ and all $K \in \{0, \ldots, N\} \setminus (\mathcal{Q}(k, x, P, N) \cup \mathcal{Q}(k, x, P, \infty))$.
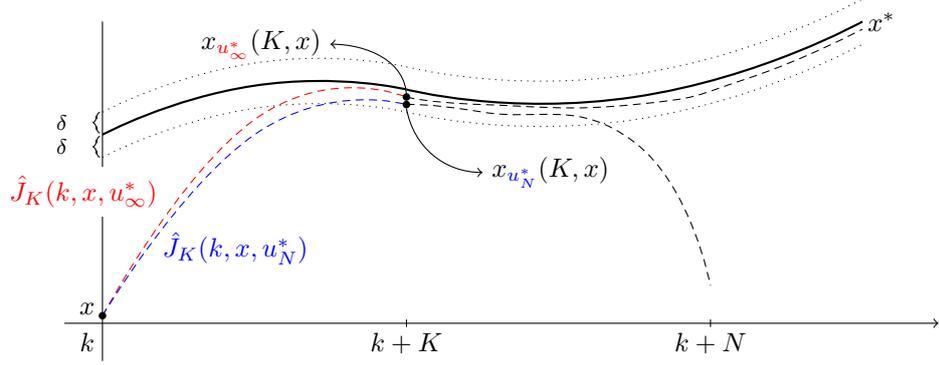
Figure 4.5: Illustration of Lemma 4.15.

Proof. Figure 4.5 contains an illustration of the key idea of the proof. It consists of the observation that under the turnpike assumption both the solution of infinite (depicted in red) and finite open-loop trajectories (depicted in blue) are close to the turnpike at some time instant $k + K$. At this point, we will exploit the continuity of the optimal value function at $x^*(k + K)$. Then, using the dynamic programming principle together with Lemma 4.14 it can be concluded that the cost of the initial pieces of the finite and infinite horizon optimal control sequences are approximately the same:

Consider $R_2(k, x, K, N) = \hat{V}_{N-K}(k+K, x_{u_N^*}(K, x)) - \hat{V}_{N-K}(k+K, x^*(k+K))$ from Lemma 4.14 (b)) and define

$$\tilde{R}_1(k, x, K, N) := \hat{V}_{N-K}(k + K, x_{u_\infty^*}(K, x)) - \hat{V}_{N-K}(k + K, x^*(k + K)).$$

Those expressions satisfy $|R_2(k, x, K, N)| \leq \gamma_V(N - K, \sigma(P))$ for $K \in \{0, \ldots, N\} \setminus \mathcal{Q}(k, x, P, N)$ and $|\tilde{R}_1(k, x, K, N)| \leq \gamma_V(N - K, \rho(P))$ for $K \in \mathbb{N}_0 \setminus \mathcal{Q}(k, x, P, \infty)$ as one sees similarly to the proof of Lemma 4.14 (b)).

The finite horizon dynamic programming principle from Theorem 4.2 implies that $u = u_N^*$ minimizes the expression $\hat{J}_K(k, x, u) + \hat{V}_{N-K}(k + K, x_u(K, x))$, in particular it holds that

$$\hat{J}_K(k, x, u_N^*) + \hat{V}_{N-K}(k + K, x_{u_N^*}(K, x)) \leq \hat{J}_K(k, x, u_\infty^*) + \hat{V}_{N-K}(k + K, x_{u_\infty^*}(K, x)).$$

This, together with the definition of R_2 and $\tilde{R}_1$ implies that

$$\begin{aligned}
&\hat{J}_K(k, x, u_N^*) + \hat{V}_{N-K}(k + K, x^*(k + K)) \\
&= \hat{J}_K(k, x, u_N^*) + \hat{V}_{N-K}(k + K, x_{u_N^*}(K, x)) - R_2(k, x, K, N) \\
&\leq \hat{J}_K(k, x, u_\infty^*) + \hat{V}_{N-K}(k + K, x_{u_\infty^*}(K, x)) - R_2(k, x, K, N) \\
&= \hat{J}_K(k, x, u_\infty^*) + \hat{V}_{N-K}(k + K, x^*(k + K)) + \tilde{R}_1(k, x, K, N) - R_2(k, x, K, N),
\end{aligned}$$

i.e. we have

$$\hat{J}_K(k, x, u_N^*) \leq \hat{J}_K(k, x, u_\infty^*) + \tilde{R}_1(k, x, K, N) - R_2(k, x, K, N) \tag{4.17}$$

for all $K \in \{0, \ldots, N\} \setminus (\mathcal{Q}(k, x, P, N) \cup \mathcal{Q}(k, x, P, \infty))$.

To show the converse inequality consider $R_1(k, x, K) = \hat{V}_\infty(k+K, x_{u_\infty^*}(K, x))$ from Lemma 4.14 (a) for which we obtained the bound $|R_1(k, x, K)| \le \omega_V(\rho(P))$ for $K \in \mathbb{N}_0 \setminus \mathcal{Q}(k, x, P, \infty)$, and define $\tilde{R}_2(k, x, K, N) := \hat{V}_\infty(k + K, x_{u_N^*}(K, x))$ for which the bound $\tilde{R}_2(k, x, K, N) \le \omega_V(\sigma(P))$ holds, given that $K \in \{0, \ldots, N\} \setminus \mathcal{Q}(k, x, P, N)$.

The infinite horizon dynamic programming principle (Theorem 4.3) implies

$$\hat{J}_K(k, x, u_\infty^*) + \hat{V}_\infty(k + K, x_{u_\infty^*}(K, x)) \le \hat{J}_K(k, x, u_N^*) + \hat{V}_\infty(k + K, x_{u_N^*}(K, x))$$

from which we get that

$$
\begin{aligned}
\hat{J}_K(k, x, u_\infty^*) &= \hat{J}_K(k, x, u_\infty^*) + \hat{V}_\infty(k + K, x_{u_\infty^*}(K, x)) - R_1(k, x, K) \\
&\le \hat{J}_K(k, x, u_N^*) + \hat{V}_\infty(k + K, x_{u_N^*}(K, x)) - R_1(k, x, K) \\
&= \hat{J}_K(k, x, u_N^*) + \tilde{R}_2(k, x, K, N) - R_1(k, x, K).
\end{aligned}
$$

In summary, we have

$$\hat{J}_K(k, x, u_\infty^*) \le \hat{J}_K(k, x, u_N^*) + \tilde{R}_2(k, x, K, N) - R_1(k, x, K) \tag{4.18}$$

for all $K \in \{0, \ldots, N\} \setminus (\mathcal{Q}(k, x, P, N) \cup \mathcal{Q}(k, x, P, \infty))$.

Combining the two inequalities (4.17) and (4.18) we obtain

$$
\begin{aligned}
|R_3(k, x, K, N)| &= |\hat{J}_K(k, x, u_N^*) - \hat{J}_K(k, x, u_\infty^*)| \\
&\le \max\{|\tilde{R}_1(k, x, K, N)| + |R_2(k, x, K, N)|, |\tilde{R}_2(k, x, K, N)| + |R_1(k, x, K)|\} \\
&= \max\{\gamma_V(N - K, \rho(P)) + \gamma_V(N - K, \sigma(P)), \omega_V(\sigma(P)) + \omega_V(\rho(P))\} \\
&\le \gamma_V(N - K, \rho(P)) + \gamma_V(N - K, \sigma(P)) + \omega_V(\sigma(P)) + \omega_V(\rho(P))
\end{aligned}
$$

which concludes the proof.

$\square$

The following theorem gives an estimate of how the closed-loop cost of the MPC trajectory compares to the best possible cost of a solution to the problem on an infinite horizon.

Theorem 4.16

Let Assumptions 4.10, 4.11 and 4.12 hold. Then for each $k \in \mathbb{N}_0$, and each sufficiently large N, the closed-loop cost satisfies

$$\hat{J}_L^{cl}(k, x, \mu_N) \le \hat{V}_\infty(k, x) - \hat{V}_\infty(k + L, x_{\mu_N}(L, x)) + L\delta(N) \tag{4.19}$$

with a function $\delta \in \mathcal{L}$.

Proof. Let $k \in \mathbb{N}_0$. For $i \ge k$ pick $x \in \mathbb{X}(i)$ and abbreviate $x^+ := f(i, x, \mu_N(i, x))$. By the dynamic programming principle (cf. Theorem 4.2), and the definition of μ_N we know that

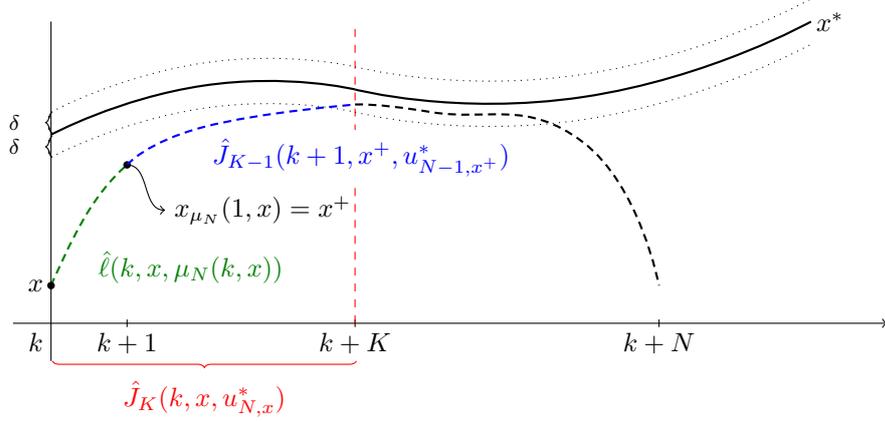$$\hat{\ell}(i, x, \mu_N(i, x)) = \hat{V}_N(i, x) - \hat{V}_{N-1}(i + 1, x^+). \tag{4.20}$$

Figure 4.6: Graphical illustration of equations (4.20) and (4.21) from the proof of Theorem 4.16.

Using the definition of the optimal value function and the fact that $u_{N,x}^*(\cdot + 1)$ and $u_{N-1,x^+}^*(\cdot)$ coincide we obtain

$$
\begin{aligned}
\hat{V}_N(i,x) - \hat{V}_{N-1}(i+1,x^+) &= \hat{J}_N(i,x,u_{N,x}^*) - \hat{J}_{N-1}(i+1,x^+,u_{N-1,x^+}^*) \\
&= \hat{J}_K(i,x,u_{N,x}^*) - \hat{J}_{K-1}(i+1,x^+,u_{N-1,x^+}^*),
\end{aligned}
\tag{4.21}
$$

which holds for each $K = \{1,\ldots,N\}$ (see also Figure 4.6 for a graphical illustration of this relation).

Now let $K \in \{1,\ldots,N\}$ such that $K \notin \mathcal{Q}(i,x,P,N) \cup \mathcal{Q}(i,x,P,\infty)$ and $K-1 \notin \mathcal{Q}(i+1,x^+,P,N-1) \cup \mathcal{Q}(i+1,x^+,P,\infty)$. In each of the four sets there are at most P elements, thus for $N > 8P$ there is at least one such K with $K \le \frac{N}{2}$, i.e. we set $P = \lfloor \frac{N-1}{8} \rfloor$ and choose N sufficiently large.

This means we can apply Lemma 4.15 twice with $K = K$, $N = N$ and $K = K-1$, $N = N-1$, respectively, to conclude that

$$
\hat{J}_K(i,x,u_{N,x}^*) - \hat{J}_{K-1}(i+1,x^+,u_{N-1,x^+}^*)
$$
$$
= \hat{J}_K(i,x,u_{\infty,x}^*) - \hat{J}_{K-1}(i+1,x^+,u_{\infty,x^+}^*) - R_3(i,x,K,N) + R_3(i+1,x^+,K-1,N-1).
$$

Proceeding further, by applying Lemma 4.14 (a) for $K = K$ and $K = K-1$ we conclude that

$$
\begin{aligned}
\hat{J}_K(i,x,u_{\infty,x}^*) &- \hat{J}_{K-1}(i+1,x^+,u_{\infty,x^+}^*) \\
&= \hat{V}_\infty(i,x) - \hat{V}_\infty(i+1,x^+) - R_1(i,x,K) + R_1(i+1,x^+,K-1).
\end{aligned}
$$

In summary, we have

$$
\hat{\ell}(i,x,\mu_N(i,x)) = \hat{V}_\infty(i,x) - \hat{V}_\infty(i+1,x^+) + R_4(i,x,K,N),
\tag{4.22}
$$

with

$$R_4(i, x, K, N) = -R_3(i, x, K, N) + R_3(i + 1, x^+, K - 1, N - 1) - R_1(i, x, K)$$
$$+ R_1(i + 1, x^+, K - 1).$$

In addition, from Lemma 4.15 and Lemma 4.14 (a) together with the monotonicity of γ_V we obtain the bound

$$|R_4(i, x, K, N)| \leq 2\gamma_V(N - K, \rho(P)) + 4\omega_V(\rho(P)) + 2\gamma_V(N - K, \sigma(P)) + 2\omega_V(\sigma(P)). \tag{4.23}$$

Recall that for $P = \lfloor \frac{N-1}{8} \rfloor$ we have $K \leq \frac{N}{2}$ and thus $N - K \geq \frac{N}{2}$. Because of the monotonicity of γ_V in its first argument, we can bound the right hand side of (4.23) by

$$|R_4(i, x, K, N, S)| \leq 2\gamma_V(\lfloor \frac{N}{2} \rfloor, \rho(\lfloor \frac{N-1}{8} \rfloor)) + 2\gamma_V(\lfloor \frac{N}{2} \rfloor, \sigma(\lfloor \frac{N-1}{8} \rfloor)) + 2\omega_V(\sigma(\lfloor \frac{N-1}{8} \rfloor))$$
$$+ 4\omega_V(\rho(\lfloor \frac{N-1}{8} \rfloor))$$
$$=: \quad \delta(N). \tag{4.24}$$

Finally, note that equation (4.22) was shown for all $i \geq k$, which means we can apply it to $\hat{J}_L^{cl}(k, x, \mu_N)$ with $i = k + j$, $x = x_{\mu_N}(j, x)$, and in each summand the estimate (4.24) holds. This yields

$$\hat{J}_L^{cl}(k, x, \mu_N) = \sum_{j=0}^{L-1} \hat{\ell}(k + j, x_{\mu_N}(j, x), \mu_N(k + j, x_{\mu_N}(j, x)))$$

$$= \sum_{j=0}^{L-1} \hat{V}_\infty(k + j, x_{\mu_N}(j, x)) - \hat{V}_\infty(k + j + 1, x_{\mu_N}(j + 1, x)) + \underbrace{R_4(k + j, x_{\mu_N}(j, x), K, N)}_{\leq \delta(N)}$$

$$\leq \hat{V}_\infty(k, x) - \hat{V}_\infty(k + L, x_{\mu_N}(L, x)) + L\delta(N)$$

and thus the assertion. □

The result from this theorem states that on finite horizons L the MPC closed-loop trajectory approximates an infinite horizon overtaking optimal trajectory. We will clarify this in the following by giving two different interpretations of the result.

The first interpretation considers a composite trajectory and shows that it is approximately an overtaking optimal trajectory. For an initial state x_0 at time k consider the control sequence $\bar{u}$ consisting for the first L steps of the MPC feedback solution and after that of the solution of the infinite horizon problem starting in $\tilde{x} = x_{\mu_N}(L, x_0)$ at time $k + L$:

$$\bar{u}(j) := \begin{cases} \mu_N(k + j, x_{\mu_N}(j, x_0)), & j = 0, \ldots, L - 1 \\ u^*_{\infty, \tilde{x}}(j), & j \geq L. \end{cases}$$

An illustration of the resulting trajectories resulting from this control sequence is depicted in Figure 4.7, together with an infinite horizon optimal state trajectory. The cost of the
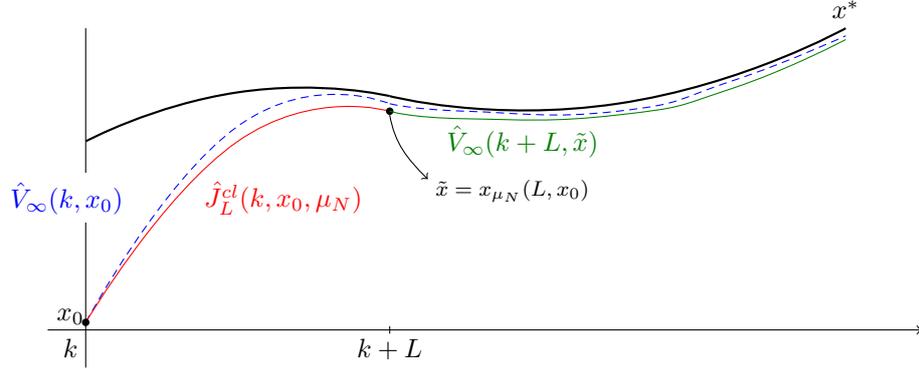
Figure 4.7: Illustration of trajectory resulting form constructed control sequence $\bar{u}$ (composed of the red and green trajectories) together with an infinite horizon optimal trajectory (shown in blue).

trajectory corresponding to $\bar{u}$ is given by

$$\hat{J}_\infty(k, x_0, \bar{u}) = \sum_{j=0}^\infty \hat{\ell}(k+j, x_{\bar{u}}(j, x_0), \bar{u}(j))$$

$$= \underbrace{\hat{J}_L^{cl}(k, x_0, \mu_N)}_{\leq \hat{V}_\infty(k, x_0) - \hat{V}_\infty(k+L, \tilde{x}) + L\delta(N)} + \hat{V}_\infty(k+L, \tilde{x})$$

$$\leq \hat{V}_\infty(k, x_0) + L\delta(N).$$

Because $\hat{V}_\infty(k, x_0) = \hat{J}_\infty(k, x_0, u^*_{\infty, x_0})$ this is equivalent to

$$L\delta(N) \geq \sum_{j=0}^\infty \hat{\ell}(k+j, x_{\bar{u}}(j, x_0), \bar{u}(j)) - \sum_{j=0}^\infty \hat{\ell}(k+j, x_{u^*_{\infty, x_0}}(j, x_0), u^*_{\infty, x_0}(j))$$

$$\Leftrightarrow \quad \sum_{j=0}^\infty \hat{\ell}(k+j, x_{u^*_{\infty, x_0}}(j, x_0), u^*_{\infty, x_0}(j)) - \sum_{j=0}^\infty \hat{\ell}(k+j, x_{\bar{u}}(j, x_0), \bar{u}(j)) \geq -L\delta(N).$$

From this inequality and the definition of $\hat{\ell}$ it follows that

$$\liminf_{K \to \infty} \left(\sum_{j=0}^{K-1} \ell(k+j, x_{u^*_{\infty, x_0}}(j, x_0), u^*_{\infty, x_0}(j)) - \ell(k+j, x_{\bar{u}}(j, x_0), \bar{u}(j)) \right) \geq -L\delta(N).$$

This means that in terms of the overtaking optimality criterion the initial piece of the MPC closed-loop trajectory approximates the initial piece of the optimal trajectory $x_{u^*_{\infty, x_0}}(\cdot, x_0)$. An alternative interpretation of Theorem 4.16 is provided in the following corollary.

Corollary 4.17
Let $k \in \mathbb{N}_0$ and $x \in \mathbb{X}(k)$ and let the assumptions of Theorem 4.16 hold. Then for each

$N \in \mathbb{N}$ *the MPC closed-loop trajectory is an approximately overtaking optimal trajectory in the sense that the inequality*

$$\liminf_{L \to \infty} \left(\sum_{j=0}^{L-1} \left(\ell(k+j, x_u(j,x), u(j)) - \ell(k+j, x_{\mu_N}(j,x_0), \mu_N(k+j, x_{\mu_N}(j,x_0))) \right) + L\delta(N) \right) \geq 0$$
(4.25)

holds for all $u \in \mathbb{U}^\infty(k,x)$.

Proof. From closed-loop cost estimate (4.19) of Theorem 4.16 and the fact that $\hat{V}_\infty(k+L, x_{\mu_N}(L,x)) \geq 0$ (cf. (4.12)) it follows that

$$\hat{J}_L^{cl}(k,x,\mu_N) \leq \hat{V}_\infty(k,x) + L\delta(N).$$
(4.26)

By inserting the definition of the closed-loop cost and replacing the infinite horizon optimal value function $\hat{V}_\infty(k,x)$ by $\lim_{M \to \infty} \sum_{j=0}^{M-1} \hat{\ell}(k+j, x_{u_\infty^*}(j,x), u_\infty^*(j))$ we obtain:

$$\lim_{M \to \infty} \left(\sum_{j=0}^{M-1} \hat{\ell}(k+j, x_{u_\infty^*}(j,x), u_\infty^*(j)) \right) - \sum_{j=0}^{L-1} \hat{\ell}(k+j, x_{\mu_N}(j,x_0), \mu_N(k+j, x_{\mu_N}(j,x_0))) + L\delta(N) \geq 0.$$
(4.27)

Since this inequality holds for all L it remains true if we take the $\liminf_{L \to \infty}$ (note that the first term in the above inequality is independent of L):

$$\lim_{M \to \infty} \left(\sum_{j=0}^{M-1} \hat{\ell}(k+j, x_{u_\infty^*}(j,x), u_\infty^*(j)) \right)$$
$$+ \liminf_{L \to \infty} \left(-\sum_{j=0}^{L-1} \hat{\ell}(k+j, x_{\mu_N}(j,x_0), \mu_N(k+j, x_{\mu_N}(j,x_0))) + L\delta(N) \right) \geq 0.$$
(4.28)

Applying the computation rules for the $\liminf$ from Lemma A.1 in the appendix it follows that

$$\liminf_{L \to \infty} \left(\sum_{j=0}^{L-1} \left(\hat{\ell}(k+j, x_{u_\infty^*}(j,x), u_\infty^*(j)) - \hat{\ell}(k+j, x_{\mu_N}(j,x_0), \mu_N(k+j, x_{\mu_N}(j,x_0))) \right) + L\delta(N) \right) \geq 0.$$
(4.29)

By the definition of the shifted stage cost function (Definition 4.8) this is equivalent to:

$$\liminf_{L \to \infty} \left(\sum_{j=0}^{L-1} \left(\ell(k+j, x_{u_\infty^*}(j,x), u_\infty^*(j)) - \ell(k+j, x_{\mu_N}(j,x_0), \mu_N(k+j, x_{\mu_N}(j,x_0))) \right) + L\delta(N) \right) \geq 0.$$
(4.30)

Let $u \in \mathbb{U}^\infty(k,x)$ denote an arbitrary infinite horizon control sequence. Because u_∞^* is an overtaking optimal trajectory, the inequality

$$\liminf_{L \to \infty} \left(\sum_{j=0}^{L-1} \ell(k+j, x_u(j,x_0), u(j)) - \ell(k+j, x_{u_\infty^*}(j,x), u_\infty^*(j)) \right) \geq 0$$
(4.31)

holds. Finally, applying Lemma A.2 to the two inequalities (4.30) and (4.31) yields the inequality

$$\liminf_{L \to \infty} \left(\sum_{j=0}^{L-1} \left(\ell(k+j, x_u(j,x_0), u(j)) - \ell(k+j, x_{u_\infty^*}(j,x), u_\infty^*(j)) + \ell(k+j, x_{u_\infty^*}(j,x), u_\infty^*(j)) \right. \right.$$
$$\left. \left. -\ell(k+j, x_{\mu_N}(j,x_0), \mu_N(k+j, x_{\mu_N}(j,x_0)))) + L\delta(N) \right) \geq 0 \right.$$

$$(4.32)$$

which simplifies to

$$\liminf_{L \to \infty} \left(\sum_{j=0}^{L-1} \left(\ell(k+j, x_u(j,x_0), u(j)) - \ell(k+j, x_{\mu_N}(j,x_0), \mu_N(k+j, x_{\mu_N}(j,x_0))) \right) + L\delta(N) \right) \geq 0.$$

$$(4.33)$$

This concludes the proof. $\qquad\square$

Ideally, we would have a result that states that the MPC closed loop trajectory is an overtaking optimal trajectory, i.e. that

$$\liminf_{L \to \infty} \left(\sum_{j=0}^{L-1} \left(\ell(k+j, x_u(j,x_0), u(j)) - \ell(k+j, x_{\mu_N}(j,x_0), \mu_N(k+j, x_{\mu_N}(j,x_0))) \right) \right) \geq 0.$$

$$(4.34)$$

holds. Although it is not exactly (4.34), the corollary at least shows that the MPC closed loop trajectory satisfies the overtaking optimality criterion if we include the additional term $L\delta(N)$.

4.4.2 Averaged performance

At first glance, it may appear that the error term $L\delta(N)$ from the performance estimate in Theorem 4.16 causes the performance to deteriorate if the MPC algorithm is run for large times L. However, if we analyze the averaged closed-loop cost functionals

$$\bar{J}_L^{cl}(k, x, u) := \frac{1}{L} J_L^{cl}(k, x, u) \tag{4.35}$$

along the closed-loop it becomes obvious that the situation is not quite as bad: from (4.19) and the fact that $\hat{V}_\infty(k+L, x_{\mu_N}(L,x)) \geq 0$ we get

$$\hat{J}_L^{cl}(k, x, \mu_N) \leq \hat{V}_\infty(k, x) + L\delta(N)$$

or equivalently

$$\frac{1}{L} \hat{J}_L^{cl}(k, x, \mu_N) \leq \frac{1}{L} \hat{V}_\infty(k, x) + \delta(N). \tag{4.36}$$

Consider the average performance of the optimal trajectory starting at time k

$$\bar{J}_L^*(k) := \frac{1}{L} \sum_{j=0}^{L-1} \ell(k+j, x^*(k+j), u^*(k+j)). \tag{4.37}$$

Then from the definition of the shifted stage cost together with (4.35) and (4.37) for the left-hand side of inequality (4.36) we obtain

$$\frac{1}{L} \hat{J}_L^{cl}(k, x, \mu_N) = \frac{1}{L} \sum_{j=0}^{L-1} \ell(k, x_{\mu_N}(j, x), \mu_N(k+j, x_{\mu_N}(j, x)) - \ell(k+j, x^*(k+j), u^*(k+j))$$

$$= \bar{J}_L^{cl}(k, x, \mu_N) - \bar{J}_L^*(k)$$

Thus, inequality (4.36) is equivalent to

$$\bar{J}_L^{cl}(k, x, \mu_N) \le \bar{J}_L^*(k) + \frac{1}{L} \hat{V}_\infty(k, x) + \delta(N).$$

Taking the $\limsup_{L\to\infty}$ yields

$$\limsup_{L\to\infty} \bar{J}_L^{cl}(k, x, \mu_N) \le \limsup_{L\to\infty} \bar{J}_L^*(k) + \delta(N).$$

Thus, for sufficiently long horizons the average cost of the MPC closed-loop is approximately the same as the average cost of the trajectory of optimal operation. This demonstrates that in this averaged sense the closed-loop performs well on arbitrarily long time horizons.

The following example illustrates the results presented so far.

Example 4.18 (Cost convergence for scalar example)
Consider the system

$$x(k+1) = x(k) + u(k) + w(k)$$

where $w(k) = -2\sin(\frac{k\pi}{12}) + a_k$ and $(a_k)_{k\in\mathbb{N}_0} \subset [-\frac{1}{4}, \frac{1}{4}]$ is a sequence of random numbers. Let

$$\mathbb{X}(k) = \begin{cases} [-2, 2], & \text{for } k \in [24j, 24j+12), \\ [-\frac{1}{2}, \frac{1}{2}], & \text{for } k \in [24j+12, 24(j+1)), \end{cases} \quad j \in \mathbb{N}_0, \tag{4.38}$$

and let $\mathbb{U}(k) = [-3, 3]$, $k \in \mathbb{N}_0$. The goal in this example is to keep the state x within the set $\mathbb{X}(k)$ with minimal control effort. We thus use the stage cost $\ell(k, x, u) = u^2$.
The setting could be interpreted as keeping the temperature of a room within a certain range while spending as little energy as possible. In this setting, the sequence $w(k)$ would correspond to influence of the time-varying outside temperature, which can be predicted.
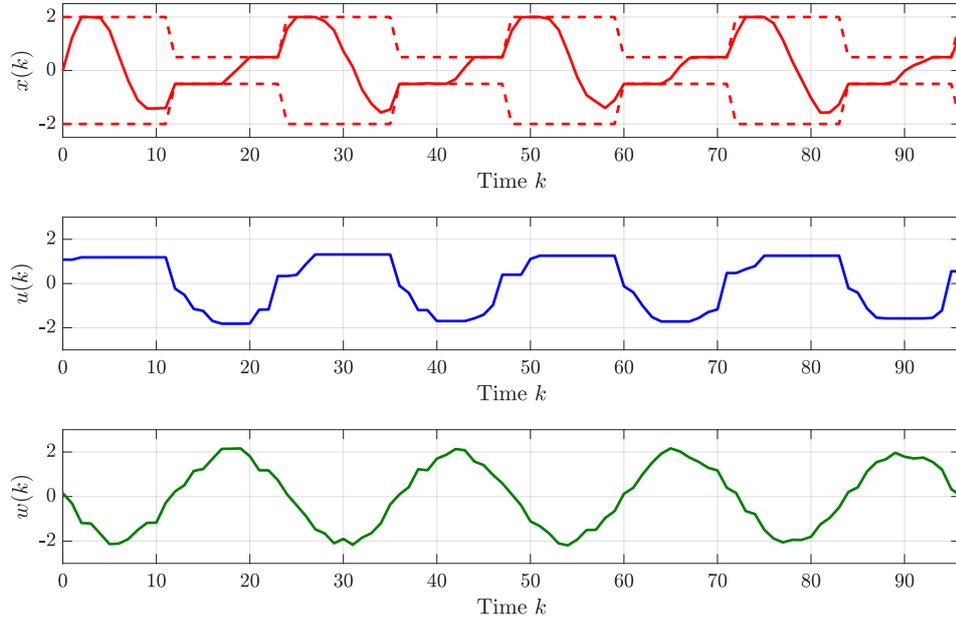
Figure 4.8: MPC solution starting from the initial state $x(0) = 0$ for a horizon length of $N = 10$.

Figure 4.8 shows in red the closed-loop solution of the economic MPC algorithm, as well as the corresponding control sequence in blue and the time-varying sequence w in green. Obviously, the state remains within the constraints.

Next, Figure 4.9 illustrates how the closed-loop cost evolves as the simulation time L is increased. The different colors represent the cumulative cost for different MPC horizons N. First of all, it is noticeable that the closed-loop costs grow indefinitely as L increases. Although initially, the cost can be lower for short horizons, ultimately longer horizons will lead to a lower overall cost. One could say that the long horizons overtake the short horizons at some point, which in a way indicates the connection to overtaking optimality. In addition, looking at the gap between the different lines the figure confirms that the error term $L\delta(N)$ evolves linearly in L and decreases as the horizon N is increased (cf. Theorem 4.16).

In Figure 4.10 the final value at $k = 96$ of the closed-loop cost from Figure 4.9 for the different MPC horizons N is shown. For increasing horizon the closed-loop cost $J_{96}(0, 0, \mu_N)$ converges to some value, according to our theory to the (unknown) value of the initial piece of the infinite horizon optimal trajectory, i.e. $J_{96}(0, 0, u_\infty^*)$.

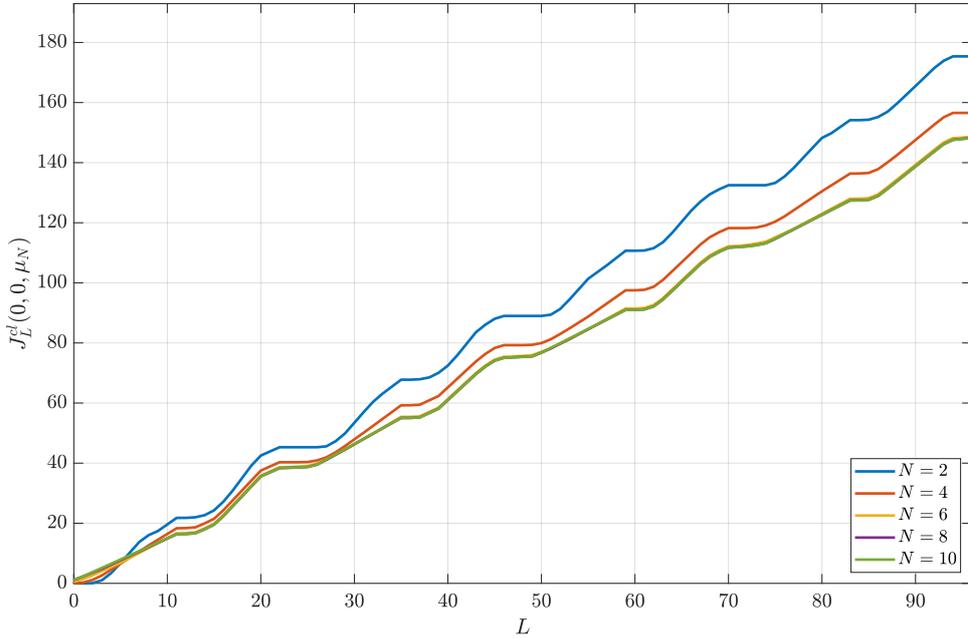*Thus, the numerical simulations from the example confirm our theoretical results from the*

Figure 4.9: Cumulative closed-loop cost for increasing simulation horizon L and different MPC horizon lengths N.

first part of this chapter.

4.5   Trajectory convergence

So far we only derived estimates for the *cost* of the MPC closed-loop trajectory. Now we turn our attention to the trajectories themselves. We want to investigate under what conditions they will converge to the optimal trajectory (x^*, u^*).

The way to formalize this is by using the notion of $\mathbb{P}$-practical asymptotic stability which we will introduce below. For proving convergence we will then show the existence of a Lyapunov function using a construction relying on modified costs and a dissipation inequality. In this regard, the approach bears resemblance to the stability proofs for time-invariant MPC in Chapter 8 of [50]. However, the arguments needed to be modified to account for the time-variance in the problem.

4.5.1   Stability notion

For the definition of stability, we substitute the feedback for the control in system (4.1), i.e. we consider the feedback-controlled system

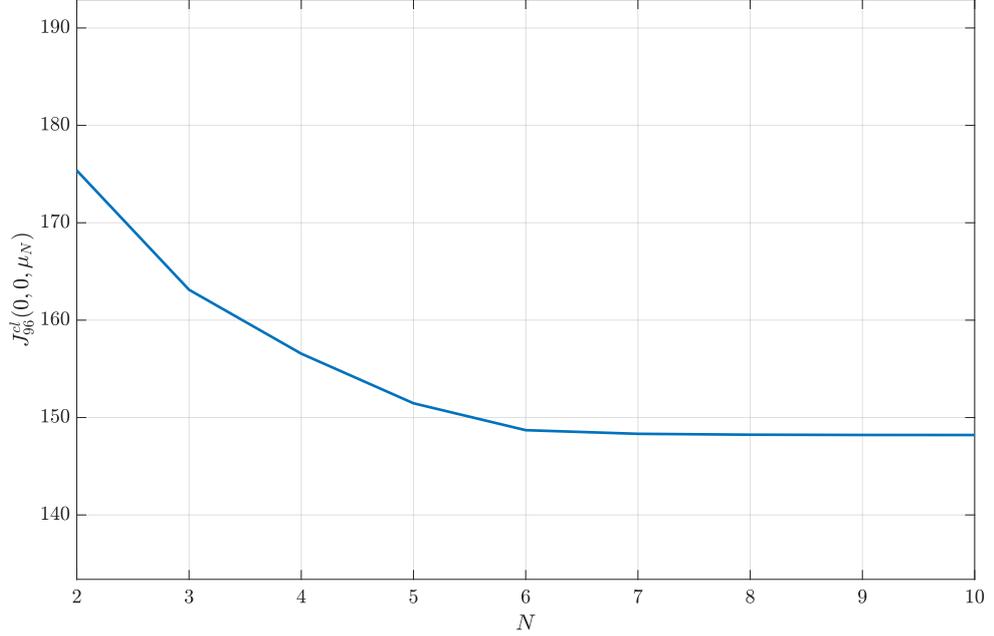$$x^+ = f(k, x, \mu_N(k, x)) =: g(k, x). \tag{4.39}$$

Figure 4.10: Closed-loop cost for Example 4.18 for different MPC horizon lengths N.

The following definitions and the theorem are taken from [50].

Definition 4.19 (Forward invariance)
We say a family of sets $Y(k) \subseteq X$, $k \in \mathbb{N}_0$ is forward invariant if $g(k, x) \in Y(k+1)$ for all $k \in \mathbb{N}_0$ and all $x \in Y(k)$.

Definition 4.20 (Uniform $\mathbb{P}$-practical asymptotic stability, [50, Definition 2.17])
Let $Y(k)$ be a forward invariant family of sets and let $\mathbb{P}(k) \subset Y(k)$ be subsets of $Y(k)$. Then we say that a trajectory x^* with $x^*(k) \in Y(k)$ is $\mathbb{P}$-practically uniformly asymptotically stable on $Y(k)$ if there exists $\beta \in \mathscr{KL}$ such that

$$|x(k; k_0, x_0)|_{x^*(k)} \leq \beta(|x_0|_{x^*(k_0)}, k - k_0) \tag{4.40}$$

holds for all $x_0 \in Y(k_0)$ and all k_0, $k \in \mathbb{N}_0$ with $k \geq k_0$ and $x(k; k_0, x_0) \notin \mathbb{P}(k)$.

A graphical illustration of Definition 4.20 can be found in Figure 4.11. The definition demands that it is possible to put a bound on the distance between the state trajectory $x(\cdot; k_0, x_0)$ and the optimal trajectory x^*. The bound depends on the initial distance of the two trajectories $|x_0|_{x^*(k_0)}$ as well as the elapsed time $k - k_0$. Since β is a $\mathscr{KL}$ function the bound on the distance continually decreases for increasing time k, at least until the trajectory enters the sets $\mathbb{P}(k)$ where it then remains.
A way to prove uniform asymptotic stability is to ensure the existence of a Lyapunov function defined as follows.
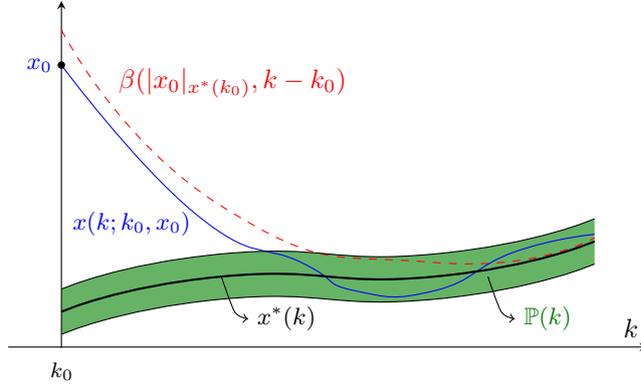
Figure 4.11: Schematic illustration of $\mathbb{P}$-practical asymptotic stability.

Definition 4.21 (Uniform time-varying Lyapunov function, [50, Definition 2.21])
Let subsets $S(k) \subseteq X$ and define $\mathcal{S} := \{(k,x) | k \in \mathbb{N}_0, x \in S(k)\}$. A function $V : \mathcal{S} \to \mathbb{R}_0^+$ is called uniform time-varying Lyapunov function on $S(k)$ if the following conditions are satisfied:

1. *There exist functions $\alpha_1, \alpha_2 \in \mathcal{K}_\infty$ such that*

$$\alpha_1(|x|_{x^*(k)}) \leq V(k,x) \leq \alpha_2(|x|_{x^*(k)}) \tag{4.41}$$

   holds for all $k \in \mathbb{N}_0$ and all $x \in S(k)$.

2. *There exists a function $\alpha_V \in \mathcal{K}$ such that*

$$V(k+1, g(k,x)) \leq V(k,x) - \alpha_V(|x|_{x^*(k)}) \tag{4.42}$$

   holds for all $k \in \mathbb{N}_0$ and all $x \in S(k)$ with $g(k,x) \in S(n+1)$.

Inequality (4.42) from the previous definition essentially states that a Lyapunov function decays along the solution trajectory of the system. This can be combined with the first two inequalities in (4.41) to conclude that also the solution trajectory itself converges to the trajectory x^*. In other words, the existence of a Lyapunov function guarantees asymptotic stability as stated in the following theorem.

Theorem 4.22 (Lyapunov function implies $\mathbb{P}$-practical asymptotic stability, [50, Theorem 2.23])
Consider forward invariant families of sets $Y(k)$ and $\mathbb{P}(k) \subset Y(k)$, $k \in \mathbb{N}_0$, and $x^*(k) \in \mathbb{P}(k)$. If there exists a uniform time-varying Lyapunov function V on $S(k) = Y(k) \setminus \mathbb{P}(k)$ then x^* is uniformly $\mathbb{P}$-practically asymptotically stable on $Y(k)$.

4.5.2   Construction of a Lyapunov function based on modified costs

In this section, we will show that a modified optimal value function related to the optimal value function of the original MPC problem is a Lyapunov function for the feedback-controlled system. This will then allow us to conclude convergence of the MPC closed-loop trajectory to an optimal trajectory.

An essential assumption we impose is strict dissipativity of the system as introduced in the following.

Assumption 4.23 (Strict dissipativity)
The system (4.1) is strictly dissipative with respect to the supply rate $s(k, x, u) = \hat{\ell}(k, x, u)$ and the optimal trajectory (x^*, u^*), i.e. there exists a storage function $\lambda : \mathbb{N}_0 \times X \to \mathbb{R}$ bounded from below on X and $\alpha \in \mathscr{K}_\infty$ such that the inequality

$$\lambda(k + 1, f(k, x, u)) - \lambda(k, x) \leq s(k, x, u) - \alpha(|(x, u)|_{(x^*(k), u^*(k))}) \tag{4.43}$$

holds for all $k \in \mathbb{N}_0$ and all $(x, u) \in \mathbb{X}(k) \times \mathbb{U}(k, x)$.

Remark 4.24 (Relevance of dissipativity theory)
Dissipativity was first introduced by Willems in the two pioneering works [106] and [107]. The classical definition considers dissipativity with respect to equilibria. In our setting we replace the equilibrium by an optimal trajectory in Assumption 4.23.
For our purposes, dissipativity is applied mainly as a tool for the construction of a Lyapunov function in order to prove asymptotic stability of the MPC closed-loop trajectory. Beyond that, dissipativity is a widely used concept in many areas of control theory. Applications of dissipativity include controller synthesis and feedback design [29] or classification of a system's regime of optimal operation [28]. Moreover, there exists a strong connection between dissipativity and the turnpike property [45, 48]. We will explore this connection for time-varying systems in more detail in the next chapter.
Finally, for many systems, the storage function and the supply rate carry a physical interpretation because they describe the amount of "energy" currently stored in the system and the amount that is fed to the system from the outside. ◇

Remark 4.25 (Alternative versions of dissipativity)
Other notions of dissipativity than the one introduced in Assumption 4.23 have been proposed by Müller [81]. It is argued that in the time-varying setting there may not exist a single distinct optimal trajectory but a whole set of optimal trajectories. The dissipativity notion should account for this by defining the dissipativity margin α in such a way that it treats all the possible optimal trajectories equally. For periodic orbits (where orbits with shifted phase can be regarded equivalent) this was explored in [84] by considering the distance of all points $(\tilde{x}, \tilde{u})$ of a P-step trajectory to the optimal orbit Π.
In the more general non-periodic case comparable results do not yet exist. However, it is conjectured (see [82]) that a promising extension of the dissipation inequality (4.43) could

take the shape

$$\lambda(k+1, f(k,x,u)) - \lambda(k,x) \leq s(k,x,u) - \alpha(|(x,u)|_{\Omega(k)}) \qquad (4.44)$$

in which

$$\Omega(k) := \{(x,u) \in \mathbb{X}(k) \times \mathbb{U}(k) : \exists \; an \; optimal \; trajectory \; (x^*(\cdot), u^*(\cdot))$$
$$s.t. \; x^*(k) = x \; and \; u^*(k) = u\} \qquad (4.45)$$

is the set of all points located on an optimal trajectory at time k.
In this work, we will use the version introduced above, which presents a more straight-forward extension to the classical dissipativity notion of Willems [106]. However, there certainly is potential for generalizing our results in this regard. $\diamond$

Using the storage function λ from Assumption 4.23 we introduce a modified MPC stage cost and cost functional.

Definition 4.26 (Modified MPC cost functional)
Consider the modified stage cost $\tilde{\ell}$ given by

$$\tilde{\ell}(k,x,u) := \hat{\ell}(k,x,u) + \lambda(k,x) - \lambda(k+1, f(k,x,u)). \qquad (4.46)$$

The modified MPC cost functional is defined as

$$\tilde{J}_N(k,x,u) := \sum_{j=0}^{N-1} \tilde{\ell}(k+j, x_u(j;k,x), u(j)). \qquad (4.47)$$

Correspondingly, we define a modified MPC problem and the modified optimal value function.

Definition 4.27 (Modified MPC optimal control problem)
We consider the modified MPC problem

$$\min_{u \in \mathbb{U}^N(k,x)} \tilde{J}_N(k,x,u) \qquad (4.48)$$

and the corresponding modified optimal value function

$$\tilde{V}_N(k,x) := \inf_{u \in \mathbb{U}^N(k,x)} \tilde{J}_N(k,x,u). \qquad (4.49)$$

We denote the optimal control sequence corresponding to the solution of (4.48) by $\tilde{u}_N^*$.

Below we will make several assumptions for this modified problem in order to facilitate the proofs. In addition to the turnpike property for the original MPC problem from Assumption 4.10, we demand that the *modified* problem also has the turnpike property.

Assumption 4.28 (Turnpike property for the modified MPC problem)
The modified optimal control problem from Definition 4.27 has the turnpike property. For the modified problem we will denote the set Q by $\tilde{Q}$ and the bound σ by $\tilde{\sigma}$.

Moreover, we make two assumptions for the modified stage cost and the modified optimal value function.

Assumption 4.29 (Modified cost bounded from above)
We assume there exists $\alpha_u \in \mathscr{K}_\infty$ such that the modified stage cost satisfies

$$\tilde{\ell}(k, x, u) \leq \alpha_u(|(x, u)|_{(x^*(k), u^*(k))}) \tag{4.50}$$

for all $k \in \mathbb{N}_0$ and all $(x, u) \in \mathbb{X}(k) \times \mathbb{U}(k, x)$.

Assumption 4.30 (Continuity of $\tilde{V}_N$ at x^*)
We assume there exists $\gamma_{\tilde{V}}$ such that for each $k \in \mathbb{N}_0$, $N \in \mathbb{N}$ and $x \in \mathbb{X}$ the following holds

$$|\tilde{V}_N(k, x) - \tilde{V}_N(k, x^*(k))| \leq \gamma_{\tilde{V}}(|x|_{x^*(k)}) \tag{4.51}$$

In the next chapter, we will discuss in more detail why the above assumptions are meaningful and when they can be fulfilled.

Remark 4.31 (Modified cost along optimal trajectory)
From Assumptions 4.23 and 4.29 it follows that the modified cost along the optimal trajectory pair (x^*, u^*) satisfies

$$\tilde{\ell}(k, x^*(k), u^*(k)) = 0 \tag{4.52}$$

for all $k \in \mathbb{N}_0$. Note that this implies that

$$\tilde{V}_N(k, x^*(k)) = 0 \tag{4.53}$$

for all $k \in \mathbb{N}_0$ and for every $N \in \mathbb{N}$. $\diamond$

Remark 4.32 (Difference between different continuity assumptions)
Note the difference between the two continuity assumptions from Assumption 4.12 and Assumption 4.30. The continuity assumption for the modified problem is independent of the horizon N. $\diamond$

The following preparatory lemma shows that the initial cost (up to some time instant M) of two optimal trajectories with different horizon length of the modified problem is nearly identical.

Lemma 4.33
Let Assumptions 4.28 and 4.30 hold. Then

$$\tilde{J}_M(k, x, \tilde{u}_N^*) = \tilde{J}_M(k, x, \tilde{u}_{N+1}^*) + R_5(k, x, M, N)$$

where the error term satisfies $|R_5(k, x, M, N)| \leq 2\gamma_{\tilde{V}}(\tilde{\sigma}(P))$ for all $k \in \mathbb{N}_0$, all $N \in \mathbb{N}$, all $P \in \mathbb{N}$ sufficiently large, all $x \in \mathbb{X}(k)$ and all $M \in \{0, \ldots, N\} \setminus (\tilde{Q}(k, x, P, N) \cup \tilde{Q}(k, x, P, N + 1))$.

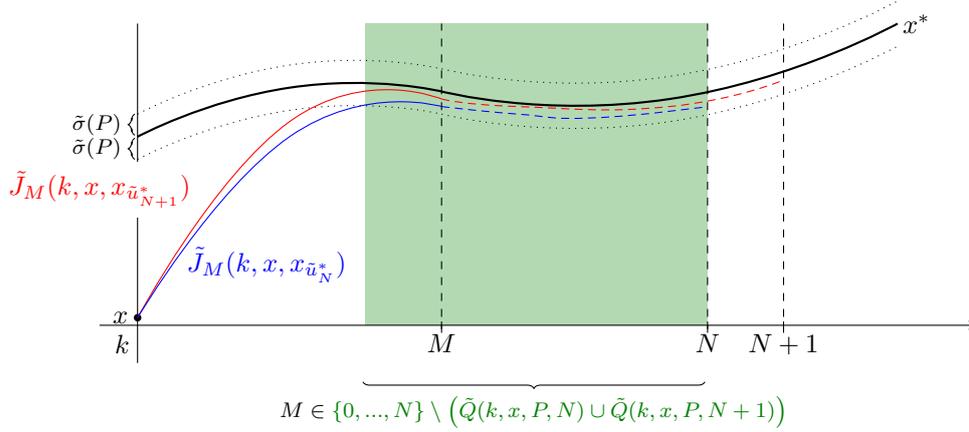$$M \in \{0, ..., N\} \setminus \left(\tilde{Q}(k, x, P, N) \cup \tilde{Q}(k, x, P, N+1) \right)$$

Figure 4.12: Illustration of Lemma 4.33

Proof. The intuition behind this proof is as follows. We consider two optimal control trajectories of different horizon length starting at the same initial state. Because of the turnpike assumption we know that both trajectories will at some point be close to the optimal trajectory as illustrated in Figure 4.12. At that point, we exploit the continuity property of $\tilde{V}_N$ to switch from one trajectory to the other without changing the overall cost too much.

More formally, let $\tilde{u}_N^*$ and $\tilde{u}_{N+1}^*$ denote the optimal solutions of problem (4.48) with horizon N and $N+1$, respectively. From the finite horizon dynamic programming principle (cf. Theorem 4.2) we obtain that $u = \tilde{u}_N^*$ is a minimizer of $\tilde{J}_M(k, x, u) + \tilde{V}_{N-M}(k + M, x_u(M, x))$. In particular it holds that

$$\tilde{J}_M(k, x, \tilde{u}_N^*) + \tilde{V}_{N-M}(k + M, x_{\tilde{u}_N^*}(M, x)) \leq \tilde{J}_M(k, x, \tilde{u}_{N+1}^*) + \tilde{V}_{N-M}(k + M, x_{\tilde{u}_{N+1}^*}(M, x)). \tag{4.54}$$

Now consider

$$R_1(k, x, M, N) := \tilde{V}_{N-M}(k + M, x_{\tilde{u}_N^*}(M, x)) - \tilde{V}_{N-M}(k + M, x^*(k + M))$$

and

$$R_2(k, x, M, N) := \tilde{V}_{N-M}(k + M, x_{\tilde{u}_{N+1}^*}(M, x)) - \tilde{V}_{N-M}(k + M, x^*(k + M)).$$

Inserting the definition of R_1 and R_2 into (4.54) we obtain

$$\tilde{J}_M(k, x, \tilde{u}_N^*) + \tilde{V}_{N-M}(k + M, x^*(k + M)) + R_1(k, x, M, N)$$
$$\leq \tilde{J}_M(k, x, \tilde{u}_{N+1}^*) + \tilde{V}_{N-M}(k + M, x^*(k + M)) + R_2(k, x, M, N)$$

which is equivalent to

$$\tilde{J}_M(k, x, \tilde{u}_N^*) \leq \tilde{J}_M(k, x, \tilde{u}_{N+1}^*) - R_1(k, x, M, N) + R_2(k, x, M, N). \tag{4.55}$$

The above equations are true for every $M \in \{0, \ldots, N\}$. For $M \in \{0, \ldots, N\} \backslash (\tilde{\bar{Q}}(k, x, P, N) \cup \tilde{\bar{Q}}(k, x, P, N+1))$ we know from Assumption 4.28 that $|(x_{\tilde{u}_N^*}(M, x), \tilde{u}_N^*(M))|_{(x^*(k+M), u^*(k+M))} \leq \tilde{\sigma}(P)$, and in particular $|x_{\tilde{u}_N^*}(M, x)|_{x^*(k+M)} \leq \tilde{\sigma}(P)$, i.e. we have a bound on the distance of $x_{\tilde{u}_N^*}(M, x)$ to the optimal trajectory x^*. Using Assumption 4.30 we obtain

$$|R_1(k, x, M, N)| \leq \gamma_{\tilde{V}}(\tilde{\sigma}(P)).$$

The same holds when considering the optimal trajectory $\tilde{u}_{N+1}^*$ yielding the estimate

$$|R_2(k, x, M, N)| \leq \gamma_{\tilde{V}}(\tilde{\sigma}(P)).$$

For the converse inequality we use the dynamic programming principle from Theorem 4.2 once more together with the fact that $u = \tilde{u}_{N+1}^*$ minimizes the expression $\tilde{J}_M(k, x, u) + \tilde{V}_{N+1-M}(k+M, x_u(M, x))$ which implies that

$$\tilde{J}_M(k, x, \tilde{u}_{N+1}^*) + \tilde{V}_{N+1-M}(k+M, x_{\tilde{u}_{N+1}^*}(M, x)) \leq \tilde{J}_M(k, x, \tilde{u}_N^*) + \tilde{V}_{N+1-M}(k+M, x_{\tilde{u}_N^*}(M, x)).$$

Defining

$$R_3(k, x, M, N) := \tilde{V}_{N+1-M}(k+M, x_{\tilde{u}_{N+1}^*}(M, x)) - \tilde{V}_{N+1-M}(k+M, x^*(k+M))$$

and

$$R_4(k, x, M, N) := \tilde{V}_{N+1-M}(k+M, x_{\tilde{u}_N^*}(M, x)) - \tilde{V}_{N+1-M}(k+M, x^*(k+M))$$

we can estimate

$$\tilde{J}_M(k, x, \tilde{u}_{N+1}^*) + \tilde{V}_{N+1-M}(k+M, x^*(k+M)) + R_3(k, x, M, N)$$
$$\leq \tilde{J}_M(k, x, \tilde{u}_N^*) + \tilde{V}_{N+1-M}(k+M, x^*(k+M)) + R_4(k, x, M, N)$$
$$\Leftrightarrow \tilde{J}_M(k, x, \tilde{u}_{N+1}^*) \leq \tilde{J}_M(k, x, \tilde{u}_N^*) - R_3(k, x, M, N) + R_4(k, x, M, N). \tag{4.56}$$

Analogously to the above discussion we obtain the bounds

$$|R_3(k, x, M, N)| \leq \gamma_{\tilde{V}}(\tilde{\sigma}(P))$$

and

$$|R_4(k, x, M, N)| \leq \gamma_{\tilde{V}}(\tilde{\sigma}(P))$$

for every $M \in \{0, \ldots, N\} \backslash (\tilde{\bar{Q}}(k, x, P, N) \cup \tilde{\bar{Q}}(k, x, P, N+1))$. Finally, combining the inequalities (4.55) and (4.56) leads to

$$|R_5(k, x, M, N)| = |\tilde{J}_M(k, x, \tilde{u}_N^*) - \tilde{J}_M(k, x, \tilde{u}_{N+1}^*)|$$
$$\leq \max\{|-R_1(k, x, M, N) + R_2(k, x, M, N)|, |-R_3(k, x, M, N) + R_4(k, x, M, N)|\}$$
$$\leq \max\{|R_1(k, x, M, N)| + |R_2(k, x, M, N)|, |R_3(k, x, M, N)| + |R_4(k, x, M, N)|\}$$
$$\leq \max\{2\gamma_{\tilde{V}}(\tilde{\sigma}(P)), 2\gamma_{\tilde{V}}(\tilde{\sigma}(P))\}$$
$$= 2\gamma_{\tilde{V}}(\tilde{\sigma}(P)).$$

This concludes the proof. $\qquad \square$

Using this result we can prove the following lemma, which states that the optimal value functions for the modified problem yield almost the same value for different horizons N and $N + 1$.

Lemma 4.34

Let Assumption 4.29 and those of Lemma 4.33 hold. Then the equation

$$\tilde{V}_{N+1}(k, x) = \tilde{V}_N(k, x) + R_6(k, x, M, N)$$

holds with $|R_6(k, x, M, N)| \leq 4\gamma_{\tilde{V}}(\tilde{\sigma}(P))$ for all $k \in \mathbb{N}_0$, all $N \in \mathbb{N}$, all $P \in \mathbb{N}$ sufficiently large, all $x \in \mathbb{X}(k)$ and all $M \in \{0, \ldots, N\} \setminus (\tilde{\tilde{\mathcal{Q}}}(k, x, P, N) \cup \tilde{\tilde{\mathcal{Q}}}(k, x, P, N + 1))$.

Proof. The proof exploits the special construction of the rotated optimal value function $\tilde{V}_N$. As explained in Remark 4.31, for any point on the optimal trajectory the rotated optimal value function vanishes. Combining this with the turnpike and continuity properties, we can conclude that the cost of the whole trajectory is approximately the cost of the initial piece of the trajectory. The same reasoning applies if the horizon is one step longer. Consequently, by applying Lemma 4.33, we can conclude that the initial pieces for horizon N and $N + 1$ also have approximately the same cost and thus the assertion follows. To make these arguments precise, let $k \in \mathbb{N}_0$ and let $x \in \mathbb{X}(k)$. We first consider the optimal value function with horizon length N. From the dynamic programming principle (Theorem 4.2) it follows for every $M \in \{0, \ldots, N\}$ that

$$\tilde{V}_N(k, x) = \tilde{J}_M(k, x, \tilde{u}_N^*) + \tilde{V}_{N-M}(k + M, x_{\tilde{u}_N^*}(M, x)). \tag{4.57}$$

We define

$$R_1(k, x, M, N) := \tilde{V}_{N-M}(k + M, x_{\tilde{u}_N^*}(M, x)) - \tilde{V}_{N-M}(k + M, x^*(k + M))$$

which can be bounded by

$$|R_1(k, x, M, N)| \leq \gamma_{\tilde{V}}(\tilde{\sigma}(P))$$

for $M \in \{0, \ldots, N\} \setminus \tilde{\tilde{\mathcal{Q}}}(k, x, P, N)$ as seen in the proof of Lemma 4.33.
Using the definition of R_1 we rewrite (4.57) to

$$\begin{aligned}
\tilde{V}_N(k, x) &= \tilde{J}_M(k, x, \tilde{u}_N^*) + \tilde{V}_{N-M}(k + M, x^*(k + M)) + R_1(k, x, M, N) \\
&= \tilde{J}_M(k, x, \tilde{u}_N^*) + R_1(k, x, M, N)
\end{aligned} \tag{4.58}$$

where we used Remark 4.31 in the last equality.
Now consider the optimal value function for horizon length $N + 1$. Again, we apply the dynamic programming principle from Theorem 4.2 which yields

$$\tilde{V}_{N+1}(k, x) = \tilde{J}_M(k, x, \tilde{u}_{N+1}^*) + \tilde{V}_{N+1-M}(k + M, x_{\tilde{u}_{N+1}^*}(M, x)) \tag{4.59}$$

for every $M \in \{0, \ldots, N + 1\}$. We define

$$R_3(k, x, M, N) := \tilde{V}_{N+1-M}(k + M, x_{\tilde{u}_{N+1}^*}(M, x)) - \tilde{V}_{N+1-M}(k + M, x^*(k + M))$$

with the bound

$$|R_3(k, x, M, N)| \le \gamma_{\tilde{V}}(\tilde{\sigma}(P))$$

for $M \in \{0, \dots, N\} \setminus \tilde{\mathcal{Q}}(k, x, P, N+1)$ (cf. Lemma 4.33).

Inserting the definition of R_3 into (4.59) and using Remark 4.31, we obtain

$$\tilde{V}_{N+1}(k, x) = \tilde{J}_M(k, x, \tilde{u}^*_{N+1}) + \tilde{V}_{N+1-M}(k + M, x^*(k + M)) + R_3(k, x, M, N)$$
$$= \tilde{J}_M(k, x, \tilde{u}^*_{N+1}) + R_3(k, x, M, N).$$

For $M \in \{0, \dots, N\} \setminus (\tilde{\mathcal{Q}}(k, x, P, N) \cup \tilde{\mathcal{Q}}(k, x, P, N+1))$ we apply Lemma 4.33 to get

$$\tilde{V}_{N+1}(k, x) = \tilde{J}_M(k, x, \tilde{u}^*_{N+1}) + R_3(k, x, M, N)$$
$$= \tilde{J}_M(k, x, \tilde{u}^*_N) + R_3(k, x, M, N) - R_5(k, x, M, N)$$
$$= \tilde{V}_N(k, x) - R_1(k, x, M, N) + R_3(k, x, M, N) - R_5(k, x, M, N)$$

where the last equation follows with equation (4.58).

Finally, we define

$$R_6(k, x, M, N) := -R_1(k, x, M, N) + R_3(k, x, M, N) - R_5(k, x, M, N)$$

and from the bounds on R_1, R_3 and R_5 we get the bound

$$|R_6(k, x, M, N)| = |-R_1(k, x, M, N) + R_3(k, x, M, N) - R_5(k, x, M, N)|$$
$$\le |R_1(k, x, M, N)| + |R_3(k, x, M, N)| + |R_5(k, x, M, N)|$$
$$\le \gamma_{\tilde{V}}(\tilde{\sigma}(P)) + \gamma_{\tilde{V}}(\tilde{\sigma}(P)) + 2\gamma_{\tilde{V}}(\tilde{\sigma}(P))$$
$$= 4\gamma_{\tilde{V}}(\tilde{\sigma}(P)).$$

This shows the assertion. $\qquad\square$

Remark 4.35
In the next theorem, we will use both the turnpike property for the modified and the unmodified MPC problem. Note however, that Assumption 4.10 and Assumption 4.28 express two different turnpike properties with different bounds σ and $\tilde{\sigma}$ and associated sets $\mathcal{Q}$ and $\tilde{\mathcal{Q}}$. To prove the next lemma, we will need a common bound and a single set for both problems. This can be achieved by defining

$$\bar{\sigma} := \max\{\sigma, \tilde{\sigma}\}$$

and

$$\bar{\mathcal{Q}}(k, x, P, N) := \mathcal{Q}(k, x, P, N) \cup \tilde{\mathcal{Q}}(k, x, P, N).$$

Then the optimal trajectories of both problems (4.3) and (4.48) satisfy

$$|(x_{u^*_{N,x}}(M, x), u^*_{N,x}(M))|_{(x^*(k+M), u^*(k+M))} \le \bar{\sigma}(P)$$

and

$$|(x_{\tilde{u}^*_{N,x}}(M, x, \tilde{u}^*_{N,x}(M))|_{(x^*(k+M), u^*(k+M))} \le \bar{\sigma}(P)$$

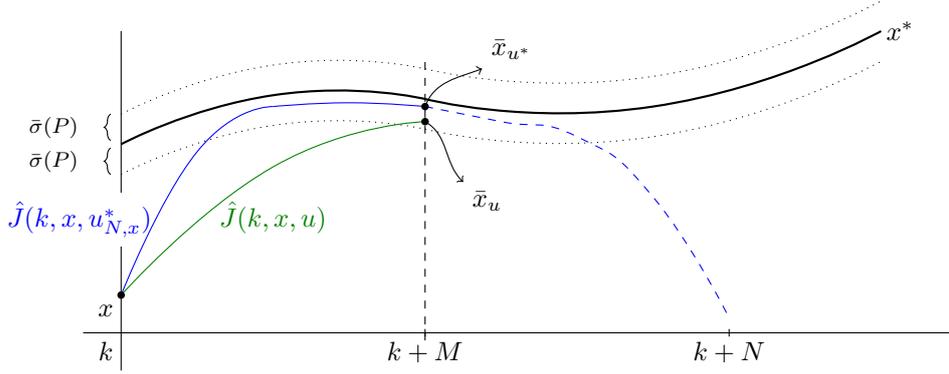*for all $M \in \{0, \dots, N\} \setminus \bar{\mathcal{Q}}(k, x, P, N)$ and $\#\bar{\mathcal{Q}}(k, x, P, N) \le 2P$.* $\qquad\diamond$

Figure 4.13: Illustration of Theorem 4.36 depicting the optimal control sequence $u^*_{N,x}$ (in blue) and a suboptimal control u (in green).

The next theorem shows that the initial piece of an optimal control trajectory which ends in a neighborhood of the optimal trajectory of the unmodified MPC problem yields approximately lower cost than all other trajectories ending in that neighborhood.

Theorem 4.36 (Initial piece of optimal trajectory ending near turnpike is approximately optimal)
Let $u^*_{N,x}$ denote the optimal trajectory of problem (4.3) *and let Assumptions 4.10, 4.12 and 4.28 hold. Then for all $k \in \mathbb{N}_0$, all $x \in \mathbb{X}(k)$, all $N \in \mathbb{N}$, all $P \in \mathbb{N}$, all $M \in \{0, \ldots, N\} \setminus \bar{\bar{\mathcal{Q}}}(k,x,P,N)$ and all $u \in \mathbb{U}^M(k,x)$ with $|x_u(M,x)|_{x^*(k+M)} \leq \bar{\sigma}(P)$ the estimate*

$$\hat{J}_M(k,x,u^*_{N,x}) \leq \hat{J}_M(k,x,u) + R_7(k,x,M,N) \tag{4.60}$$

holds with $|R_7(k,x,M,N)| \leq 2\gamma_V(N-M,\bar{\sigma}(P))$.

Proof. We prove the theorem by contradiction. Let $u^*_{N,x}$ denote the optimal solution of problem (4.3) and let $\bar{x}_{u^*} := x_{u^*_{N,x}}(M,x)$ for $M \in \{0, \ldots, N\} \setminus \bar{\bar{\mathcal{Q}}}(k,x,P,N)$. Then from Remark 4.35 we know that $|\bar{x}_{u^*}|_{x^*(k+M)} \leq \bar{\sigma}(P)$.
Now assume there exists a control sequence $u \in \mathbb{U}^M(k,x)$ with $\bar{x}_u := x_u(M,x)$ satisfying $|\bar{x}_u|_{x^*(k+M)} \leq \bar{\sigma}(P)$ and

$$\hat{J}_M(k,x,u) + R_1(k,x,M,N) + R_2(k,x,M,N) < \hat{J}_M(k,x,u^*_{N,x}). \tag{4.61}$$

with

$$R_1(k,x,M,N) := \hat{V}_{N-M}(k+M,\bar{x}_u) - \hat{V}_{N-M}(k+M,x^*(k+M))$$

and

$$R_2(k,x,M,N) := \hat{V}_{N-M}(k+M,x^*(k+M)) - \hat{V}_{N-M}(k+M,\bar{x}_{u^*}).$$

Using Assumption 4.12 R_1 and R_2 can be bounded by

$$\begin{aligned}|R_1(k,x,M,N)| &\leq \gamma_V(N-M,\bar{\sigma}(P)) \\ |R_2(k,x,M,N)| &\leq \gamma_V(N-M,\bar{\sigma}(P)).\end{aligned} \tag{4.62}$$

Consider

$$
\begin{aligned}
\hat{J}_M(k, x, u) + \hat{V}_{N-M}(k + M, \bar{x}_u) &= \hat{J}_M(k, x, u) + \hat{V}_{N-M}(k + M, x^*(k + M)) + R_1(k, x, M, N) \\
&= \hat{J}_M(k, x, u) + \hat{V}_{N-M}(k + M, \bar{x}_{u^*}) \\
&\quad + R_1(k, x, M, N) + R_2(k, x, M, N) \\
&\overset{(4.61)}{<} \hat{J}_M(k, x, u_{N,x}^*) + \hat{V}_{N-M}(k + M, \bar{x}_{u^*}) \\
&= \hat{V}_N(k, x)
\end{aligned}
$$

where we used the dynamic programming principle from Theorem 4.2 for the last equation. But this contradicts the optimality of $u_{N,x}^*$ and thus the inequality

$$
\hat{J}_M(k, x, u_{N,x}^*) \leq \hat{J}_M(k, x, u) + R_1(k, x, M, N) + R_2(k, x, M, N)
$$

follows. Finally, define

$$
R_7(k, x, M, N) := R_1(k, x, M, N) + R_2(k, x, M, N)
$$

which can be bounded by

$$
|R_7(k, x, M, N)| \leq |R_1(k, x, M, N)| + |R_2(k, x, M, N)| \overset{(4.62)}{\leq} 2\gamma_V(N - M, \bar{\sigma}(P)).
$$

This concludes the proof. $\qquad\square$

So far we did not impose any assumptions on the storage function λ from the strict dissipativity of the system. For the next lemma, we will need that this function is continuous at the optimal trajectory.

Assumption 4.37 (Continuity of storage function λ at x^*)
Assume that the storage function λ is continuous in the following sense: There exists $\gamma_\lambda \in \mathscr{K}_\infty$ such that for all $k \in \mathbb{N}$ and all $x \in \mathbb{X}$ it holds that

$$
|\lambda(k, x) - \lambda(k, x^*(k))| \leq \gamma_\lambda(|x|_{x^*(k)}). \tag{4.63}
$$

In our final preparatory lemma, we consider a control sequence $\hat{u}$ that for the first part consists of the optimal control sequence $u_{N,x}^*$ of the unmodified problem until it is close to the optimal trajectory x^*. Then we control from the final point using the optimal control sequence of the modified problem. The lemma states that the resulting composite control sequence has almost the same cost as if we had controlled using the optimal control sequence of the modified problem for the whole horizon.
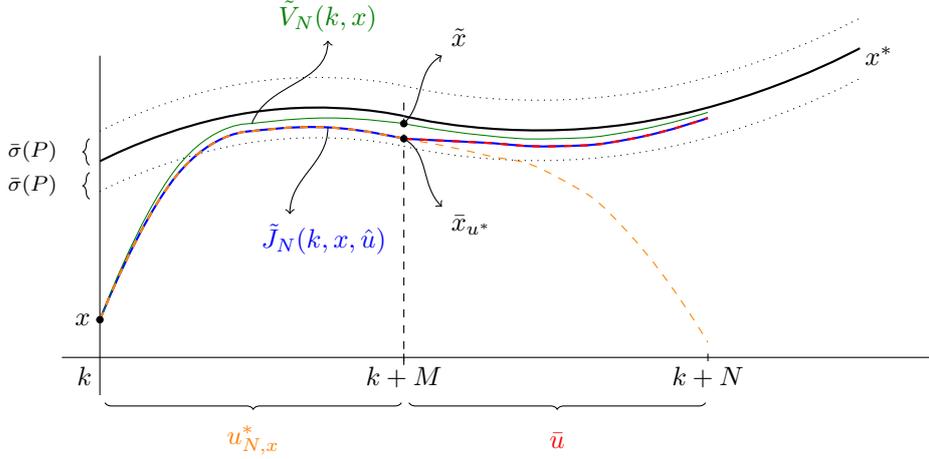
Figure 4.14: Illustration of the proof of Lemma 4.38.

Lemma 4.38

Let Assumptions 4.10, 4.12, 4.28, 4.30 and 4.37 hold and let $u^*_{N,x}$ and $\tilde{u}^*_{N,x}$ denote the optimal control sequences corresponding to problems (4.3) and (4.48). Let $N, P \in \mathbb{N}$ be arbitrary and for $M \in \{0, \ldots, N\} \setminus \bar{\mathcal{Q}}(k, x, P, N)$ define $\bar{x}_{u^*} := x_{u^*_{N,x}}(M, x)$ and denote by $\bar{u}$ the solution of the optimal control problem

$$\min_{u \in \mathbb{U}^{N-M}(k+M, \bar{x}_{u^*})} \tilde{J}_{N-M}(k+M, \bar{x}_{u^*}, u). \tag{4.64}$$

Then the composite control sequence $\hat{u} \in \mathbb{U}^N(k, x)$ defined by $\hat{u}(k) = u^*_{N,x}(k)$ for $k = \{0, \ldots, M-1\}$ and $\hat{u}(k+M) = \bar{u}(k)$ for $k = \{0, \ldots, N-M\}$ satisfies

$$\tilde{J}_N(k, x, \hat{u}) = \tilde{V}_N(k, x) + R_8(k, x, M, N)$$

with

$$|R_8(k, x, M, N)| \leq \gamma_{\tilde{V}}(\sigma(P)) + \gamma_\lambda(\sigma(P)) + \gamma_{\tilde{V}}(\tilde{\sigma}(P)) + \gamma_\lambda(\tilde{\sigma}(P)) + 2\gamma_V(N-M, \bar{\sigma}(P))$$

for all $k \in \mathbb{N}_0$ and for all $x \in \mathbb{X}(k)$.

Proof. We start with a brief outline of the proof. Refer to Figure 4.14 for an illustration of the construction of the composite control sequence $\hat{u}$ (depicted in blue) which consists of the concatenation of two trajectories (orange and red). The first part of the proof shows that the cost of $\hat{u}$ is upper bounded by the cost of the optimal solution of the modified MPC problem (depicted in green) up to some error term. The central assumption in this step is that there exists a time point M at which both the solution of the modified and the unmodified MPC problem are close to the turnpike. Using continuity of the optimal value function and the storage function it then becomes possible to conclude that the values of

the final pieces of the modified trajectory $\tilde{u}_{N,x}^*$ and of the composite trajectory $\hat{u}$ cannot differ by much. Adding to this the statement from Theorem 4.36, that also the initial piece of the unmodified trajectory has approximately lower cost than the initial piece of the modified trajectory, we get that the cost of the composite trajectory is bounded by the cost of the modified trajectory, up to error terms. On the other hand, the modified trajectory is optimal thus the reverse inequality also holds and we can construct an error term such that the assertion holds.

We first prove "$\tilde{J}_N(k,x,\hat{u}) \leq \tilde{V}_N(k,x) + \varepsilon(N)$": Using the definition of $\hat{u}$, noting that $\bar{u}$ is an optimal solution and inserting the definition of $\tilde{J}_M$ we obtain

$$
\begin{aligned}
\tilde{J}_N(k,x,\hat{u}) &= \tilde{J}_M(k,x,u_{N,x}^*) + \tilde{J}_{N-M}(k+M,\bar{x}_{u^*},\bar{u}) \\
&= \tilde{J}_M(k,x,u_{N,x}^*) + \tilde{V}_{N-M}(k+M,\bar{x}_{u^*}) \qquad (4.65) \\
&= \hat{J}_M(k,x,u_{N,x}^*) + \lambda(k,x) - \lambda(k+M,\bar{x}_{u^*}) + \tilde{V}_{N-M}(k+M,\bar{x}_{u^*})
\end{aligned}
$$

Define
$$
R_1(k,x,M,N) := \tilde{V}_{N-M}(k+M,\bar{x}_{u^*}) - \tilde{V}_{N-M}(k+M,x^*(k+M))
$$
and
$$
R_2(k,x,M,N) := \lambda(k+M,x^*(k+M)) - \lambda(k+M,\bar{x}_{u^*}).
$$

Because of Assumption 4.10 we know the bound $|\bar{x}_{u^*}|_{x^*(k+M)} \leq \sigma(P)$ for $M \in \{0,\dots,N\} \setminus \mathcal{Q}(k,x,P,N)$. Thus we can use the continuity of $\tilde{V}_{N-M}$ from Assumption 4.30 and the continuity of λ from Assumption 4.37 to obtain the bounds
$$
|R_1(k,x,M,N)| \leq \gamma_{\tilde{V}}(\sigma(P))
$$
and
$$
|R_2(k,x,M,N)| \leq \gamma_\lambda(\sigma(P)).
$$

Inserting R_1 and R_2 into (4.65) leads to

$$
\begin{aligned}
&\hat{J}_M(k,x,u_{N,x}^*) + \lambda(k,x) - \lambda(k+M,\bar{x}_{u^*}) + \tilde{V}_{N-M}(k+M,\bar{x}_{u^*}) \\
&= \hat{J}_M(k,x,u_{N,x}^*) + \lambda(k,x) - \lambda(k+M,x^*(k+M)) + \tilde{V}_{N-M}(k+M,x^*(k+M)) \quad (4.66) \\
&\quad + R_1(k,x,M,N) + R_2(k,x,M,N)
\end{aligned}
$$

Now consider the optimal solution $\tilde{u}_{N,x}^*$ of problem (4.27), denote $\tilde{x} := x_{\tilde{u}_{N,x}^*}(M,x)$ and define
$$
R_3(k,x,M,N) := \tilde{V}_{N-M}(k+M,x^*(k+M)) - \tilde{V}_{N-M}(k+M,\tilde{x})
$$
and
$$
R_4(k,x,M,N) := \lambda(k+M,\tilde{x}) - \lambda(k+M,x^*(k+M)).
$$

For $M \in \{0,\dots,N\} \setminus \tilde{\mathcal{Q}}(k,x,P,N)$ we have the bound $|\tilde{x}| \leq \tilde{\sigma}(P)$ from Assumption 4.28. Using again the continuity of $\tilde{V}_{N-M}$ and λ from Assumptions 4.30 and 4.37, we can bound R_3 and R_4 by
$$
|R_3(k,x,M,N)| \leq \gamma_{\tilde{V}}(\tilde{\sigma}(P))
$$

and
$$|R_4(k, x, M, N)| \leq \gamma_\lambda(\tilde{\sigma}(P)).$$

Continuing from (4.66) by inserting R_3 and R_4 yields

$$\hat{J}_M(k, x, u^*_{N,x}) + \lambda(k, x) - \lambda(k + M, x^*(k + M)) + \tilde{V}_{N-M}(k + M, x^*(k + M))$$
$$+ R_1(k, x, M, N) + R_2(k, x, M, N)$$
$$= \hat{J}_M(k, x, u^*_{N,x}) + \lambda(k, x) - \lambda(k + M, \tilde{x}) + \tilde{V}_{N-M}(k + M, \tilde{x})$$
$$+ R_1(k, x, M, N) + R_2(k, x, M, N) + R_3(k, x, M, N) + R_4(k, x, M, N)$$

Finally, using Theorem 4.36 for the control sequence $u = \tilde{u}^*_{N,x}$, we obtain for $M \in \{0, \ldots, N\} \setminus \bar{\bar{Q}}(k, x, P, N)$ (with the set $\bar{\bar{Q}}(k, x, P, N)$ from Remark 4.35)

$$\hat{J}_M(k, x, u^*_{N,x}) + \lambda(k, x) - \lambda(k + M, \tilde{x}) + \tilde{V}_{N-M}(k + M, \tilde{x})$$
$$+ R_1(k, x, M, N) + R_2(k, x, M, N) + R_3(k, x, M, N) + R_4(k, x, M, N)$$
$$\leq \hat{J}_M(k, x, \tilde{u}^*_{N,x}) + \lambda(k, x) - \lambda(k + M, \tilde{x}) + \tilde{V}_{N-M}(k + M, \tilde{x})$$
$$+ \underbrace{R_1(k, x, M, N) + R_2(k, x, M, N) + R_3(k, x, M, N) + R_4(k, x, M, N) + R_7(k, x, M, N)}_{=:\tilde{R}_8(k,x,M,N)}$$
$$= \tilde{J}_M(k, x, \tilde{u}^*_{N,x}) + \tilde{V}_{N-M}(k + M, \tilde{x}) + \tilde{R}_8(k, x, M, N)$$
$$= \tilde{V}_N(k, x) + \tilde{R}_8(k, x, M, N)$$

To summarize, we have shown that

$$\tilde{J}_N(k, x, \hat{u}) \leq \tilde{V}_N(k, x) + \tilde{R}_8(k, x, M, N) \tag{4.67}$$

with

$$|\tilde{R}_8(k, x, M, N)| \leq |R_1(k, x, M, N)| + |R_2(k, x, M, N)| + |R_3(k, x, M, N)| + |R_4(k, x, M, N)|$$
$$+ |R_7(k, x, M, N)|$$
$$\leq \gamma_{\tilde{V}}(\sigma(P)) + \gamma_\lambda(\sigma(P)) + \gamma_{\tilde{V}}(\tilde{\sigma}(P)) + \gamma_\lambda(\tilde{\sigma}(P)) + 2\gamma_V(N - M, \bar{\sigma}(P))$$

which holds for all $M \in \{0, \ldots, N\} \setminus \bar{\bar{Q}}(k, x, P, N)$.

To prove the reverse inequality, note that from the definition of the optimal value function we know that

$$\tilde{V}_N(k, x) \leq \tilde{J}_N(k, x, u)$$

for all $u \in \mathbb{U}^N(k, x)$ and in particular, for $u = \hat{u}$. Combining this inequality with inequality (4.67) from above, it follows that

$$\tilde{J}_N(k, x, \hat{u}) \leq \tilde{V}_N(k, x) + \tilde{R}_8(k, x, M, N) \leq \tilde{J}_N(k, x, \hat{u}) + \tilde{R}_8(k, x, M, N)$$

and thus $\tilde{R}_8(k, x, M, N) \geq 0$. In addition, we know that

$$\tilde{V}_N(k, x) \leq \tilde{J}_N(k, x, \hat{u}) \leq \tilde{V}_N(k, x) + \tilde{R}_8(k, x, M, N).$$

With this, we can conclude the existence of R_8 with $|R_8(k, x, M, N)| \leq \tilde{R}_8(k, x, M, N)$ such that

$$\tilde{J}_N(k, x, \hat{u}) = \tilde{V}_N(k, x) + R_8(k, x, M, N). \tag{4.68}$$

This finishes the proof. □

Using the results from Lemmas 4.33 - 4.38, we can now prove that the modified optimal value function $\tilde{V}_N$ is a Lyapunov function for the system controlled by the MPC feedback μ_N obtained by solving the original (unmodified) MPC problem.

Theorem 4.39 ($\tilde{V}_N$ Lyapunov function for MPC with unmodified cost)
Let Assumptions 4.10, 4.12, 4.23, 4.28, 4.29, 4.30 and 4.37 hold. Then for each $\Theta > 0$ there exists $\delta_1 \in \mathscr{L}$ such that the optimal value function $\tilde{V}_N$ is a Lyapunov function for the closed-loop system $g(k, x) = f(k, x, \mu_N(k, x))$ on $S(k) = Y(k) \setminus \mathbb{P}(k)$ for the families of forward invariant sets $Y(k) = \tilde{V}_N^{-1}(k, [0, \Theta])$ and $\mathbb{P}(k) = \tilde{V}_N^{-1}(k, [0, \delta_1(N)])$.

Proof. [1] Let $\Theta > 0$, $k \in \mathbb{N}_0$ and $x \in \mathbb{X}(k)$. We first prove the existence of lower and upper bounds for $\tilde{V}_N(k, x)$ in inequality (4.41). To obtain a lower bound, observe that from Assumption 4.23 it follows that

$$\tilde{\ell}(k, x, u) \geq \alpha(|x|_{x^*(k)}) \tag{4.69}$$

for all $(x, u) \in \mathbb{X}(k) \times \mathbb{U}(k, x)$. With this, we can estimate

$$\tilde{V}_N(k, x) = \inf_{u \in \mathbb{U}^N(k,x)} \sum_{j=0}^{N-1} \tilde{\ell}(k+j, x_u(j; x), u(j)) \geq \inf_{u \in \mathbb{U}^N(k,x)} \sum_{j=0}^{N-1} \alpha(|x_u(j; x)|_{x^*(k+j)})$$

$$\geq \alpha(|x|_{x^*(k)})$$

This yields the lower bound $\alpha_1 = \alpha$. The upper bound follows from Assumption 4.30 since $\tilde{V}_N(k, x^*(k)) = 0$ with $\alpha_2 = \gamma_{\tilde{V}}$.

Now we turn to the inequality (4.42). Consider the control sequence $\hat{u} \in \mathbb{U}^N(k, x)$ defined in Lemma 4.38 and let $x^+ := x_{\hat{u}}(1, x)$. From the definition of the cost functional we have

$$\tilde{J}_N(k, x, \hat{u}) = \tilde{\ell}(k, x, \hat{u}) + \tilde{J}_{N-1}(k + 1, x^+, \hat{u}(\cdot + 1)).$$

We can apply Lemma 4.38 to $\tilde{J}_N(k, x, \hat{u})$ because $\hat{u}$ exactly corresponds to the control sequence from the lemma. Furthermore, we can apply the lemma to $\tilde{J}_{N-1}(k + 1, x^+, \hat{u}(\cdot + 1))$. The reason for this is that the control sequence $\hat{u}(\cdot + 1)$ coincides with the control sequence u^*_{N-1,x^+} up to time $M - 1$. This follows from the dynamic programming principle and the fact that tails of optimal control sequences are again optimal control sequences, cf. [50, Corollary 4.5]. From this we obtain

$$\tilde{V}_N(k, x) + R_8(k, x, M, N) = \tilde{\ell}(k, x, \hat{u}) + \tilde{V}_{N-1}(k + 1, x^+) + R_8(k + 1, x^+, M - 1, N - 1)$$

---

[1]Parts of the proof are analogous to the proof of Proposition 8.32 in [50]

Using Lemma 4.34 on the right-hand side of the equation for $k = k+1$, $x = x^+$, $M = M-1$ and $N = N - 1$, we get

$$\tilde{V}_N(k,x) + R_8(k,x,M,N) = \tilde{\ell}(k,x,\hat{u}) + \tilde{V}_N(k+1,x^+) + R_6(k+1,x^+,M-1,N-1)$$
$$+ R_8(k+1,x^+,M-1,N-1)$$

or equivalently

$$\tilde{V}_N(k+1,x^+) = \tilde{V}_N(k,x) - \tilde{\ell}(k,x,\hat{u}) - R_6(k+1,x^+,M-1,N-1)$$
$$- R_8(k+1,x^+,M-1,N-1) + R_8(k,x,M,N).$$

From Lemma 4.34 and Lemma 4.38 we obtain a bound for the residuals

$$- R_6(k+1,x^+,M-1,N-1) - R_8(k+1,x^+,M-1,N-1) + R_8(k,x,M,N)$$
$$\leq |R_6(k+1,x^+,M-1,N-1)| + |R_8(k+1,x^+,M-1,N-1)| + |R_8(k,x,M,N)|$$
$$\leq 2\gamma_{\tilde{V}}(\sigma(P)) + 2\gamma_\lambda(\sigma(P)) + 6\gamma_{\tilde{V}}(\tilde{\sigma}(P)) + 2\gamma_\lambda(\tilde{\sigma}(P)) + 4\gamma_V(N-M,\bar{\sigma}(P))$$

$$(4.70)$$

which holds for all $M \in \{0,\ldots,N\} \setminus \{\bar{\bar{\mathcal{Q}}}(k,x,P,N) \cup \bar{\bar{\mathcal{Q}}}(k+1,x^+,P,N-1)\}$. Because each of the sets $\bar{\bar{\mathcal{Q}}}$ contains at most $2P$ elements we can choose $P = \lfloor \frac{N}{8} \rfloor$ to guarantee that there is at least one such M satisfying $M \leq \frac{N}{2}$ which implies $N - M \geq \frac{N}{2}$. With this, we can find an upper bound $\nu(N)$ of (4.70) only depending on N that is given by

$$\nu(N) := 8\gamma_{\tilde{V}}(\sigma(\lfloor \tfrac{N}{8} \rfloor)) + 2\gamma_\lambda(\sigma(\lfloor \tfrac{N}{8} \rfloor)) + 2\gamma_\lambda(\tilde{\sigma}(\lfloor \tfrac{N}{8} \rfloor)) + 4\gamma_V(\tfrac{N}{2},\bar{\sigma}(\lfloor \tfrac{N}{8} \rfloor))$$

using the properties of comparison functions. Thus we arrive at the inequality

$$\tilde{V}_N(k+1,x^+) \leq \tilde{V}_N(k,x) - \tilde{\ell}(k,x,\hat{u}) + \nu(N)$$
$$= \tilde{V}_N(k,x) - \tilde{\ell}(k,x,\mu_N(k,x)) + \nu(N).$$

$$(4.71)$$

In addition, from Assumption 4.23 it follows that

$$-\tilde{\ell}(k,x,u) \leq -\alpha(|x|_{x^*(k)})$$

for all $(x,u) \in \mathbb{X}(k) \times \mathbb{U}(k,x)$, in particular for $u = \mu_N(k,x)$. This leads to the inequality

$$\tilde{V}_N(k+1,x^+) \leq \tilde{V}_N(k,x) - \alpha(|x|_{x^*(k)}) + \nu(N).$$

Since we have the upper bound $\tilde{V}_N(k,x) \leq \alpha_2(|x|_{x^*(k)})$, we can further estimate

$$\tilde{V}_N(k+1,x^+) \leq \tilde{V}_N(k,x) - \alpha(|x|_{x^*(k)}) + \nu(N)$$
$$\leq \tilde{V}_N(k,x) - \alpha(\alpha_2^{-1}(\tilde{V}_N(k,x))) + \nu(N) \qquad (4.72)$$
$$= \tilde{V}_N(k,x) - \chi(\tilde{V}_N(k,x))) + \nu(N)$$

with $\chi := \alpha \circ \alpha_2^{-1}$. Define $\delta_1(N) := \max\{\chi^{-1}(2\nu(N)), \chi^{-1}(\nu(N)) + \nu(N)\}$ and let $\mathbb{P}(k) := \tilde{V}_N^{-1}(k, [0, \delta_1(N)])$. Then for $x \in Y(k) \setminus \mathbb{P}(k)$ it holds that

$$\tilde{V}_N(k, x) \geq \delta_1(N) \geq \chi^{-1}(2\nu(N)).$$

This implies

$$\nu(N) \leq \frac{\chi(\tilde{V}_N(k, x))}{2}$$

and it follows that

$$\tilde{V}_N(k+1, x^+) \leq \tilde{V}_N(k, x) - \chi(\tilde{V}_N(k, x))) + \nu(N)$$
$$\leq \tilde{V}_N(k, x) - \frac{\chi(\tilde{V}_N(k, x)))}{2}$$

and using the lower bound $\alpha_1(|x|_{x^*(k)}) \leq \tilde{V}_N(k, x)$ we get

$$\tilde{V}_N(k+1, x^+) \leq \tilde{V}_N(k, x) - \frac{\chi(\tilde{V}_N(k, x)))}{2} \leq \tilde{V}_N(k, x) - \frac{\chi(\alpha_1(|x|_{x^*}))}{2}.$$

Thus, we have shown the inequality (4.42) with $\alpha_V(r) = \frac{\chi(\alpha_1(r))}{2}$. What remains to be shown is the forward invariance of the sets $Y(k)$ and $\mathbb{P}(k)$. For $x \in Y(k)$ it holds that $\tilde{V}_N(k, x) \leq \Theta$. Now consider x^+ for which it holds

$$\tilde{V}_N(k, x) \leq \tilde{V}_N(k, x) - \alpha_V(|x|_{x^*}) < \tilde{V}_N(k, x) \leq \Theta$$

and thus $x^+ \in \tilde{V}_N^{-1}(k+1, [0, \Theta]) = Y(k+1)$. This shows the forward invariance of $Y(k)$. To prove forward invariance of $\mathbb{P}(k)$ let $x \in \mathbb{P}(k)$ which implies that $\tilde{V}_N(k, x) \leq \delta_1(N)$. Distinguish two cases:

1. case: $\chi(\tilde{V}_N(k, x)) \geq \nu(N)$
   Here it follows from (4.72) that

   $$\tilde{V}_N(k+1, x^+) \leq \tilde{V}_N(k, x) - \chi(\tilde{V}_N(k, x)) + \nu(N) \leq \tilde{V}_N(k, x) \leq \delta_1(N).$$

2. case: $\chi(\tilde{V}_N(k, x)) \leq \nu(N)$
   In this case, it follows

   $$\tilde{V}_N(k+1, x^+) \leq \tilde{V}_N(k, x) - \chi(\tilde{V}_N(k, x)) + \nu(N)$$
   $$\leq \tilde{V}_N(k, x) + \nu(N) < \chi^{-1}(\nu(N)) + \nu(N) \leq \delta_1(N).$$

So in both cases $x^+ \in \mathbb{P}(k+1)$ and thus the forward invariance holds. $\qquad\square$

Remark 4.40
The proof of Theorem 4.39 uses the same basic idea as the proof of Proposition 8.32 in [50].
However, due to the time-variance a different route for establishing a relation between

$\tilde{V}_N(k+1, x^+)$ *and* $\tilde{V}_N(k, x)$ *in inequality (4.71) had to be taken. The reason for this is that in the time-invariant case the cost of the optimal equilbrium* $\ell(x_e, u_e)$ *is constant in time whereas in the time-varying case the cost of the optimal trajectory at two time instances* k_1 *and* k_2 *may differ, i.e. in general* $\ell(k_1, x^*(k_1), u^*(k_1)) \neq \ell(k_2, x^*(k_2), u^*(k_2))$. *Because of this, a straightforward generalization of Lemma 8.26, which was used in the original proof of Proposition 8.32, is not possible. The problem was circumvented by the preliminary Lemmas 4.33 - 4.38.* $\diamond$

Together with Theorem 4.22, Theorem 4.39 shows that the MPC closed-loop is practically asymptotically stable at the optimal trajectory. In particular, this means that the closed-loop trajectory will converge to a neighborhood $\mathbb{P}(k)$ of the optimal trajectory. Furthermore, since the bounds α_1, α_2 as well as the function α_V are independent of N, the size of this neighborhood tends to zero as the optimization horizon N tends to infinity. In addition, Theorem 4.16 ensures that the closed-loop trajectory approaches this neighborhood in an approximately optimal way.

4.6   Illustrative examples

To conclude this chapter, we illustrate the essential results by a number of examples. Even though they are simple they point out the possible behavior of the MPC solutions in the time-varying context.

We first give two examples that show by means of numerical simulations that both the MPC closed-loop cost and the MPC closed-loop trajectories converge to the optimal cost and the optimal trajectory (x^*, u^*), respectively. In a third example, we consider a case where MPC fails to converge to the optimal trajectory.

Here we restrict ourselves to presenting the simulation results without investigating why MPC works as expected (or does not). This will be done in the next chapter where we will revisit these examples and explain their behavior in more detail by checking the assumptions we used in our convergence results.

Example 4.41 (Trajectory convergence for scalar example)
Consider again the system from Example 4.18. There, we already saw that the cost of the MPC closed-loop trajectories converges to the cost of an overtaking optimal trajectory as the horizon is increased. Now we want to investigate what happens to the trajectories themselves.

To the best of our knowledge, it is not possible to compute the optimal trajectory (x^*, u^*) *analytically for this example. Instead, an approximation to the optimal trajectory was computed by solving an optimal control problem on a long finite horizon with free initial value.*

Figure 4.15 shows the MPC closed-loops for different initial values. We see that all solutions converge towards a single unique trajectory, which is the approximation of the optimal trajectory (x^*, u^*), *at which the system is optimally operated. Thus, this example demon-*
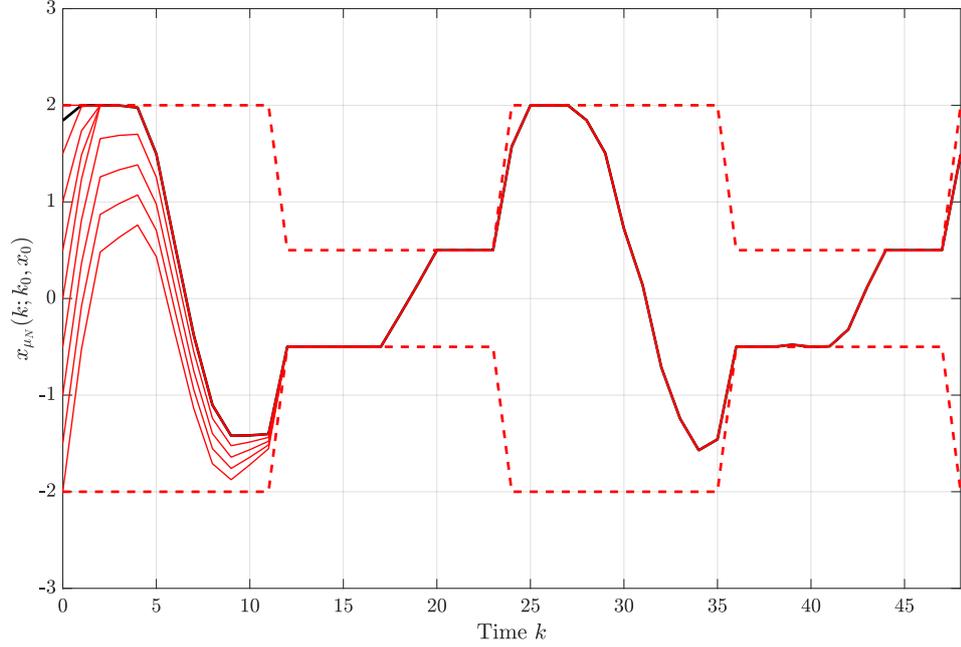
Figure 4.15: MPC closed-loop trajectories for different initial values of the system using a fixed horizon of $N = 10$.

strates that MPC works in the time-varying setting and produces a closed-loop solution which approximates the optimal trajectory (x^*, u^*).

As a second example, we investigate a problem involving a partial differential equation (PDE). The example demonstrates that MPC not only works for finite but also infinite dimensional systems.

Example 4.42 (PDE example)
Consider the convection diffusion equation

$$\frac{\partial y}{\partial t} - \alpha \nabla^2 y + w \nabla y = 0 \;\; on \; Q := \Omega \times [0, T],$$
$$y(0) = y_0 \;\; on \; \Omega, \tag{4.73}$$

where $y : Q \to \mathbb{R}$ is the temperature, $\alpha > 0$ is the diffusion coefficient, $w : \Omega \times [0, T] \to \mathbb{R}$ is a velocity field and $y_0 : \Omega \to \mathbb{R}$ is the initial condition at time zero. Let the boundary of the domain be separated in two parts Γ_{out} and Γ_c and consider boundary conditions of Robin type:

$$\frac{\partial y}{\partial n} + \gamma_{out} y = \delta_{out} y_{out} \;\; on \; \Sigma_{out} := \Gamma_{out} \times [0, T],$$
$$\frac{\partial y}{\partial n} + \gamma_c y = \delta_c u \;\; on \; \Sigma_c := \Gamma_c \times [0, T]. \tag{4.74}$$

In the above equations $\frac{\partial y}{\partial n}$ is the derivative of y in normal direction, $y_{out} : \Sigma_{out} \to \mathbb{R}$ is the outside temperature, $u : \Sigma_c \to \mathbb{R}$ is a control function, and $\gamma_c, \delta_c : \Sigma_c \to \mathbb{R}$, $\gamma_{out}, \delta_{out} : \Sigma_{out} \to \mathbb{R}$ are coefficient functions.

The optimal control problem is given by:

$$\min_{y,u,w} J(y, u, w) = \frac{1}{2}\|u\|^2_{L^2(\Sigma_c)} + \frac{1}{2}\|w\|^2_{L^2(Q)} \tag{4.75}$$

subject to equations (4.73), (4.74) and the constraints

$$\underline{u} \leq u \leq \overline{u} \text{ on } \Sigma_c, \tag{4.76}$$

$$\underline{y} \leq y \leq \overline{y} \text{ on } \Omega_y \times [0, T], \tag{4.77}$$

with lower and upper bounds for state and control where $\Omega_y \subseteq \Omega$ is a subdomain.

The physical interpretation of this setting is similar to Example 4.18 but now with an underlying PDE. The example is motivated by the application of HVAC (heating, ventilation, air conditioning). The state y models the spatial distribution of the temperature within a room. The temperature is subject to time-dependent variations at the boundary Γ_{out} due to changing outside temperature y_{out}. On the controlled part of the boundary Γ_c, the temperature can be influenced by the control u representing heating and cooling. In addition, a second control w can be used to affect the convection, similar to controllable airflow (ventilation) inside the room. The goal is to keep the temperature of the room within lower and upper bounds $\underline{y}$ and $\overline{y}$ on the subdomain Ω_y, using as little energy as possible.

For simplicity, we consider the unit interval as domain Ω. Similar results can be obtained also in higher dimensions, see also [78]. The boundary Γ is partitioned into an uncontrolled boundary Γ_{out} at $x = 0$ and a controlled boundary Γ_c at $x = 1$, see Figure 4.16. Furthermore, we assume the controlled convection w is constant in space. The numerical
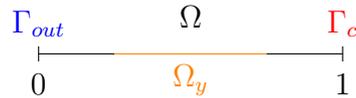

Figure 4.16: Illustration of domain Ω and subdomain Ω_y, as well as controlled (Γ_c) and uncontrolled (Γ_{out}) parts of the boundary.

implementation of the example was described in more detail in Chapter 3.

Like in Example 4.41 the optimal trajectory (y^*, u^*) has been computed from an optimization with a free initial value on a long horizon.

We apply the MPC algorithm (Algorithm 4.1) to the problem. Figure 4.17 shows an exemplary MPC closed-loop with a horizon of $N = 50$. The state on the subdomain Ω_y is kept between the lower and upper bounds. The control u alternates between cooling and heating in order to counteract the rising and falling temperature at the uncontrolled boundary. As seen in Figure 4.18, we can observe the convergence of the closed-loop

Parameter	Value	Description
Ω_y	$[0.25, 0.75]$	subdomain
h	0.01	sampling rate
n_y	100	dof for FEM discretization
$-\underline{y}, \overline{y}$	0.15	state constraints
$-\underline{u}, \overline{u}$	0.25	control constraints
y_0	-0.1	initial value of the state
α	1	diffusion coefficient
$\gamma_{out}, \delta_{out}$	10^6	parameters at outside boundary
γ_c	0	parameter at control boundary
δ_c	10	parameter at control boundary
$y_{out}(t)$	$0.3\sin(10t)$	time-varying outside temperature

Table 4.1: Overview of parameters used in the simulations.

cost of the MPC solutions for increasing horizon length, as well as the convergence of the MPC closed-loop trajectories to the optimal trajectory in Figure 4.19. An interesting observation is that in this example the cost converges much quicker than the state. While there is hardly any change in the value of the closed-loop cost for $N = 20$ the closed loop trajectories themselves only come close to the optimal trajectory around relatively long horizons of $N = 70$.
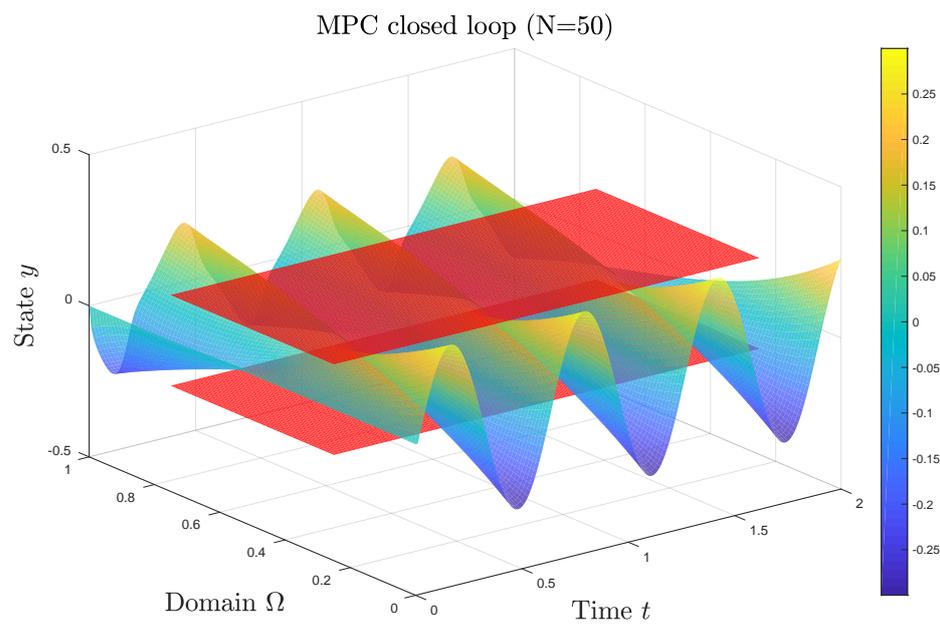
Figure 4.17: Temporal and spatial evolution of an MPC closed-loop trajectory for horizon length $N = 50$. The state constraints on the subdomain $\Omega_y = [0.25, 0.75]$ are plotted in red.
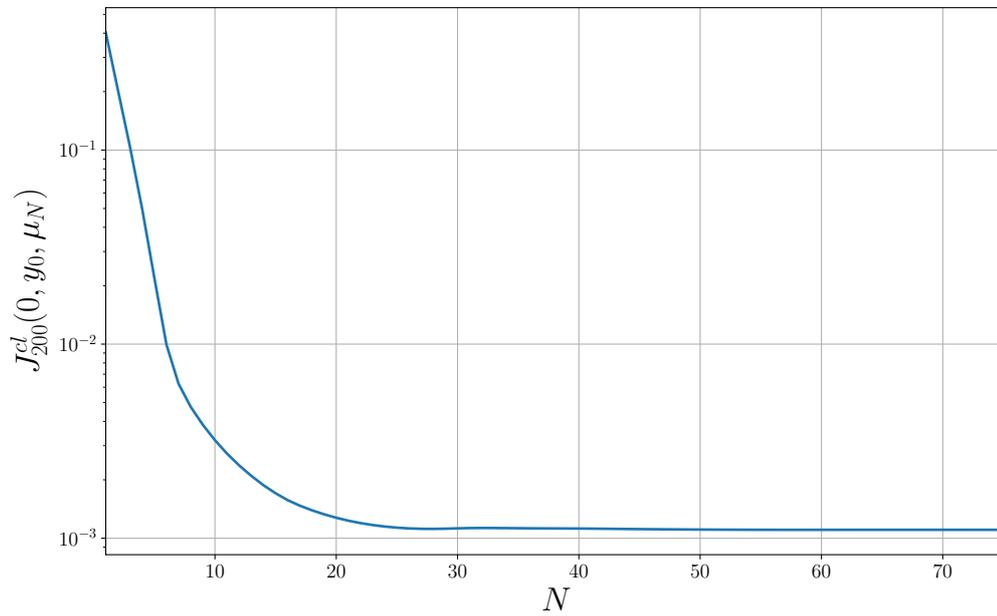
Figure 4.18: Evolution of the closed-loop cost $J_{200}^{cl}(0, y_0, \mu_N)$ for $L = 200$ time steps with different horizon lengths N.
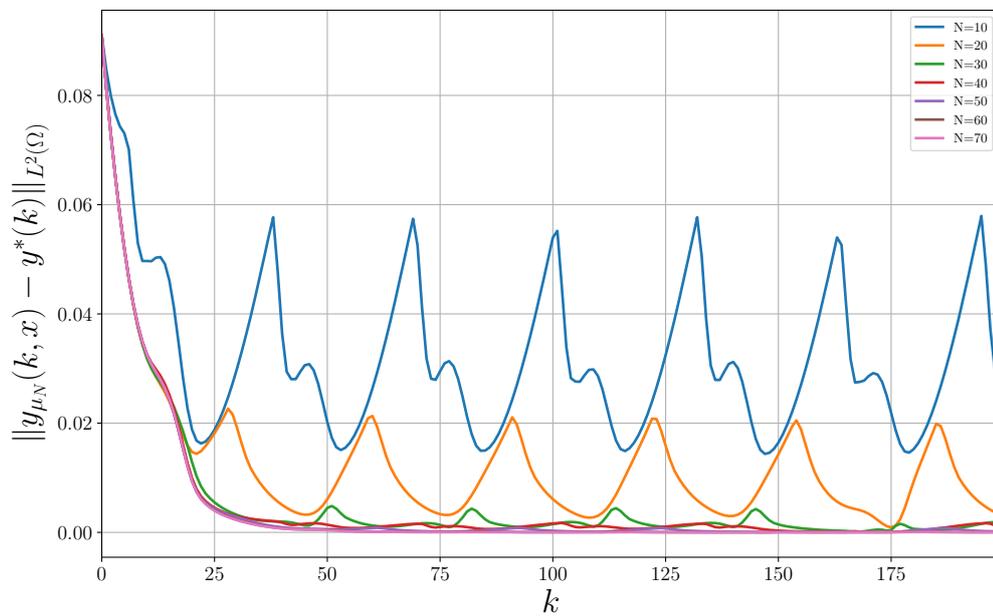
Figure 4.19: Norm difference $\|y_{\mu_N}(k, x) - y^*(k)\|_{L^2(\Omega)}$ between MPC closed-loop trajectories and the optimal trajectory at each time point for different horizon lengths N.

As a final example, we investigate a case where MPC fails to converge to the optimal trajectory.

Example 4.43
Consider the system

$$x(k+1) = \begin{cases} u(k), & \text{if } k = 0, \\ x(k), & \text{if } k \geq 1, \end{cases}$$

with discrete state and control spaces $X = U = \mathbb{N}_0$ starting at the initial state $x(0) = 0$ together with the stage cost

$$\ell(k, x, u) = \begin{cases} 1, & \text{if } k \geq 0, x = 0, u = 0, \\ 0, & \text{if } k = 0, x = 0, u \neq 0, \\ 0, & \text{if } 1 \leq k < x, \\ 2, & \text{if } k \geq x. \end{cases}$$

An illustration of this system and the possible state transitions is depicted in Figure 4.20.
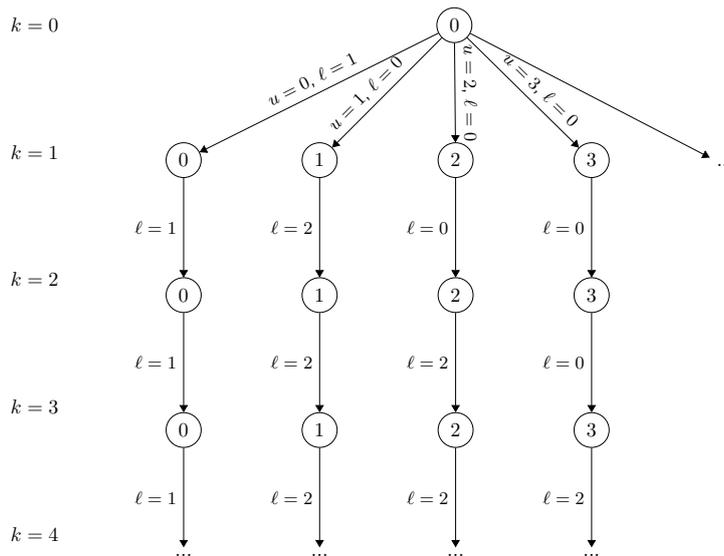
Figure 4.20: Possible state transitions for Example 4.43 together with the corresponding cost $\ell = \ell(k, x, u)$.

The only control action happens at the initial state $x(0)$. Here the control $u(0)$ determines which branch of the state space the solution will follow. The system has been constructed in such a way that the optimal trajectory is the sequence $(x^*, u^*) = \{(0,0), (0,0), \ldots\}$ which produces a cost of $\ell(k, x^*(k), u^*(k)) = 1$ for each $k \geq 0$.
However, for each finite horizon $N \in \mathbb{N}$ a control sequence with lower cost can be found,

namely by choosing the initial control such that $u(0) > N$. This means that the MPC will never converge to the optimal trajectory independently of the horizon length N and the closed-loop cost $\hat{J}_L^{cl}(k, 0, \mu_N)$ will exceed that of the optimal trajectory for all $L > 2u(0)$. As will be shown in the next chapter, the reason for the failure of MPC is that both the turnpike and strict dissipativity assumptions are violated.

5 | Analytical and numerical approaches for checking turnpike and continuity assumptions

In the previous Chapter 4 we analyzed the performance and convergence for time-varying economic MPC schemes. To arrive at our results, we posed a number of assumptions to the underlying problem statement, first and foremost the turnpike property and continuity of the optimal value functions. While these assumptions are convenient for the construction of approximately optimal trajectories, it was not addressed if they are reasonable and can be expected to hold for practical systems. Likewise, it was not explained how to verify them in practice. This is what this chapter will be about.

Generally speaking, the turnpike property is a rather qualitative statement, expressing that open-loop trajectories are most of the time close to what we called the *optimal trajectory* in the previous chapter. In Definition 4.9 this was formalized by putting bounds on the distance to the turnpike and counting the number of time-instances when the open-loop trajectory violates these bounds. Still, it is difficult to quantify and thus check the definition directly, as we will also see in the second part of this chapter.

In contrast to this, dissipativity (cf. Assumption 4.23) is a more tractable condition from a computational point of view, since it is expressed by a set of inequalities that need to hold for each pair of state and control. While still challenging, in principle it is possible to verify dissipativity algorithmically. Examples of how the dissipation inequality can be checked for time-invariant systems can be found in [75, 98], relying on Linear Matrix Inequality techniques, or [29, 92] with approaches based on Sum-of-Squares. Unfortunately, so far these methods have not been extended to time-varying systems. Nevertheless, in the first part of this chapter we will derive alternative sufficient conditions for the turnpike property based on dissipativity, expecting that these conditions will become easier to verify in the future. Similarly, we will show that also the continuity property is implied by strict dissipativity when imposing additional controllability assumptions.

In contrast to the analytical approach of the first part, the second part of this chapter deals with numerical ways to verify the turnpike and continuity assumptions. Here we will look at ways to check if a given system exhibits turnpike and continuity properties. The system we consider is related to a practical application. The fact that it is possible to find

numerical evidence of our central assumptions for this system demonstrates that they are not unreasonably restrictive.

The results presented here encompass the contents of the publications [52] and [54].

5.1 Sufficient conditions for turnpike and continuity properties

In this first part we will show that both the turnpike and the continuity property hold for strictly dissipative systems if we impose additional reachability and controllability assumptions. In addition, we will see that strict dissipativity, in turn, can be concluded if appropriate optimality conditions of the infinite horizon problem hold. We will then revisit one of the examples of the previous chapter and go through all the necessary steps for verification of our assumptions.

5.1.1 Alternative conditions for the turnpike property

We begin by deriving alternative sufficient conditions for the turnpike property from Definition 4.9, given that the system is strictly dissipative, i.e. Assumption 4.23 holds, and the optimal trajectory from Definition 4.5 satisfies the following reachability condition.

Assumption 5.1 (Cheap reachability)
We assume that the trajectory pair (x^*, u^*) is cheaply reachable, i.e. there exists $E \in \mathbb{R}$ such that for each $k \in \mathbb{N}_0$ and for all $x \in \mathbb{X}(k)$, $N \in \mathbb{N} \cup \{\infty\}$ the inequality

$$\hat{V}_N(k, x) \leq E \tag{5.1}$$

holds.

This assumption essentially demands that the optimal trajectory x^* can be reached from any initial state with bounded cost. Since the shifted cost along x^* is zero, this can be expressed via a bound on the shifted optimal value functions. This allows us to prove the following theorem.

Theorem 5.2 (Strict dissipativity and cheap reachability imply turnpike)
Let (x^*, u^*) be an optimal trajectory. If the optimal control problem is strictly dissipative with respect to the supply rate $s(k, x, u) = \hat{\ell}(k, x, u) = \ell(k, x, u) - \ell(k, x^*(k), u^*(k))$ with bounded storage function λ for the trajectory pair (x^*, u^*) and (x^*, u^*) is cheaply reachable, then the turnpike property from Definition 4.9 holds.

Proof. We first prove the finite-horizon turnpike property from Definition 4.9 (a). Let $k \in \mathbb{N}_0$, $x \in \mathbb{X}(k)$ and consider a control sequence $u \in \mathbb{U}(k, x)$ with corresponding state trajectory $x_u(\cdot; k, x)$. From strict dissipativity we have

$$\hat{\ell}(k+j, x_u(j; k, x), u(j)) \geq \lambda(k+j+1, f(k+j, x_u(j; k, x), u(j))) - \lambda(k+j, x_u(j))$$
$$+ \alpha(|(x_u(j; k, x), u(j))|_{(x^*(j), u^*(j))})$$

for all $j \in \mathbb{N}_0$. This yields

$$
\begin{aligned}
\hat{J}_N(k, x, u) &= \sum_{j=0}^{N-1} \hat{\ell}(k+j, x_u(j; k, x), u(j)) \\
&\geq \lambda(k+N, f(k+N-1, x_u(N-1; k, x), u(N-1))) - \lambda(k, x_u(k; k, x)) \\
&\quad + \sum_{j=0}^{N-1} \alpha(|(x_u(j; k, x), u(j))|_{(x^*(j), u^*(j))}).
\end{aligned} \tag{5.2}
$$

We prove the finite-horizon turnpike property by contradiction. Suppose the turnpike property does not hold for

$$
\sigma(P) := \alpha^{-1}\left(\frac{2M_\lambda + E}{P}\right),
$$

in which $M_\lambda > 0$ is a bound on $|\lambda|$ and with E from Assumption 5.1. This means that there are $N \in \mathbb{N}$, $x \in \mathbb{X}(k)$ and $P \in \mathbb{N}$ such that the number of elements $j \in \mathcal{Q}(k, x, P, N)$, i.e. those elements for which $|(x_{u_N^*}(j; k, x), u_N^*(j))|_{(x^*(j), u^*(j))} > \sigma(P)$ is larger than P. Using (5.2) with the optimal control sequence $u = u_N^*$ and taking only those elements in the sum into account for which $|(x_{u_N^*}(j; k, x), u_N^*(j))|_{(x^*(j), u^*(j))} > \sigma(P)$ holds (the other summands are lower-bounded by zero), this implies

$$
\hat{V}_N(k, x) = \hat{J}_N(k, x, u_N^*) > -2M_\lambda + P\alpha(\sigma(P)) = -2M_\lambda + 2M_\lambda + E = E.
$$

However, this contradicts Assumption 5.1.

The proof for the infinite horizon follows analogously with

$$
\rho(P) := \alpha^{-1}\left(\frac{2M_\lambda + E}{P}\right).
$$

$\qquad \square$

5.1.2 Conditions for the continuity property

Next, we show that not only the turnpike property but also continuity of the optimal value function can be deduced from strict dissipativity. For this we need some additional assumptions, first of all local controllability near the optimal trajectory of the system.

Assumption 5.3 (Local controllability)
The system is locally controllable along the trajectory pair (x^*, u^*), i.e. there exists a time $d \in \mathbb{N}$, $\delta_c > 0$, and functions $\gamma_x, \gamma_u, \gamma_c \in \mathcal{K}_\infty$ such that for each $k \in \mathbb{N}_0$ and for any two points $x \in \mathcal{B}_{\delta_c}(x^*(k))$, $y \in \mathcal{B}_{\delta_c}(x^*(k+d))$ there exists a control sequence $u \in \mathbb{U}^d(x)$ satisfying $x_u(d, x) = y$ and for all $j = 0, \ldots, d-1$ the estimates

$$
\begin{aligned}
\|x_u(j; k, x) - x^*(k+j)\| &\leq \gamma_x(\delta), \\
\|u(j) - u^*(k+j)\| &\leq \gamma_u(\delta)
\end{aligned}
$$

and

$$|\hat{\ell}(j + k, x_u(j; k, x), u(j))| \leq \gamma_c(\delta)$$

hold, where $\delta := \max\{\|x - x^*(k)\|, \|y - x^*(k + d)\|\}$.

Clearly, local controllability means that any two points within a tube along the optimal trajectory can be connected in forward time by a trajectory close to (x^*, u^*) as illustrated in Figure 5.1.
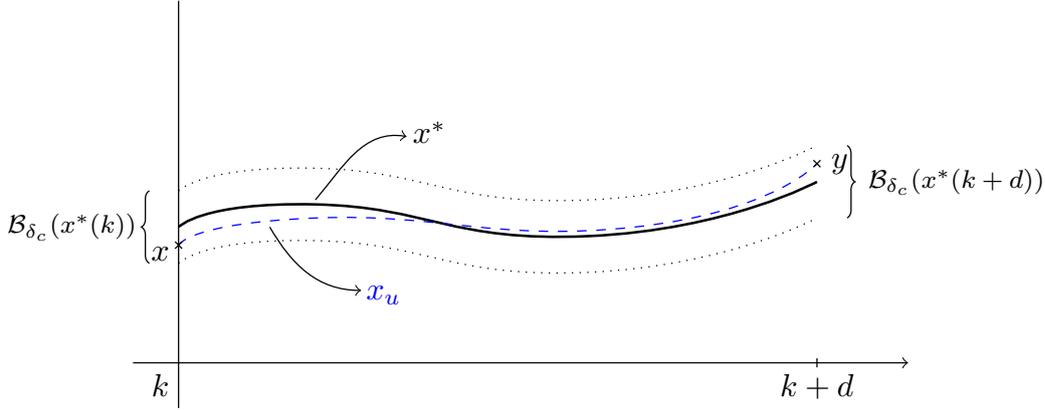

Figure 5.1: Local controllability along the optimal trajectory.

For the subsequent results we will make use once more of the modified stage cost function, which we have introduced in Definition 4.26 of the previous chapter. In inequality (4.69) in the proof of Theorem 4.39 we already saw that the modified stage cost is bounded from below by a function $\alpha_l := \alpha$ (where α is the dissipativity margin from Definition 4.23), i.e.

$$\tilde{\ell}(k, x, u) \geq \alpha_l(|(x, u)|_{(x^*(k), u^*(k))}) \tag{5.3}$$

with $\alpha_l \in \mathscr{K}_\infty$ holds for all $(x, u) \in \mathbb{X}(k) \times \mathbb{U}(k, x)$. If, in addition, Assumption 4.29 is satisfied we also have an upper bound $\alpha_u \in \mathscr{K}_\infty$

$$\tilde{\ell}(k, x, u) \leq \alpha_u(|(x, u)|_{(x^*(k), u^*(k))}) \tag{5.4}$$

with for all $k \in \mathbb{N}_0$ and all $(x, u) \in \mathbb{X}(k) \times \mathbb{U}(k, x)$.
One easily sees that for the modified cost functional the following identity holds:

$$\tilde{J}_N(k, x, u) = \hat{J}_N(k, x, u) + \lambda(k, x) - \lambda(k + N, x_u(N; k, x)). \tag{5.5}$$

The following preliminary result shows that an optimal trajectory starting in a neighborhood of the optimal pair (x^*, u^*) will stay near the optimal pair for some time.

Lemma 5.4
Suppose that the system (4.1) *is strictly dissipative and that Assumptions 4.29, 5.1 and 5.3 hold. Then there exist $N_1 > 0$, $R \geq N/2$ and $\eta : \mathbb{N} \times \mathbb{R}_0^+ \to \mathbb{R}_0^+$ with $\eta(N, r) \to 0$ if $N \to \infty$ and $r \to 0$, such that for each $k > 0$ the open-loop optimal trajectories with horizon $N \geq N_1$ starting in $x_1 \in \mathscr{B}_{\delta_c}(x^*(k))$ satisfy*

$$|(x_{u_{N,x_1}^*}(j; k, x_1), u_{N,x_1}^*(j))|_{(x^*(k+j), u^*(k+j))} \leq \eta(N, \|x_1 - x^*(k)\|)$$

for all $j \in \{0, \ldots, R\}$ and δ_c from Assumption 5.3.

Proof. [1] Let $k \in \mathbb{N}_0$. We choose an arbitrary $x_1 \in \mathscr{B}_{\delta_c}(x^*(k))$, i.e. a point close to the optimal trajectory. By Theorem 5.2 we know that for the optimal open-loop trajectory $x_{u_{N,x_1}^*}(\cdot; k, x_1)$ the finite horizon turnpike property holds. Consider $d \in \mathbb{N}$ and $\delta_c > 0$ from Assumption 5.3, i.e. the number for which local controllability of $x^*(k)$ to $x^*(k + d)$ holds, and the size of the balls around $x^*(k)$ and $x^*(k + d)$. Then, because of the turnpike property we can choose ε satisfying $0 < \varepsilon \leq \delta_c$ and N, P with $P \leq N - 2d$, such that there are at least $N - P \geq 2d$ time instants $j \in \{0, \ldots, N\}$ at which

$$|(x_{u_{N,x_1}^*}(j; k, x_1), u_{N,x_1}^*(j))|_{(x^*(k+j), u^*(k+j))} \leq \sigma(P) \leq \varepsilon$$

holds. In particular, for those time instants we also have

$$\|x_{u_{N,x_1}^*}(j; k, x_1) - x^*(k + j)\| \leq \varepsilon \leq \delta_c.$$

Let R denote the largest such time index and note that $R \geq N - P \geq 2d$. We now construct a control sequence $\bar{u} \in \mathbb{U}^N$ as follows: By applying Assumption 5.3 with $x = x_1$, $y = y_1 := x^*(k + d)$ we know that there exists a control sequence $u_1 \in \mathbb{U}^d$ with $x_{u_1}(d; k, x_1) = x^*(k + d)$. We define $\bar{u}(j) = u_1(j)$ for $j \in \{0, \ldots, d-1\}$. For $j \in \{d, \ldots, R - d - 1\}$ we choose $\bar{u}(j) = u^*(k + j)$, and thus get $x_{\bar{u}}(R - d) = x^*(k + R - d)$. Using Assumption 5.3 again, this time with $x = x_2 := x^*(k + R - d) \in \mathscr{B}_{\delta_c}(x^*(k + R - d))$ and $y = y_2 := x_{u_{N,x_1}^*}(R, x_1) \in \mathscr{B}_{\delta_c}(x^*(k + R))$, we obtain the control sequence $u_2 \in \mathbb{U}^d$. We finish by defining $\bar{u}(j) = u_2(j - R + d)$ for $j \in \{R - d, \ldots, R - 1\}$ and $\bar{u}(j) = u_{N,x_1}^*(j)$ for $j \in \{R, \ldots, N - 1\}$. To summarize, we constructed the following control sequence

$$\bar{u}(j) = \begin{cases} u_1(j), & \text{for } 0 \leq j \leq d - 1 \\ u^*(k + j), & \text{for } d \leq j \leq R - d - 1 \\ u_2(j), & \text{for } R - d \leq j \leq R - 1 \\ u_{N,x_1}^*(j), & \text{for } R \leq j \leq N - 1 \end{cases} \tag{5.6}$$

The corresponding state trajectory is sketched in Figure 5.2.
Next, we show that the modified cost of the initial R steps for the control $\bar{u}$ cannot be smaller than the cost of the optimal control u_{N,x_1}^*. Observe that by construction

---
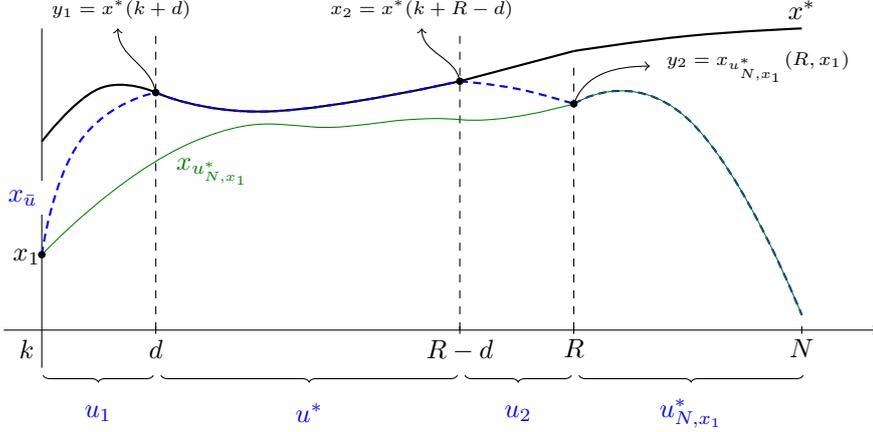[1] The proof uses a construction similar to the one of Lemma 6.3 in [43].

Figure 5.2: Illustration of the state trajectory resulting from the control sequence $\bar{u}$ (dashed blue).

the trajectories $x_{\bar{u}}(j; k, x_1)$ and $x_{u^*_{N,x_1}}(j; k, x_1)$ coincide for $j \in \{R, \ldots, N\}$. Due to the optimality principle, and because $x_{u^*_{N,x_1}}(j; k, x_1)$ is the tail of an optimal trajectory for $j \in \{R, \ldots, N\}$, the initial pieces of the control sequences u^*_{N,x_1} and $\bar{u}$ up to time $R - 1$ satisfy

$$J_R(k, x_1, u^*_{N,x_1}) \leq J_R(k, x_1, \bar{u})$$

as well as

$$\hat{J}_R(k, x_1, u^*_{N,x_1}) \leq \hat{J}_R(k, x_1, \bar{u}). \tag{5.7}$$

Now consider the modified cost functionals $\tilde{J}_R$. From (5.5) with $N = R$ and the fact that $x_{\bar{u}}(R, x_1) = x_{u^*_{N,x_1}}(R, x_1)$ it follows that

$$
\begin{aligned}
\tilde{J}_R(k, x_1, u^*_{N,x_1}) &= \hat{J}_R(k, x_1, u^*_{N,x_1}) + \lambda(k, x_1) - \lambda(k + R, x_{u^*_{N,x_1}}(R; k, x_1)) \\
&\overset{(5.7)}{\leq} \hat{J}_R(k, x_1, \bar{u}) + \lambda(k, x_1) - \lambda(k + R, x_{u^*_{N,x_1}}(R; k, x_1)) \\
&= \hat{J}_R(k, x_1, \bar{u}) + \lambda(k, x_1) - \lambda(k + R, x_{\bar{u}}(R; k, x_1)) = \tilde{J}_R(k, x_1, \bar{u}).
\end{aligned}
\tag{5.8}
$$

This observation will be used in the following in order to prove by contradiction that the optimal open-loop trajectory must stay close to the optimal trajectory for at least R time steps. Otherwise with $\bar{u}$ we would have constructed a better control sequence than u^*_{N,x_1}, violating the optimality of u^*_{N,x_1}. We abbreviate $r := \|x_1 - x^*(k)\|$. From the construction of $\bar{u}$ we know that

$$\|x_{\bar{u}}(j; k, x_1) - x^*(k + j)\| \leq \gamma_x(r) \text{ and } \|\bar{u}(j) - u^*(k + j)\| \leq \gamma_u(r)$$

for $j = \{0, \ldots, d - 1\}$, and similarly $\|x_{\bar{u}}(j; k, x_1) - x^*(k + j)\| \leq \gamma_x(\varepsilon)$ as well as $\|\bar{u}(j) - u^*(k+j)\| \leq \gamma_u(\varepsilon)$ for $j \in \{R-d, \ldots, R-1\}$. Additionally, we have $x_{\bar{u}}(j; k, x_1) = x^*(k+j)$

and $\bar{u}(j) = u^*(k + j)$ for $j \in \{d, \ldots, R - d - 1\}$. Recalling that the modified stage cost satisfies $\tilde{\ell}(k, x^*(k), u^*(k)) = 0$ (cf. Remark 4.31) and using Assumption 4.29, we thus get the following estimate for the modified cost functional with the control sequence $\bar{u}$:

$$
\begin{aligned}
\tilde{J}_R(k, x_1, \bar{u}) &= \sum_{j=0}^{R-1} \tilde{\ell}(k + j, x_{\bar{u}}(j; k, x_1), \bar{u}(j)) \\
&= \sum_{j=0}^{d-1} \underbrace{\tilde{\ell}(k + j, x_{\bar{u}}(j; k, x_1), \bar{u}(j))}_{\leq \alpha_u(|(x_{\bar{u}}(j;k,x_1),\bar{u}(j))|_{(x^*(k+j),u^*(k+j))})} + \underbrace{\sum_{j=d}^{R-d-1} \tilde{\ell}(k + j, x_{\bar{u}}(j; k, x_1), \bar{u}(j))}_{= 0} \\
&\quad + \sum_{j=R-d}^{R-1} \underbrace{\tilde{\ell}(k + j, x_{\bar{u}}(j; k, x_1), \bar{u}(j))}_{\leq \alpha_u(|(x_{\bar{u}}(j;k,x_1),\bar{u}(j))|_{(x^*(k+j),u^*(k+j))})} \\
&\leq \sum_{j=0}^{d-1} \alpha_u(\underbrace{|(x_{\bar{u}}(j; k, x_1), \bar{u}(j))|_{(x^*(k+j),u^*(k+j))}}_{\leq \gamma_x(r)+\gamma_u(r)}) \\
&\quad + \sum_{j=R-d}^{R-1} \alpha_u(\underbrace{|(x_{\bar{u}}(j; k, x_1), \bar{u}(j))|_{(x^*(k+j),u^*(k+j))}}_{\leq \gamma_x(\varepsilon)+\gamma_u(\varepsilon)}) \\
&\leq d\alpha_u(\gamma_x(r) + \gamma_u(r)) + d\alpha_u(\gamma_x(\varepsilon) + \gamma_u(\varepsilon))
\end{aligned}
\tag{5.9}
$$

Now assume that $|(x_{u^*_{N,x_1}}(\tilde{j}; k, x_1), u^*_{N,x_1}(\tilde{j}))|_{(x^*(k+\tilde{j}),u^*(k+\tilde{j}))} \geq \Delta$ holds for some $\tilde{j} \in \{0, \ldots, R - 1\}$ and $\Delta > \alpha_l^{-1}(d\alpha_u(\gamma_x(r) + \gamma_u(r)) + d\alpha_u(\gamma_x(\varepsilon) + \gamma_u(\varepsilon)))$. By adding up the modified stage cost of the control sequence u^*_{N,x_1} for R steps and using (4.69) and (5.9) we get the estimate

$$
\begin{aligned}
\tilde{J}_R(k, x_1, u^*_{N,x_1}) &= \sum_{j=0}^{R-1} \tilde{\ell}(k + j, x_{u^*_{N,x_1}}(j; k, x_1), u^*_{N,x_1}(j)) \\
&\overset{(4.69)}{\geq} \sum_{j=0}^{R-1} \alpha_l(|(x_{u^*_{N,x_1}}(j; k, x_1), u^*_{N,x_1}(j))|_{(x^*(k+j),u^*(k+j))}) \\
&\geq \alpha_l(\underbrace{|(x_{u^*_{N,x_1}}(\tilde{j}; k, x_1), u^*_{N,x_1}(\tilde{j}))|_{(x^*(k+\tilde{j}),u^*(k+\tilde{j}))}}_{>\Delta}) \\
&> d\alpha_u(\gamma_x(r) + \gamma_u(r)) + d\alpha_u(\gamma_x(\varepsilon) + \gamma_u(\varepsilon)) \overset{(5.9)}{\geq} \tilde{J}_R(k, x_1, \bar{u}).
\end{aligned}
$$

But this contradicts (5.8) and thus we get $\Delta \leq \alpha_l^{-1}(d\alpha_u(\gamma_x(r) + \gamma_u(r)) + d\alpha_u(\gamma_x(\varepsilon) + \gamma_u(\varepsilon)))$. Finally, choose $\varepsilon = \sigma(\frac{N}{2})$, which satisfies $\varepsilon \to 0$ for $N \to \infty$, and define $\eta(N, r) := \alpha_l^{-1}(d\alpha_u(\gamma_x(r) + \gamma_u(r)) + d\alpha_u(\gamma_x(\varepsilon) + \gamma_u(\varepsilon)))$. By choice of R we know that $R \geq N - P$, which for $P = \frac{N}{2}$ yields the assertion, i.e. $R \geq \frac{N}{2}$. It remains to ensure that $N - P = \frac{N}{2} \geq 2d$ as well as $\varepsilon \leq \delta_c$, which can be achieved by setting $N_1 \geq \max\{4d, 2\sigma^{-1}(\delta_c)\}$. $\qquad \square$

As a final assumption in order to prove continuity of the optimal value function we require the stage cost to be continuous.

Assumption 5.5 (Continuity of the stage cost)
We assume that the stage cost function ℓ is continuous at the optimal trajectory (x^*, u^*) in the sense that there exists $\eta_\ell \in \mathscr{K}_\infty$ such that for each $k \in \mathbb{N}_0$ and each compact set $\mathbb{Y} \subseteq \mathbb{X}(k) \times \mathbb{U}(k)$ the inequality

$$|\ell(k, x, u) - \ell(k, x^*(k), u^*(k))| \leq \eta_\ell(|(x, u)|_{(x^*(k), u^*(k))}) \tag{5.10}$$

holds for all $(x, u) \in \mathbb{Y}$.

The next theorem gives alternative conditions for the continuity property of the optimal value function $\hat{V}_N$ from Assumption 4.12.

Theorem 5.6 (Continuity property of the optimal value function)
Assume the optimal control problem (4.9) is strictly dissipative and Assumptions 4.29, 5.1, 5.3 and 5.5 are satisfied. Then for sufficiently large $N \in \mathbb{N}$ the finite horizon optimal value function $\hat{V}_N$ is continuous in the sense of Assumption 4.12.

Proof. [2] We start with a brief outline of the proof. We need to show that the value of $\hat{V}_N$ changes only slightly if we consider states close to the optimal trajectory x^*. For this we pick a point x_1 on the optimal trajectory and another point x_2 in a neighborhood of x_1. Then, we construct a control sequence that steers the state from x_2 to a state x_3 on the optimal open-loop trajectory starting at x_1 (cf. Figure 5.3). We can show that the cost of this specially constructed control sequence can be (approximately) bounded by the optimal value function at x_1. This also transfers to the optimal value function at x_2. Let $k \geq 0$ and pick $\delta \in (0, \delta_c]$ with δ_c from Assumption 5.3. To shorten the notation we write $x_1 = x^*(k)$ and choose $x_2 \in \mathscr{B}_\delta(x_1) \cap \mathbb{X}(k)$. Let $N \in \mathbb{N}$ and denote the optimal control sequence for N steps starting in x_1 by u^*_{N,x_1}, and the one starting in x_2 by u^*_{N,x_2}. According to Lemma 5.4 we can choose $N \geq N_1$ sufficiently large and $\delta \in (0, \delta_c]$ such that both

$$|(x_{u^*_{N,x_1}}(j; k, x_1), u^*_{N,x_1}(j))|_{(x^*(k+j), u^*(k+j))} \leq \eta(N, \|x_1 - x^*(k)\|) \leq \eta(N, \delta) \leq \delta_c$$

and

$$|(x_{u^*_{N,x_2}}(j; k, x_2), u^*_{N,x_2}(j))|_{(x^*(k+j), u^*(k+j))} \leq \eta(N, \|x_2 - x^*(k)\|) \leq \eta(N, \delta) \leq \delta_c$$

hold for all $j \in \{0, \ldots, R\}$. This means both trajectories $x_{u^*_{N,x_1}}$ and $x_{u^*_{N,x_2}}$ will initially be close to the optimal trajectory (for at least R steps). From the proof of Lemma 5.4 we also know that $R \geq 2d > d$.
Next, we show that the cost of the initial piece (for d steps) of the optimal trajectory starting in x_1 is approximately the same as the cost along the optimal trajectory (x^*, u^*).

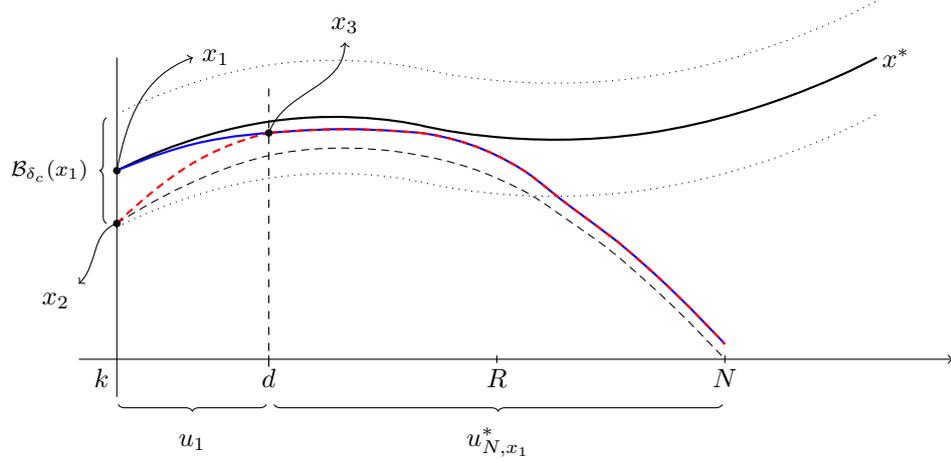[2]The idea is similar to the proof of Theorem 16 in [84].

Figure 5.3: Illustration for the proof of the continuity property of Theorem 5.6.

Define $\varepsilon := \eta(N, \delta)$, $\hat{\delta} := \max\{\delta, \varepsilon\}$ and let $x_3 := x_{u^*_{N,x_1}}(d; k, x_1)$. Because of Assumption 5.5 we know that

$$|\ell(k + j, x_{u^*_{N,x_1}}(j; k, x_1), u^*_{N,x_1}(j)) - \ell(k + j, x^*(k + j), u^*(k + j))|$$
$$\leq \eta_\ell(|(x_{u^*_{N,x_1}}(j; k, x_1), u^*_{N,x_1}(j))|_{(x^*(k+j), u^*(k+j))}) \leq \eta_\ell(\varepsilon).$$

This leads to the estimate

$$\sum_{j=0}^{d-1} \underbrace{\ell(k + j, x_{u^*_{N,x_1}}(j; k, x_1), u^*_{N,x_1}(j))}_{\geq \ell(k+j, x^*(k+j), u^*(k+j)) - \eta_\ell(\varepsilon)} \geq J^*_d(k) - d\eta_\ell(\varepsilon). \tag{5.11}$$

A similar relation holds for a control sequence that steers the state from x_2 to the optimal open-loop trajectory starting in x_1: We can apply Assumption 5.3 with $x = x_2$, $y = x_3$ to conclude that there exists a control sequence $u_1 \in \mathbb{U}^d$ such that $x_{u_1}(d, x_2) = x_3$ and the estimate

$$|\ell(k + j, x_{u_1}(j, x_2), u_1(j)) - \ell(k + j, x^*(k + j), u^*(k + j))|$$
$$\leq \gamma_c(\max\{\|x_2 - x^*(k)\|, \|x_3 - x^*(k + d)\|\}) \leq \gamma_c(\hat{\delta})$$

holds for all $j \in \{0, \dots, d - 1\}$. This yields

$$\sum_{j=0}^{d-1} \underbrace{\ell(k + j, x_{u_1}(j; k, x_2), u_1(j))}_{\leq \ell(k+j, x^*(k+j), u^*(k+j)) + \gamma_c(\hat{\delta})} \leq J^*_d(k) + d\gamma_c(\hat{\delta}). \tag{5.12}$$

Now we construct a control sequence $\bar{u} \in \mathbb{U}^N$ as follows:

$$\bar{u}(j) = \begin{cases} u_1(j), & \text{for } j \in \{0, \dots, d - 1\}, \\ u^*_{N,x_1}(j), & \text{for } j \in \{d, \dots, N - 1\}. \end{cases} \tag{5.13}$$

Note that by construction of $\bar{u}$ the trajectories $x_{\bar{u}}(j;k,x_2)$ and $x_{u_{N,x_1}^*}(j;k,x_1)$ coincide for $j \in \{d,\dots,N\}$. For the cost of this composite control sequence we obtain

$$V_N(k,x_2) \leq J_N(k,x_1,\bar{u})$$

$$= \sum_{j=0}^{d-1} \ell(k+j,x_{\bar{u}}(j;k,x_2),\bar{u}(j)) + \sum_{j=d}^{N-1} \ell(k+j,x_{\bar{u}}(j;k,x_2),\bar{u}(j))$$

$$= \underbrace{\sum_{j=0}^{d-1} \ell(k+j,x_{u_1}(j;k,x_2),u_1(j))}_{\overset{(5.12)}{\leq} J_d^*(k)+d\gamma_c(\hat{\delta})} - \underbrace{\sum_{j=0}^{d-1} \ell(k+j,x_{u_{N,x_1}^*}(j;k,x_1),u_{N,x_1}^*(j))}_{\overset{(5.11)}{\geq} J_d^*(k)-d\eta_\ell(\varepsilon)}$$

$$+ \sum_{j=0}^{N-1} \ell(k+j,x_{u_{N,x_1}^*}(j;k,x_1),u_{N,x_1}^*(j))$$

$$\leq V_N(k,x_1) + d(\gamma_c(\hat{\delta}) + \eta_\ell(\varepsilon)),$$

where the last and the first inequality follow from the optimality of u_{N,x_1}^* and suboptimality of $\bar{u}$, respectively. Setting $\tilde{\gamma}_V(N,\delta) = d(\gamma_c(\hat{\delta}) + \eta_\ell(\varepsilon)))$ and using the definition of $\hat{V}_N$ then yields

$$\hat{V}_N(k,x_2) \leq \hat{V}_N(k,x_1) + \tilde{\gamma}_V(N,\delta). \tag{5.14}$$

Observe that $\tilde{\gamma}_V \to 0$ if both $N \to \infty$ and $\delta \to 0$. Finally, to get the required monotonicity we define

$$\gamma_V(N,r) := \sup_{\tilde{N} \geq N, \tilde{\delta} \leq r} \tilde{\gamma}_V(\tilde{N},\tilde{\delta}),$$

for which (5.14) remains true. The converse inequality follows by exchanging the roles of x_1 and x_2 which concludes the proof.   □

5.1.3 From optimality conditions to dissipativity

The previous section used strict dissipativity as a key ingredient to establish both the turnpike property and continuity of the optimal value function. In this section we show how strict dissipativity, in turn, can be established from optimality conditions for the infinite horizon optimal control problem (4.9).

The proof extends those for discounted and non-discounted time-invariant optimal control problems, see [46] and [23]. The optimality conditions in the literature which most easily lead to the desired result are those derived in [17, Theorem 2.2], which we will hence use in the sequel. However, we believe that using other optimality conditions strict dissipativity can be proved, too. We will elaborate more on this with respect to the results stated in [11] at the end of the section.

To be consistent with [17, Theorem 2.2], let us assume that $X = \mathbb{R}^n$ and $U = \mathbb{R}^m$ and that no constraints are imposed on the state and control variables. We first define the Hamiltonian which is essential for deriving optimality conditions.

Definition 5.7 (Hamiltonian)
For all times $k \in \mathbb{N}_0$ the Hamiltonian $H_k : X \times U \times \mathbb{R}^n \times \mathbb{R} \to \mathbb{R}$ of problem (4.9) is defined by

$$H_k(x, u, p, \eta) := -\eta \ell(k, x, u) + p^T f(k, x, u).$$

Below, we state [17, Theorem 2.2] in our notation. Note that the sign of ℓ has been changed in the definition above and theorem below because we are considering minimization problems here.

Theorem 5.8 (Optimality conditions, cf. [17, Theorem 2.2])
Let (x^*, u^*) be an overtaking optimal pair for (4.9). If it holds:

1. *For all $k \in \mathbb{N}_0$ the functions $\ell(k, \cdot, \cdot)$ and $f(k, \cdot, \cdot)$ are continuous on a neighborhood of (x^*, u^*) and differentiable at (x^*, u^*).*

2. *For all $k \in \mathbb{N}_0$ the partial differential $\frac{\partial f}{\partial x}(k, x^*(k), u^*(k)) \in \mathbb{R}^{n \times n}$ is invertible.*

Then, there are $\eta_0 \in \mathbb{R}$, and $p_{k+1} \in \mathbb{R}^n$ for all $k \in \mathbb{N}_0$ satisfying the following conditions:

1. *$(\eta_0, p_1) \neq (0, 0)$.*

2. *$\eta_0 \geq 0$.*

3. *For all $k \in \mathbb{N}_0$ it holds*

$$p_k = p_{k+1}^T \frac{\partial f}{\partial x}(k, x^*(k), u^*(k)) - \eta_0 \frac{\partial \ell}{\partial x}(k, x^*(k), u^*(k)).$$

4. *For all $k \in \mathbb{N}_0$ it holds $\frac{\partial H_k}{\partial u}(x^*(k), u^*(k), p_{k+1}, \eta_0) = 0$.*

In what follows, structural assumptions on the optimal control problems are imposed.

Assumption 5.9 (Uniform strict convexity)
We assume that the dynamics $f(k, \cdot, \cdot)$ are affine for each $k \in \mathbb{N}_0$. We also assume that there is $\kappa \in \mathbb{R}_{>0}$ and $F \in \mathscr{K}_\infty$ such that for all $k \in \mathbb{N}_0$ it holds

$$\ell(k, t(x_1, u_1) + (1-t)(x_2, u_2)) \leq t\ell(k, x_1, u_1) + (1-t)\ell(k, x_2, u_2)$$
$$- \frac{\kappa}{2} t(1-t) F(\|(x_1, u_1) - (x_2, u_2)\|) \tag{5.15}$$

for all $(x_1, u_1), (x_2, u_2) \in X \times U$ and $t \in [0, 1]$.

Remark 5.10
It follows from the definitions, that strong convexity *(see e.g. [87] for a definition) implies* (5.15) *and this property itself implies strict convexity.* ◇

Theorem 5.11 (Optimality conditions imply strict dissipativity)
Let Assumption 5.9 and those of Theorem 5.8 hold. If $\eta_0 \neq 0$ and $\sup_{k \in \mathbb{N}_0} \|p_k\| < \infty$, then the optimal control problem (4.9) *is strictly dissipative on every bounded set[3] $\mathbb{X}_0$ with respect to the supply rate $s(k, x, u) = \hat{\ell}(k, x, u)$ and the optimal pair (x^*, u^*).*

Proof. In order to prove strict dissipativity we have to verify that there exists $\alpha \in \mathcal{K}_\infty$ and a storage function λ such that (4.43) holds. We claim that the candidate $\lambda(k, x) = \frac{1}{\eta_0} p_k^T (x - x^*(k))$ yields the desired property. Note that the restriction to bounded sets $\mathbb{X}_0$ is needed here in order to ensure that λ is bounded from below as required in Assumption 4.23.

Let $\mathbb{X}_0$ be an arbitrary bounded set in $\mathbb{R}^n$. This yields boundedness of λ. Conditions (3.) and (4.) in Theorem 5.8 read

(3.) $\forall k \in \mathbb{N}_0 : p_k = -\eta_0 \frac{\partial \ell}{\partial x}(k, x^*(k), u^*(k)) + p_{k+1}^T \frac{\partial f}{\partial x}(k, x^*(k), u^*(k))$ and

(4.) $\forall k \in \mathbb{N}_0 : -\eta_0 \frac{\partial \ell}{\partial u}(k, x^*(k), u^*(k)) + p_{k+1}^T \frac{\partial f}{\partial u}(k, x^*(k), u^*(k)) = 0.$

Let us consider the modified stage cost $\tilde{\ell}$ (cf. Definition 4.26) using our ansatz for the storage function:

$$
\begin{aligned}
\tilde{\ell}(k, x, u) &= \hat{\ell}(k, x, u) + \frac{1}{\eta_0} p_k^T (x - x^*(k)) - \frac{1}{\eta_0} p_{k+1}^T (f(k, x, u) - x^*(k+1)) \\
&= \ell(k, x, u) - \ell(k, x^*(k), u^*(k)) \\
&\quad + \frac{1}{\eta_0} p_k^T (x - x^*(k)) - \frac{1}{\eta_0} p_{k+1}^T (f(k, x, u) - x^*(k+1))
\end{aligned}
$$

Since ℓ is uniformly strictly convex with respect to κ and F, p_k linear and f affine for each k, the modified cost $\tilde{\ell}$ is uniformly strictly convex with respect to κ and F (and in particular strictly convex for all $k \in \mathbb{N}_0$). This means that a point $(\bar{x}(k), \bar{u}(k))$ satisfying $\frac{\partial \tilde{\ell}}{\partial x}(k, \bar{x}(k), \bar{u}(k)) = \frac{\partial \tilde{\ell}}{\partial u}(k, \bar{x}(k), \bar{u}(k)) = 0$ is a unique strict minimizer of $\tilde{\ell}(k, \cdot, \cdot)$. Let us therefore consider the partial derivatives of $\tilde{\ell}$. For all $k \in \mathbb{N}_0$ we have

$$
\begin{aligned}
\frac{\partial \tilde{\ell}}{\partial x}(k, x, u) &= \frac{\partial \ell}{\partial x}(k, x, u) + \frac{1}{\eta_0} p_k - \frac{1}{\eta_0} p_{k+1}^T \frac{\partial f}{\partial x}(k, x, u) \text{ and} \\
\frac{\partial \tilde{\ell}}{\partial u}(k, x, u) &= \frac{\partial \ell}{\partial u}(k, x, u) - \frac{1}{\eta_0} p_{k+1}^T \frac{\partial f}{\partial u}(k, x, u).
\end{aligned}
$$

Now plugging in $(x^*(k), u^*(k))$ and conditions (3.) and (4.) for the first and second equation, respectively, we obtain

$$
\frac{\partial \tilde{\ell}}{\partial x}(k, x^*(k), u^*(k)) = 0 \text{ and } \frac{\partial \tilde{\ell}}{\partial u}(k, x^*(k), u^*(k)) = 0.
$$

---

[3]This means that dissipativity holds for all $x \in \mathbb{X}_0$.

For each $k \in \mathbb{N}_0$ the point $(x^*(k), u^*(k))$ is thus the unique strict minimizer of $\tilde{\ell}$ at time k. By definition of the modified stage cost $\tilde{\ell}$ we have

$$\tilde{\ell}(k, x^*(k), u^*(k)) = \hat{\ell}(k, x^*(k), u^*(k)) + \lambda(k, x^*(k)) - \lambda(k+1, f(k, x^*(k), u^*(k)))$$

$$= \frac{1}{\eta_0} p_k^T (x^*(k) - x^*(k)) - \frac{1}{\eta_0} p_{k+1}^T (f(k, x^*(k), u^*(k)) - x^*(k+1))$$

$$= 0.$$

Fix an arbitrary $t \in (0, 1)$. For $k \in \mathbb{N}_0$ consider an arbitrary point $(x, u) \in X \times U$. We define $(\bar{x}, \bar{u}) := t(x, u) + (1-t)(x^*(k), u^*(k)) \in X \times U$. Assumption 5.9 implies

$$\tilde{\ell}(k, \bar{x}, \bar{u}) + \frac{\kappa}{2} t(1-t) F(\|(x, u) - (x^*(k), u^*(k))\|)$$

$$\leq t\tilde{\ell}(k, x, u) + (1-t)\tilde{\ell}(k, x^*(k), u^*(k)) = t\tilde{\ell}(k, x, u)$$

$$\Rightarrow \tilde{\ell}(k, x, u) > \frac{1}{t}\tilde{\ell}(k, x^*(k), u^*(k)) + \frac{\kappa}{2}(1-t) F(\|(x, u) - (x^*(k), u^*(k))\|)$$

$$= \frac{\kappa}{2}(1-t) F(\|(x, u) - (x^*(k), u^*(k))\|).$$

This implies (4.43) if we set $\alpha(r) := \frac{\kappa}{2}(1-t)F(r)$, which is of class $\mathscr{K}_\infty$ because $F \in \mathscr{K}_\infty$ and $\frac{\kappa}{2}(1-t) \in \mathbb{R}_{>0}$. $\qquad\square$

Remark 5.12
The assumption of ℓ being uniformly strictly convex is needed in order to establish that $\alpha \in \mathscr{K}_\infty$ in (4.43) does not depend on the time k. $\qquad\diamond$

Discussion

As indicated at the beginning of the section the optimality conditions of the reference [17, Theorem 2.2] fit our purpose very well but are just exemplary and we conjecture that alternative conditions can also be taken to establish strict dissipativity and thus the turnpike property. We will point out similarities and differences of the conditions above with those in [11]. Firstly, let us mention that an important part of [11] is that the authors are able to establish a *transversality condition.* Such conditions are a valuable tool to restrict the set of candidates of optimal solutions to the infinite-horizon optimal control problem and, moreover, can be used in order to ensure $\sup_{k \in \mathbb{N}_0} \|p_k\| < \infty$ in Theorem 5.11. A comparable result does not exist in [17, Section 2.2] (but in other results in that reference).

The assumptions that are imposed in [11, 17] are in general difficult to compare. However, the main assumption (Assumption A) in [11] can be simplified if Condition 2 in Theorem 5.8 holds. Moreover, reference [11] assumes weakly overtaking optimality whereas the theorem we used from [17] assumes overtaking optimality. The statements in the theorems are strongly related: Condition (3.) in Theorem 5.8 is the same as [11, Corollary 2.3],

and Condition (4.) is similar to the maximum condition in [11, Theorem 2.2], that reads (adapted to our notation)

$$\forall\, k \in \mathbb{N}_0 : \left(-\frac{\partial \ell}{\partial u}(k, x^*(k), u^*(k)) + p_{k+1}^T \frac{\partial f}{\partial u}(k, x^*(k), u^*(k)) \right) v \leq 0 \qquad (5.16)$$

$\forall v \in T_{U_k}(u^*(k))$. The set $T_{U_k}(u^*(k))$ denotes the Bouligand tangent cone of U_k (the constraint set for u at time k in [11]) at point $u^*(k)$. Certainly, (5.16) is obtained under weaker assumptions than [17, Theorem 2.2], yet it also yields a weaker statement and it is currently an open question whether it is still sufficient to prove strict dissipativity.

To summarize, in the previous sections we have established alternative conditions for our essential assumptions, namely the turnpike and the continuity property. Admittedly, the question might arise what we have gained by seemingly replacing those conditions by others. To demonstrate that the alternative conditions can be verified rigorously we will consider two examples in the following section.

5.1.4 Examples

We revisit Example 4.18 which was already considered in Chapter 4. Before, we only showed that the MPC closed-loop cost and the trajectories converge using numerical simulations. This time we verify that the example meets the assumptions needed for strict dissipativity as well as the continuity and turnpike properties. The latter will also be illustrated by numerical simulations.

Example 5.13 (Turnpike for scalar example)
Consider again the system from Example 4.18, i.e.

$$x(k + 1) = f(k, x(k), u(k)) = x(k) + u(k) + w(k)$$

with $w(k) = -2 \sin\left(\frac{k\pi}{12}\right) + a_k$ and in which the a_k are random numbers on the interval $[-\frac{1}{4}, \frac{1}{4}]$. We consider a regularized stage cost

$$\ell(k, x, u) = u^2 + \varepsilon x^2,$$

for $0 < \varepsilon \ll 1$. The regularization term εx^2 renders the original cost u^2, that was used in Example 4.18, strictly convex with respect to x and u. However, numerical experiments show, that the optimal trajectories for both the original version of ℓ from Example 4.18 and the regularized stage cost do not differ perceptibly for sufficiently small ε.
Recall that the system has to be operated subject to the control constraints $\mathbb{U}(k) = [-3, 3]$ and the state constraints $\mathbb{X}(k) = [-1/2, 1/2]$ if $k \in [24j + 12, 24(j + 1))$, $j \in \mathbb{N}_0$ and $\mathbb{X}(k) = [-2, 2]$ if $k \in [24j, 24j + 12)$. We assume that we have a perfect prediction of the external influence $w(k)$, which means that its values are known beforehand whenever we optimize. Since a correct weather forecast is hardly possible for a few days, let alone on an

infinite horizon, this may not be realistic. However, a verification of the turnpike property allows us to apply the MPC algorithm, and so only finite horizon problems of moderate horizon length have to be solved.

Strict dissipativity*:*
We will first show that the system is strictly dissipative. For this we show that Assumption 5.9 is satisfied and optimality conditions of Theorem 5.8 hold, from which we then conclude strict dissipativity by Theorem 5.11.

Since the results were stated for unconstrained problems, we first rewrite the example above using penalty functions $b_1 : \mathbb{N}_0 \times \mathbb{R} \to \mathbb{R}_{\geq 0}$ and $b_2 : \mathbb{N}_0 \times \mathbb{R} \to \mathbb{R}_{\geq 0}$. Then, the reformulated stage cost is given as follows (the dynamics remain unchanged):

$$L(k, x, u) := \ell(k, x, u) + b_1(k, x) + b_2(k, u), \tag{5.17}$$

$$b_1(k, x) = \begin{cases} c_x(|x| - 2)^4 & , x \notin [-2, 2] \\ 0 & , x \in [-2, 2] \end{cases}, \ k \in [24j, 24j + 12), \ j \in \mathbb{N}_0,$$

$$b_1(k, x) = \begin{cases} c_x(|x| - 1/2)^4 & , x \notin [-1/2, 1/2] \\ 0 & , x \in [-1/2, 1/2] \end{cases}, \ k \in [24j + 12, 24(j + 1)), \ j \in \mathbb{N}_0,$$

$$b_2(k, u) = \begin{cases} c_u(|u| - 3)^4 & , u \notin [-3, 3] \\ 0 & , u \in [-3, 3] \end{cases}, \ k \in \mathbb{N}_0,$$

with c_x and $c_u \in \mathbb{R}_{>0}$.
We claim, that the reformulated optimal control problem satisfies Assumption 5.9, i.e. uniform strict convexity. It is clear that for predictable a_k the dynamics are affine for each $k \in \mathbb{N}_0$. The Hessian of the stage cost reads

$$H_{(x,u)}L(k, x, u) = \begin{pmatrix} 2\varepsilon + \frac{d^2 b_1}{dx^2}(k, x) & 0 \\ 0 & 2 + \frac{d^2 b_2}{du^2}(k, u) \end{pmatrix}.$$

It is easily seen, that $\frac{d^2 b_1}{dx^2}(k, x) \geq 0$ and $\frac{d^2 b_2}{du^2}(k, u) \geq 0$ for all $k \in \mathbb{N}_0$, $x \in \mathbb{R}$ and $u \in \mathbb{R}$ such that we can conclude positive semidefiniteness of the matrix $H_{(x,u)}L(k, x, u) - 2\varepsilon I$, in which I is the identity matrix of dimension 2. For twice continuously differentiable functions this property is equivalent to L being strongly convex with respect to 2ε (see e.g. [87]) for all $k \in \mathbb{N}_0$ and this implies uniform strict convexity of L with respect to $\kappa = 2\varepsilon$ and $F(r) = r^2$.
Let us now check the assumptions of Theorem 5.8. Clearly, the continuity and differentiability requirements are met. The second condition also holds because $\frac{\partial f}{\partial x}(k, x, u) = 1$. For this example it moreover holds that $\eta_0 \neq 0$: If $\eta_0 = 0$ then Theorem 5.8 yields that $p_1 \neq 0$. From condition (3.) applied to this example we get $p_k = p_{k+1}$ for all $k \in \mathbb{N}_0$. This contradicts (4.), which in case $\eta_0 = 0$ implies $p_{k+1} = 0$. It is left to show that the adjoints p_k are bounded. A formal proof appears technically involved, however, we can give evidence why it is reasonable to expect bounded p_k. The adjoint p_k is a measure of how much

the value of the trajectory differs from the optimal value if the trajectory value at time k differs (slightly) from $x^*(k)$. In our example the absence of constraints allows to steer the trajectory to $x^*(k+1)$ in one step after having been disturbed at time k. Thus, the value of the disturbed trajectory and the optimal trajectory only differ in the first term and this difference can be estimated on bounded sets by a bound which is independent of k. This implies boundedness of the p_k and thus by Theorem 5.8 strict dissipativity for our example.

Turnpike property:
Next, we will investigate Assumption 5.1, i.e. cheap reachability, to conclude by Theorem 5.2 that the example exhibits the turnpike property on any compact set $\mathbb{X}_0 \subset \mathbb{R}^n$. We first show that the optimal pair (x^*, u^*) satisfies the (uniform) estimates

$$|x^*(k)| \leq \sqrt[4]{\frac{81 - 4\varepsilon}{16c_x}} + 2 \tag{5.18}$$

and

$$|u^*(k)| \leq \sqrt[4]{\frac{81 - 4\varepsilon}{16c_u}} + 3. \tag{5.19}$$

The idea of the proof is as follows: We compare the cost of an admissible trajectory that is constructed such that it is constantly zero after the first time step, to the cost of the optimal pair. If the estimates above are violated this contradicts the fact that (x^*, u^*) is overtaking optimal. For cheap reachability we need to show that there exists $E \in \mathbb{R}$ such that for all $k \in \mathbb{N}_0$, $x \in \mathbb{X}_0$ and $N \in \mathbb{N} \cup \{\infty\}$ it holds $\hat{V}_N(k, x) \leq E$. To see this we consider a control sequence $\tilde{u}(\cdot)$ of length N given by $\tilde{u}(0) = -x + x^*(k+1) - w(k)$, $\tilde{u}(j) = u^*_{N-1, x^*(k+1)}(j-1)$, $j \in \{1, \ldots, N-1\}$. This yields

$$\hat{V}_N(k, x) \leq \hat{\ell}(k, x, \tilde{u}(0)) + \underbrace{\hat{V}_{N-1}(k+1, x^*(k+1))}_{\leq 0} \leq \ell(k, x, \tilde{u}(0)) - \underbrace{\ell(k, x^*(k), u^*(k))}_{\geq 0}$$

$$\leq \varepsilon x^2 + (-x + x^*(k+1) - w(k))^2 + b_1(k, x) + b_2(k, -x + x^*(k+1) - w(k)).$$

Using compactness of $\mathbb{X}_0$, boundedness of $(w(k))_{k \in \mathbb{N}_0}$, $(x^*(k))_{k \in \mathbb{N}_0}$ and $(u^*(k))_{k \in \mathbb{N}_0}$, the fact that the b_i can be bounded uniformly in k using (5.18), (5.19) we obtain a bound E that does not depend on k, x and N and conclude the assertion. To summarize, this means by Theorem 5.2 the turnpike property holds for this problem.

Continuity of the optimal value function:
Finally, we check if the continuity property is also satisfied by checking the assumptions of Theorem 5.6. We claim, that Assumption 5.3 holds with $d = 1$ and arbitrary but fixed $\delta_c > 0$. Let $x \in \mathscr{B}_{\delta_c}(x^*(k))$ and $y \in \mathscr{B}_{\delta_c}(x^*(k+1))$ and consider $\delta := \max\{|x - x^*(k)|, |y - x^*(k+1)|\}$. Since no constraints are imposed in the example (after the reformulation in (5.17)), any two points x and y in a δ_c-ball around the optimal trajectory at time k and $k+1$, respectively, can be connected in one step applying the control $u = y - x - w(k)$.

For $\gamma_x(r) := r$ the estimate

$$|x_u(0; k, x) - x^*(k)| = |x - x^*(k)| \leq \delta = \gamma_x(\delta) \tag{5.20}$$

is obviously satisfied. In addition, it holds

$$
\begin{aligned}
|u - u^*(k)| &= |y - x - w(k) - u^*(k)| \\
&\leq |y - x^*(k+1)| + |x^*(k) - x| + |\underbrace{x^*(k+1) - x^*(k) - w(k) - u^*(k)}_{=0}| \\
&\leq 2\delta,
\end{aligned}
$$

which means that we can choose $\gamma_u(r) := 2r$. The stage cost L is locally Lipschitz with constant $L_c > 0$ and hence

$$
\begin{aligned}
|\hat{\ell}(k, x, u)| &= |L(k, x, u) - L(k, x^*(k), u^*(k))| \leq L_c\|(x, u) - (x^*(k), u^*(k))\| \\
&\leq L_c \delta \sqrt{5}.
\end{aligned}
$$

Choosing $\gamma_c(r) := L_c\sqrt{5}\,r$ now yields that all requirements of Assumption 5.3 are met. Assumption 4.29 holds on compact sets under the assumption that the p_k are bounded. This assumption is justified as explained above in the proof of strict dissipativity. In conjunction with the previous considerations, we have thus verified all the assumptions of Theorem 5.6 from which continuity of the optimal value function $\hat{V}_N$ follows.

Alternatively, the continuity assumption of the optimal value functions can also be proved directly as follows: Consider $x_1 := x^*(k)$ and the corresponding optimal control sequence u^*_{N,x_1}. Let $x \in \mathcal{B}_\varepsilon(x_1) \cap \mathbb{X}(k)$ and construct a control sequence $\tilde{u} \in U^N$ by

$$
\tilde{u}(j) := \begin{cases} x_1 - x + u^*_{N,x_1}(0), & j = 0 \\ u^*_{N,x_1}(j), & j = 1, \ldots, N-1. \end{cases}
$$

By construction, the trajectories $x_{\tilde{u}}$ and $x_{u^*_{N,x_1}}$ coincide for all except the first time instant. Thus, we have

$$
\begin{aligned}
\hat{V}_N(k, x) - \hat{V}_N(k, x_1) &\leq J_N(k, x, \tilde{u}) - J_N(k, x_1, u^*_{N,x_1}) \\
&= (\underbrace{x_1 - x}_{=:r} + u^*_{N,x_1}(0))^2 - u^*_{N,x_1}(0)^2 = r^2 + 2r u^*_{N,x_1}(0) \\
&\leq r^2 + (6 + 2\sqrt[4]{\frac{81 - 4\varepsilon}{16 c_u}})|r| := \gamma_V(N, r),
\end{aligned}
$$

using that $u^*_{N,x_1}(0)$ is uniformly bounded for all $N \in \mathbb{N}$ and fixed $c_u > 0$, $0 < \varepsilon < 1$. Observing that $\gamma_V(N, r) \to 0$ for $r \to 0$ yields the desired continuity. The continuity of $\hat{V}_\infty$ follows similarly.

Consequently, since both the turnpike and the continuity properties are satisfied, from Theorem 4.16 we can conclude that the MPC closed loop cost approximates the cost of an infinite horizon optimal trajectory.

Numerical simulations:
On top of the numerical results from Examples 4.18 and 4.41 here we present several simulations illustrating that the system in the example has the turnpike property. For the purpose of the simulations the trajectory of optimal operation on an infinite horizon has been approximated by computing an optimal trajectory on a large finite horizon of $N = 100$ and leaving the initial value free. In the figures this trajectory is depicted in black. The regularization factor was chosen as $\varepsilon = 10^{-10}$ and the penalty parameters as $c_x = c_u = 10^{10}$. Figure 5.4 depicts open-loop trajectories of the state for different horizon lengths. As one can see the trajectories are close to the trajectory of optimal operation most of the time. It is also visible that the finite horizon trajectories will at some point turn away from the optimal trajectory and hit the constraints. This is due to the fact that it is cheaper to deviate from the infinite horizon optimal trajectory than it would be to stay close to it. Such a behavior is characteristic for the turnpike property.
In Figure 5.5 open-loop trajectories for different initial values and fixed horizon length of $N = 48$ are shown. One observes that the open-loop solutions quickly converge to the trajectory of optimal operation.

With our additional insight gained from this chapter we can also take another look at Example 4.43 in order to investigate in more detail, why MPC does not work there.

Example 5.14 (Example 4.43 revisited)
Consider again the system from Example 4.43. It is obvious that the turnpike assumption is violated since all finite optimal open-loop trajectories immediately leave the optimal trajectory (x^*, u^*) and can never return. Thus, from Theorem 5.2 we know that dissipativity or cheap reachability are violated. In fact, in this example neither assumption holds:

Strict dissipativity:
To see that strict dissipativity does not hold let $N > 0$ be arbitrary and consider the dissipation inequality (4.43) at the initial state $x = x(0) = 0$ and a control $u(0) \neq 0$ such that $u(0) > N$. The dissipation inequality then reads

$$\lambda(1, \underbrace{f(0, x, u)}_{=:x(1)}) - \lambda(0, x) \leq \ell(0, x, u) - \ell(0, x^*(0), u^*(0)) - \alpha(|(x, u)|_{(x^*(0), u^*(0))}).$$

Without loss of generality we can assume that $\lambda(0, 0) = 0$, otherwise λ can just be shifted such that this holds. Substituting the values for the stage cost function yields

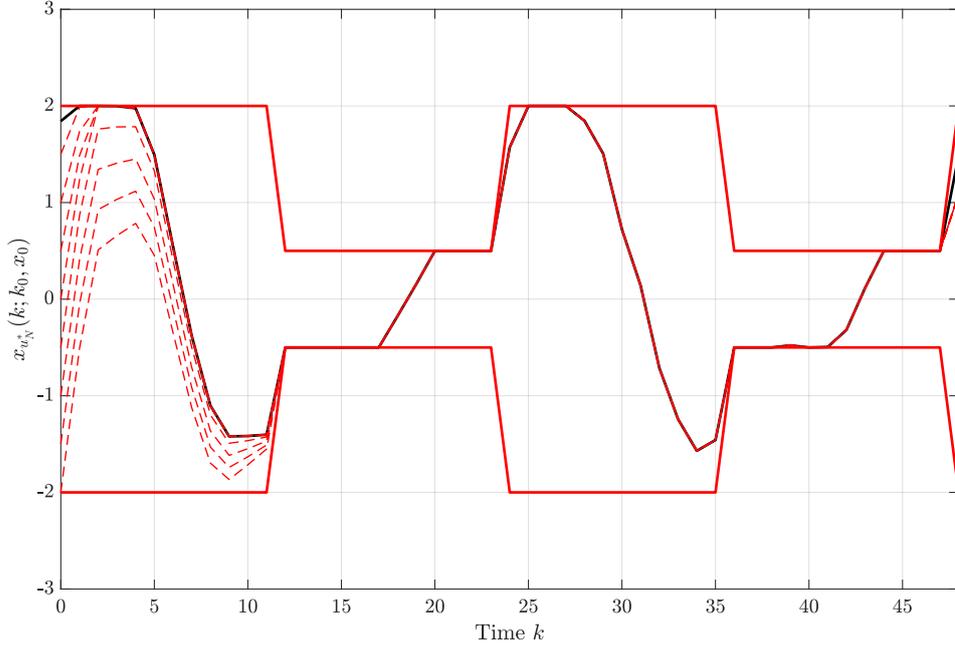$$\lambda(1, x(1)) \leq 0 - 1 - \underbrace{\alpha(|(x, u)|_{(x^*(0), u^*(0))})}_{\geq 0} \leq -1.$$
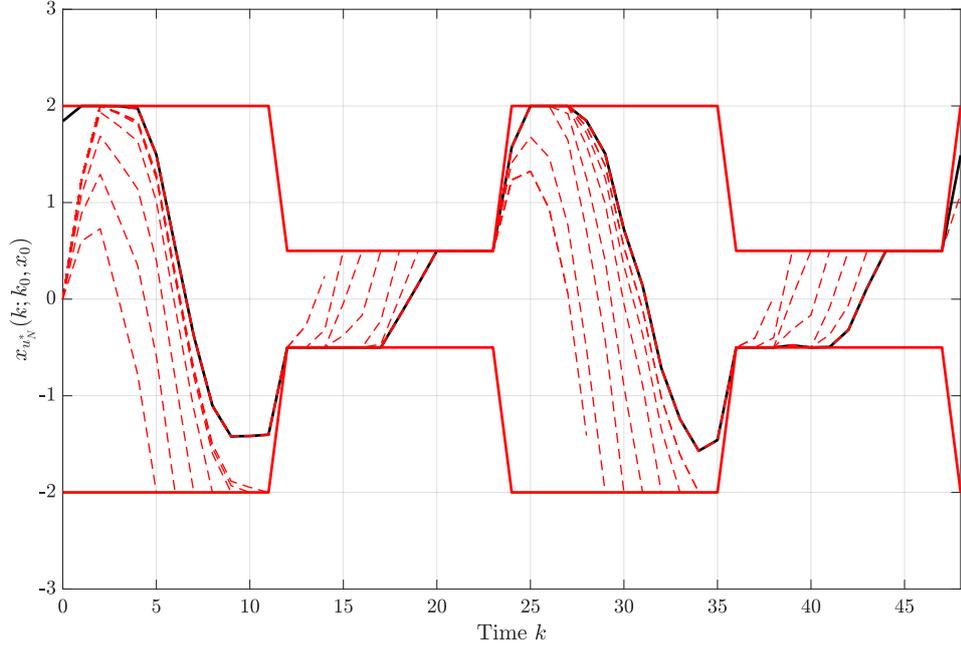
Figure 5.4: Numerical simulations of the trajectory of optimal operation (black line) and open-loop trajectories of the state (dashed red lines) with different fixed initial value $x_0 = 0$ and different horizon lengths of N.

At the next time step from the dissipation inequality we have

$$\lambda(2, \underbrace{f(1, x(1), u(1))}_{=:x(2)}) - \lambda(1, x(1)) \leq \ell(1, x(1), u(1)) - \ell(1, x^*(1), u^*(1)) - \alpha(|(x(1), u(1))|_{(x^*(1), u^*(1))})$$

for some arbitrary control $u(1)$ or equivalently

$$\lambda(2, x(2)) \leq \lambda(1, x(1)) + \ell(1, x(1), u(1)) - \ell(1, x^*(1), u^*(1)) - \alpha(|(x(1), u(1))|_{(x^*(1), u^*(1))}).$$

Because of the choice of $u(0)$ in the initial step we have $\ell(1, x(1), u(1)) = 0$. This means we can estimate

$$\lambda(2, x(2)) \leq \underbrace{\lambda(1, x(1))}_{\leq -1} + \underbrace{\ell(1, x(1), u(1))}_{=0} - \underbrace{\ell(1, x^*(1), u^*(1))}_{=1} - \underbrace{\alpha(|(x(1), u(1))|_{(x^*(1), u^*(1))})}_{\geq 0} \leq -2.$$

Proceeding in this fashion up to the time point N we obtain the bound

$$\lambda(N, x(N)) \leq -N.$$

Since N was chosen as an arbitrary number this contradicts our assumption that the storage function is bounded from below and thus strict dissipativity does not hold.

Figure 5.5: Numerical simulations of the trajectory of optimal operation (black line) and open-loop trajectories of the state (dashed red lines) with different initial values x_0 and fixed horizon length of $N = 48$.

Cheap reachability:

The violation of cheap reachability is also proved by contradiction: Assume cheap reachability holds, i.e. there exists $E \geq 0$ such that

$$\hat{V}_N(k, x) \leq E \tag{5.21}$$

for all $k \in \mathbb{N}$ and $x \in \mathbb{X}(k)$. Consider $N \in \mathbb{N}$ with $N > E$. Then by construction the cost of the N-step trajectory starting in the state $x = N$ at time $k = N$ is given by

$$J_N(k, x, u) = \sum_{j=0}^{N-1} \underbrace{\ell(k + j, x_u(j; x), u)}_{=2} = 2N \tag{5.22}$$

which is equal to the optimal value function , i.e. it holds $J_N(k, x, u) = V_N(k, x)$, since there is only one possible control sequence. Thus, by the definition of the shifted optimal value function it follows that

$$\hat{V}_N(k, x) = V_N(k, x) - \sum_{j=0}^{N-1} \underbrace{\ell(k + j, x^*(k + j), u^*(k + j))}_{=1} = 2N - N = N > E. \tag{5.23}$$

But this contradicts (5.21) and thus cheap reachability cannot hold.

5.2 Numerical approaches

In this section, we will present numerical evidence that for the convection diffusion equation from Example 4.42 the turnpike and continuity properties are satisfied. Unfortunately, this system which is governed by a partial differential equation (PDE) eludes an analytical examination.

While there is a growing literature on turnpike properties of PDEs [55, 56, 60, 61, 100], none of these results directly applies to Example 4.42. The proofs of turnpike properties are based on a combination of optimality conditions of the static (for the equilibrium) and dynamic (for the open-loop trajectories) optimal control problems. Most of the results are limited to linear dynamics and time-invariant problems, with the exception of [56] where time-varying operators are possible. The two main reasons why the approaches are unsuitable for the problem at hand are that they only treat steady-state turnpikes (except for [100] where also periodic turnpikes are possible) and that state constraints are not considered.

Still, in order to illustrate that turnpike and continuity properties are meaningful assumptions that can be expected to hold for practical systems we want to find numerical evidence of these properties. This will be the aim of the second part of this chapter and helps explaining why MPC works for the system from Example 4.42.

For convenience, we write down the system once more:

$$\frac{\partial y}{\partial t} - \alpha \nabla^2 y + w \nabla y = 0 \text{ on } Q := \Omega \times [0, \infty),$$
$$y(0) = y_0 \text{ on } \Omega, \tag{5.24}$$

with boundary conditions

$$\frac{\partial y}{\partial n} + \gamma_{out} y = \delta_{out} y_{out} \text{ on } \Sigma_{out} := \Gamma_{out} \times [0, \infty),$$
$$\frac{\partial y}{\partial n} + \gamma_c y = \delta_c u \text{ on } \Sigma_c := \Gamma_c \times [0, \infty). \tag{5.25}$$

Recall that we want to compute an approximate solution to the infinite horizon optimal control problem

$$\min_{y,u,w} J(y, u, w) = \frac{1}{2} \|u\|^2_{L^2(\Sigma_c)} + \frac{1}{2} \|w\|^2_{L^2(Q)} \tag{5.26}$$

subject to equations (5.24), (5.25) and the constraints

$$\underline{u} \leq u \leq \overline{u} \text{ on } \Sigma_c, \tag{5.27}$$
$$\underline{y} \leq y \leq \overline{y} \text{ on } \Omega \times [0, \infty), \tag{5.28}$$

with lower and upper bounds for state and control where $\Omega_y \subseteq \Omega$ is a subdomain.
As domain we consider again the unit interval, i.e. $\Omega = [0, 1]$, and as subdomain $\Omega_y = [\frac{1}{4}, \frac{3}{4}]$.

Control and state constraints are chosen as $\overline{u} = -\underline{u} = \frac{1}{4}$,

$$\overline{y}(x,t) = -\underline{y}(x,t) = \begin{cases} \frac{3}{20}, & \text{for } x \in \Omega_y, \\ 10, & \text{for } x \in \Omega \setminus \Omega_y. \end{cases}$$

Further parameters are $\alpha = 1$, $\gamma_{out} = \delta_{out} = 10^6$, $\gamma_c = 0$ and $\delta_c = 10$. For y_{out} we choose the periodic function $y_{out}(t) = \frac{3}{10}\sin(10t)$.

The problem is discretized and the resulting finite dimensional optimization problems are solved as described in Chapter 3.

5.2.1   Approximate computation of an optimal operation trajectory

To check Assumptions 4.10 and 4.12, it is first necessary to compute an optimal operation trajectory pair (x^*, u^*) from Definition 4.5, called (y^*, u^*) in the notation of this section. To the best of our knowledge this cannot be done analytically. Computing it numerically is also impossible since this would involve solving an optimal control problem on an infinite horizon. Instead we compute a surrogate by choosing a large (but finite) L and solve a single open-loop problem where the initial value y_0 is left as a free variable. We denote this approximation by $(\tilde{y}_L^*, \tilde{u}_L^*)$.

Numerical evidence suggests that for decreasing sampling rate $h \to 0$ the initial state of the optimal operation trajectory y^* is not a regular function in space but rather a distribution (see Figure 5.6). This implies that the initial value of the computed approximation $\tilde{y}_L^*(0)$ may not be close to the initial value of the optimal operation trajectory $y^*(0)$. In practice this is not an issue because the smoothing property of the convection diffusion equation causes solutions to be sufficiently regular for each $t > 0$. In fact it can be observed in simulations that for decreasing sampling rate h the approximate optimal operation trajectories quickly converge to what we presume is the *true* optimal operation trajectory if the time horizon is sufficiently large (see Figure 5.7). Moreover, for fixed sampling rate h and varying L the initial pieces of open-loop solutions $\tilde{y}_L^*$ are close which also suggests convergence to the optimal operation trajectory y^* (see Figure 5.8).

For these reasons it seems justified to choose the sampling rate $h = 10^{-2}$ and the horizon of $L = 500$ to obtain an approximation of the optimal operation trajectory (y^*, u^*) for the purpose of the following simulations.

5.2.2   Verifying the turnpike property

In order to demonstrate that the turnpike property from Assumption 4.10 holds we check if solutions $y_{u_N^*}$ of the open-loop problem

$$\underset{u \in \mathbb{U}^N(k, y_0)}{\text{minimize}} \quad J_N(k, y_0, u) \tag{5.29}$$

starting from some initial state $y_0 \in L_2(\Omega)$ are most of the time in a neighborhood of the optimal operation trajectory y^*. For our purposes the optimal trajectory is replaced by $\tilde{y}_L^*$.
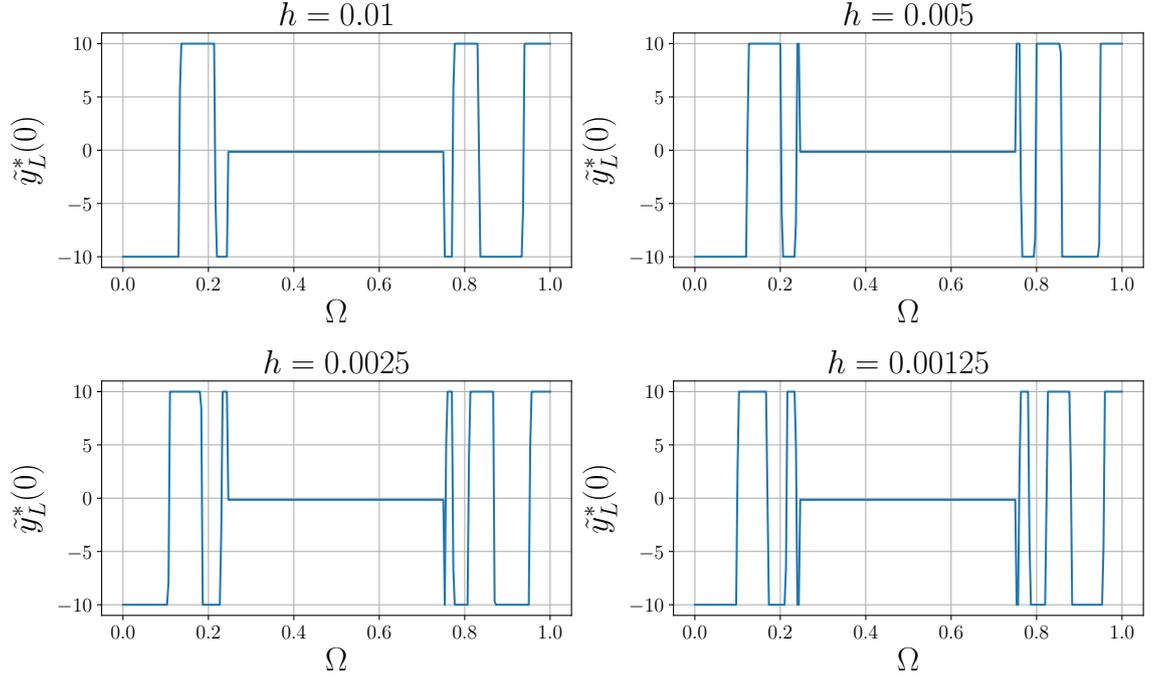
Figure 5.6: Initial state $\tilde{y}_L^*(0)$ of the numerically computed optimal operation trajectories for decreasing sampling rate h. The results indicate a lack of regularity of the initial state of the optimal operation trajectory as a function in space.

The assumption also demands that as the horizon increases the size of the neighborhood shrinks, i.e. the open-loop solutions get closer to the optimal operation trajectory. It should be noted that numerically we can only verify the finite horizon turnpike property in this way since for the infinite horizon turnpike we would need access to solutions of the problem on the infinite horizon.

In order to avoid the issue of the lacking regularity of the initial state $y^*(0)$ (cf. Section 5.2.1) we pick as initial time $t_0 = 0.4$ for the computation of open-loop trajectories $y_{u_N^*}$. We set the initial state $y_0 \equiv 0$ and vary the horizon length N. Figure 5.9a shows that the open-loop trajectories $y_{u_N^*}$ approach the optimal operation trajectory $\tilde{y}_L^*$. The trajectories exhibit an approaching and a leaving arc, which is typical for the turnpike property. It can also be observed that for longer horizons the distance to the turnpike is smaller.

Next, we fix a horizon of $N = 100$ and investigate how the open-loop trajectories for different initial values look like. Figure 5.9b shows the distance between the turnpike $y_{u_N^*}$ and open-loop trajectories starting from constant (in space) initial states $y(x, t_0) \equiv -0.15 + 0.05i, i = \{0, \ldots, 6\}$. The results presented are exemplary and similar behavior also occurs at other initial values and initial times. The plots demonstrate that all trajectories approach the same optimal operation trajectory.

Finally, Figure 5.10 shows the intermediate open-loop trajectories for an MPC closed-loop
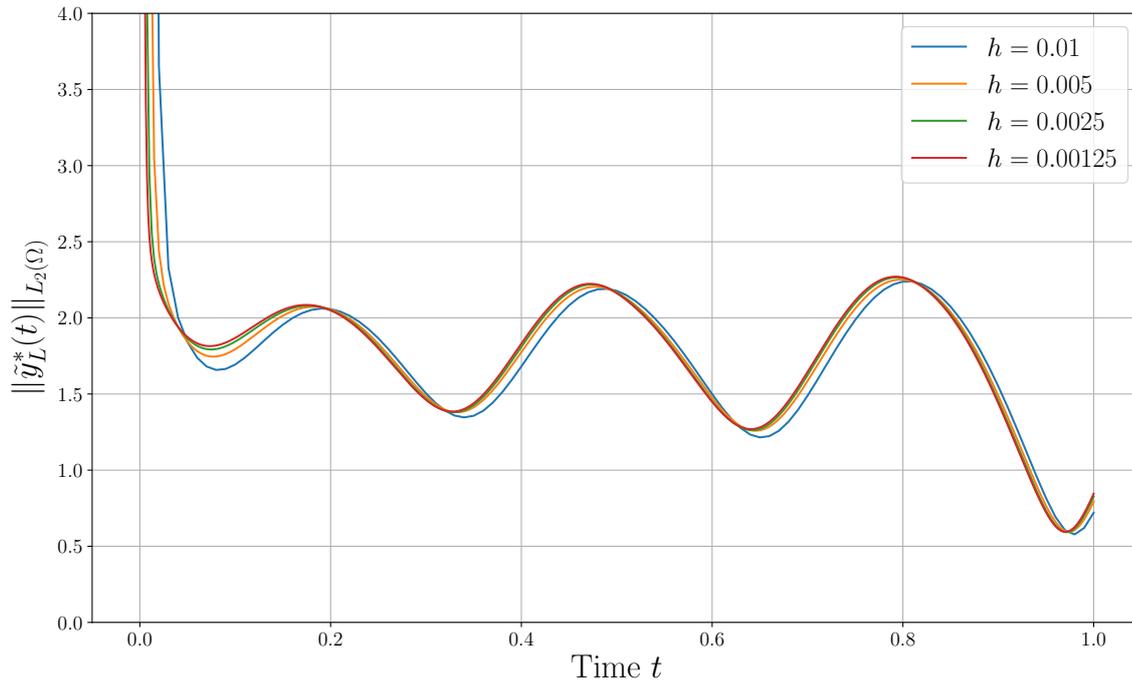
Figure 5.7: L_2 norms of the approximate optimal operation trajectories $\tilde{y}_L^*$ for different sampling rates h over a fixed time horizon of $T = 1.0$.
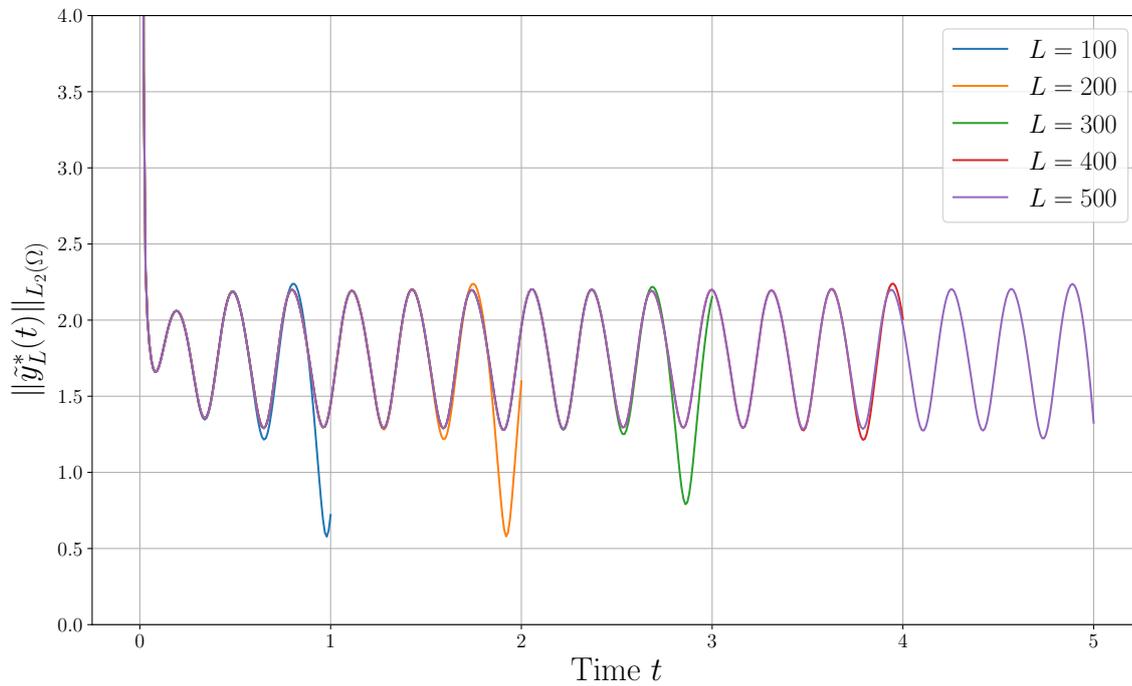
Figure 5.8: L_2 norms of the approximate optimal operation trajectories $\tilde{y}_L^*$ with fixed sampling rate $h = 10^{-2}$ and different horizon lengths L.

simulation up to time $k = 50$ for two different MPC horizons. Again, it can be seen that the open-loop trajectories approach the turnpike and after a while turn away. Since the MPC closed-loop implements only the very first control of each open-loop it is not affected by the "leaving arc" (at least for sufficiently large horizon).
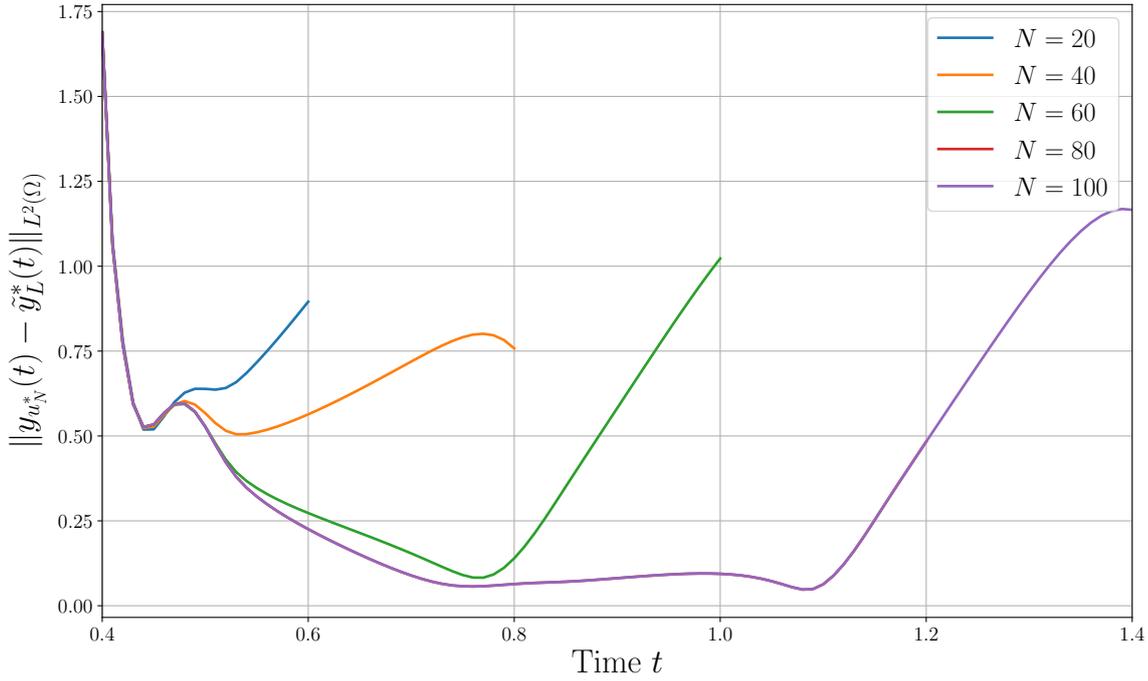
(a) L_2 distance between the optimal operation trajectory $\tilde{y}_L^*$ and open-loop trajectories $y_{u_N^*}$ of the MPC algorithm starting at time $t_0 = 0.4$ and initial state $y_0 \equiv 0$ for different horizon lengths N.
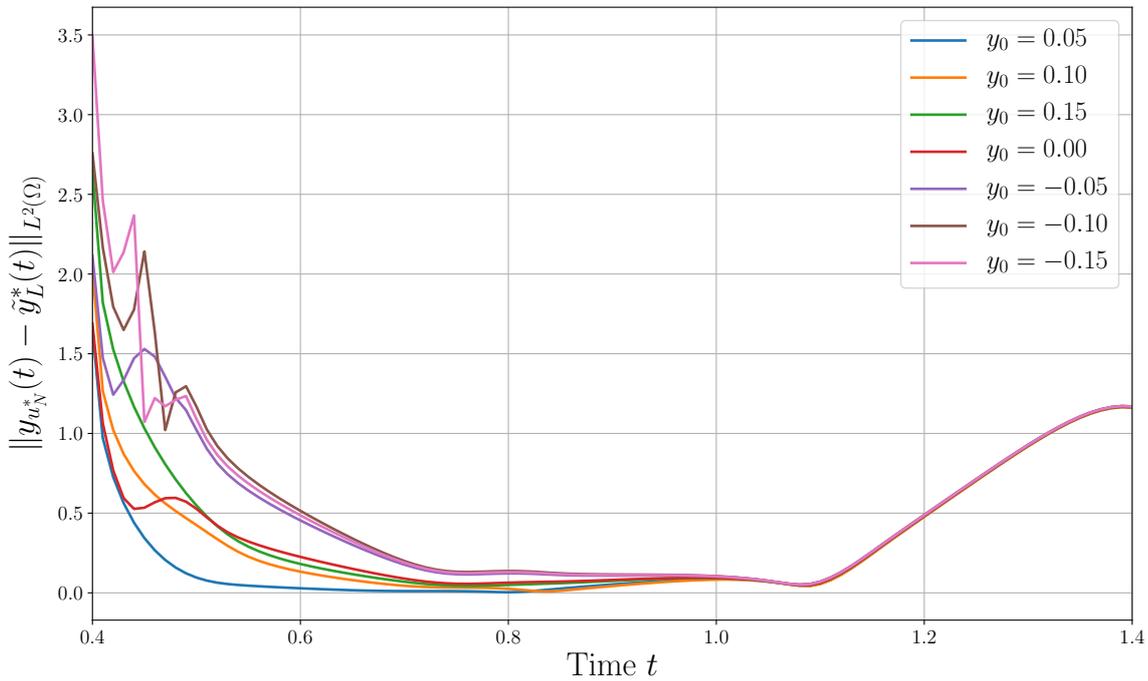
(b) L_2 distance between the optimal operation trajectory $\tilde{y}_L^*$ and open-loop trajectories $y_{u_N^*}$ of the MPC algorithm with fixed horizon $N = 100$ and different constant initial states $y(x, t_0) \equiv y_0$ at time $t_0 = 0.4$.

Figure 5.9: Simulations showing that the turnpike property holds.
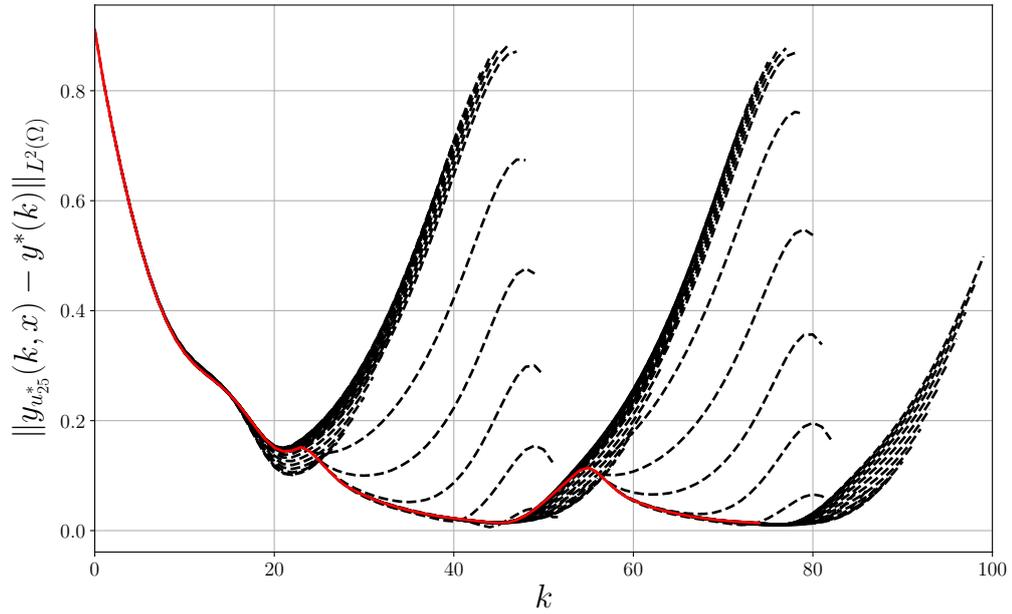
(a) Norm difference $\|y_{u_N^*}(k,x) - y^*(k)\|_{L^2(\Omega)}$ between open-loop predictions $y_{u_N^*}$ starting at time k with initial values on the closed loop $y_{\mu_N}(k)$ and the optimal trajectory y^* for horizon length $N = 25$.
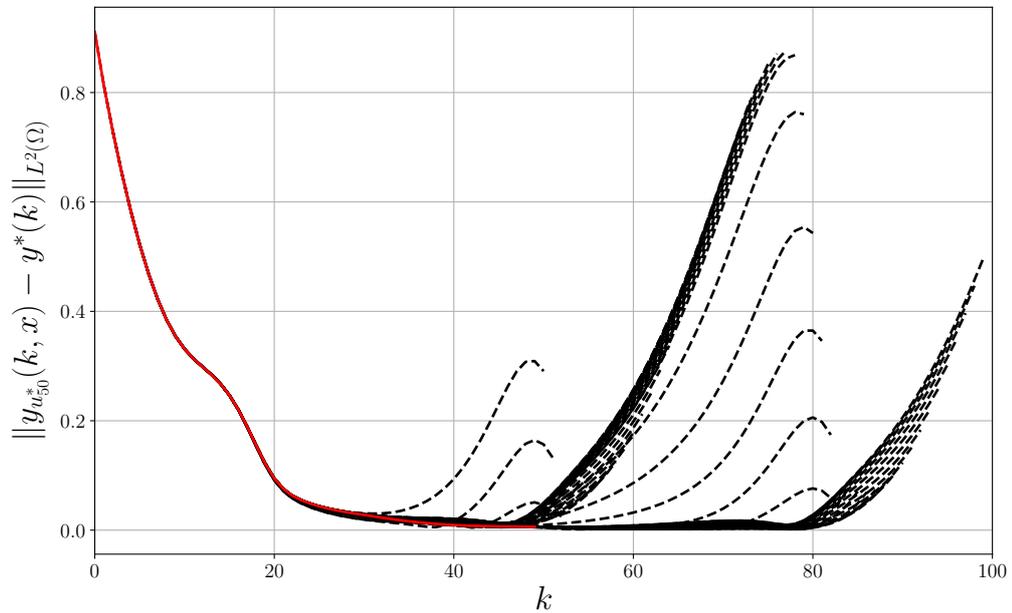
(b) Norm difference $\|y_{u_N^*}(k,x) - y^*(k)\|_{L^2(\Omega)}$ between open-loop predictions $y_{u_N^*}$ starting at time k with initial values on the closed loop $y_{\mu_N}(k)$ and the optimal trajectory y^* for horizon length $N = 50$. In addition the norm difference of the closed loop y_{μ_N} to the optimal trajectory y^* is shown.

Figure 5.10: Successive open-loop predictions exhibiting turnpike convergence (dashed black lines) together with closed-loop (solid red line).

5.2.3   Verifying the continuity property

In order to verify the continuity property from Assumption 4.12 we need to check that the optimal value function for an initial state on the optimal operation trajectory does not change too much when we disturb this initial state. We note that state constraints are active in the solutions, thus we cannot conclude continuity of the optimal value function simply from the continuity of the stage cost and dynamics. As in the previous section, we can only check the continuity assumption of the finite horizon problem numerically. Formally, for each time point k and optimal state $y^*(k)$ we consider the quantity

$$\delta_k(N,\varepsilon) := |\hat{V}_N(k,y^*(k)) - \hat{V}_N(k,y_\varepsilon)| \tag{5.30}$$

for different horizon lengths N and disturbed states $y_\varepsilon \in \mathscr{B}_\varepsilon(y^*(k))$. Since the shifted optimal value function for finite horizons satisfies

$$\hat{V}_N(k,y) = V_N(k,y) - \sum_{j=0}^{N-1} \ell(k+j, y^*(k+j), u^*(k+j)) \tag{5.31}$$

it holds that

$$\begin{aligned} \delta_k(N,\varepsilon) &= |\hat{V}_N(k,y^*(k)) - \hat{V}_N(k,y_\varepsilon)| \\ &= |V_N(k,y^*(k)) - V_N(k,y_\varepsilon)|. \end{aligned} \tag{5.32}$$

where V_N is the optimal value function of problem (5.29) given by

$$V_N(k,y) := \inf_{u \in \mathbb{U}^N(k,y)} J_N(k,y,u). \tag{5.33}$$

As it turns out, in this example an alternative stronger continuity condition for the condition from Assumption 4.12 is valid, at least numerically: inequality (4.13) can be replaced by

$$|\hat{V}_N(k,y) - \hat{V}_N(k,y^*(k))| \le \varphi_V(|y|_{y^*(k)}) \tag{5.34}$$

with a function $\varphi_V \in \mathscr{K}_\infty$. This means the function δ_k from (5.30) can be bounded by a $\mathscr{K}_\infty$ function that is independent of N. To check this numerically we fix a time point $t = kh$ and consider the state $\tilde{y}_L^*(t)$ on the optimal operation trajectory at that time point. Then, for decreasing $\varepsilon_i := \varepsilon_0 \frac{1}{2^i}$, $i \in \{0, \cdots, n\}$, we generate a number of random disturbances $y_{\varepsilon_i}^j$, $j \in \{1, \ldots, m\}$ of the optimal state such that $\varepsilon_i = \|y_{\varepsilon_i}^j - \tilde{y}_L^*(t)\|_{L^2(\Omega)}$. For each of the initial conditions $y_{\varepsilon_i}^j$ generated in this way we solve the optimal control problem (5.29) for different horizon lengths $N \in \{N_1, \ldots, N_l\}$. Thus we obtain samples of optimal value functions V_N for varying N in a neighborhood of the optimal operation trajectory. Out of all samples we choose the ones with maximum deviation from the optimal value function at the optimal operation trajectory, i.e.

$$\tilde{\delta}_k(N,\varepsilon) := \max_j |V_N(k,\tilde{y}_L^*(t)) - V_N(k,y_{\varepsilon_i}^j)|. \tag{5.35}$$

For a sufficiently large number of samples this gives a good approximation of δ_k in a neighborhood of the optimal operation trajectory. Finally, we remark that of course we would have to check the conditions on δ_k for all time instances k. Because the optimal operation trajectory of the example exhibits periodic behavior (cf. Figure 5.8) we could restrict ourselves to checking one period.

In the following we show exemplary results for a single time point $k = 50$ corresponding to the time $t = 0.5$. The chosen results are representative for all time points. The parameters from the above discussion were chosen as $\varepsilon_0 = 10^{-2}$, $n = 5$, $m = 10$, $N_i = 10i$, $i \in \{1, \dots, 10\}$.

Figure 5.11 shows the computed function $\tilde{\delta}_k$ as a function in its first and second component. The top figure 5.11a shows that $\tilde{\delta}_k(N, \varepsilon)$ is indeed bounded in N and thus it is possible to find a modulus of continuity φ_V that satisfies the required assumptions. Similarly, the bottom figure 5.11b demonstrates that the required upper bound for $\tilde{\delta}_k(N, \cdot)$ exists and satisfies the monotonicity assumptions. Thus we can conclude that, at least according to our numerical evidence, the continuity property holds for this example.

5.2.4 Discussion of the numerical approach

The numerical approach presented in this section is not restricted to the specific PDE we considered but can in principle be extended to other types of systems. It offers a possibility to directly verify the occurrence of turnpike and continuity properties, especially when alternative conditions like dissipativity are out of reach.

The only requirement is that the solution of open-loop optimal control problems can be computed. At the same time, this is probably the biggest disadvantage: Checking the assumptions numerically involves solving optimal control problems for a variety of parameters (horizon length, initial values and initial time). Although these problems are independent and the process can be (and has been) carried out in parallel it is still a computationally intensive task.

Moreover, we are limited to investigate problems for which the open-loop solutions can be solved within a reasonable amount of time. In practice, we can only verify the assumptions for small horizons (up to $N \approx 200$) because the solution of the optimal control problems for larger horizons takes prohibitively long. However, if we are only interested in checking the presence of the assumptions in order to justify the application of MPC, the method is still helpful since MPC typically only uses relatively small horizons anyway.

Finally, it should be remarked that this does not constitute a formal proof and in particular, we can neither explicitly identify the set $\mathcal{Q}(k, x, P, N)$ and the bound $\sigma \in \mathcal{L}$ for the distance to the turnpike from Definition 4.9 nor the modulus of continuity φ_V from the continuity property. Nonetheless, the numerical results strongly indicate that the turnpike and continuity properties are satisfied for the example. This gives us confidence that they are the 'right' type of assumptions, which we presume to hold for a large class of systems.
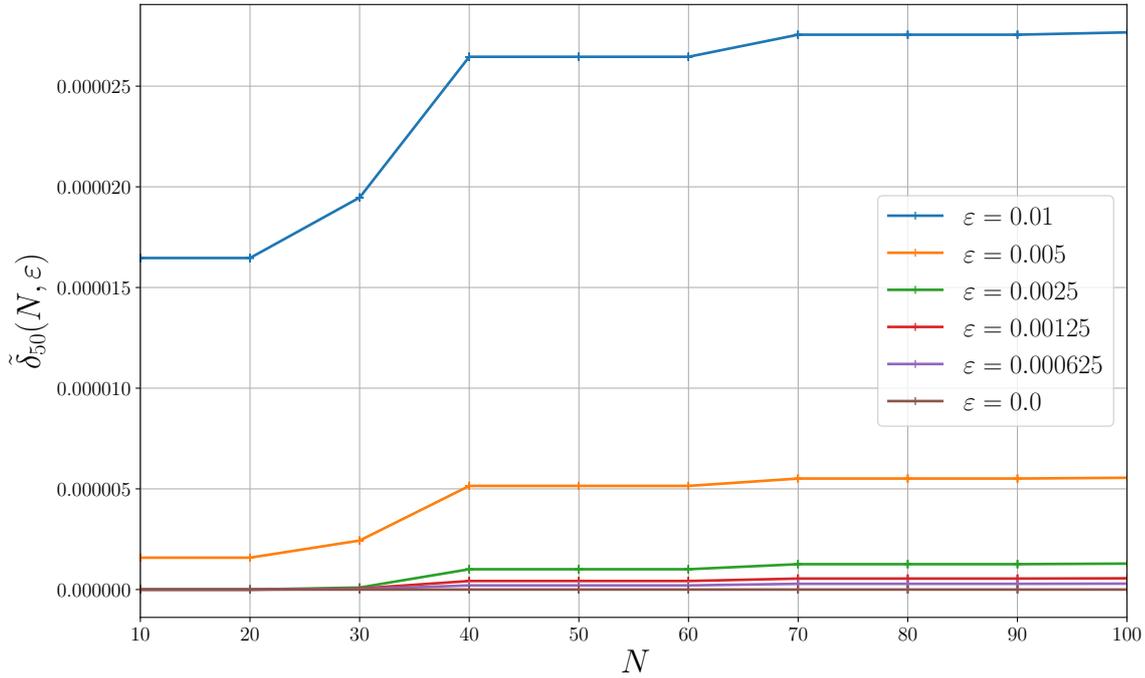
(a) Plot the difference between the optimal value function V_N at an initial value on the optimal operation trajectory $\tilde{y}_L^*$ and the optimal value function at the disturbed states y_ε as a function in the horizon length N and for different magnitude of the disturbance ε. It can be observed that for each ε the function is bounded by a constant for increasing N.
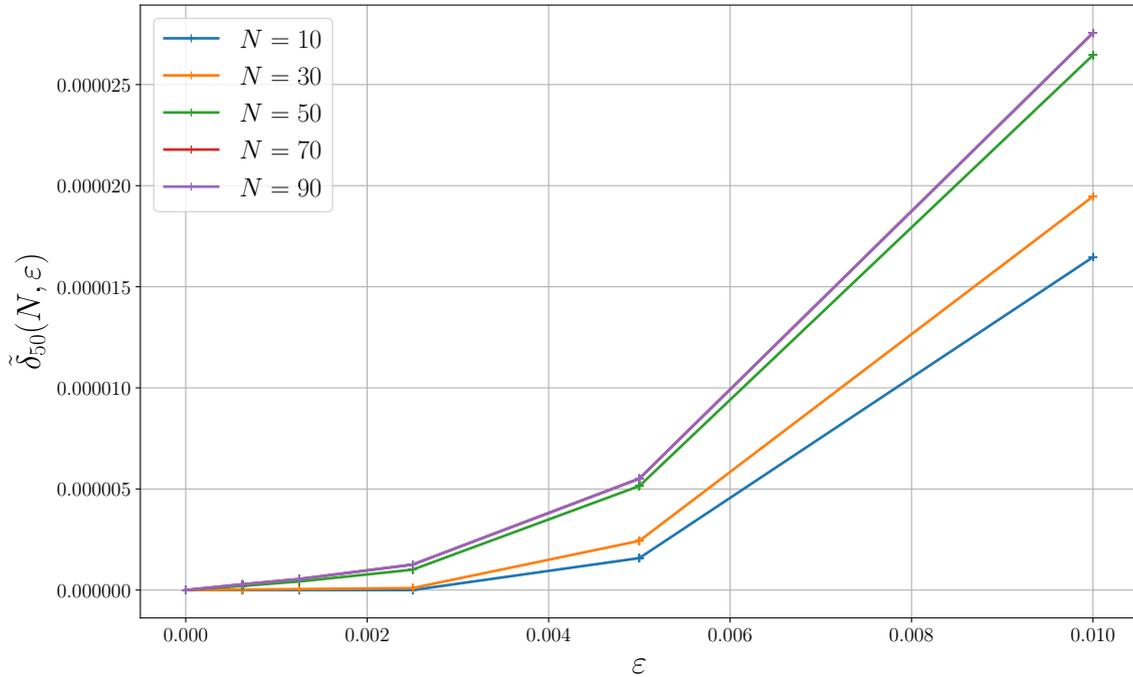
(b) Difference between the optimal value function V_N at an initial value on the optimal operation trajectory $\tilde{y}_L^*$ and the optimal value function at the disturbed states y_ε as a function in the magnitude of the disturbance ε for a selection different horizon lengths N. Obviously, the function can be upper bounded by a $\mathscr{K}_\infty$ function.

Figure 5.11: Simulation results that show that the continuity property holds.

6 | Online MPC performance estimates

In this chapter, we will develop error estimates which allow to monitor the quality of the resulting MPC closed-loop solution at run time. We base our investigations on online performance estimation of tracking type MPC controllers, which have been studied in [58]. In order to verify that the tracking works as expected, one can consider the MPC closed-loop cost because for tracking type cost functionals it corresponds to the tracking error. Using suboptimality estimates along the MPC trajectory, an a posteriori error estimator for the MPC performance can be derived. This estimator relates the MPC performance to the cost of an optimal trajectory on an infinite horizon which indicates how the MPC for a given horizon performs compared to the longest possible (i.e. infinite) horizon.

Performance estimates can be exploited in various algorithmic ways, for example, to reduce the length of the MPC horizon as in [91]. Moreover, as shown in other research [5], not only can these estimates be used as a measure for the error resulting from the truncation of the optimization horizon, but also to quantify the errors caused by numerical approximation and model reduction.

So far, this theory is available only for stabilizing MPC but not for economic MPC or MPC with tracking type functionals for which perfect tracking is not possible, either because the system is not controllable to the desired reference or because exact tracking causes persistent nonzero control costs. In these situations, the error estimator from [58] does not work. The reason for this is the lack of sign definiteness of the stage cost in economic MPC, rendering the relative suboptimality indices α used in stabilizing MPC unsuitable.

Still, a performance estimate that also works for economic MPC is highly desirable, for example in order to tune its parameters or to gain some insight into what the controller is doing. We will see that an appropriate absolute definition of such indices provides a remedy. The estimates compare the cost of the solution produced by the MPC to the cost of a partially optimal trajectory. This gives a criterion that shows if the controller is performing as desired. As in the stabilizing case, the estimate can also be used to decide if adjustments to the parameters used in the MPC implementations have to be made, e.g. by changing the length of the MPC horizon or other discretization parameters.

This chapter is based on the publication [47].

6.1   Setting

Unlike in the previous chapters, we limit our investigations to time-invariant systems as introduced in Chapter 2, i.e. we consider systems

$$x(k + 1) = f(x(k), u(k)),$$
$$x(0) = x_0 \tag{6.1}$$

with stage cost function $\ell : X \times U \to \mathbb{R}$.

The optimal operating cost of the system will enter as a key ingredient in the formulation of the proposed absolute error indices. As seen in the previous chapters, for time-variant systems the optimal operating behavior can be quite complex and, in particular, the cost of the optimal trajectory is generally unknown. While in principle it would be possible to extend our approach to more general regimes of optimal operation, for ease of presentation we will assume that the optimal operation happens at an equilibrium whose cost is readily computed.

Assumption 6.1

The system (6.1) *with stage cost function ℓ exhibits an optimal equilibrium (x_e^*, u_e^*) as introduced in Definition 2.7.*

Recall that we use the notation

$$\hat{\ell}(x, u) = \ell(x, u) - \ell(x_e^*, u_e^*) \tag{6.2}$$

for the shifted stage cost.

6.2   Relative performance index

We will first revisit a relative performance index initially proposed in [58] and explain why it does not deliver a meaningful estimate of the MPC performance for cases other than stabilizing MPC. This performance index has been derived for nonnegative stage cost, i.e. it is assumed that $\ell(x, u) \geq 0$ for all $(x, u) \in X \times U$. The performance index is based on the Theorem 2.6. The central result of this theorem is that we can obtain a bound of the infinite horizon closed-loop performance from the inequality

$$J_\infty^{cl}(x, \mu_N) \leq \frac{1}{\alpha} V_N(x). \tag{6.3}$$

In order to use this for evaluating the performance of the MPC closed-loop we have to check if $\alpha \in (0, 1]$ can be found such that

$$V_N(x(k)) \geq \alpha \ell(x(k), \mu_N(x(k))) + V_N(f(x(k), \mu_N(x(k)))) \tag{6.4}$$

holds for each $k \in \mathbb{N}_0$. The closer α is to 1 the better the performance of the MPC controller will be. In practice, we compute the performance index by

$$\alpha(k) := \frac{V_N(x(k)) - V_N(f(x(k), \mu_N(x(k))))}{\ell(x(k), \mu_N(x(k)))} \tag{6.5}$$

for all times $k \in \mathbb{N}_0$. This can be accomplished online, however, the performance index for time step k becomes available only after the open-loop problem at time step $k+1$ has been solved. In that sense, we obtain an *a posteriori* estimator.

The relative performance index was originally designed with stabilizing MPC controllers in mind, where the stage cost is positive definite w.r.t. the stabilized equilibrium, i.e. it holds that

$$\ell(x_e, u_e) = 0 \text{ and } \ell(x, u) > 0 \text{ for all } x \in X, u \in U \text{ with } x \neq x_e. \tag{6.6}$$

In a more general setting where this assumption is violated, we have $\ell(x_e, u_e) \neq 0$. As a consequence, for any MPC trajectory that converges to the optimal equilibrium the performance index satisfies $\alpha(k) \to 0$ as $k \to \infty$ since the numerator in (6.5) approaches zero while the denominator approaches some positive number. This means the relative performance estimate does not give a meaningful value of the true performance.

A remedy could be to work with the shifted stage cost $\hat{\ell}$ instead, i.e., to consider the modified relaxed dynamic programming inequality

$$\alpha \hat{\ell}(x(k), \mu_N(x(k))) \leq \hat{V}_N(x(k)) - \hat{V}_N(f(x(k), \mu_N(x(k)))) \\ = V_N(x(k)) - V_N(f(x(k), \mu_N(x(k)))). \tag{6.7}$$

Then by summing up, we can estimate

$$\alpha \underbrace{\sum_{j=0}^{K-1} \hat{\ell}(x(j), \mu_N(x(j)))}_{=: \hat{J}_K^{cl}(x, \mu_N)} \leq \sum_{j=0}^{K-1} V_N(x(j)) - V_N(x(j+1)) \tag{6.8}$$

$$= V_N(x(0)) - V_N(x(K)).$$

Since ℓ is nonnegative, we can further estimate

$$V_N(x(0)) - V_N(x(K)) \leq V_N(x(0)) \tag{6.9}$$

which implies that

$$\hat{J}_K^{cl}(x, \mu_N) \leq \frac{1}{\alpha} V_N(x(0)). \tag{6.10}$$

Alternatively, it also holds that

$$V_N(x(0)) \leq V_K(x(0)) \tag{6.11}$$

for $K \geq N$, yielding the estimate

$$\hat{J}_K^{cl}(x, \mu_N) \leq \frac{1}{\alpha} V_K(x(0)). \tag{6.12}$$

This upper bound for the closed-loop cost is useful only if $\ell(x_e^*, u_e^*)$ is close to zero (and thus $\hat{J}_K^{cl}(x, \mu_N) \approx J_K^{cl}(x, \mu_N)$). In the general case the estimate will be too conservative.

6.3   Absolute performance index

Since the relative performance index is of limited use if the stage cost is not positive definite, we propose an absolute performance index that overcomes these limitations.

Theorem 6.2 (Absolute performance index)
Consider the dynamical system (6.1) with general stage cost $\ell : X \times U \to \mathbb{R}$. Let Assumption 6.1 hold and consider the MPC feedback μ_N. For P in $\{0, \ldots, N-1\}$ and $K \geq N$ define the quantities

$$\varepsilon_N^1(k) := V_N(x(k)) - V_N(x(k+1)) - \hat{\ell}(x(k), \mu_N(x(k))), \tag{6.13a}$$

$$\varepsilon_{N,P}^2(K) := V_{N-P}(x_{u_{N,x}^*}(P, x)) - V_{N-P}(x_{u_{N,x(K)}^*}(P, x(K))), \tag{6.13b}$$

$$\varepsilon_{N,P}^3(K) := P\ell(x_e^*, u_e^*) - J_P(x(K), u_{N,x(K)}^*) \tag{6.13c}$$

and let

$$E_{N,P}(K) := \sum_{k=0}^{K-1} \varepsilon_N^1(k) - \varepsilon_{N,P}^3(K) - \varepsilon_{N,P}^2(K). \tag{6.14}$$

Then the equation

$$E_{N,P}(K) = J_P(x, u_{N,x}^*) + (K - P)\ell(x_e^*, u_e^*) - J_K^{cl}(x, \mu_N) \tag{6.15}$$

holds.

Proof. Summing up (6.13a) along the MPC closed-loop trajectory yields

$$\sum_{k=0}^{K-1} \varepsilon_N^1(k) = \sum_{k=0}^{K-1} \left[V_N(x(k)) - V_N(x(k+1)) + \ell(x_e^*, u_e^*) - \ell(x(k), \mu_N(x(k))) \right]$$

$$= V_N(x) - V_N(x(K)) + K\ell(x_e^*, u_e^*) - \underbrace{\sum_{k=0}^{K-1} \ell(x(k), \mu_N(x(k)))}_{= J_K^{cl}(x, \mu_N)} \tag{6.16}$$

or equivalently

$$V_N(x) - V_N(x(K)) = J_K^{cl}(x, \mu_N) - K\ell(x_e^*, u_e^*) + \sum_{k=0}^{K-1} \varepsilon_N^1(k). \tag{6.17}$$

By the dynamic programming principle, for any $P \in \{0, \ldots, N-1\}$ we can rewrite the terms on the left-hand side as

$$V_N(x) = J_P(x, u^*_{N,x}) + V_{N-P}(x_{u^*_{N,x}}(P, x)) \tag{6.18}$$

and

$$V_N(x(K)) = J_P(x(K), u^*_{N,x(K)}) + V_{N-P}(x_{u^*_{N,x(K)}}(P, x(K))). \tag{6.19}$$

Now consider

$$
\begin{aligned}
V_N(x) - V_N(x(K)) &= J_P(x, u^*_{N,x}) - J_P(x(K), u^*_{N,x(K)}) + V_{N-P}(x_{u^*_{N,x}}(P, x)) \\
&\quad - V_{N-P}(x_{u^*_{N,x(K)}}(P, x(K))) \\
&= J_P(x, u^*_{N,x}) - P\ell(x^*_e, u^*_e) \\
&\quad + \underbrace{V_{N-P}(x_{u^*_{N,x}}(P, x)) - V_{N-P}(x_{u^*_{N,x(K)}}(P, x(K)))}_{=\varepsilon^2_{N,P}(K)} \\
&\quad + \underbrace{P\ell(x^*_e, u^*_e) - J_P(x(K), u^*_{N,x(K)})}_{=\varepsilon^3_{N,P}(K)}.
\end{aligned}
\tag{6.20}
$$

Combining (6.17) and (6.20) yields

$$J_P(x, u^*_{N,x}) - P\ell(x^*_e, u^*_e) + \varepsilon^3_{N,P}(K) + \varepsilon^2_{N,P}(K) = J^{cl}_K(x, \mu_N) - K\ell(x^*_e, u^*_e) + \sum_{k=0}^{K-1} \varepsilon^1_N(k)$$

and by reordering we obtain

$$
\begin{aligned}
J_P(x, u^*_{N,x}) + (K-P)\ell(x^*_e, u^*_e) - J^{cl}_K(x, \mu_N) &= \sum_{k=0}^{K-1} \varepsilon^1_N(k) - \varepsilon^3_{N,P}(K) - \varepsilon^2_{N,P}(K) \\
&= E_{N,P}(K).
\end{aligned}
$$

This concludes the proof. $\qquad\qquad\qquad\qquad\qquad\qquad\qquad\qquad\qquad\qquad\quad$ $\square$

Theorem 6.2 states that the quantity $E_{N,P}(K)$ measures the difference between the MPC closed-loop cost for K steps and the cost of a trajectory that consists for the first P steps of a finite horizon open-loop and after that of the cost of the optimal equilibrium. The quantities ε^1_N, $\varepsilon^2_{N,P}$ and $\varepsilon^3_{N,P}$ that compose the error estimate can all be computed online (assuming that the cost of the optimal equilibrium $\ell(x^*_e, u^*_e)$ is known).

Remark 6.3
It should be noted that $E_{N,P}(K)$ could also be determined by just computing the right-hand side of equation (6.15) directly. However, the error estimate $E_{N,P}(K)$ offers the advantages that the step-by-step data provides more detailed information about the error. It could be that the individual error estimates are large, but partially cancel out each other and then deliver a small error after P steps. This would mean, however, that MPC only provides a good solution "by chance", which one would not recognize without the error estimator. $\qquad\qquad\qquad\qquad\qquad\qquad\qquad\qquad\qquad\qquad\qquad\qquad\qquad\quad$ $\diamondsuit$

6.3.1   Interpretation of the absolute performance index

In this section, we give a more in-depth insight into what the individual terms of performance index from Theorem 6.2 tell us about the quality of the MPC closed-loop solution. The following analysis is based on Assumption 2.8 (turnpike property) and Assumption 2.9 (continuity property), which we already introduced in Chapter 2. Under these assumptions the following lemma can be proved.

Lemma 6.4 (cf. Lemma 8.26 in [50])
Let Assumption 2.8 and Assumption 2.9 hold. Then the equation

$$V_N(x) = V_{N-1}(x) + \ell(x_e^*, u_e^*) + R_2(x, N) \tag{6.21}$$

holds with $|R_2(x, N)| \leq \nu_2(\|x - x_e^*\|, N) = 2\gamma_V(\sigma_\delta(\lfloor N/2 \rfloor)) + 2\omega(\lfloor N/2 \rfloor - 1)$ for all $x \in \mathbb{X}$, all $N \in \mathbb{N}$ with γ_V, ω from Assumption 2.9 and σ_δ from [50, Proposition 8.15] with $\delta = \gamma_V(\|x - x_e^*\|) + \omega(N - 1)$.

The above lemma explains the first error term ε_N^1 in equation (6.13): consider the following relation for the MPC closed-loop cost, which directly follows from the dynamic programming principle.

$$V_N(x(k)) = \ell(x(k), \mu_N(x(k))) + V_{N-1}(x(k+1)). \tag{6.22}$$

Applying Lemma 6.4 to this equation yields

$$V_N(x(k)) = \ell(x(k), \mu_N(x(k))) + V_N(x(k+1)) - \ell(x_e^*, u_e^*) - R_2(x(k), N). \tag{6.23}$$

By rearranging the previous equation to

$$-R_2(x(k), N) = V_N(x(k)) - V_N(x(k+1)) + \ell(x_e^*, u_e^*) - \ell(x(k), \mu_N(x(k))) = \varepsilon_N^1(k), \tag{6.24}$$

we immediately see that ε_N^1 corresponds exactly to the error term from Lemma 6.4. This means we can interpret ε_N^1 as a measure for the improvement that an optimal trajectory with horizon length N offers compared to a shorter trajectory with length $N - 1$ that is augmented with the cost of one step on the optimal equilibrium. Moreover, the bound $|\varepsilon_N^1(k)| = |R_2(x(k), N)| \leq 2\gamma_V(\sigma_\delta(\lfloor N/2 \rfloor)) + 2\omega(\lfloor N/2 \rfloor - 1)$ tells us that the magnitude of the error will decrease as the horizon is increased.

The other error terms can be interpreted as follows: $\varepsilon_{N,P}^2(K)$ measures the difference between the final piece of optimal trajectories starting in x and $x(K)$, respectively, cf. Figure 6.1. If Assumption 2.8 is satisfied and we choose P such that the final pieces of the optimal trajectories start near the turnpike, this means the performance index $\varepsilon_{N,P}^2$ measures the difference of the so-called leaving arcs. This can be used as an indicator of how much the leaving cost has improved between the first and current step of the MPC algorithm. In other words, it is a measure of how much progress towards the optimal equilibrium the closed-loop has made until now.
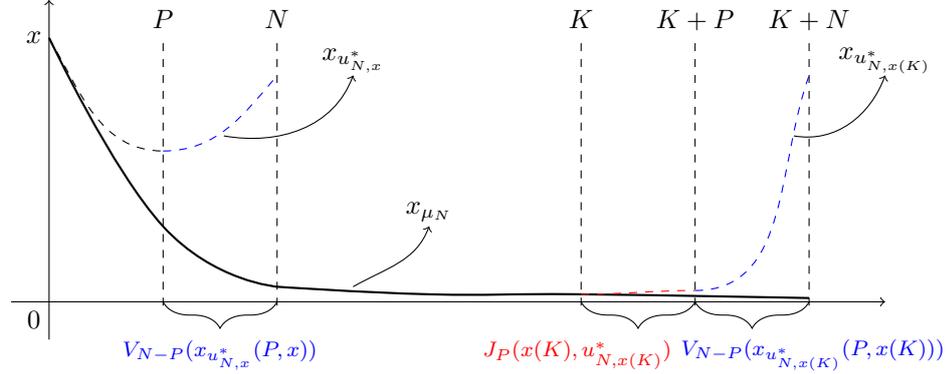
Figure 6.1: Illustration of the quantities used for the computation of the performance indices $\varepsilon_{N,P}^2(K)$ (in blue) and $\varepsilon_{N,P}^3(K)$ (in red).

In contrast, the error term $\varepsilon_{N,P}^3(K)$ measures the difference between the initial piece of the optimal trajectory starting in $x(K)$ and the cost of the optimal equilibrium for P steps. This is motivated by an observation from Lemma 6.3 in [43], which states that an optimal trajectory originating near the optimal equilibrium will stay near the optimal equilibrium for some time because this is the cheapest option. A "good" MPC controller will drive the state $x(K)$ to a neighborhood of the optimal equilibrium. If this is not the case it can be detected by performance index $\varepsilon_{N,P}^3$ which will yield a larger error.

We now investigate the influence of P on the performance estimate. Figure 6.2 shows different choices of P for an MPC horizon N that has been chosen sufficiently large such that the open-loop trajectory is very close to the optimal equilibrium x_e^*. If we chose P too small, e.g. $P = P_1$ in the topmost figure, then we will compare the MPC closed-loop (shown in green) trajectory to a trajectory (shown in blue) that first follows the open-loop for P steps and then suddenly jumps to the optimal equilibrium, thus making it an unfair comparison. The quantity $E_{N,P}(K)$ will reflect this by attaining a large negative value. Similarly, if P is too large, e.g. $P = P_3$ in the bottom figure, the trajectory we compare against will include part of the leaving arc of the open-loop, which also results in a large negative value. Ideally, P is chosen such that the open-loop state at time P is very close to the turnpike, so somewhere near P_2 which is shown in the middle figure. This choice would lead to a small absolute value of $|E_{N,P}(K)| \approx 0$ which is desirable since it implies "good" closed-loop performance according to (6.15).

We conjecture that a safe choice for P is in the middle of the horizon. In fact, for continuous time systems there exist estimates for the distance of open-loop solutions to the turnpike which are of the form

$$||x_{u_{T,x}^*}(t,x) - x_e^*|| \leq C_1(e^{-C_2 t} + e^{-C_2(T-t)}) \tag{6.25}$$
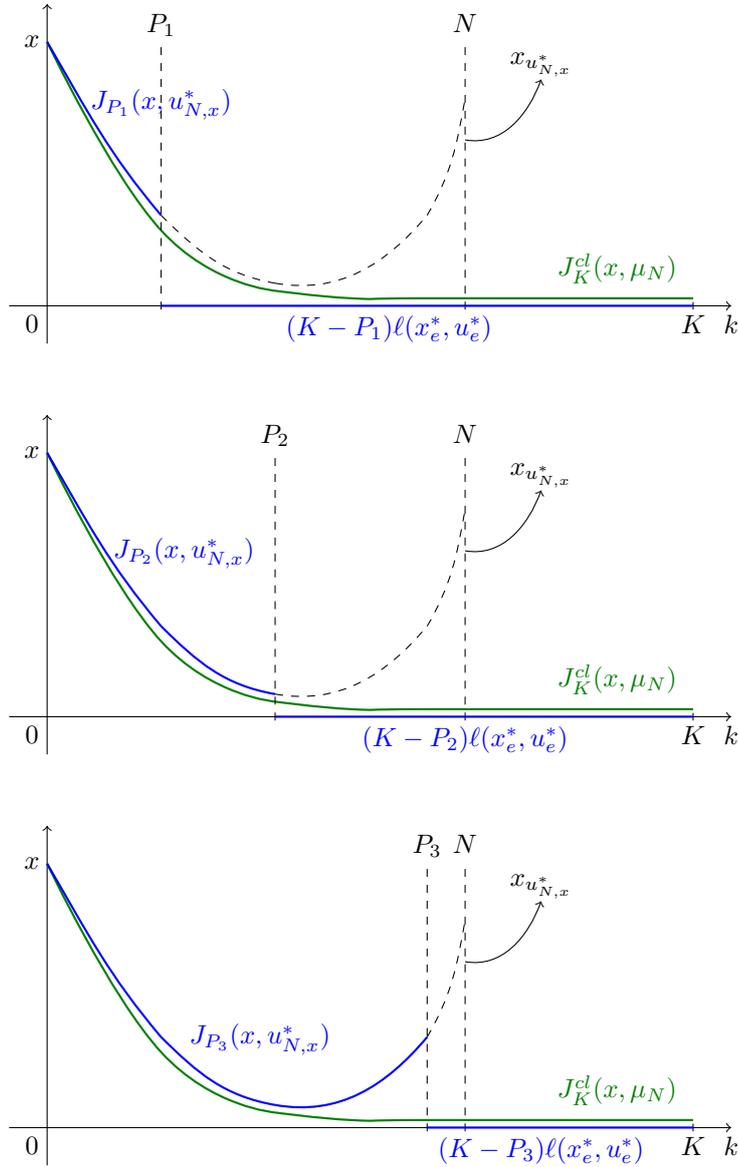
Figure 6.2: Illustration of how the choice of P influences the quantity $E_{N,P}$.

with constants C_1, C_2, cf. [101, Theorem 1]. Consequently, the tightest bound from these estimates is obtained for $t = \frac{T}{2}$. Although this does not exclude that there are time instances where the trajectory is closer to the turnpike, choosing $P \approx \frac{N}{2}$ should yield enough information to capture the improvement of both the leaving arcs described by $\varepsilon_{N,P}^2$ and the proximity to the optimal equilibrium from $\varepsilon_{N,P}^3$.

6.3.2 Possible improvements of the performance index

While in the setting of economic MPC the absolute performance index is more useful than the relative one, there is still room for improvement. Ideally, we would have an estimate that relates the MPC closed-loop cost to the cost of an infinite horizon optimal trajectory as it was for the relative performance estimate (cf. Theorem 2.6).
For this the following two options could be considered:

1. The first idea is to apply the following lemma from [44], which states that values of initial pieces of finite and infinite horizon trajectories are approximately the same.

   Lemma 6.5 (cf. [44, Lemma 4.3])
   Let Assumption 2.8 and Assumption 2.9 hold. Then the equation

   $$J_K(x, u_\infty^*) = J_K(x, u_N^*) + R_3(x, K, N) \tag{6.26}$$

   holds with $|R_3(x, K, N)| \leq \eta(\rho(P)) + \eta(\sigma(P)) + 2\omega(N - K)$ for all sufficiently large $P \in \mathbb{N}$, all $x \in \mathbb{X}$ and all $K \in \{0, \ldots, N\} \setminus (\mathcal{Q}(x, P, N) \cup \mathcal{Q}(x, P, \infty))$.

   This lemma allows us to replace the finite horizon optimal control sequence $u_{N,x}^*$ by the infinite horizon control sequence $u_{\infty,x}^*$. Consequently, (6.15) becomes

   $$J_P(x, u_{\infty,x}^*) + (K - P)\ell(x_e^*, u_e^*) - J_K^{cl}(x, \mu_N) = E_{N,P}(K) + R_3(x, P, N). \tag{6.27}$$

   The transition from u_N^* to u_∞^* introduces an additional unknown error $R_3(x, P, N)$, i.e. now $E_{N,P}(K)$ does not exactly describe the difference but is only an approximation. The quality of the approximation depends on both the choice of P and N which is inconvenient if the estimate should be used for tuning the horizon. For large P the error estimate $E_{N,P}(K)$ also contains the cost of the leaving arc while $J_P(x, u_{\infty,x}^*)$ does not.

2. Alternatively, one could directly consider the difference

   $$J_K(x, u_{\infty,x}^*) - J_K^{cl}(x, \mu_N) \tag{6.28}$$

   and try to derive an error estimate for this quantity. This would be the most powerful tool for rating the MPC performance. Unfortunately, a direct extension of the ideas in the previous section seems out of reach.

6.4 Numerical example

In this section, we will present a numerical example to demonstrate the capabilities of the online performance estimators. To this end, we consider a convection-diffusion equation with boundary control. Note that in the following the state variable will be indicated by
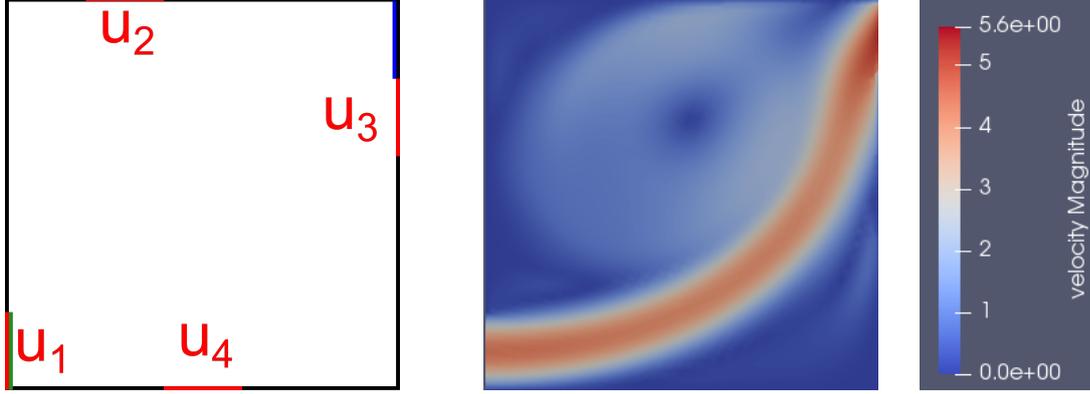
(a) Domain Ω and boundaries the $\Gamma = \Gamma_{\text{out}} \cup \Gamma_{\text{c}}$ as well as inlets (green) and outlets (blue) used in the computation of the velocity field.

(b) Velocity field $\boldsymbol{v}(\boldsymbol{x})$ used in equation (6.29) which is computed by the solution of Navier-stokes equations (6.30).

Figure 6.3: Illustration of the domain and velocity field.

the letter y, due to the fact that the letter $\boldsymbol{x}$ is used to represent the spatial coordinates in $\mathbb{R}^2$.

We consider the state equation

$$
\begin{aligned}
y_t(t, \boldsymbol{x}) - \Delta y(t, \boldsymbol{x}) + \boldsymbol{v}(\boldsymbol{x}) \cdot \nabla y(t, \boldsymbol{x}) &= 0, & \text{a.e. in } [0, +\infty) \times \Omega, \\
\frac{\partial y}{\partial \boldsymbol{n}}(t, \boldsymbol{s}) + y(t, \boldsymbol{s}) &= \sum_{i=1}^{4} u_i(t) b_i(\boldsymbol{s}), & \text{a.e. on } [0, +\infty) \times \Gamma_{\text{c}}, \\
\frac{\partial y}{\partial \boldsymbol{n}}(t, \boldsymbol{s}) + 5000 y(t, \boldsymbol{s}) &= 5000 y_{\text{out}}, & \text{a.e. on } [0, +\infty) \times \Gamma_{\text{out}}, \\
y(0, \boldsymbol{x}) &= y_\circ(\boldsymbol{x}), & \text{a.e. in } \Omega,
\end{aligned}
\tag{6.29}
$$

where $\Omega := [0, 5] \times [0, 5] \subset \mathbb{R}^2$ is a bounded set with Lipschitz-continuous boundary $\Gamma = \Gamma_{\text{c}} \cup \Gamma_{\text{out}}$, with $\Gamma_{\text{c}} \cap \Gamma_{\text{out}} = \emptyset$. This setting represents a squared room Ω, where four controls u_i, $i = \{1, \dots, 4\}$, are placed on the boundary Γ_{c} with the following shape functions

$$
b_1(\boldsymbol{x}) = \begin{cases} 1 & \text{if } \boldsymbol{x} \in \{0\} \times [0.0, 1.0], \\ 0 & \text{otherwise}, \end{cases} \qquad
b_2(\boldsymbol{x}) = \begin{cases} 1 & \text{if } \boldsymbol{x} \in [1.0, 2.0] \times \{1\}, \\ 0 & \text{otherwise}, \end{cases}
$$

$$
b_3(\boldsymbol{x}) = \begin{cases} 1 & \text{if } \boldsymbol{x} \in \{1\} \times [3.0, 4.0], \\ 0 & \text{otherwise}, \end{cases} \qquad
b_4(\boldsymbol{x}) = \begin{cases} 1 & \text{if } \boldsymbol{x} \in [2.0, 3.0] \times \{0\}, \\ 0 & \text{otherwise}. \end{cases}
$$

as shown in Figure 6.3a. On the boundary Γ_{out} the exchange of heat between the outside and the inside of the room is parametrized through Robin boundary conditions for a constant outside temperature of $y_{\text{out}} = 18.0$. The initial state is chosen as $y_\circ(\boldsymbol{x}) := 15 + \sin(2\pi x_1)\cos(2\pi x_2)$.

The (time-invariant) convection field $\boldsymbol{v}(\boldsymbol{x})$ shown in Figure 6.3a is a stationary velocity field. It is generated by a forward solution of the incompressible Navier-Stokes equation

$$
\begin{aligned}
v_t + (v \cdot \nabla)v - \nu\Delta v &= -\nabla p && \text{in } [0,6) \times \Omega, \\
\nabla \cdot v &= 0 && \text{in } [0,6) \times \Omega, \\
p &= 0 && \text{in } [0,6) \times \Gamma_{\text{outlet}} = \{x_1 = 5.0, x_2 \in [4,5]\} \\
v &= \tilde{v} && \text{in } [0,6) \times \Gamma_{\text{inlet}} = \{x_1 = 0.0, x_2 \in [0,1]\} \\
v &= 0 && \text{in } \Gamma \setminus (\Gamma_{\text{outlet}} \cup \Gamma_{\text{inlet}}) \\
v(0) &= 0 && \text{in } \Omega
\end{aligned}
\tag{6.30}
$$

up to the time $t = 6.0$ and setting $\boldsymbol{v}(\boldsymbol{x}) := v(5.0, \boldsymbol{x})$. In (6.30), p is the pressure of the air in the room, $\nu = 0.01$ is the kinematic viscosity and

$$
\tilde{v}(t, \boldsymbol{x}) = (4.5(4.0x_2(1 - x_2)), 0.0).
$$

In this scenario, we have an inflow $\tilde{v}(t, \boldsymbol{x})$ on the bottom left side of Ω, which is constant in time and has maximum magnitude of 4.5, and an outflow on the top right part of the domain. The numerical solution of the Navier-Stokes equation is described in detail in [9, Chapter 3].

After discretization of the state equation (6.29), we define the stage cost

$$
\ell(y_u(k; y_\circ), u(k)) := \frac{1}{2} \sum_{i=1}^{4} \Delta t \, |u_i(k)|^2 + \frac{100}{2} \Delta t \|y_u(k; y_\circ) - y_Q(k)\|_{H^1(\Omega)}^2
$$

with $y_Q(k) = 18.0$ for all $k \in \mathbb{N}$, where $\Delta t = 0.05$ is the time discretization step. The setting can be described as reaching a constant temperature distribution (i.e. tracking the target state y_Q) while spending as little energy (i.e. control effort u) as possible. The discretization and the subsequent numerical solution of the optimal control problems is carried out as described in Chapter 3. The desired temperature distribution y_Q can only be maintained if the control is constantly kept at a non-zero value, which implies positive cost even in the optimal equilibrium of the system. As discussed in Section 6.2, this indicates that the relative performance index will not work correctly. In the following, we will confirm this by numerical simulations and also demonstrate that the absolute performance estimate achieves superior results.

Results

We present simulations of the MPC algorithm applied to the optimal control problem above. Figure 6.4 shows the closed-loop cost of the MPC (top) and the relative error estimate α (bottom) that was discussed in Section 6.2. It can be observed that the closed-loop cost at time $k = 400$ in Figure 6.4a still improves if we increase the MPC horizon N but this is not reflected by the performance index depicted in Figure 6.4b, which for

all horizon lengths quickly decays to zero. These observations confirm our claim that the relative performance index is not helpful in this setting.

The absolute performance indices shown in Figures 6.5 and 6.6, on the other hand, clearly demonstrate that the performance improves when the MPC horizon is increased. Figure 6.5a shows the sum of the performance indices ε_N^1 up to time K. Recall that the individual values $\varepsilon_N^1(k)$ correspond to the improvement a larger horizon offers over a smaller horizon. Accordingly, the sum measures the accumulated improvement of the performance that would be gained by increasing the horizon.

In Figure 6.5b the quantity $\varepsilon_{N,P}^2(k)$ for a fixed $P = 30$ is depicted. As stated in Section 6.3.1 this can be interpreted as the improvement of the leaving arc of the MPC open-loop trajectories compared to the very first leaving arc. Up to a horizon of $N = 120$ a huge improvement is visible, while for even longer horizon it seems to saturate. This is in accordance with the observations in Figure 6.4a.

Next, in Figure 6.6a we show the performance index $\varepsilon_{N,P}^3(k)$, again for $P = 30$, whose absolute value can be interpreted as a measure of the proximity of the initial part of the MPC open-loop to the optimal equilibrium. Again, we see that for sufficiently long horizons ($N \geq 120$) we arrive in close proximity to the optimal equilibrium. Moreover, as the simulation time continues to increase, Figure 6.7a shows that the error estimate can still effectively distinguish the convergence for different horizon lengths.

Finally, the last plot in Figure 6.6 shows the quantity $E_{N,P}(K)$ which is composed of the other error estimates in Figure 6.5a, 6.5b and 6.6a. According to Theorem 6.2, this tells us how the MPC closed-loop performance compares to the performance of a composite trajectory consisting by parts of the very first open-loop and of the optimal equilibrium. We can see from the plot that for sufficiently long simulation time $E_{N,P}$ settles at some value and as the MPC horizon N increases we also observe convergence. Ideally, we would see a convergence to zero, but this can in general not be expected if the P has not been chosen in the right way (cf. the discussion to Figure 6.2). In fact the value of the performance index $E_{N,P}$ is heavily influenced by the choice of P as seen in Figure 6.7b. The figure also shows that for every horizon N choosing a P that is somewhere in the middle of the horizon seems to offer the best results, because then the absolute value of $E_{N,P}$ nicely captures the turnpike behavior of the initial open-loop we compare against. This observation is subject to further investigation.
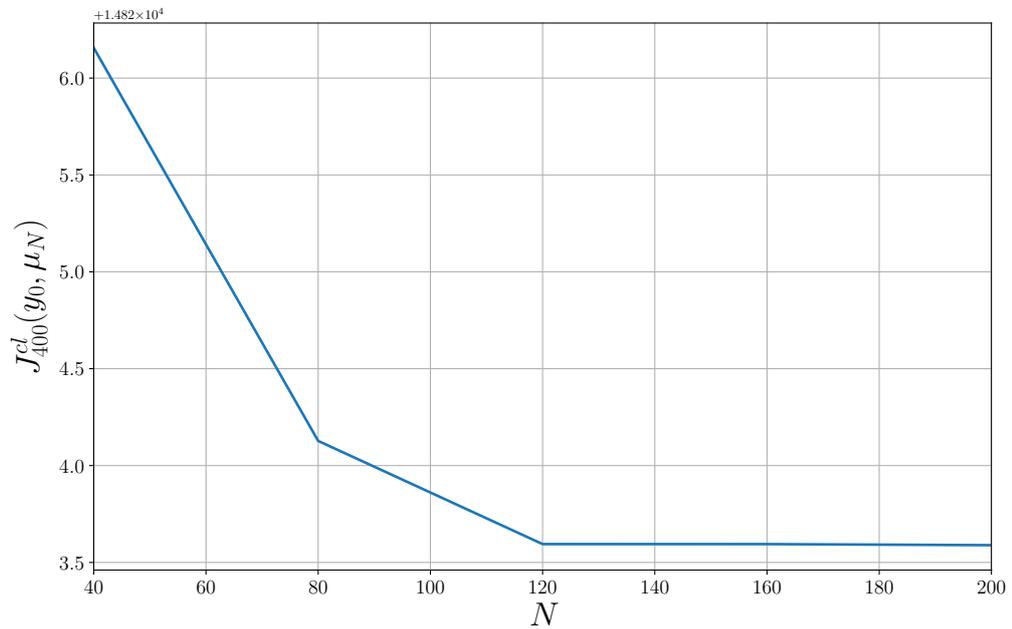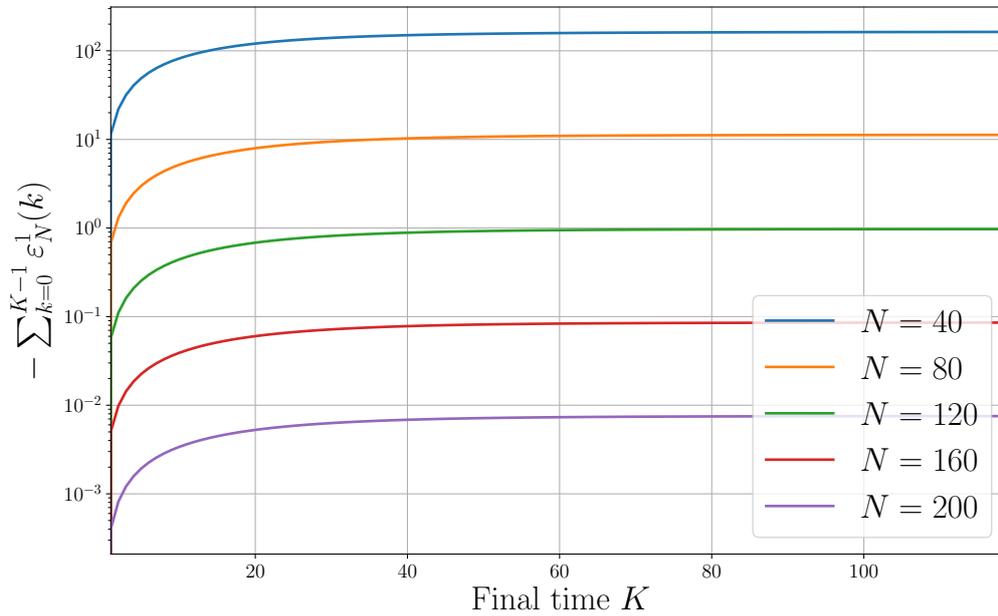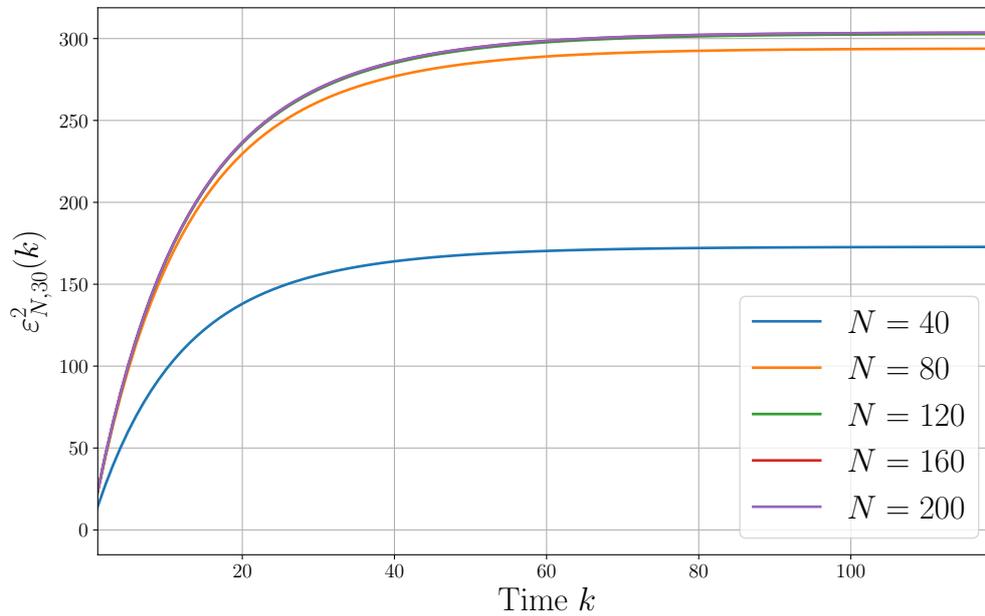
(a) MPC closed-loop cost at the final time $k = 400$ for different horizon lengths N.
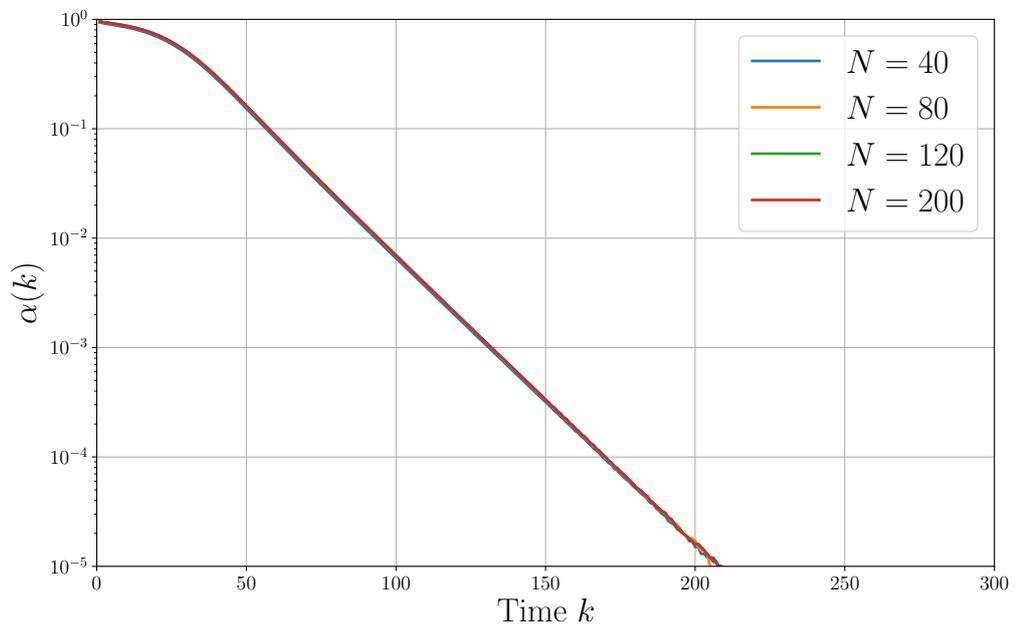
(b) Logarithmic plot of the evolution of the relative performance index α for different horizon lengths N.

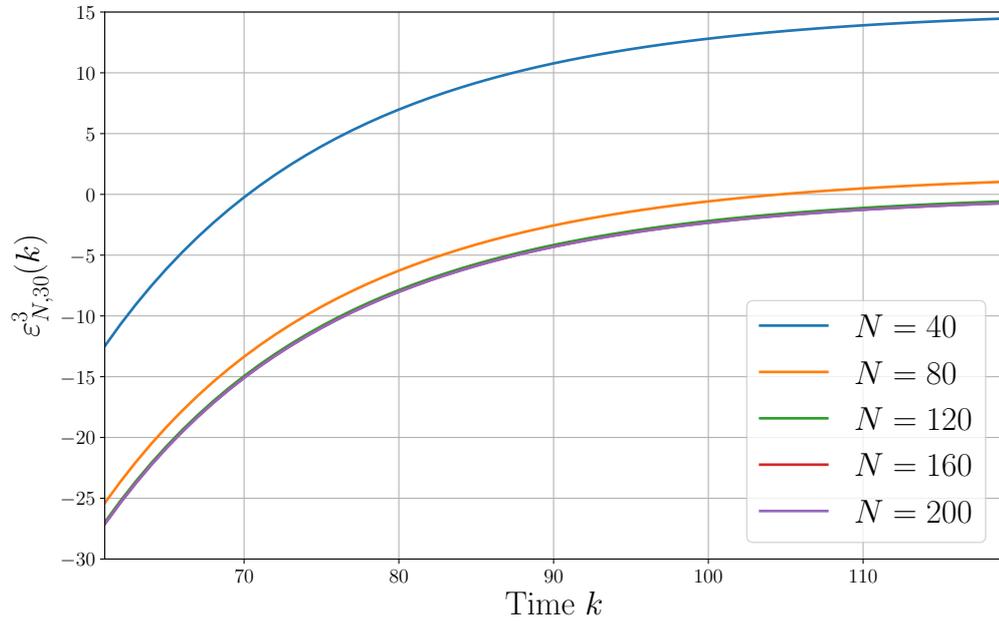Figure 6.4: MPC closed-loop cost and relative performance index

(a) Logarithmic plot of the cumulative performance index ε_N^1 over time k for different horizon lengths N.
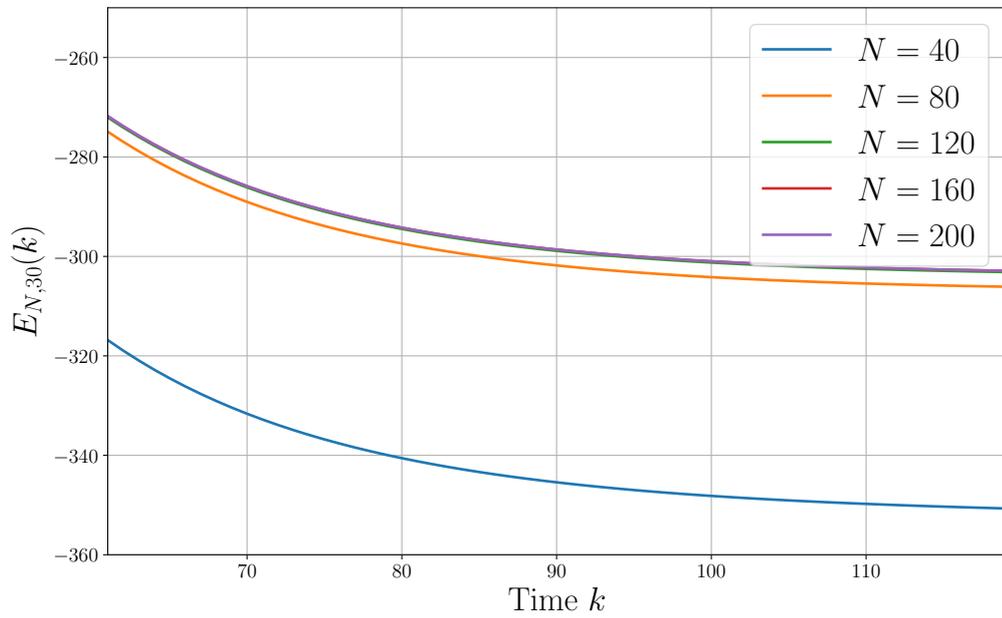

(b) Plot of the performance index $\varepsilon_{N,P}^2$ for $P = 30$ over time k for different horizon lengths N.

Figure 6.5: Plots of the individual components of the absolute performance index.

(a) Plot of the performance index $\varepsilon_{N,P}^3$ for $P = 30$ over a selected time window and for different horizon lengths N.

(b) Plot of the quantity $E_{N,P}$ over time k for $P = 30$ and different horizon lengths N.

Figure 6.6: Plots of the individual components of the absolute performance index.
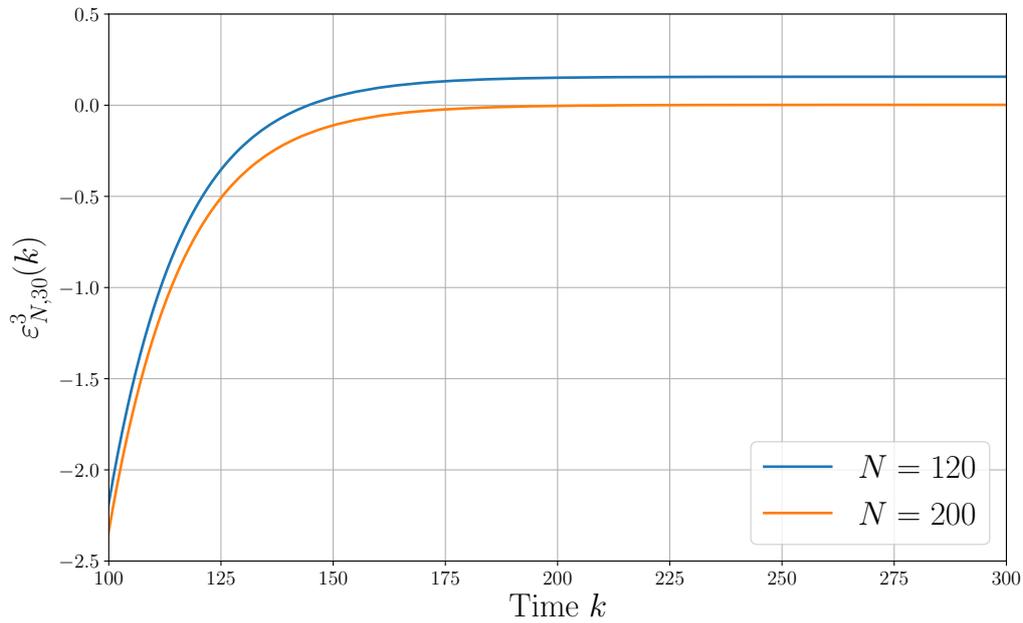
(a) Performance index ε_N^3 converging to different values for longer simulation times.
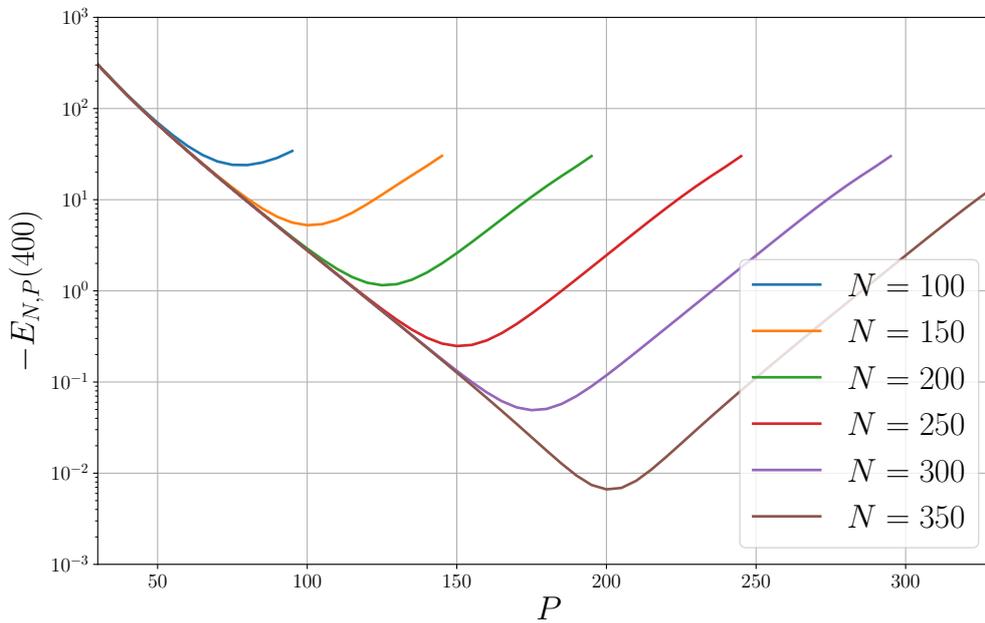
(b) Performance index $E_{N,P}(K)$ at the final time $K = 400$ for varying P and N.

Figure 6.7: Plots of performance index $\varepsilon_{N,P}^3$ for longer simulation times and of the influence of P on the value of $E_{N,P}$.

7 | Future research

To conclude the thesis, we outline some possibilities for future research.

Transient optimality
In Chapter 4, we have seen that the results for the performance and stability of the closed-loop for time-invariant economic MPC can be extended to time-varying systems. This tells us two things: first, the infinite horizon performance of the controller is near-optimal, and second, the MPC closed-loop will converge to a neighborhood of the optimal trajectory. However, there is no definite statement about how the controller behaves in the transient phase, i.e., what will happen as the controller approaches the optimal trajectory.
In the time-invariant case, it is known that the MPC control approaches the optimal equilibrium in an optimal way (cf. Theorem 2.17). This means that it is also nearly optimal in the transient phase in the sense that of all trajectories ending in a neighborhood of the optimal equilibrium the MPC closed-loop has the lowest cost.
We expect that it is possible to obtain a similar result in the time-varying case as well. In this context, Theorem 4.36 already provides a related result, although for open-loop trajectories instead of the MPC closed-loop.

Generalized sets of optimal operation
As mentioned in Remark 4.25, it may happen that there is not a single optimal trajectory of the system but a whole set of trajectories that are all optimal in the sense of overtaking optimality. In this case, we may no longer consider stability at a particular optimal trajectory but rather w.r.t. the set of optimal trajectories. So far, it is unclear how this extended stability concept can be adequately formalized and under what conditions we can recover convergence of the MPC closed-loop trajectory to the set of optimal trajectories. As also outlined in Remark 4.25, one idea is to consider a modified dissipativity notion that takes into account the set of optimal trajectories [81]. While it seems likely that the arguments in the stability proofs of Chapter 4 could be extended, the question remains how the modified dissipativity concept could be verified.

Improved simulation models for energy-efficient buildings
We have illustrated the analytical results in the thesis using simulations of the convection-diffusion equation. Although this equation already provides a good model for describing

the heat transfer within a building, it does not include the simulation of the airflow. Instead, the airflow was given either by prior simulations of the Navier-Stokes equations, or (in the 1D examples) it was assumed to be fully controllable. This means the airflow influences heat propagation, but not vice versa.

A more realistic building model should include the mutual coupling between heat and airflow. To this end, one could consider the fully coupled Navier-Stokes equations, but the need to solve optimal control problems online would pose considerable challenges as soon as complex 2D or even 3D geometries are involved. As a middle ground, one could use the so-called Boussinesq approximation of the Navier-Stokes equations, which simplifies the equations by only including buoyancy-driven density variations of the fluid [9]. We expect that this simplified model will present a realistic and at the same time affordable optimization model, especially in combination with POD.

State estimation for the convection-diffusion equation

The first step of the MPC Algorithm 2.1 is to measure the current state of the system, which is required as the initial state for the open-loop optimal control problem. So far, it was not addressed how this step can be realized in practical applications. In the case of convection-diffusion systems, the state of the system consists of the temperature at each point in the domain. Besides, the velocity field describing the airflow also needs to be known.

From a practical point of view, this presents some challenges since both temperature and airflow cannot be measured at every point but only at a few discrete locations throughout or at the boundary of the domain. Thus, for the implementation of an MPC controller in a real system, we also need to design an observer that can approximate the full state of the system based on discrete measurements of the airflow and temperatures.

The literature already offers several approaches for the design of PDE observers (see e.g. [68, 97, 108]) which will have to be assessed and then implemented for the convection-diffusion equation.

Prospective applications for the absolute performance estimate

Finally, the absolute MPC performance estimate proposed in Chapter 6 presents a versatile tool to evaluate the performance of MPC controllers online. We expect that this can be exploited in various algorithmic ways. Applications could include the automatic adjustment of the MPC horizon length whenever the performance deteriorates. This idea has already been successfully applied with the relative performance index α (see [66, 90]), and thus an extension to the absolute performance index seems within reach. In addition, we surmise that it is possible to use the method as an error estimator for POD, which in turn can be used to determine the appropriate number of POD basis functions. This means we apply the performance index as a measure of model inaccuracies which can be reduced by adding more POD basis functions. First results in this direction have been presented in [47].

A | Computation rules for the $\liminf$

Lemma A.1

Consider sequences $(a_n)_{n\in\mathbb{N}}$, $(b_n)_{n\in\mathbb{N}}$ with a_n converging to a, i.e. $\lim_{n\to\infty}(a_n) = a$. If the inequality

$$a + \liminf_{n\to\infty}(b_n) \geq 0 \tag{A.1}$$

is satisfied, then

$$\liminf_{n\to\infty}(a_n + b_n) \geq 0 \tag{A.2}$$

holds.

Proof. Let $\varepsilon > 0$. From the definition of the $\liminf$ it follows that there exists $N_0 \in \mathbb{N}$ such that

$$a + b_n \geq -\varepsilon \tag{A.3}$$

for all $n \geq N_0$. Moreover, since a is the limit of the sequence $(a_n)_{n\in\mathbb{N}}$ it holds that there exists $N_1 \in \mathbb{N}$ such that

$$a_n \geq a - \varepsilon \tag{A.4}$$

for all $n \geq N_1$. Summing up the two inequalities (A.3) and (A.4) gives

$$
\begin{aligned}
& a + b_n + a_n \geq a - 2\varepsilon \\
\Leftrightarrow \quad & b_n + a_n \geq -2\varepsilon
\end{aligned}
\tag{A.5}
$$

which holds for all $n \geq \max(N_0, N_1)$. Since ε was arbitrary it follows that

$$\liminf_{n\to\infty}(a_n + b_n) \geq 0. \tag{A.6}$$

This concludes the proof. □

Lemma A.2

Consider sequences $(a_n)_{n\in\mathbb{N}}$ and $(b_n)_{n\in\mathbb{N}}$ satisfying

$$\liminf_{n\to\infty}(a_n) \geq 0 \tag{A.7}$$

and

$$\liminf_{n\to\infty}(b_n) \geq 0. \tag{A.8}$$

Then the inequality

$$\liminf_{n\to\infty}(a_n + b_n) \geq 0 \tag{A.9}$$

holds.

Proof. We prove that

$$\liminf_{n\to\infty}(a_n) + \liminf_{n\to\infty}(b_n) \leq \liminf_{n\to\infty}(a_n + b_n). \tag{A.10}$$

From this it immediately follows that

$$\liminf_{n\to\infty}(a_n + b_n) \geq \underbrace{\liminf_{n\to\infty}(a_n)}_{\geq 0} + \underbrace{\liminf_{n\to\infty}(b_n)}_{\geq 0} \geq 0. \tag{A.11}$$

Define $a := \liminf_{n\to}(a_n)$, $b := \liminf_{n\to\infty}(b_n)$ and let $\varepsilon > 0$. Then there exist $N_1, N_2 \in N$ such that

$$a_n > a - \varepsilon \tag{A.12}$$

for all $n \geq N_1$ and

$$b_n > b - \varepsilon \tag{A.13}$$

for all $n \geq N_2$. Then for $N = \max\{N_1, N_2\}$ it holds that

$$a_n + b_n > a - \varepsilon + b - \varepsilon = a + b - 2\varepsilon. \tag{A.14}$$

Thus, taking the limit $n \to \infty$, it follows that $\liminf_{n\to\infty}(a_n + b_n) \geq a + b - 2\varepsilon$. Because ε was arbitrary, we obtain

$$\begin{aligned}
\liminf_{n\to\infty}(a_n + b_n) &\geq a + b \\
&= \liminf_{n\to}(a_n) + \liminf_{n\to\infty}(b_n)
\end{aligned} \tag{A.15}$$

This concludes the proof.

$$\square$$

List of Figures

Publications

[1] L. Grüne and S. Pirkelmann. Closed-loop performance analysis for economic model predictive control of time-varying systems. In *2017 IEEE 56th Annual Conference on Decision and Control (CDC)*, pages 5563–5569, Dec 2017.
`https://doi.org/10.1109/CDC.2017.8264485`

[2] L. Grüne, S. Pirkelmann, and M. Stieler. Strict dissipativity implies turnpike behavior for time-varying discrete time optimal control problems. In *Control Systems and Mathematical Methods in Economics: Essays in Honor of Vladimir M. Veliov*, volume 687 of *Lecture Notes in Economics and Mathematical Systems*, pages 195–218. Springer, Cham, 2018.
`http://doi.org/10.1007/978-3-319-75169-6_10`

[3] L. Grüne and S. Pirkelmann. Numerical verification of turnpike and continuity properties for time-varying PDEs. *IFAC-PapersOnLine*, **52**(2): 7–12, 2019
`http://doi.org/10.1016/j.ifacol.2019.08.002`

[4] S. Pirkelmann, D. Angeli, and L. Grüne. Approximate computation of storage functions for discrete-time systems using sum-of-squares techniques. *IFAC-PapersOnLine*, **52**(16): 508–513, 2019.
`http://doi.org/10.1016/j.ifacol.2019.12.012`

[5] L. Grüne and S. Pirkelmann. Economic model predictive control for time-varying system: Performance and stability results, *Optimal Control Applications and Methods*, **41**(1): 42-64, 2020.
`https://doi.org/10.1002/oca.2492`

[6] L. Grüne, L. Mechelli, S. Pirkelmann, S. Volkwein. Performance estimates for economic model predictive control and their application in proper orthogonal decomposition-based implementations. Accepted for publication in *AIMS' Journals*, 2020.
Available at: `http://nbn-resolving.de/urn:nbn:de:bsz:352-2-ywxqb2eru5d19`

Bibliography

[1] Quadrennial technology review: an assessment of energy technologies and research opportunities. Technical report, US Department of Energy, Washington, DC, 2015.

[2] Global status report for buildings and construction: Towards a zero-emissions, efficient and resilient buildings and construction sector. Technical report, International Energy Agency, 2019.

[3] A. Alessandretti, A. P. Aguiar, and C. N. Jones. On convergence and performance certification of a continuous-time economic model predictive control scheme with time-varying performance index. *Automatica*, 68:305 – 313, 2016.

[4] A. Alessandretti, A. P. Aguiar, and C. N. Jones. An input-to-state-stability approach to economic optimization in model predictive control. *IEEE Transactions on Automatic Control*, 62(12):6081–6093, 2017.

[5] A. Alla and S. Volkwein. Asymptotic stability of POD based model predictive control for a semilinear parabolic PDE. *Advances in Computational Mathematics*, 41(5):1073–1102, 2015.

[6] M. S. Alnæs, J. Blechta, J. Hake, A. Johansson, B. Kehlet, A. Logg, C. Richardson, J. Ring, M. E. Rognes, and G. N. Wells. The FEniCS project version 1.5. *Archive of Numerical Software*, 3(100), 2015.

[7] N. Altmüller. *Model Predictive Control for Partial Differential Equations*. PhD thesis, Universtität Bayreuth, Bayreuth, December 2014.

[8] R. Amrit, J. B. Rawlings, and D. Angeli. Economic optimization using model predictive control with a terminal cost. *Annual Rev. Control*, 35:178–186, 2011.

[9] J. Andrej. *Modeling and optimal control of multiphysics problems using the finite element method*. PhD thesis, Universität Kiel, Kiel, 2019.

[10] D. Angeli, R. Amrit, and J. B. Rawlings. On average performance and stability of economic model predictive control. *IEEE Trans. Autom. Control*, 57(7):1615–1626, 2012.

[11] S. Aseev, M. Krastanov, and V. Veliov. Optimality conditions for discrete-time optimal control on infinite horizon, November 2016. SWM/ORCOS Research Report 2016-09.

[12] A. Atangana. *Fractional Operators with Constant and Variable Order with Application to Geo-Hydrology.* Academic Press, 2018.

[13] S. Banholzer and D. Beermann. Optimal control and model-order reduction of an abstract parabolic system containing a controlled bilinear form : Applied to the example of a controlled advection term in an advection-diffusion equation. Technical report, Universität Konstanz, 2016.

[14] R. Becker, D. Meidner, and B. Vexler. Efficient numerical solution of parabolic optimization problems by finite element methods. *Optimization Methods and Software*, 22(5):813–833, 2007.

[15] J. Berberich, J. Köhler, F. Allgöwer, and M. A. Müller. Indefinite linear quadratic optimal control: Strict dissipativity and turnpike properties. *IEEE Control Systems Letters*, 2(3):399–404, July 2018.

[16] M. Bergounioux, K. Ito, and K. Kunisch. Primal-dual strategy for constrained optimal control problems. *SIAM Journal on Control and Optimization*, 37(4):1176–1194, 1999.

[17] J. Blot and N. Hayek. *Infinite-horizon optimal control in the discrete-time framework.* Springer, 2014.

[18] S. Brenner and R. Scott. *The mathematical theory of finite element methods*, volume 15. Springer Science & Business Media, third edition, 2008.

[19] A. Britzelmeier and M. Gerdts. Non-linear model predictive control of connected, automatic cars in a road network using optimal control methods. *IFAC-PapersOnLine*, 51(2):168 – 173, 2018. 9th Vienna International Conference on Mathematical Modelling.

[20] W. A. Brock and L. J. Mirman. Optimal economic growth and uncertainty: The discounted case. *Journal of Economic Theory*, 4(3):479 – 513, 1972.

[21] C. Chen, J. Wang, Y. Heo, and S. Kishore. MPC-based appliance scheduling for residential building energy management controller. *IEEE Transactions on Smart Grid*, 4(3):1401–1410, 2013.

[22] D. B. Crawley, C. O. Pedersen, L. K. Lawrie, and F. C. Winkelmann. Energyplus: Energy simulation program. *ASHRAE Journal*, 42:49–56, 2000.

[23] T. Damm, L. Grüne, M. Stieler, and K. Worthmann. An exponential turnpike theorem for dissipative discrete time optimal control problems. *SIAM Journal on Control and Optimization*, 52(3):1935–1957, 2014.

[24] P. A. Davidson. *An Introduction to Magnetohydrodynamics*. Cambridge Texts in Applied Mathematics. Cambridge University Press, 2001.

[25] M. Diehl, R. Amrit, and J. B. Rawlings. A Lyapunov function for economic optimizing model predictive control. *IEEE Transactions on Automatic Control*, 56(3):703–707, 2010.

[26] K. Dietl and K. Link. Start up optimization of combined cycle power plants: Controller development and real plant test results. pages 599–604, 04 2018.

[27] B. Dong and K. P. Lam. A real-time model predictive control for building heating and cooling systems based on the occupancy behavior pattern detection and local weather forecasting. *Building Simulation*, 7(1):89–106, Feb 2014.

[28] Z. Dong and D. Angeli. Analysis of economic model predictive control with terminal penalty functions on generalized optimal regimes of operation. *International Journal of Robust and Nonlinear Control*, 28(16):4790–4815, 2018.

[29] C. Ebenbauer and F. Allgöwer. Analysis and design of polynomial control systems using dissipation inequalities and sum of squares. *Computers and Chemical Engineering*, 30:1590–1602, 2006.

[30] M. Ellis, H. Durand, and P. D. Christofides. A tutorial review of economic model predictive control methods. *Journal of Process Control*, 24(8):1156 – 1178, 2014. Economic nonlinear model predictive control.

[31] M. Ellis, J. Liu, and P. D. Christofides. *Economic Model Predictive Control: Theory, Formulations and Chemical Process Applications*. Springer, Berlin, 2017.

[32] T. Erez, K. Lowrey, Y. Tassa, V. Kumar, S. Kolev, and E. Todorov. An integrated system for real-time model predictive control of humanoid robots. In *2013 13th IEEE-RAS International Conference on Humanoid Robots (Humanoids)*, pages 292–299, Oct 2013.

[33] K. Eriksson, C. Johnson, and V. Thomée. Time discretization of parabolic problems by the discontinuous Galerkin method. *ESAIM: Mathematical Modelling and Numerical Analysis*, 19(4):611–643, 1985.

[34] T. Faulwasser, K. Flaßkamp, S. Ober-Blöbaum, and K. Worthmann. Towards velocity turnpikes in optimal control of mechanical systems. *arXiv preprint arXiv:1907.01786*, 2019.

[35] T. Faulwasser, L. Grüne, and M. A. Müller. Economic nonlinear model predictive control. *Foundations and Trends® in Systems and Control*, 5(1):1–98, 2018.

[36] T. Faulwasser, M. Korda, C. N. Jones, and D. Bonvin. On turnpike and dissipativity properties of continuous-time optimal control problems. *Automatica*, 81:297–304, 2017.

[37] K. Flaßkamp, S. Ober-Blöbaum, and K. Worthmann. Symmetry and motion primitives in model predictive control. *Mathematics of Control, Signals, and Systems*, 31(4):455–485, Dec 2019.

[38] A. Foucquier, S. Robert, F. Suard, L. Stéphan, and A. Jay. State of the art in building modelling and energy performances prediction: A review. *Renewable and Sustainable Energy Reviews*, 23:272 – 288, 2013.

[39] D. Gale. On optimal development in a multi-sector economy. *Rev. Econ. Studies*, 34(1):1–18, 1967.

[40] C. E. García, D. M. Prett, and M. Morari. Model predictive control: Theory and practice—a survey. *Automatica*, 25(3):335 – 348, 1989.

[41] M. S. Gockenbach. *Understanding and implementing the finite element method*, volume 97. Society for Industrial and Applied Mathematics (SIAM), 2006.

[42] H. Goosse. *Climate system dynamics and modeling.* Cambridge University Press, 2015.

[43] L. Grüne. Economic receding horizon control without terminal constraints. *Automatica*, 49(3):725–734, 2013.

[44] L. Grüne. Approximation properties of receding horizon optimal control. *Jahresber. DMV*, 118(1):3–37, 2016.

[45] L. Grüne and R. Guglielmi. Turnpike properties and strict dissipativity for discrete time linear quadratic optimal control problems. *SIAM Journal on Control and Optimization*, 56(2):1282–1302, 2018.

[46] L. Grüne, C. M. Kellett, and S. R. Weller. On a discounted notion of strict dissipativity. *IFAC-PapersOnLine*, 49(18):247–252, August 2016.

[47] L. Grüne, L. Mechelli, S. Pirkelmann, and S. Volkwein. Performance estimates for economic model predictive control and their application in proper orthogonal decomposition-based implementations, May 2019.

[48] L. Grüne and M. A. Müller. On the relation between strict dissipativity and turnpike properties. *Systems & Control Letters*, 90:45 – 53, 2016.

[49] L. Grüne, M. A. Müller, C. M. Kellett, and S. R. Weller. Strict dissipativity for discrete time discounted optimal control problems, September 2019.

[50] L. Grüne and J. Pannek. *Nonlinear Model Predictive Control. Theory and Algorithms.* Springer, second edition, 2017.

[51] L. Grüne and S. Pirkelmann. Closed-loop performance analysis for economic model predictive control of time-varying systems. In *2017 IEEE 56th Annual Conference on Decision and Control (CDC)*, pages 5563–5569, Dec 2017.

[52] L. Grüne and S. Pirkelmann. Numerical verification of turnpike and continuity properties for time-varying PDEs. *IFAC-PapersOnLine*, 52(2):7–12, 2019.

[53] L. Grüne and S. Pirkelmann. Economic model predictive control for time-varying system: Performance and stability results. *Optimal Control Applications and Methods*, 41(1):42–64, 2020.

[54] L. Grüne, S. Pirkelmann, and M. Stieler. Strict dissipativity implies turnpike behavior for time-varying discrete time optimal control problems. In *Control Systems and Mathematical Methods in Economics: Essays in Honor of Vladimir M. Veliov*, volume 687 of *Lecture Notes in Economics and Mathematical Systems*, pages 195–218. Springer, Cham, 2018.

[55] L. Grüne, M. Schaller, and A. Schiela. Exponential sensitivity and turnpike analysis for linear quadratic optimal control of general evolution equations. *Journal of Differential Equations*, 2019.

[56] L. Grüne, M. Schaller, and A. Schiela. Sensitivity analysis of optimal control for a class of parabolic PDEs motivated by model predictive control. *SIAM Journal on Control and Optimization*, 57(4):2753–2774, 2019.

[57] L. Grüne and M. Stieler. Asymptotic stability and transient optimality of economic MPC without terminal conditions. *J. Proc. Control*, 24(8):1187–1196, 2014.

[58] L. Grüne and J. Pannek. Practical NMPC suboptimality estimates along trajectories. *Systems & Control Letters*, 58(3):161 – 168, 2009.

[59] M. Gubisch and S. Volkwein. Proper orthogonal decomposition for linear-quadratic optimal control. Technical report, Universität Konstanz, 2013.

[60] M. Gugat. A turnpike result for convex hyperbolic optimal boundary control problems. *Pure and Applied Functional Analysis*, 4(4):849–866, 11 2019.

[61] M. Gugat and F. Hante. On the turnpike phenomenon for optimal boundary control problems with hyperbolic systems. *SIAM Journal on Control and Optimization*, 57(1):264–289, 2019.

[62] B. Gutjahr, L. Gröll, and M. Werling. Lateral vehicle trajectory optimization using constrained linear time-varying MPC. *IEEE Transactions on Intelligent Transportation Systems*, 18(6):1586–1595, 2016.

[63] M. Hintermüller, K. Ito, and K. Kunisch. The primal-dual active set strategy as a semismooth newton method. *SIAM Journal on Optimization*, 13(3):865–888, 2002.

[64] D. Hrovat, S. Di Cairano, H. E. Tseng, and I. V. Kolmanovsky. The development of model predictive control in automotive industry: A survey. In *2012 IEEE International Conference on Control Applications*, pages 295–302, Oct 2012.

[65] K. Ito and K. Kunisch. *Lagrange Multiplier Approach to Variational Problems and Applications*. Society for Industrial and Applied Mathematics, 2008.

[66] T. U. Jahn and J. Pannek. Stability of constrained adaptive model predictive control algorithms. In *Proceedings of the 18th IFAC World Congress 2011 Held in Milano, Italy*, volume 18 of *World Congress*, pages 9272–9277. International Federation of Automatic Control (IFAC), Milano, Italy, 2011.

[67] H. Khalil. *Nonlinear Systems*. Pearson Education. Prentice Hall, 2002.

[68] M. Krstic and A. Smyshlyaev. *Boundary control of PDEs: A course on backstepping designs*, volume 16. Siam, 2008.

[69] K. Krumbiegel and A. Rösch. A virtual control concept for state constrained optimal control problems. *Computational Optimization and Applications*, 43(2):213–233, Jun 2009.

[70] K. Kunisch and S. Volkwein. Galerkin proper orthogonal decomposition methods for parabolic problems. *Numerische Mathematik*, 90(1):117–148, Nov 2001.

[71] A. Logg, K.-A. Mardal, and G. Wells. *Automated solution of differential equations by the finite element method: The FEniCS book*, volume 84. Springer Science & Business Media, 2012.

[72] V. Lykina and S. Pickenhain. Weighted functional spaces approach in infinite horizon optimal control problems: A systematic analysis of hidden opportunities and advantages. *Journal of Mathematical Analysis and Applications*, 454(1):195 – 218, 2017.

[73] T. Martin, P. N. Köhler, and F. Allgöwer. Dissipativity and economic model predictive control for optimal set operation. In *2019 American Control Conference (ACC)*, pages 1020–1026, July 2019.

[74] D. Mayne. An apologia for stabilising terminal conditions in model predictive control. *International Journal of Control*, 86, 11 2013.

[75] M. J. McCourt and P. J. Antsaklis. Demonstrating passivity and dissipativity using computational methods. *ISIS*, 8, 2013.

[76] L. Mechelli. *POD-based State-Constrained Economic Model Predictive Control of Convection-Diffusion Phenomena*. PhD thesis, Universität Konstanz, Konstanz, 2019.

[77] L. Mechelli and S. Volkwein. POD-based economic optimal control of heat-convection phenomena. In M. Falcone, R. Ferretti, L. Grüne, and W. McEneaney, editors, *Numerical Methods for Optimal Control Problems*, pages 63–87. Springer International Publishing, 2018.

[78] L. Mechelli and S. Volkwein. POD-based economic model predictive control for heat-convection phenomena. In F. A. Radu, K. Kumar, I. Berre, J. M. Nordbotten, and I. S. Pop, editors, *Numerical Mathematics and Advanced Applications ENUMATH 2017*, pages 663–671. Springer International Publishing, 2019.

[79] D. Meidner and B. Vexler. Adaptive space-time finite element methods for parabolic optimization problems. *SIAM Journal on Control and Optimization*, 46(1):116–142, 2007.

[80] D. Meidner and B. Vexler. A priori error estimates for space-time finite element discretization of parabolic optimal control problems part i: Problems without control constraints. *SIAM Journal on Control and Optimization*, 47(3):1150–1177, 2008.

[81] M. A. Müller. Dissipativity in economic model predictive control: beyond steady-state optimality. arXiv:1911.09908, 2019.

[82] M. A. Müller. Dissipativity in economic MPC: time-varying case. Personal communication, 2019.

[83] M. A. Müller, D. Angeli, and F. Allgöwer. On necessity and robustness of dissipativity in economic model predictive control. *IEEE Transactions on Automatic Control*, 60(6):1671–1676, June 2015.

[84] M. A. Müller and L. Grüne. Economic model predictive control without terminal constraints for optimal periodic behavior. *Automatica*, 70:128–139, August 2016.

[85] M. A. Müller, L. Grüne, and F. Allgöwer. On the role of dissipativity in economic model predictive control. *IFAC-PapersOnLine*, 48(23):110 – 116, 2015. 5th IFAC Conference on Nonlinear Model Predictive Control NMPC 2015.

[86] M. Muratori and G. Rizzoni. Residential demand response: Dynamic energy management and time-varying electricity pricing. *IEEE Transactions on Power systems*, 31(2):1108–1117, 2015.

[87] Y. Nesterov. *Introductory Lectures on Convex Optimization: A Basic Course*, volume 87 of *Applied Optimization*. Springer US, 1 edition, 2004.

[88] J. Nocedal and S. Wright. *Numerical optimization.* Springer Science & Business Media, 2006.

[89] F. Oldewurtel, A. Ulbig, A. Parisio, G. Andersson, and M. Morari. Reducing peak electricity demand in building climate control using real-time pricing and model predictive control. In *49th IEEE conference on decision and control (CDC)*, pages 1927–1932. IEEE, 2010.

[90] J. Pannek. *Receding Horizon Control: A Suboptimality-based Approach.* PhD thesis, Bayreuth, 2009.

[91] J. Pannek and K. Worthmann. Stability and performance guarantees for model predictive control algorithms without terminal constraints. *ZAMM - Journal of Applied Mathematics and Mechanics / Zeitschrift für Angewandte Mathematik und Mechanik*, 94(4):317–330, 2014.

[92] S. Pirkelmann, D. Angeli, and L. Grüne. Approximate computation of storage functions for discrete-time systems using sum-of-squares techniques. *IFAC-PapersOnLine*, 52(16):508–513, 2019.

[93] S. Qin and T. Badgwell. An overview of nonlinear model predictive control applications. In F. Allgöwer and A. Zheng, editors, *Nonlinear Model Predictive Control*, pages 369–392, Basel, 2000. Birkhäuser Basel.

[94] S. Qin and T. Badgwell. A survey of industrial model predictive control technology. *Control Engineering Practice*, 11(7):733 – 764, 2003.

[95] F. Rathgeber, D. A. Ham, L. Mitchell, M. Lange, F. Luporini, A. T. T. Mcrae, G.-T. Bercea, G. R. Markall, and P. H. J. Kelly. Firedrake. *ACM Transactions on Mathematical Software*, 43(3):1–27, Dec 2016.

[96] J. Rawlings, D. Mayne, and M. Diehl. *Model Predictive Control: Theory and Design.* Nob Hill Pub., second edition, 2017.

[97] A. Schaum, T. Meurer, and J. A. Moreno. Dissipative observers for coupled diffusion–convection–reaction systems. *Automatica*, 94:307 – 314, 2018.

[98] C. Scherer and S. Weiland. Linear matrix inequalities in control. *Lecture Notes, Dutch Institute for Systems and Control, Delft, The Netherlands*, 2015.

[99] E. D. Sontag. *Mathematical control theory: deterministic finite dimensional systems*, volume 6. Springer Science & Business Media, 2013.

[100] E. Trélat, C. Zhang, and E. Zuazua. Steady-state and periodic exponential turnpike property for optimal control problems in Hilbert spaces. *SIAM Journal on Control and Optimization*, 56(2):1222–1252, 2018.

[101] E. Trélat and E. Zuazua. The turnpike property in finite-dimensional nonlinear optimal control. *Journal of Differential Equations*, 258(1):81–114, 2015.

[102] M. Ulbrich. *Semismooth Newton Methods for Variational Inequalities and Constrained Optimization Problems in Function Spaces*. Society for Industrial and Applied Mathematics, USA, 2011.

[103] M. Vukov, S. Gros, G. Horn, G. Frison, K. Geebelen, J. Jørgensen, J. Swevers, and M. Diehl. Real-time nonlinear MPC and MHE for a large-scale mechatronic application. *Control Engineering Practice*, 45:64 – 78, 2015.

[104] A. Wächter and L. T. Biegler. On the implementation of an interior-point filter line-search algorithm for large-scale nonlinear programming. *Mathematical Programming*, 106(1):25–57, March 2006.

[105] M. Wetter, W. Zuo, T. S. Nouidui, and X. Pang. Modelica buildings library. *Journal of Building Performance Simulation*, 7(4):253–270, 2014.

[106] J. C. Willems. Dissipative dynamical systems part I: General theory. *Archive for Rational Mechanics and Analysis*, 45(5):321–351, 1972.

[107] J. C. Willems. Dissipative dynamical systems part II: Linear systems with quadratic supply rates. *Archive for Rational Mechanics and Analysis*, 45(5):352–393, Jan 1972.

[108] A. V. Wouwer and M. Zeitz. State estimation in distributed parameter systems. *Encyclopedia of Life Support Systems (EOLSS), chap. Control Systems, Robotics and Automation, article*, (6.43):19–3, 2001.

[109] M. Zanon, S. Gros, and M. Diehl. A Lyapunov function for periodic economic optimizing model predictive control. In *Proceedings of the 52nd IEEE Conference on Decision and Control — CDC2013*, pages 5107–5112, Florence, Italy, 2013.

[110] M. Zanon, L. Grüne, and M. Diehl. Periodic optimal control, dissipativity and MPC. *IEEE Transactions on Automatic Control*, 62(6):2943–2949, June 2017.

[111] H.-X. Zhao and F. Magoulès. A review on the prediction of building energy consumption. *Renewable and Sustainable Energy Reviews*, 16(6):3586 – 3592, 2012.

Eidesstattliche Versicherung

Hiermit versichere ich an Eides statt, dass ich die vorliegende Arbeit selbstständig verfasst und keine anderen als die von mir angegebenen Quellen und Hilfsmittel verwendet habe.

Weiterhin erkläre ich, dass ich die Hilfe von gewerblichen Promotionsberatern bzw. Promotionsvermittlern oder ähnlichen Dienstleistern weder bisher in Anspruch genommen habe, noch künftig in Anspruch nehmen werde.

Zusätzlich erkläre ich hiermit, dass ich keinerlei früheren Promotionsversuche unternommen habe.

Bayreuth,

_____

Simon Pirkelmann